

Quasi Deterministic Radio Channel Generator User Manual and Documentation



Document Revision: v1.4.8-571
September 5, 2016

Fraunhofer Heinrich Hertz Institute
Wireless Communications and Networks
Einsteinufer 37, 10587 Berlin, Germany

e-mail: quadriga@hhi.fraunhofer.de
<http://www.quadriga-channel-model.de>



Contributors

Editor: Fraunhofer Heinrich Hertz Institute
Wireless Communications and Networks
Einsteinufer 37, 10587 Berlin, Germany

Contributing Authors: Stephan Jaeckel, Leszek Raschkowski, Kai Börner and Lars Thiele
Fraunhofer Heinrich Hertz Institute

Frank Burkhardt and Ernst Eberlein
Fraunhofer Institute for Integrated Circuits IIS

Grants and Funding

This work was supported by

- the European Space Agency (ESA) in the Advanced Research in Telecommunications Systems (ARTES) programme under contract AO/1-5985/09/08/NL/LvH (Acronym: MIMOSA), [1]
<http://artes.esa.int/projects/mimosa-characterisation-mimo-channel-mobile-satellite-systems>
- the German Federal Ministry of Economics and Technology (BMWi) in the national collaborative project IntelliSpektrum under contract 01ME11024
<http://www.intellispektrum.de>
- the European Commission co-funded the project METIS as an Integrated Project under the Seventh Framework Programme for research and development (FP7)
<http://www.metis2020.com>
- the GreenTouch consortium within the funded project “LSAS Channel Modelling”
<http://www.greentouch.org>
- the European Commission co-funded the project mmMAGIC as an Integrated Project under the Horizon 2020 Programme for research and development (FP7)
<https://5g-mmagic.eu/>

Acknowledgements

The authors thank G. Sommerkorn, C. Schneider, M. Kaeske [Ilmenau University of Technology (IUT), Ilmenau, Germany] and V. Jungnickel [Heinrich Hertz Institute (HHI), Berlin, Germany] for the fruitful discussions on the QuaDRiGa channel model and the manuscript of this document.

How to Cite QuaDRiGa

- [2] S. Jaeckel, L. Raschkowski, K. Börner, and L. Thiele, “QuaDRiGa: A 3-D multi-cell channel model with time evolution for enabling virtual field trials,” *IEEE Trans. Antennas Propag.*, vol. 62, pp. 3242-3256, 2014.
- [3] S. Jaeckel, L. Raschkowski, K. Börner, L. Thiele, F. Burkhardt and E. Eberlein, ”QuaDRiGa - Quasi Deterministic Radio Channel Generator, User Manual and Documentation”, Fraunhofer Heinrich Hertz Institute, Tech. Rep. v1.4.8-571, 2016.

Contents

| | |
|--|-----------|
| 1 Introduction and Overview | 12 |
| 1.1 Installation and System Requirements | 12 |
| 1.2 General Remarks | 12 |
| 1.3 Introduction to QuaDRiGa | 14 |
| 1.4 Continuous time evolution | 16 |
| 1.5 QuaDRiGa Program Flow | 17 |
| 1.6 Description of modeling of different reception conditions by means of a typical drive course . | 18 |
| 2 Software Structure | 22 |
| 2.1 Overview | 22 |
| 2.2 Description of Classes, Properties, and Methods | 23 |
| 2.2.1 Class “simulation_parameters” | 25 |
| 2.2.2 Class “array” | 27 |
| 2.2.3 Class “track” | 34 |
| 2.2.4 Class “layout” | 39 |
| 2.2.5 Class “parameter_set” | 45 |
| 2.2.6 Class “channel_builder” | 48 |
| 2.2.7 Class “channel” | 50 |
| 2.3 Data Flow | 54 |
| 2.4 Scenario Specific Parameters | 55 |
| 2.4.1 Description of the Parameter Table | 55 |
| 2.4.2 Adding New Scenarios | 59 |
| 3 Technical Documentation | 61 |
| 3.1 Correlated Large-Scale Parameter Maps | 62 |
| 3.2 Initial Delays and Path Powers | 65 |
| 3.3 Departure and Arrival Angles | 66 |
| 3.4 Drifting | 69 |
| 3.5 Antennas and Polarization | 73 |
| 3.5.1 Relation between the Polarization Model and the Jones Calculus | 73 |
| 3.5.2 Changing the Orientation of Antennas | 75 |
| 3.5.3 Constructing the Polarization Transfer Matrix | 77 |
| 3.6 Combining Sub-Paths into Paths | 79 |
| 3.7 Path Gain, Shadow Fading and K-Factor | 79 |
| 3.8 Transitions between Segments | 80 |
| 3.9 Postprocessing / Variable Speeds | 80 |
| 4 3GPP-3D calibration results | 81 |
| A Tutorials | 92 |
| A.1 Network Setup and Parameter Generation | 92 |
| A.2 Simulating a Measured Scenario | 96 |
| A.3 Generation of Satellite Channels | 100 |
| A.4 Drifting Phases and Delays | 108 |
| A.5 Time Evolution and Scenario Transitions | 112 |
| A.6 Applying Varying Speeds (Channel Interpolation) | 117 |
| A.7 Geometric Polarization | 121 |
| A.8 Visualizing RHCP/LHCP Patterns | 125 |
| A.9 How to manually set LSPs in QuaDRiGa | 127 |

B Departure and Arrival Angles (Adopted WINNER Method)

131

List of Figures

| | | |
|----|---|-----|
| 1 | Evolution of GSCMs | 13 |
| 2 | Simplified overview of the modeling approach used in QuaDRiGa | 15 |
| 3 | Typical driving course | 18 |
| 4 | UML class diagram of the model software. | 24 |
| 5 | QuaDRiGa Data Flow | 54 |
| 6 | Steps for the calculation of time-evolving channel coefficients | 61 |
| 7 | Principle of the generation of channel coefficients based on correlated LSPs | 63 |
| 8 | Map-based 2-D autocorrelation shaping using FIR filters | 64 |
| 9 | Maximal achievable angular spread depending on the K-factor | 68 |
| 10 | Scatterer positions and arrival angles (single-bounce model) | 69 |
| 11 | Scatterer positions and arrival angles (multi-bounce model) | 71 |
| 12 | Example showing the effect of the new polarization rotation method | 74 |
| 13 | Example patterns for a dipole antenna | 75 |
| 14 | Illustration of overlapping segments and variable MT speeds | 81 |
| 15 | 3GPP-3D Calibration Results: Coupling Loss (Phase 1) | 84 |
| 16 | 3GPP-3D Calibration Results: Geometry Factor (Phase 1) | 84 |
| 17 | 3GPP-3D Calibration Results: Zenith of Departure Angle (Phase 1) | 85 |
| 18 | 3GPP-3D Calibration Results: Coupling Loss (Phase 2) | 86 |
| 19 | 3GPP-3D Calibration Results: Wideband SINR (Phase 2) | 87 |
| 20 | 3GPP-3D Calibration Results: Zenith of Departure Spread (Phase 2) | 88 |
| 21 | 3GPP-3D Calibration Results: Zenith of Arrival Spread (Phase 2) | 88 |
| 22 | 3GPP-3D Calibration Results: Largest Singular Value (Phase 2) | 90 |
| 23 | 3GPP-3D Calibration Results: Smallest Singular Value (Phase 2) | 90 |
| 24 | 3GPP-3D Calibration Results: Ratio of Singular Values (Phase 2) | 91 |
| 25 | Distribution of the users in the scenario. | 93 |
| 26 | Comparison of input values and simulation results | 94 |
| 27 | Scenario setup for the comparison of simulated and measured data | 97 |
| 28 | 2D PDP of the simulated track | 97 |
| 29 | Results for the measurement based simulation tutorial | 99 |
| 30 | Receiver track for the satellite channel tutorial | 101 |
| 31 | Antenna patterns for the satellite channel tutorial | 102 |
| 32 | Results for the satellite channel tutorial | 107 |
| 33 | Scenario setup for the drifting phases tutorial | 108 |
| 34 | Cluster delays vs. Rx position (drifting phases tutorial) | 109 |
| 35 | Drifting phases and Tx power vs. Rx position (drifting phases tutorial) | 110 |
| 36 | Phases and Tx power vs. Rx position without drifting (drifting phases tutorial) | 111 |
| 37 | Scenario setup for the time evolution tutorial | 113 |
| 38 | Received power on the circular track (time evolution tutorial) | 114 |
| 39 | Received power on the linear track (time evolution tutorial) | 116 |
| 40 | Scenario setup for the speed profile tutorial | 118 |
| 41 | Received power and 2D PDP for the speed profile tutorial | 118 |
| 42 | Movement profile (left) and interpolated PDP (right) | 120 |
| 43 | Polarimetric dipole antenna patterns for different orientations | 121 |
| 44 | Scenario layout | 122 |
| 45 | Results from the geometric polarization tutorial | 123 |
| 46 | RHCP / LHCP antenna patterns | 126 |
| 47 | Scenario overview (manual parameter selection) | 128 |

| | | |
|----|--|-----|
| 48 | Power along the track (manual parameter selection) | 130 |
| 49 | DS along the track (manual parameter selection) | 130 |
| 50 | Visualization of the angular spread correction function $C_\phi(L, K)$ | 132 |

List of Tables

| | | |
|----|---|-----|
| 1 | QuaDRiGa System Requirements | 12 |
| 2 | System Compatibility Tests | 12 |
| 10 | Parameter sets provided together with the standard software | 55 |
| 12 | Offset Angle of the m^{th} Sub-Path from [4] | 69 |
| 13 | Simulation assumptions for 3GPP-3D calibration | 83 |
| 14 | Correction values from [4] for different numbers of paths | 133 |
| 15 | Comparison of the correction functions | 133 |

List of Acronyms

| | |
|--------|---|
| 2-D | two-dimensional |
| 3-D | three-dimensional |
| 3GPP | 3rd generation partnership project |
| AoA | azimuth angle of arrival |
| AoD | azimuth angle of departure |
| AS | angular spread |
| ASA | azimuth spread of arrival |
| ASD | azimuth spread of departure |
| BS | base station |
| CIR | channel impulse response |
| DS | delay spread |
| EoA | elevation angle of arrival |
| EoD | elevation angle of departure |
| ESA | elevation angle spread of arrival |
| ESD | elevation angle spread of departure |
| FBS | first-bounce scatterer |
| FIR | finite impulse response |
| FWHM | full width at half maximum |
| GCS | global coordinate system |
| GF | geometry factor |
| GSCM | geometry-based stochastic channel model |
| i.i.d. | independent and identically distributed |
| KF | Ricean K-factor |
| LBS | last-bounce scatterer |
| LHCP | left hand circular polarized |
| LOS | line of sight |
| LSF | large-scale fading |
| LSP | large-scale parameter |
| MIMO | multiple-input multiple-output |
| MIMOSA | MIMO over satellite |
| MPC | multipath component |
| MT | mobile terminal |
| NLOS | non-line of sight |

| | |
|----------|---|
| O2I | outdoor-to-indoor |
| PAS | power-angular spectrum |
| PDP | power delay profile |
| PG | path gain |
| PL | path loss |
| QuaDRiGa | quasi deterministic radio channel generator |
| RB | resource block |
| RHCP | right hand circular polarized |
| RSRP | reference signal received power |
| Rx | receiver |
| SCM | spatial channel model |
| SF | shadow fading |
| SINR | signal to interference and noise ratio |
| SISO | single input single output |
| SSF | small-scale-fading |
| SSG | state sequence generator |
| STD | standard deviation |
| Tx | transmitter |
| UMa | urban-macrocell |
| UMi | urban-microcell |
| UML | unified modeling language |
| WGS | world geodetic system |
| WINNER | Wireless World Initiative for New Radio |
| WSS | wide-sense stationary |
| WSSUS | wide sense stationary uncorrelated scattering |
| XPR | cross polarization ratio |
| ZoA | zenith angle of arrival |
| ZoD | zenith angle of departure |
| ZSA | zenith angle spread of arrival |
| ZSD | zenith angle spread of departure |

Glossary

| | |
|--|----------------|
| base station (BS) | 61 |
| The term base station (BS) refers to a fixed transmitter which utilizes one or more transmit antennas to serve one or more MTs . BSs might further use <i>sectors</i> to increase the capacity. Usually, BSs operate independent of each other which might lead to inter-BS interference if they use the same time and frequency resource. | |
| cell | 62 |
| Synonym for <i>sector</i> . | |
| cluster | 77, 80 |
| A cluster describes an area where many scattering events occur simultaneously, e.g. at the foliage of trees or at a rough building wall. In the channel model, each scattering cluster is approximated by 20 single reflections. Each of those reflections has the same propagation delay. | |
| drifting | 69 |
| Drifting occurs within a small area (about 20-30 m diameter) in which a specific “ <i>cluster</i> ” can be seen from the MT . Within this area the cluster position is fixed. Due to the mobility of the terminal the path length (resulting in a path delay) and the arrival angles change slowly, i.e. they “ <i>drift</i> ”. | |
| large-scale parameter (LSP) | 62 |
| The term “ <i>large scale parameter</i> ” refers to a set of specific properties of the propagation channel. Those are the “ <i>delay spread</i> ”, the “ <i>K-factor</i> ”, the “ <i>shadow fading</i> ”, the “ <i>cross-polarization ratio</i> ”, and four “ <i>angular spread</i> ”-values. Those properties can be extracted from channel sounding data. If a large amount of channel measurements is available for a specific propagation <i>scenario</i> and the LSPs can be calculated from those channels, statistics of the LSPs , e.g. their distribution and correlation properties can be obtained. A complete set of such statistical properties forms a “parameter table” that characterizes the <i>scenario</i> . | |
| mobile terminal (MT) | 61 |
| Mobile terminals (MTs) are mobile receivers with one or more receive antennas. They are usually assigned to a serving BS which delivers data to the terminal. | |
| multipath component (MPC) | 61 |
| Synonym for <i>path</i> . | |
| path | 66, 69, 79, 80 |
| A path describes the way that a signal takes from the transmitter to the receiver. In the channel model, there is usually a direct, or LOS path, and several indirect, or NLOS paths. Indirect paths involve one or more scattering events which are described by clusters. However, paths do not describe single reflections but combine sub-paths that can not be separated in the delay domain. Usually, the channel model uses 6-25 paths to describe the propagation channel. | |
| scatterer | 69, 77 |
| A scatterer describes a single reflection along a NLOS propagation path. Usually, several scatterers with a similar propagation delay and a narrow angular spread are combined into a “(<i>scattering cluster</i>)”. | |

| | |
|---|------------|
| scattering cluster | 61 |
| Synonym for <i>cluster</i> . | |
| scenario | 62 |
| In this thesis, the term <i>scenario</i> refers to a specific propagation environment such as “Urban macro-cell”, “Urban satellite”, “Indoor hotspot”, etc. Usually, each propagation environment can be further split into LOS and NLOS propagation (e.g. “Urban macro-cell LOS” and “Urban macro-cell NLOS”), both of which might have very different properties. In the channel model, each <i>scenario</i> is fully specified by a parameter table. | |
| segment | 62, 69, 80 |
| Segments are parts of a user trajectory in which the LSPs do not change considerably and where the channel keeps its WSS properties. Typical segment lengths are 5-30 m. It is assumed that within a segment, the scattering clusters are fixed. | |
| sub-path | 68, 79 |
| A sub-path is the exact way that a signal takes from the transmitter to the receiver. It contains at least one reflection. However, normally the channel model uses two scatterers (resulting in two reflections) to create a sub-path. 20 sub-paths are combined to a path. The LOS path has no sub-paths. | |
| time evolution | 61, 69 |
| Time evolution describes how the propagation channel changes (or evolves) with time. In the channel model, two effects are used to describe this time-dependency: <i>drifting</i> and the birth and death of scattering clusters during the transition between <i>segments</i> . The propagation environment is considered static and, thus, the model includes time-evolution only when the receiver is moving. | |
| user | 63 |
| Synonym for <i>mobile terminal</i> . | |

List of Symbols

| | | |
|---------------|--|----------------------|
| γ | Polarization rotation angle for the linear NLOS polarization in [rad] | 78 |
| λ | Wavelength in units of [m] | 61, 70 |
| ϕ | Azimuth angle in [rad]. ϕ can be used for ϕ^d or ϕ^a | 66, 67, 73, 131, 132 |
| ϕ^a | Azimuth angle of arrival (AoA) in [rad] | 66, 68, 69 |
| ϕ^d | Azimuth angle of departure (AoD) in [rad] | 66, 68, 69 |
| $\hat{\phi}$ | The offset angle between the path angle ϕ of the m^{th} sub-path in [degree] | 68 |
| ψ | Phase of a path in [rad] | 70, 79 |
| ρ | Correlation coefficient | 65 |
| σ_ϕ | The RMS angular spread in [rad] | 67, 131, 132 |
| σ_τ | The RMS delay spread in units of [s] | 62, 65, 66 |
| τ | Delay of a MPC in units of [s] | 65, 66, 69, 70 |
| θ | Elevation angle in [rad]. θ can be used for θ^d or θ^a | 67, 73 |
| ϑ | Polarization rotation angle in [rad] | 76, 77 |
| θ^a | Elevation angle of arrival (EoA) in [rad] | 66–69 |
| θ^d | Elevation angle of departure (EoD) in [rad] | 66–69 |
| ζ | A coefficient describing additional shadowing within a PDP | 65 |
| a | Vector pointing from the position of the LBS to the Rx position | 70, 77 |
| B | Bandwidth in units of [Hz] | 61 |
| B | LSP map represented as a matrix with real-valued coefficients | 63 |

| | | |
|--------------------|--|----------------------|
| b | Vector pointing from the Tx position to the position of the LBS | 70 |
| <i>c</i> | Speed of Light | 69, 70 |
| c | Representation of the departure or arrival angle in Cartesian coordinates | 75 |
| c_ϕ | The scenario-dependent cluster-wise RMS angular spread in [degree] | 68 |
| <i>d</i> | Length of a propagation path in [m] | 69, 79 |
| d_λ | Decorrelation distance in [m] where the autocorrelation falls below e^{-1} | 63 |
| $\mathbf{e}_{r,s}$ | Vector from the Rx position to Rx antenna element <i>r</i> at snapshot <i>s</i> | 70 |
| F | Polarimetric antenna response | 73, 76 |
| f_S | Sampling Rate in [samples per meter] | 62 |
| f_T | Sampling Rate in [samples per second] | 61 |
| <i>g</i> | Channel coefficient in time domain | 73 |
| J | Jones vector | 73 |
| <i>K</i> | Ricean K-Factor, linear scale | 65, 131 |
| <i>k</i> | Filter coefficient index | 64 |
| $K^{[\text{dB}]}$ | Ricean K-Factor, logarithmic scale | 132 |
| <i>L</i> | Number of paths | 65, 66, 131, 132 |
| <i>l</i> | Path index, $l \in \{1, 2, \dots, L\}$ | 65, 66, 69 |
| <i>m</i> | Sub-path index, $m \in \{1, 2, \dots, M\}$ | 68, 69 |
| M | Polarization coupling matrix | 73 |
| \mathcal{N} | Normal distribution $\mathcal{N}(\mu, \sigma^2)$ with mean μ and STD σ | 65–68, 78, 79, 131 |
| <i>P</i> | Power | 65, 66, 79, 131, 132 |
| <i>r</i> | Receive antenna index; $r \in \{1, 2, \dots, n_r\}$ | 69 |
| R | Rotation matrix | 76 |
| r | Vector pointing from the Tx position to the Rx position | 69, 70, 72, 77 |
| r_τ | Proportionality factor to trade between delays and path powers | 65 |
| <i>s</i> | Snapshot index $s \in \{1, 2, \dots, S\}$ | 69 |
| <i>t</i> | Transmit antenna index; $t \in \{1, 2, \dots, n_t\}$ | 69 |
| \mathcal{U} | Continuous uniform distribution $\mathcal{U}(a, b)$ with minimum a and maximum b | 65, 73 |
| <i>v</i> | Speed in [m/s] | 61 |
| <i>X</i> | A random variable | 65, 78, 131 |
| X | Matrix containing the inter-parameter correlation values | 65 |
| <i>Y</i> | A random variable | 131 |
| <i>Z</i> | A random variable | 65, 73 |

References

- [1] E. Eberlein, T. Heyn, F. Burkhardt, S. Jaeckel, L. Thiele, T. Haustein, G. Sommerkorn, M. Käske, C. Schneider, M. Dominguez, and J. Grotz, “Characterisation of the MIMO channel for mobile satellite systems (acronym: MIMOSA), TN8.2 – final report,” Fraunhofer Institute for Integrated Circuits (IIS), Tech. Rep. v1.0, 2013.
- [2] S. Jaeckel, L. Raschkowski, K. Börner, and L. Thiele, “QuaDRiGa: A 3-D multi-cell channel model with time evolution for enabling virtual field trials,” *IEEE Trans. Antennas Propag.*, vol. 62, pp. 3242–3256, 2014.
- [3] S. Jaeckel, L. Raschkowski, K. Börner, L. Thiele, F. Burkhardt, and E. Eberlein, “QuaDRiGa - Quasi Deterministic Radio Channel Generator, User Manual and Documentation,” Fraunhofer Heinrich Hertz Institute, Tech. Rep. v1.4.1-551, 2016.
- [4] P. Kyösti, J. Meinilä, L. Hentilä *et al.*, “IST-4-027756 WINNER II D1.1.2 v.1.1: WINNER II channel models,” Tech. Rep., 2007. [Online]. Available: <http://www.ist-winner.org>

- [5] P. Heino, J. Meinilä, P. Kyösti *et al.*, “CELTIC / CP5-026 D5.3: WINNER+ final channel models,” Tech. Rep., 2010. [Online]. Available: <http://projects.celtic-initiative.org/winner+>
- [6] C. Schneider, M. Narandzic, M. Käske, G. Sommerkorn, and R. Thomä, “Large scale parameter for the WINNER II channel model at 2.53 GHz in urban macro cell,” *Proc. IEEE VTC '10 Spring*, 2010.
- [7] M. Narandzic, C. Schneider, M. Käske, S. Jaeckel, G. Sommerkorn, and R. Thomä, “Large-scale parameters of wideband MIMO channel in urban multi-cell scenario,” *Proc. EUCAP '11*, 2011.
- [8] 3GPP TR 36.873, “Study on 3D channel model for LTE,” Tech. Rep., 2015.
- [9] H. Xiao, A. Burr, and L. Song, “A time-variant wideband spatial channel model based on the 3gpp model,” *Proc. IEEE VCT '06 Fall*, 2006.
- [10] D. Baum, J. Hansen, and J. Salo, “An interim channel model for beyond-3G systems,” *Proc. IEEE VCT '05 Spring*, vol. 5, pp. 3132–3136, 2005.
- [11] [Online]. Available: <http://www.quadriga-channel-model.de>
- [12] S. Jaeckel, K. Börner, L. Thiele, and V. Jungnickel, “A geometric polarization rotation model for the 3-D spatial channel model,” *IEEE Trans. Antennas Propag.*, vol. 60, no. 12, pp. 5966–5977, 2012.
- [13] A. Algans, K. Pedersen, and P. Mogensen, “Experimental analysis of the joint statistical properties of azimuth spread, delay spread, and shadow fading,” *IEEE J. Sel. Areas Commun.*, vol. 20, no. 3, pp. 523–531, 2002.
- [14] K. Bakowski and K. Wesolowski, “Change the channel,” *IEEE Veh. Technol. Mag.*, vol. 6, pp. 82–91, 2011.
- [15] S. Szyszkowicz, H. Yanikomeroglu, and J. Thompson, “On the feasibility of wireless shadowing correlation models,” *IEEE Trans. Veh. Technol.*, vol. 59, pp. 4222–4236, 2010.
- [16] M. Gudmundson, “Correlation model for shadow fading in mobile radio systems,” *IET Electron Lett.*, vol. 27, no. 23, pp. 2145–2146, November 1991.
- [17] 3GPP TR 25.996 v10.0.0, “Spatial channel model for multiple input multiple output (MIMO) simulations,” Tech. Rep., 3 2011.
- [18] K. Pedersen, P. Mogensen, and B. Fleury, “Power azimuth spectrum in outdoor environments,” *Electronics Letters*, vol. 33, no. 18, pp. 1583–1584, 1997.
- [19] G. F. Masters and S. F. Gregson, “Coordinate system plotting for antenna measurements,” *AMTA Annual Meeting & Symposium*, 2007.
- [20] R. C. Jones, “A new calculus for the treatment of optical systems, i. description and discussion of the calculus,” *Journal of the Optical Society of America*, vol. 31, pp. 488–493, July 1941.
- [21] M. Narandzic, M. Käske, C. Schneider, M. Milojevic, M. Landmann, G. Sommerkorn, and R. Thomä, “3D-antenna array model for IST-WINNER channel simulations,” *Proc. IEEE VTC '07 Spring*, pp. 319–323, 2007.
- [22] S. Gregson, J. McCormick, and C. Parini, *Principles of Planar Near-Field Antenna Measurements*. IET, 2007.
- [23] T. Svantesson, “A physical MIMO radio channel model for multi-element multi-polarized antenna systems,” *Proc. IEEE VTC' 01 Fall*, vol. 2, pp. 1083–1087, 2001.
- [24] L. Materum, J. Takada, I. Ida, and Y. Oishi, “Mobile station spatio-temporal multipath clustering of an estimated wideband MIMO double-directional channel of a small urban 4.5 GHz macrocell,” *EURASIP J. Wireless Commun. Netw.*, no. 2009:804021, 2009.

- [25] F. Quitin, C. Oestges, F. Horlin, and P. De Doncker, "A polarized clustered channel model for indoor multiantenna systems at 3.6 GHz," *IEEE Trans. Veh. Technol.*, vol. 59, no. 8, pp. 3685–3693, 2010.
- [26] J. Poutanen, K. Haneda, L. Liu, C. Oestges, F. Tufvesson, and P. Vainikainen, "Parameterization of the COST 2100 MIMO channel model in indoor scenarios," *Proc. EUCAP '11*, pp. 3606–3610, 2011.
- [27] Y. Zhou, S. Rondineau, D. Popovic, A. Sayeed, and Z. Popovic, "Virtual channel space-time processing with dual-polarization discrete lens antenna arrays," *IEEE Trans. Antennas Propag.*, vol. 53, pp. 2444–2455, Aug. 2005.
- [28] C. Oestges, B. Clerckx, M. Guillaud, and M. Debbah, "Dual-polarized wireless communications: From propagation models to system performance evaluation," *IEEE Trans. Wireless Commun.*, vol. 7, no. 10, pp. 4019–4031, 2008.
- [29] M. Hata, "Empirical formula for propagation loss in land mobile radio services," *IEEE Trans. Veh. Technol.*, vol. 29, no. 3, pp. 317–325, 1980.
- [30] 3GPP TDOC R1-143469, "Summary of 3D-channel model calibration results," Nokia Networks, Nokia Corporation, Tech. Rep., 2014. [Online]. Available: <http://www.3gpp.org/DynaReport/TDocExMtg--R1-78--30657.htm>

1 Introduction and Overview

1.1 Installation and System Requirements

The installation is straightforward and it does not require any changes to your system settings. If you would like to use QuaDRiGa, just extract the ZIP-File containing the model files and add the “source”-folder from the extracted archive to your MATLAB-Path. This can be done by opening MATLAB and selecting “File” - “Set Path ...” from the menu. Then you can use the “Add folder ...” button to add QuaDRiGa to your MATLAB-Path.

Table 1: QuaDRiGa System Requirements

| Requirement | Value |
|---------------------------------|------------------------|
| Minimal required MATLAB version | 7.12 (R2011a) |
| Required toolboxes | none |
| Memory (RAM) requirement | 1 GB |
| Processing power | 1 GHz Single Core |
| Storage | 50 MB |
| Operating System | Linux, Windows, Mac OS |

The following table provides some compatibility tests for different operating systems, architectures, MATLAB versions, and QuaDRiGa versions.

Table 2: System Compatibility Tests

| Operating System | MATLAB Version | Architecture | QuaDRiGa Version | Test result |
|------------------|----------------|--------------|------------------|-------------|
| Ubuntu 14.04 | R2011a (7.12) | 64 bit | 1.3.8-491 | works |
| | R2012a (7.14) | 32 bit | 1.3.8-491 | works |
| | R2013a (8.1) | 64 bit | 1.4.0-491 | works |
| | R2014a (8.3) | 64 bit | 1.3.8-491 | works |
| | R2014b (8.4) | 64 bit | 1.3.8-491 | works |
| | R2015a (8.5) | 64 bit | 1.3.8-491 | works |
| Windows 7 | R2013a (8.1) | 64 bit | 1.3.8-491 | works |
| | R2014b (8.4) | 64 bit | 1.3.8-491 | works |
| | R2015a (8.5) | 64 bit | 1.3.8-491 | works |

1.2 General Remarks

This document gives a detailed overview of the **QuaDRiGa** channel model and its implementation details. The model has been evolved from the **Wireless World Initiative for New Radio (WINNER)** channel model described in **WINNER II** deliverable D1.1.2 v.1.1 [4]. This document covers only the model itself. Measurement campaigns covering the extraction of suitable parameters can be found in the **WINNER** documentation [4, 5] or other publications such as [6, 7]. Furthermore, the **MIMOSA** project [1] covers the model development and parameter extraction for land-mobile satellite channels.

Figure 1 gives an overview of a family of geometry-based stochastic channel models (**GSCMs**), starting with the 3rd generation partnership project (3GPP)-spatial channel model (**SCM**) in 2003. Work on QuaDRiGa started in 2011, after the end of the 3rd phase of the **WINNER** project. One year later, in 2012, 3GPP and the European-funded research project METIS started working on an evolution of the **SCM**, which later became commonly known as the **3GPP-3D** channel model [8]. However, the core components, e.g. the small-scale-fading (**SSF**) model, of this new model are in many parts identical to the **WINNER+** model, which was

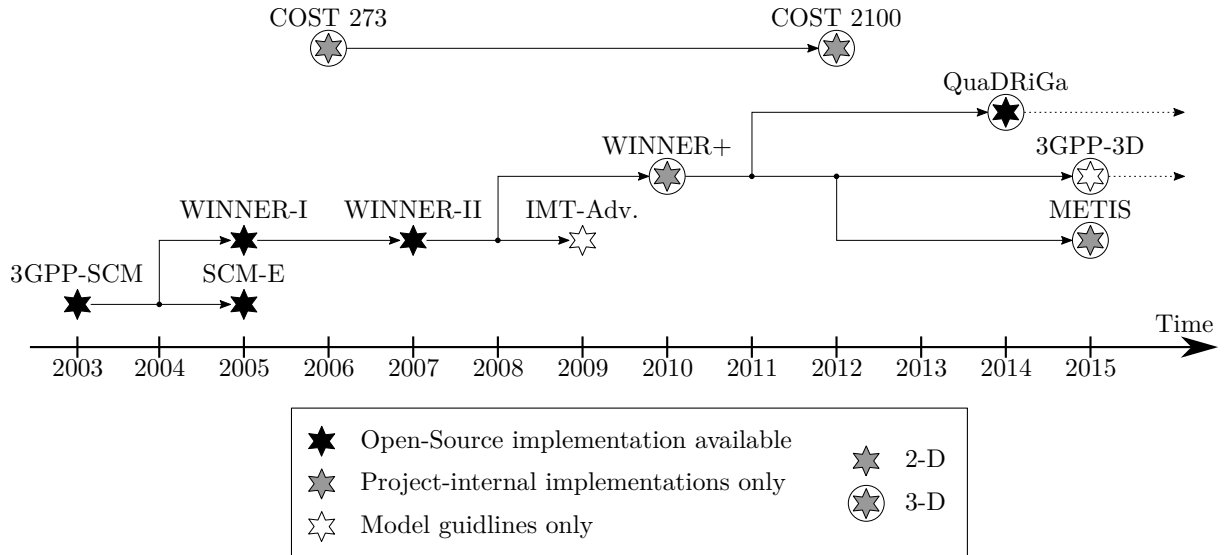


Figure 1: Evolution of GSCMs

also the baseline for quasi deterministic radio channel generator (QuaDRiGa). Hence, QuaDRiGa can be regarded a 3GPP-3D reference implementation. A mandatory part of the 3GPP-3D model is a calibration phase, were individual implementations of the 3GPP contributors have to create a set of metrics which show that the model implementation fulfills the requirements. This calibration exercise was also performed by QuaDRiGa. The results can be found in section 4.

The QuaDRiGa channel model follows a geometry-based stochastic channel modeling approach, which allows the creation of an arbitrary double directional radio channel. The channel model is antenna independent, i.e. different antenna configurations and different element patterns can be inserted. The channel parameters are determined stochastically, based on statistical distributions extracted from channel measurements. The distributions are defined for, e.g. delay spread, delay values, angle spread, shadow fading, and cross-polarization ratio. For each channel segment the channel parameters are calculated from the distributions. Specific channel realizations are generated by summing contributions of rays with specific channel parameters like delay, power, angle-of-arrival and angle-of- departure. Different scenarios are modeled by using the same approach, but different parameters. The basic features of the model approach can be summarized as follows:

- Support of freely configurable network layouts with multiple transmitters and receivers
- Scalability from a single input single output (SISO) or multiple-input multiple-output (MIMO) link to a multi-link MIMO scenario
- Same modeling approach indoor, outdoor, and satellite environments as well as combinations of them
- Support of a frequency range of 2-6 GHz with up to 100 MHz RF bandwidth (additional frequency bands can be modeled as well, if suitable parameter tables are available)
- Support of multi-antenna technologies, polarization, multi-user, multi-cell, and multi-hop networks
- Smooth time evolution of large-scale and small-scale channel parameters including the transition between different scenarios
- High accuracy for the calculation of the polarization characteristics
- 3D model of antennas and propagation environment
- Support for massive MIMO antennas, both at the BS and mobile terminal (MT)

The QuaDRiGa channel model largely extends the WINNER+ and the 3GPP-3D model to support several new features that were originally not included. These are

- Time evolution

Short term time evolution of the channel coefficients is realized by updating the delays, the departure- and arrival angles, the polarization, the shadow fading and the K-Factor based on the position of the terminal.

- Scenario transitions

When the MT moves through the fading channel, it may pass through several different scenarios. QuaDRiGa supports smooth transitions between adjacent channel segments. This is used to emulate long term time evolution and allows the simulation of e.g. handover scenarios.

- Variable speeds for mobile terminals

QuaDRiGa supports variable speeds including accelerating and slowing down of mobile terminals.

- Common framework for LOS and NLOS simulations

In WINNER, line of sight (LOS) and non-line of sight (NLOS) scenarios were treated differently. QuaDRiGa used the same method for both scenarios types. This reduces the model complexity and enables freely configurable multicell scenarios. E.g. one MT can see two BSs, one in LOS and another in NLOS.

- Geometric polarization

The polarizations for the LOS and for the NLOS case is now calculated based on a ray-geometric approach.

- Improved method for calculating correlated large-scale parameters (LSPs)

The WINNER model calculates maps of correlated parameter values using filtered random numbers. QuaDRiGa uses the same method but extends the map generation algorithm to also consider diagonal movement directions and to create smoother outputs.

- New functions for modifying antenna patterns

Antenna patterns can now be freely rotated in 3D-coordinates while maintaining the polarization properties. By default, individual antenna elements have individual antenna radiation patterns in azimuth and elevation direction. Those can also be imported from anechoic chamber measurements. The model further supports arbitrary antenna array structures where the elements can be placed in 3D coordinates. Hence, dual-polarized 2D or even 3D array structures both at the transmitter and receiver are supported.

- New MATLAB implementation

The MATLAB code was completely rewritten. The implementations now fosters object oriented programming and object handles. This increases the performance significantly and lowers the memory usage.

1.3 Introduction to QuaDRiGa

QuaDRiGa (QUAsi Deterministic RadIo channel GenerAtor) was developed to enable the modeling of MIMO radio channels for specific network configurations, such as indoor, satellite or heterogeneous configurations.

Besides being a fully-fledged three dimensional geometry-based stochastic channel model, QuaDRiGa contains a collection of features created in SCM and WINNER channel models along with novel modeling approaches which provide features to enable quasi-deterministic multi-link tracking of users (receiver) movements in changing environments.

The main features of QuaDRiGa are:

- Three dimensional propagation (antenna modeling, geometric polarization, scattering clusters),
- Continuous time evolution,
- Spatially correlated propagation parameter maps,
- Transitions between varying propagation scenarios

The QuaDRiGa approach can be understood as a “statistical ray-tracing model”. Unlike the classical ray tracing approach, it doesn’t use an exact geometric representation of the environment but distributes the positions of the scattering clusters (the sources of indirect signals such as buildings or trees) randomly. A simplified overview of the model is depicted in Figure 3. For each path, the model derives the angle of departure (the angle between the transmitter and the scattering cluster), the angle of arrival (the angle between the receiver and the scattering cluster) and the total path length which results in a delay τ of the signal. For the sake of simplicity, only two paths are shown in the figure.

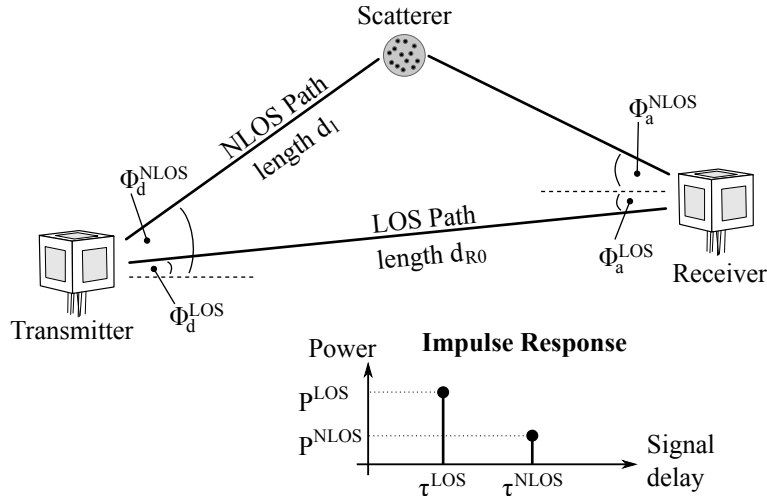


Figure 2: Simplified overview of the modeling approach used in QuaDRiGa

Terrestrial and Satellite scenarios can be modeled. For “Satellite to Earth” communication the angle of departure is identical for all clusters. The concept behind the model allows also the modeling of scenarios such as

- Earth to satellite
- Satellite systems with complementary ground components (CGC): Using several transmitters at different positions and simulating all propagation paths in one setup is supported.

The analysis of these scenarios was not in the scope of the MIMO over satellite (MIMOSA) project. This feature is not tested and especially no parameter sets are available yet.

In the following, the terms cluster, scattering cluster and scatterer are used synonymously. A cluster describes an area where many scattering events occur simultaneously, e.g. at the foliage of trees or at a rough building wall. In QuaDRiGa, each scattering cluster is approximated by 20 individual scatterers. Each one is modeled by a single reflection. The 20 signals can be resolved in spatial domain where they have a typical angular spread of 1-6°. However, they cannot be resolved in delay domain. Therefore, in the output of the channel model, these 20 signals (also named sub-paths) are combined into a single signal which is represented by a path. The difference to Rayleigh fading models, which use wide sense stationary uncorrelated scattering (WSSUS) taps instead of paths, is that each path has a very limited angular spread (1-6°) which also results in a narrow Doppler spectrum. The terms path, multipath component (MPC) and tap are also used synonymously in the QuaDRiGa documentation.

To emulate a rich scattering environment with a wider angular spread, many scattering clusters are created. QuaDRiGa supports up to 42 clusters. However, depending on the angular spread and the amount of diffuse scattering (which is approximated by discrete clusters in QuaDRiGa), typical values are around 10

cluster for LOS propagation and 20 clusters for non-LOS. The positioning of the clusters is controlled by the environment angular spread and the delay spread. The environment angular spread has values of around 20-90° and is typically much larger than the per-cluster angular spread. However, even with many clusters, the Doppler spread is narrower in QuaDRiGa than when assuming pure Rayleigh fading. This is also in line with measurement results. It can be observed in the field that the main components arrive from selected angles and the classical Doppler spectrum's "Jakes" or Butterworth filter shaped characteristics are only valid as long term average and not valid for a short time interval.

To summarize:

- A typical propagation environment requires 8-20 clusters.
- Internally, each cluster is represented by 20 sub-paths, resulting in 160 - 400 sub-paths in total.
- Each sub-path is modeled as a single reflection.
- The 160 - 400 sub-paths are weighted by the antenna response. The 20 sub-paths for each cluster are summed up which results in 8-20 paths.
- For a MIMO system with multiple antennas at the transmitter and receiver, each path has as many channel coefficients, as there are antenna pairs. Hence, at the output, there are $n_{Path} \cdot n_{Rx} \cdot n_{Tx}$ channel coefficients.

1.4 Continuous time evolution

QuaDRiGa calculates the channel for each defined reception point. To generate a "time series" a continuous track of reception points can be defined. The arrival angles of the sub-paths play a crucial role for the time evolution because the phase changes are calculated deterministically based on the arrival angles. This results in a realistic Doppler spectrum.

The temporal evolution of the channel is modeled by two effects:

- drifting and
- birth and death of clusters.

Drifting (see Section 3.4) occurs within a small area (about 20-30 m diameter) in which a specific cluster can be seen from the MT. Within this area the cluster position is fixed. Due to the mobility of the terminal the path length (resulting in a path delay) and arrival angles change slowly.

Longer time-evolving channel sequences need to consider the birth and death of scattering clusters as well as transitions between different propagation environments. We address this by splitting the MT trajectory into segments. A segment can be seen as an interval in which the LSPs, e.g. the delay and angular spread, do not change considerably and where the channel keeps its wide-sense stationary (WSS) properties. Thus, the length of a segment depends on the decorrelation distances of the LSPs. We propose to limit the segment length to the average decorrelation distance. Typical values are around 20 m for LOS and 45 m for NLOS propagation. In the case where a state does not change over a long time, adjacent segments must have the same state. For example, a 200 m NLOS segment should be split into at least 4 NLOS sub-segments.

A set of clusters is generated independently for each segment. However, since the propagation channel does not change significantly from segment to segment, we need to include correlation. This is done by so called "parameter maps" (see Section 3.1). The maps ensure that neighboring segments do not have significantly different propagation characteristics. For example, measurements show that the shadow fading (the average signal attenuation due to building, trees, etc.) is correlated over up to 100 m. Hence, we call all channel characteristics showing similarly slow changes LSPs.

With a segment length of 20 m, two neighboring segments of the same state will have similar receive-power. To get the correct correlation, QuaDRiGa calculates a map for the average received power for a large area. The received power for two adjacent segments is then obtained by reading the values of the map. This map-based approach also contains cross-correlations to other LSPs such as the delay spread. For example, a

shorter delay spread might result in a higher received power. Hence, there is a positive correlation between power and delays spread which is also reflected in the maps.

To get a continuous time-series of channel coefficients requires that the paths from different segments are combined at the output of the model. In between two segments clusters from the old segment disappear and new cluster appear. This is modeled by merging the channel coefficients of adjacent segments. The active time of a scattering cluster is confined within the combined length of two adjacent segments. The power of clusters from the old segment is ramped down and the power of new clusters is ramped up within the overlapping region of the two segments. The combination clusters to ramp up and down is modeled by a statistical process. Due to this approach, there are no sudden changes in the LSPs. For example, if the delay spread in the first segment is 400 ns and in the second it is 200 ns, then in the overlapping region, the delay spread (DS) slowly decreases till it reaches 200 ns. However, this requires a careful setup of the segments along the used trajectory. If the segments are too short, sudden changes cannot be excluded. This process is described in detail in Section 3.8.

1.5 QuaDRiGa Program Flow

For a propagation environment (e.g. urban, suburban, rural or tree-shadowing) typical channel characteristics are described by statistics of the LSPs. Those are the median and the standard deviation of the delay spread, angular spreads, shadow fading, Ricean K-Factor, as well as correlations between them. Additional parameters describe how fast certain properties of the channel change (i.e. the decorrelation distance). Those parameters are stored in configuration files which can be edited by the model user. Normally, the parameters are extracted from channel measurements. A detailed description of the model steps can be found Section 3.

1. The user of the model needs to configure the network layout. This includes:

- Setting the transmitter position (e.g. the BS positions or the satellite orbital position)
- Defining antenna properties for the transmitter and the receiver
- Defining the user trajectory
- Defining states (or segments) along the user trajectory
- Assigning a propagation environment to each state

Defining the user trajectory, states along the user trajectory and related parameters is performed by the state sequence generator (SSG). In the current implementation different SSGs are available:

- Manual definition of all parameters by the user, e.g. definition of short tracks.
- Statistical model for the “journey”. A simple model (mainly designed for demonstration and testing purpose is included in the tutorial “satellite_channel”)
- Derive trajectory and state sequence from the measurement data.

2. Configuration files define the statistical properties of the LSPs. For each state (also called scenario) a set of properties is provided. Typically two configurations files are used.

- One for the “good state” (also called LOS scenario)
- The other for the “bad state” (NLOS scenario).

For each state QuaDRiGa generates correlated “maps” for each LSP. For example, the delay spread in the file is defined as log-normal distributed with a range from 40 to 400 ns. QuaDRiGa translates this distribution in to a series of discrete values, e.g. 307 ns for segment 1, 152 ns for segment 2, 233 ns for segment 3 and so on. This is done for all LSPs.

3. The trajectory describes the position of the MT in the “maps”. For each segment of the trajectory, clusters are calculated according to the values of the LSPs at the map position. The cluster positions

are random within the limits given by the LSP. For example, a delay spread of 152 ns limits the distance between the clusters and the terminal.

4. Each cluster is split into 20 sub-paths and the arrival angles are calculated for each sub-path and for each positions of the terminal on the trajectory.
5. The antenna response for each of the arrival angels is calculated (the same holds for the departure angles). If there is more than one antenna at the transmitter- and/or receiver side, the calculation is repeated for each antenna.
6. The phases are calculated based on the position of the terminal antennas in relation to the clusters. The terminal trajectory defines how the phases change. This results in the Doppler spread.
7. The coefficients of the 20 sup-paths are summed (the output are paths). If there is more than one antenna and depending on the phase, this sum results in a different received power for each antenna-pair. At this point, the MIMO channel response is created.
8. The channel coefficients of adjacent segments are combined (merged). This includes the birth/death process of clusters. Additionally, different speeds of the terminal can be emulated by interpolation of the channel coefficients.
9. The channel coefficients together with the path delays are formatted and returned to the user for further analysis.

1.6 Description of modeling of different reception conditions by means of a typical drive course

This section describes some of the Key features of the model using a real world example. A detailed introduction with a variety of tutorials, test cases and interface descriptions then follows in section A. The later part of the document then focusses on the mathematical models behind the software and the assumptions made.

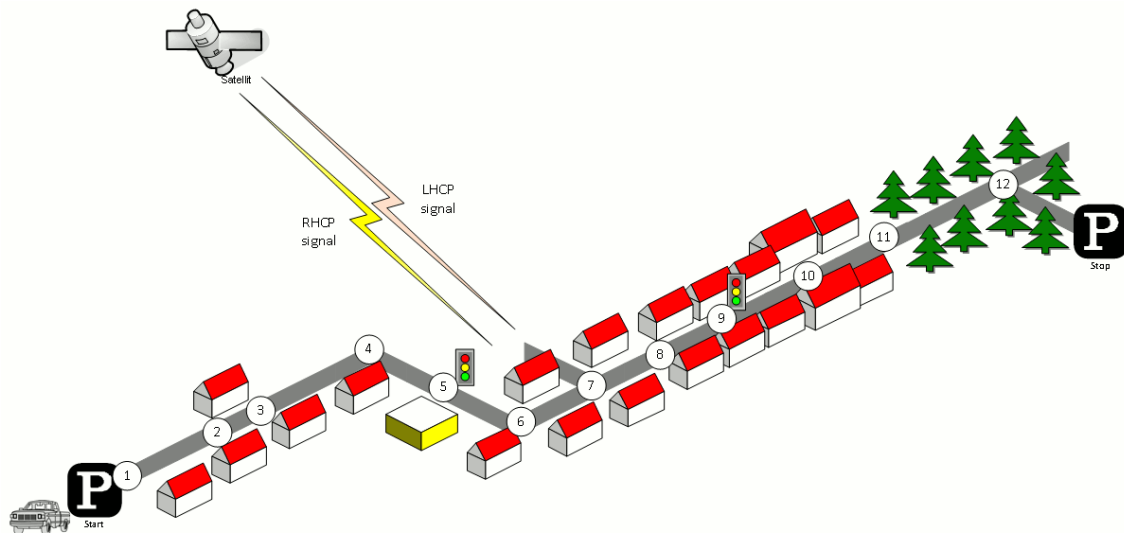


Figure 3: Typical driving course: From home to woodland parking site on the village outskirts

The different effects along the track can be summarized as follows:

1. Start Environment: Urban, LOS reception of satellite signal

2. LOS → NLOS Change
3. NLOS → LOS Change
4. Turning off without change in reception condition (LOS)
5. Stopping at traffic light (LOS)
6. Turning off with change of reception condition (LOS → NLOS)
7. Crossing side Street (NLOS → short LOS → NLOS)
8. Structural change in the environment without a change in the environment type (higher density of buildings but still the environment remains urban)
9. Stopping at traffic lights (NLOS)
10. Houses have the same characteristics as before but are further away from the street (urban environment with different reception characteristics)
11. Change of environment (Urban → Forest)
12. Turning off without change of environment (NLOS)

Each simulation run in QuaDRiGa is done in three (and an optional fourth) step.

1. Set up tracks, scenarios, antennas and network layout
2. Generate correlated LSPs
3. Calculate the channel coefficients
4. (optional) Post-processing

Those steps also need to be done for the above scenario. However, different aspects of the track are handled in different parts of the model. Additionally, the QuaDRiGa model supports two operating modes for handling the LSPs:

1. The first (default) mode generates the correlated LSPs automatically based on a scenario-specific parameter set. This is done in step 2 and involves so called parameter maps.
2. The manual mode does not generate LSPs automatically. Here, the user has to supply a list of parameters to the model. The step 2 thus to be implemented by the user.

Steps 1, 3 and 4 are identical for both modes. The following list describes the modeling of the observed effects along the track when using the automatic mode (1).

1. Start Environment: Urban, LOS reception of satellite signal

Each segment along the track gets assigned an environment. In the QuaDRiGa terminology, this is called a scenario. E.g. the first segment on the track is in the "Satellite-LOS-Urban"-scenario. The selection of the scenario is done during the first step (set up tracks, scenarios, antennas and network layout). QuaDRiGa itself does not supply functions to perform the setting up of tracks and scenarios automatically. However, external scripts can be used to perform this task. An example can be found in section A.3. A RHCP/LHCP signal is defined in the antenna setup.

After the model setup, the "automatic mode" generates a set of LSPs for this segment. I.e. the second step of the model calculates one value for each of the 7 LSPs using the map-based method. Thus, a set of seven maps is created for the scenario "Satellite-LOS-Urban". Those maps cover the entire track. Thus, the same maps are used for all "Satellite-LOS-Urban"-segments of the track.

The third step then calculates a time-series of fading coefficients for the first segment that have the properties of the LSPs from the map. E.g. if one calculates the RMS-DS from the coefficients, one gets the same value as generated by the map in step 2.

2. LOS → NLOS Change

A scenario change is defined along the track. E.g. the second segment along the track gets assigned the scenario "Satellite-NLOS-Urban". Now, a second set of maps is generated for all "Satellite-NLOS-

Urban"-segments. So in total, we now have 14 maps (seven for LOS and another seven for NLOS). The parameters for calculating the channel coefficients are drawn from the second seven maps.

We get a set of channel coefficients with different properties (e.g. more multipath components, lower K-Factor etc.). A smooth transition between the coefficients from the first segment and the second is realized by the ramping down the powers of the clusters of the old segment and ramping up the power of the new. This is implemented in step 4 (Post-processing).

3. NLOS → LOS Change

This is essentially the same as in point 2. However, since the third segment is also in the scenario "Satellite-LOS-Urban", no new maps are generated. The parameters are extracted from the same map as for the starting segment.

4. Turning off without change in reception condition (LOS)

QuaDRiGa supports free 3D-trajectories for the receiver. Thus, no new segment is needed - the terminal stays in the same segment as in point 3. However, we assume that the receive antenna is fixed to the terminal. Thus, if the car turns around, so does the antenna. Hence, the arrival angles of all clusters, including the direct path, change. This is modeled by a time-continuous update of the angles, delays and phases of each multipath component, also known as drifting. Due the change of the arrival angles and the path-lengths, the terminal will also see a change in its Doppler-profile.

5. Stopping at traffic light (LOS)

QuaDRiGa performs all internal calculations at a constant speed. However, a stop of the car at a traffic light is realized by interpolating the channel coefficients in an additional post processing step (step 4). Here, the user needs to supply a movement profile that defines all acceleration, deceleration or stopping points along the track. An example is given in section A.6. Since the interpolation is an independent step, it makes no difference if the mobile terminal is in LOS or NLOS conditions.

6. Turning off with change of reception condition (LOS → NLOS)

This is realized by combining the methods of point 2 (scenario change) and point 4 (turning without change). The scenario change is directly in the curve. Thus, the LOS and the NLOS segments have an overlapping part where the cluster powers of the LOS segment ramp down and the NLOS clusters ramp up. The update of the angles, delays and phases is done for both segments in parallel.

7. Crossing side Street (NLOS → short LOS → NLOS)

This is modeled by two successive scenario changes (NLOS-LOS and LOS-NLOS). For both changes, a new set of clusters is generated. However, since the parameters for the two NLOS-segments are extracted from the same map, they will be highly correlated. Thus, the two NLOS segments will have similar properties.

8. Structural change in the environment without a change in the environment type (higher density of buildings but still the environment remains urban)

This is not explicitly modeled. However, the "Satellite-NLOS-Urban"-map covers a typical range of parameters. E.g. in a light NLOS area, the received power can be some dB higher compared to an area with denser buildings. The placement of light/dense areas on the map is random. Thus, different characteristics of the same scenario are modeled implicit. They are covered by the model, but the user has no influence on where specific characteristics occur on the map when using the automatic mode. An alternative would be to manually overwrite the automatically generated parameters or use the manual mode.

In order to update the LSPs and use a new set of parameters, a new segment needs to be created. I.e. here, an environment change from "Satellite-NLOS-Urban" to the same "Satellite-NLOS-Urban" has to be created. Thus, a new set of LSPs is read from the map and new clusters are generated accordingly.

9. Stopping at traffic lights (NLOS)

This is the same as in point 5.

- 10. Structural change in environment.**
- Houses have the same characteristics as before but are further away from the street (urban environment with different reception characteristics)
-
- Same as point 8.

11. Change of environment (Urban → Forest)

This is the same as in point 2. The segment on the track gets assigned the scenario "Satellite-Forest" and a third set of maps (15-21) is generated for the "Satellite-Forest"-segment. The parameters are drawn from those maps, new channel coefficients are calculated and the powers of the clusters are ramped up/down.

12. Turning off without change of environment (NLOS)

Same as in point 4.

2 Software Structure

2.1 Overview

QuaDRiGa is implemented in MATLAB using an object oriented framework. The user interface is built upon classes which can be manipulated by the user. Each class contains fields to store data and methods to manipulate the data.

It is important to keep in mind that all classes in QuaDRiGa are “handle”-classes. This significantly reduces memory usage and speeds up the calculations. However, **all MATLAB variable names assigned to QuaDRiGa objects are pointers**. If you copy a variable (i.e. by assigning “**b = a**”), only the pointer is copied. “**a**” and “**b**” point to the same object in memory. If you change the values of “**b**”, the value of “**a**” is changed as well. This is somewhat different to the typical MATLAB behavior and might cause errors if not considered properly. Copying a QuaDRiGa object can be done by “**b = a.copy**”.

- **User input**

The user inputs (Point 1 in the programm flow) are provided through the classes: “simulation_parameters”, “array”, “track”, and “layout”.

“**simulation_parameters**” defines the general settings such as the center frequency and the sample density. It also enables and disables certain features of the model such as polarization rotation, sub-path output and progress bars.

“**array**” combines all functions needed to describe antenna arrays.

“**track**” is used to define user trajectories, states and segments.

“**layout**” is a object including the tracks and antenna properties together with further parameters such as the satellite position.

- **Internal processing**

All the processing is done by the classes “parameter_set” and “channel_builder”.

“**parameter_set**” is responsible for generating LSPs for the cluster generation. It also holds the parameter maps needed for generating auto- and crosscorrelation properties of the parameters. “parameter_set” implements point 2 of the program flow.

“**channel_builder**” creates the channel coefficients. This includes the cluster generation and the MIMO channels. It implements steps 3-7 of the program flow.

- **Model output**

The final two steps (8 and 9) of the program flow are implemented in the class “**channel**”. Objects of this class hold the data for the channel coefficients. The class also implements the channel merger, which creates long time evolving sequences out of the snipes produced by the channel builder. Additional function such as the transformation into frequency domain can help the user to further process the data.

- **Plugins**

The QuaDRiGa channel model can be extended by using plugins to enable additional functions. For example if you have the QuaDRiGa-source path on your MATLAB path, all functions of the core version are available to you. In order to enable the additional features provided by a plugin, you need to add the plugin-path to your MATLAB path as well. The plugin-path must be loaded after the QuaDRiGa path, i.e. it must be shown **above** the QuaDRiGa path when you call “path” on the MATLAB console. A list of available plugins is also shown when you call “**simulation_parameters**” on the MATLAB console.

An overview of the model software is depicted in Fig. 4. The unified modeling language (UML) class diagram of the QuaDRiGa channel model gives an overview of all the classes, methods and properties of the model. The class diagram serves as a reference for the following descriptions which also lists the methods that implement a specific functionality.

2.2 Description of Classes, Properties, and Methods

In the following, all properties and methods of the QuaDRiGa classes are described. For the methods, input and output variables are defined and explained. There are three types of methods: Standard methods require an instance of a class. They are printed in black without the class name:

```
par = generate_parameters ( overlap, usage, check_parfiles, verbose )
```

Static methods can be called directly from the command line without creating an instance of the class first. They are printed in blue:

```
[ h_array, mse, mse_pat ] = array.import_pattern ( fVi, fHi )
```

The constructor is a special method that is called when the class name is used as a function, e.g. when calling `a = array('dipole')`. There is only one constructor for each class. They are printed in blue.

```
h_array = array ( array_type, phi_3dB, theta_3dB, rear_gain )
```

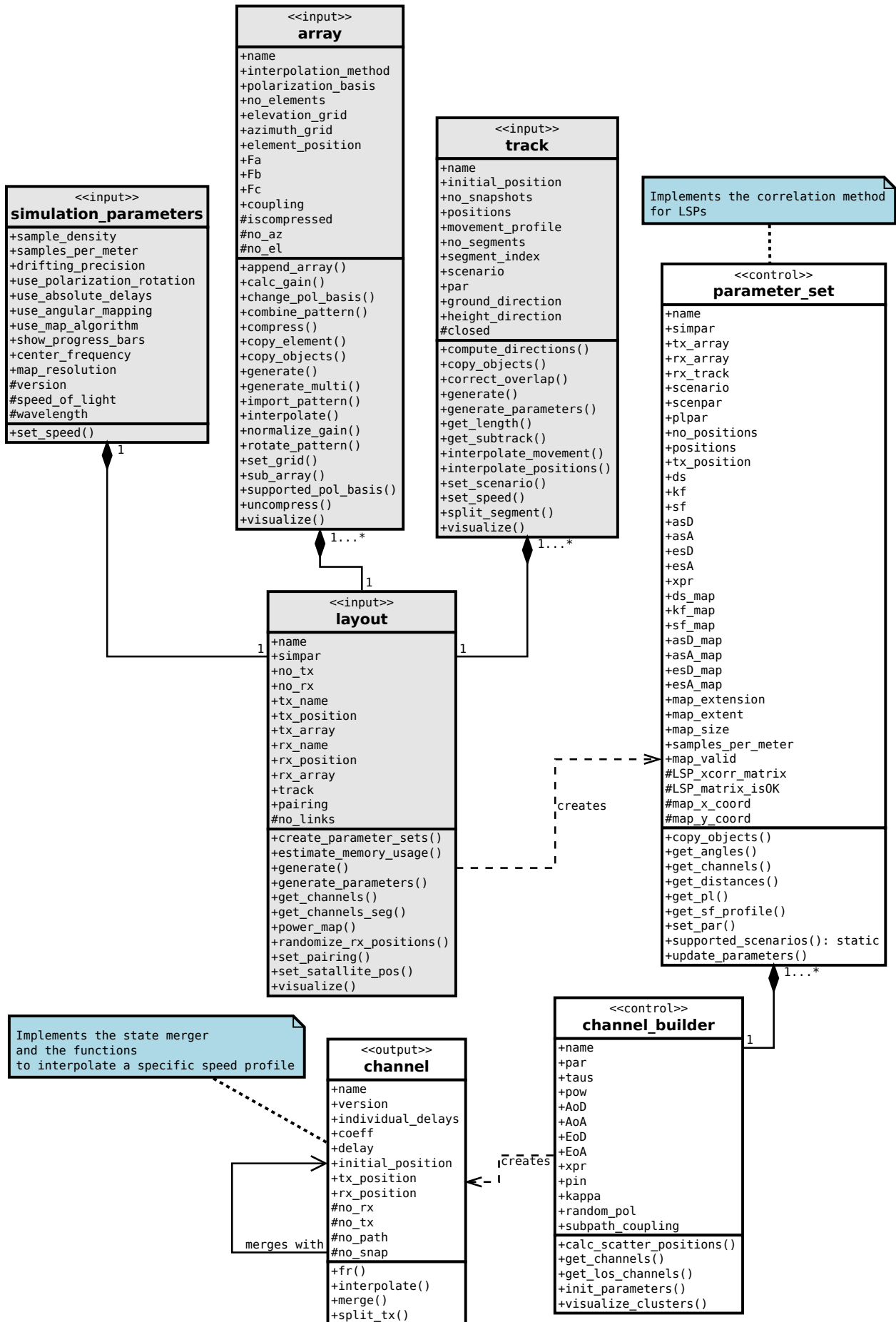


Figure 4: UML class diagram of the model software.

2.2.1 Class “simulation_parameters”

This class controls the simulation options and calculates constants for other classes.

Properties

| | |
|--------------------|---|
| sample_density | The number of samples per half-wave length Sampling density describes the number of samples per half-wave length. To fulfill the sampling theorem, the minimum sample density must be 2. For smaller values, interpolation of the channel for variable speed is not possible. On the other hand, high values significantly increase the computing time significantly. A good value is around 4. |
| samples_per_meter | Samples per meter This parameter is linked to the sample density by $f_s = 2 \cdot f_C \cdot \frac{SD}{c}$ where f_C is the carrier frequency in Hz, SD is the sample density and c is the speed of light. |
| drifting_precision | Precision of the drifting functionality drifting_precision = 0 This method applies rotating phasors to each path which emulates time varying Doppler characteristics. However, the large-scale parameters (departure and arrival angles, shadow fading, delays, etc.) are not updated in this case. This mode requires the least computing resources and may be preferred when only short linear tracks (up to several cm) are considered and the distance between transmitter and receiver is large. The phases at the antenna arrays are calculated by a planar wave approximation. drifting_precision = 1 (default) When drifting is enabled, all arrival angles, the LOS departure angle, delays, and phases are updated for each snapshot using a single-bounce model. This requires significantly more computing resources but also increases the accuracy of the results. Drifting is required when non-linear tracks are generated or the distance between transmitter and receiver is small (below 20 m). The phases at the antenna arrays are calculated by a planar wave approximation. drifting_precision = 2 The arrival angles, the LOS departure angle, delays, and phases are updated for each snapshot and for each antenna element at the receiver (spherical wave assumption). The phases at the transmitter are calculated by a planar wave approximation. This increases the accuracy for multi-element antenna arrays at the receiver. However, the computational complexity increases as well. drifting_precision = 3 [EXPERIMENTAL] This option also calculates the shadow fading, path loss and K-factor for each antenna element at the receiver separately. This feature tends to predict higher MIMO capacities since it also increases the randomness of the power for different MIMO elements. drifting_precision = 4 This option uses spherical waves at both ends, the transmitter and the receiver. This method assumes a single-bounce model and no mapping of departure and arrival angles is done. Hence, departure angular spreads are effectively ignored and results might be erroneous. drifting_precision = 5 This option uses spherical waves at both ends, the transmitter and the receiver. This method uses a multi-bounce model where the departure and arrival angles are matched such that the angular spreads stay consistent. |

| | |
|---------------------------|---|
| use_polarization_rotation | Select the polarization rotation method use_polarization_rotation = 0 Uses the polarization method from WINNER. No polarization rotation is calculated. use_polarization_rotation = 1 Uses the new polarization rotation method where the cross polarization ratio (XPR) is modeled by a rotation matrix. No change of circular polarization is assumed. use_polarization_rotation = 2 (default) Uses the polarization rotation with an additional phase offset between the H and V component of the NLOS paths. The offset angle is calculated to match the XPR for circular polarization. use_polarization_rotation = 3 Uses polarization rotation for the geometric polarization but models the NLOS polarization change as in WINNER. |
| use_absolute_delays | Returns absolute delays in channel impulse response (CIR). By default, delays are calculated such that the LOS delay is normalized to 0. By setting 'use_absolute.delays' to 1 or 'true', the absolute path delays are included in 'channel.delays' at the output of the model. |
| use_ground_reflection | Generates an additional path for the ground reflection If this variable is set to true, the channel model will create an additional path for the ground reflections (Two-Ray model). The basic assumption is that the ground reflection is not delay-resolvable and thus can be considered part of the LOS path. Hence, the LOS path gets split into two paths, the direct path and the ground reflection. |
| use_random_initial_phase | Initializes each path with a random initial phase By default, each path is initialized with a random phase (except the LOS path and the optional ground reflection). Setting "use_random_initial_phase" to false disables this function. In this case, each path gets initialized with a zero-phase. |
| use_angular_mapping | Selects the angular mapping method use_angular_mapping = 1 Maps the path powers to arrival angles by a wrapped Gaussian distribution. This method is adopted from the WINNER model. However, the generated angles show high correlations if the K-Factor is larger than 0 dB. use_angular_mapping = 2 (default) This method generates random angles for the paths. The angular spread is maintained by a scaling operation. The output angles have a more natural distribution. However, there is an upper limit for the angular spread of roughly 100 degree in NLOS conditions. |
| use_map_algorithm | Selects the parameter map generation algorithm use_map_algorithm = 1 Uses the algorithm from the WINNER model. use_map_algorithm = 2 [Default] Uses a modified version of the WINNER algorithm that also filters the diagonal directions. |
| show_progress_bars | Show a progress bar on the MATLAB prompt |
| center_frequency | Center frequency in [Hz] |
| map_resolution | Resolution of the decorrelation maps in [samples/m]. Setting a value of 0 automatically chooses the optimal map resolution depending on the values in the parameter-tables. |
| version | Version number of the current QuaDRiGa release (constant) |
| plugins | List of available plugins |
| speed_of_light | Speed of light (constant) |
| wavelength | Carrier wavelength in [m] (read only) |

Methods

| | |
|---|---|
| h_simpar = simulation_parameters | |
| Description | Creates a new 'simulation_parameters' object with default settings. |
| set_speed (speed_kmh, sampling_rate_s) | |
| Description | This method can be used to automatically calculate the sample density for a given mobile speed. |
| Input | speed_kmh speed in [km/h] sampling_rate_s channel update rate in [s] |

2.2.2 Class “array”

This class combines all functions to create and edit antenna arrays. An antenna array is a set of single antenna elements, each having a specific beam pattern, that can be combined in any geometric arrangement. A set of synthetic arrays that allow simulations without providing your own antenna patterns is provided (see generate method for more details).

Properties

| name | Name of the antenna array |
|----------------------|--|
| interpolation_method | <p>Method for interpolating the beam patterns The default is linear interpolation. Optional are:</p> <ul style="list-style-type: none"> • nearest - Nearest neighbor interpolation (QuaDRiGa optimized) • linear - Linear interpolation (QuaDRiGa optimized, Default) • spline - Cubic spline interpolation (MATLAB internal function) • nearest_int - Nearest neighbor interpolation (MATLAB internal function) • linear_int - Linear interpolation (MATLAB internal function) <p>Note: MATLAB internal routines slow down the simulations significantly.</p> |
| polarization_basis | <p>The polarization basis of the pattern The polarization basis of the pattern:</p> <ul style="list-style-type: none"> • cartesian - Ludwig 1 • az-el - Ludwig 2 - Azimuth over Elevation • el-az - Ludwig 2 - Elevation over Azimuth • polar-spheric - Ludwig 2 - Polar-Spheric [DEFAULT] <p>You can specify the polarization basis of the pattern by setting the appropriate string. By default, QuaDRiGa requires a Polar-Spheric basis. If a different basis is specified, an appropriate transformation will be carried out.</p> |
| no_elements | <p>Number of antenna elements in the array Increasing the number of elements creates new elements which are initialized as copies of the first element. Decreasing the number of elements deletes the last elements from the array.</p> |
| elevation_grid | <p>Elevation angles in [rad] were samples of the field patterns are provided The field patterns are given in spherical coordinates. This variable provides the elevation sampling angles in radians ranging from $-\frac{\pi}{2}$ (downwards) to $\frac{\pi}{2}$ (upwards).</p> |
| azimuth_grid | <p>Azimuth angles in [rad] were samples of the field patterns are provided The field patterns are given in spherical coordinates. This variable provides the azimuth sampling angles in radians ranging from $-\pi$ to π.</p> |
| element_position | <p>Position of the antenna elements in local cartesian coordinates (using units of [m])</p> |
| Fa | <p>The first component of the antenna pattern. If the polar-spheric polarization basis is used, this variable contains the vertical (or theta) component of the electric field given in spherical coordinates. This variable is a tensor with dimensions [elevation, azimuth, element] describing the theta component of the far field of each antenna element in the array.</p> |
| Fb | <p>The second component of the antenna pattern. If the polar-spheric polarization basis is used, this variable contains the horizontal (or phi) component of the electric field given in spherical coordinates. This variable is a tensor with dimensions [elevation, azimuth, element] describing the phi component of the far field of each antenna element in the array.</p> |
| Fc | <p>The third component of the antenna pattern. Currently, it is only used when the antenna pattern is using a cartesian polarization basis.</p> |

| | |
|--------------|---|
| coupling | Coupling matrix between elements This matrix describes a pre or postprocessing of the signals that are fed to the antenna elements. For example, in order to transmit a left hand circular polarized (LHCP) signal, two antenna elements are needed. They are then coupled by a matrix $\frac{1}{\sqrt{2}} \begin{pmatrix} 1 \\ j \end{pmatrix}$ The rows in the matrix correspond to the antenna elements, the columns to the signal ports. In this example, the antenna has one port, i.e. it is fed with one input signal. This signal is then split into two and fed to the two antenna elements where the second element radiates the signal with 90° phase shift. In a similar fashion, it is possible to create fixed beamforming antennas and include crosstalk between antenna elements. By default, 'coupling' is set to an identity matrix which indicates perfect isolation between the antenna elements. |
| iscompressed | Indicates if the array is compressed It is possible to compress the antenna array in memory to save storage space and reduce the memory requirements for large arrays. This property indicates if the array is compressed. |
| no_az | Number of azimuth values |
| no_el | Number of elevation values |

Methods

| | | |
|--|--|---|
| h_array = array (array_type, phi_3dB, theta_3dB, rear_gain) | | |
| Description | Creates a new array object. See 'array.generate' for a description of the input parameters and the list of supported antenna types. | |
| append_array (a) | | |
| Description | Appends an antenna array to the existing one This method appends the antenna array given in "a" to the existing array object. If the polarization basis or the sampling grid do not match, appropriate conversions or interpolations are performed. | |
| Input | a | The array object which is appended to the current array object. |
| [gain_dBi, pow_max] = calc_gain (element) | | |
| Description | Calculates the gain of the antenna array. | |
| Output | gain_dBi pow_max | Normalized Gain of the antenna Maximum power in main beam direction |
| change_pol_basis (new_basis) | | |
| Description | This method can be used to change the polarization basis of an antenna pattern. By default, QuaDRiGa uses the polar-spheric basis. However, the antenna patterns can be given in other bases as well. | |
| Input | new_basis | The basis in which the pattern should be transformed. A list of supported bases can be obtained by "array.supported_pol_basis". |
| combine_pattern (center_frequency) | | |
| Description | Calculates a virtual pattern of the given array When the inputs of an array are coupled (i.e. fed with the same signal), then it is possible to combine the elements of the array. This function calculates the virtual pattern by using the QuaDRiGa simulator. | |
| Input | center_frequency | The center frequency in [Hz]. |
| ratio = compress | | |
| Description | Stores the array in compressed form If there are many similar elements in an array, the memory and storage requirements might be high. Therefore, it is possible to compress the array to save storage space. This is done as follows: <ul style="list-style-type: none">• Patterns are stored in polar-spherical polarization basis• If multiple elements have the same patterns, the pattern is stored only once.• Patterns are stored in single precision.• If there are complex valued patterns with no imaginary part, they are converted to real values. It is recommended to call "compress" before saving an array to disk. Decompressing is done automatically when needed. | |
| Output | ratio | The compression factor in percent |

| copy_element (source, target) | | |
|--|---------------------------------------|---|
| Description | Creates a copy of an antenna element. | |
| Input | source | Index of the array object that should be copied. The value must be scalar, integer and greater than 0 and it can not exceed the array size. |
| | target | Target can be a scalar or vector with elements > 0. |

| copy_objects | | |
|---------------------|---|--|
| Description | A modified version of the standard physical copy function While the standard copy command creates new physical objects for each element of obj (in case obj is an array of object handles), copy_objects checks whether there are object handles pointing to the same object and keeps this information. | |

| par = generate (array_type, element, Ain, Bin, Cin, Din, Ein) | | |
|---|--|--|
| Description | Generates predefined arrays. | |
| Array Types | <ul style="list-style-type: none"> omni dipole half-wave-dipole patch custom parametric 3gpp-macro 3gpp-3d xpol rhcP-dipole lhCP-dipole lhCP-rhcP-dipole ula2 ula4 ula8 | <p>An isotropic radiator with vertical polarization. A short dipole radiating with vertical polarization. A half-wave dipole radiating with vertical polarization. A vertically polarized patch antenna with 90° opening in azimuth and elevation. An antenna with a custom gain in elevation and azimuth. Ain = 3dB beam width in azimuth direction Bin = 3dB beam width in elevation direction Cin = Isotropic gain (linear scale) at the back of the antenna The values A,B,C and D for the parametric antenna are returned.</p> <p>An antenna following the function</p> $F = A \cdot \sqrt{B + (1 - B) \cdot (\cos \theta)^C} \cdot \exp(-D \cdot \phi^2)$ <p>An antenna with a custom gain in elevation and azimuth. Ain = Half-Power in azimuth direction (default = 70 deg) Bin = Half-Power in elevation direction (default = 10 deg) Cin = Front-to back ratio (default = 25 dB) Din = Electrical downtilt (defult = 15 deg) See. 3GPP TR 36.814 V9.0.0 (2010-03), Table A.2.1.1-2, Page 59</p> <p>The antenna model for the 3GPP-3D channel model (TR 36.873, v12.2.0, pp.16). Ain = Number of vertical elements (M) Bin = Number of horizontal elements (N) Cin = The center frequency in [Hz] Din = Polarization indicator</p> <ol style="list-style-type: none"> 1. K=1, vertical polarization only 2. K=1, H/V polarized elements 3. K=1, +/-45 degree polarized elements 4. K=M, vertical polarization only 5. K=M, H/V polarized elements 6. K=M, +/-45 degree polarized elements <p>Ein = The electric tile angle in [deg] for Cin = 4,5,6 Fin = Element spacing in [lambda], Default: 0.5</p> <p>Two elements with ideal isotropic patterns (vertical polarization). The second element is tilted by 90°.</p> <p>Two crossed dipoles with one port. The signal on the second element (horizontal) is shifted by -90° out of phase. The two elements thus create a right hand circular polarized (RHCP) signal.</p> <p>Two crossed dipoles with one port. The signal on the second element (horizontal) is shifted by 90° out of phase. The two elements thus create a left hand circular polarized (LHCP) signal.</p> <p>Two crossed dipoles. For input port 1, the signal on the second element is shifted by +90° out of phase. For input port 2, the the signal on the second element is shifted by -90° out of phase. Port 1 thus transmits a LHCP signal and port 2 transmits a RHCP signal.</p> <p>Unified linear arrays composed of 2 omni-antennas (vertical polarization) with 10 cm element distance.</p> <p>Unified linear arrays composed of 4 omni-antennas (vertical polarization) with 10 cm element distance.</p> <p>Unified linear arrays composed of 8 omni-antennas (vertical polarization) with 10 cm element distance.</p> |
| Input | array_type element Ain - Ein | One of the above array types. The element numbers for which this functions is applied. If no element number is given, the function creates a new array and delete the old elements in the array. Additional parameters for the antenna array (see above). |
| Output | par | The parameters A, B, C, and D for the "parametric" antenna type. |

| | |
|---|--|
| <code>coupling = generate_multi (no_elements, spacing, tilt, optimize)</code> | |
|---|--|

| | | |
|--|--|---|
| Description | <p>Generates a multi-element array with electric tilt</p> <p>This function generates a vertically stacked multi-element array of the given antenna object. The element spacing is relative to the wavelength and an additional electric tilt can be applied. The output is stored in the current antenna object.</p> <p>For this method to work, you need to define a single antenna element using "array.generate". Then, you can call "array.generate_multi" to transform this element into a stacked multi-element array. The provided antenna object can only have one element. The method returns an error if a multi-element array is given.</p> | |
| Input | no_elements spacing tilt optimize | The number of "virtual" antenna elements stacked in elevation (z) direction. The element-spacing as a factor of the wavelength. Default value: 0.5 An additional electric downtilt value in [deg]. Default value: 0 If this parameter is set to 1, the optimal beamformer is calculated. Otherwise, the phases are calculated using geometric settings. Default: 0 (geometric) |
| Output | coupling | |
| The coupling matrix used to calculate the virtual antenna pattern. | | |

| | |
|--|--|
| <code>h_array = import_pattern (fVi, fHi , azimuth_grid , elevation_grid)</code> | |
|--|--|

| | | |
|--|---|---|
| Description | Converts antenna field patterns into a QuaDRiGa array object. | |
| Input | fVi fHi azimuth_grid elevation_grid | The field pattern(s) for the vertical polarization given in spherical coordinates. The first dimension corresponds to the elevation angle (ranging from -90 to 90 degrees). The second dimension is for the azimuth angle (ranging from -180 to 180 degrees). The third dimension belongs to the element number. The default resolution is 1 degree - hence, the default size of fVi is $181 \times 361 \times 1$. If a different resolution is given, the optional variables "azimuth_grid" and "elevation_grid" must be defined. The field pattern(s) for the horizontal polarization given in spherical coordinates. "fHi" can be empty if no horizontal response is given. If it is given, then "fHi" must have the same size as "fVi". A vector specifying the azimuth sampling points of the patterns in units of radians (ranging from -pi to pi). This value only needs to be defined if the patterns do not have the default size. A vector specifying the elevation sampling points of the patterns in units of radians (ranging from -pi/2 to pi/2). This value only needs to be defined if the patterns do not have the default size. |
| Output | h_array | |
| The QuaDRiGa antenna array object generated from the field patterns. | | |

| | |
|--|--|
| <code>gain_dBi = normalize_gain (element, gain)</code> | |
|--|--|

| | | |
|--------------------------------|--|---|
| Description | Normalizes all patterns to their gain. | |
| Input | element gain | A list of elements for which the normalization is done. Default: All elements. The gain that should be set in the pattern. If this variable is not given, the gain is calculated from the pattern. |
| Output | gain_dBi | |
| Normalized gain of the antenna | | |

| [V, H, CP, dist] = interpolate (azimuth, elevation, element) | | |
|--|---|---|
| Description | Interpolates the field pattern Note: Interpolation of the beam patterns is very computing intensive. It must be performed several thousands of times during a simulation run. It is highly recommended to use linear interpolation for this task since this method is optimized for speed. Spline interpolation calls the MATLAB internal interpolation function which is more than 10 times slower. To enable linear interpolation, set the ' interpolation_method ' property of the array object to ' 'linear' '. Remark: There are additional input parameters specified in the .mat-File that are not in the list below. Those parameters correspond to the properties of the ' array ' class. Passing those variables during the function call takes less time than reading them from the object properties. This is used internally in ' channel_builder.get_channels ' but is irrelevant here. | |
| Input | azimuth elevation element | A vector of azimuth angles in [rad]. A vector of elevation angles in [rad]. The element numbers for which this interpolation is done is applied. If no element number is given, the interpolation is done for all elements in the array. |
| Output | V H CP dist | The interpolated vertical field pattern. The interpolated horizontal field pattern. The interpolated common phase field pattern. The effective distances between the antenna elements when seen from the direction of the incident path. The distance is calculated by an projection of the array positions on the normale plane of the incident path. |

| cp = rotate_pattern (deg, rotaxis, element, usage) | | |
|---|---|---|
| Description | Rotates antenna patterns Pattern rotation provides the option to assemble antenna arrays out of single elements. By setting the ' element_position ' property of an array object, elements can be placed at different coordinates. In order to freely design arbitrary array configurations, however, elements often need to be rotated (e.g. to assemble a +/- 45° crosspolarized array out of single dipoles). This functionality is provided here. Note: Calling ' rotate_pattern ' will always remove the common phase from the field patterns. Call ' estimate_common_phase ' before calling ' rotate_pattern ' to extract the common phase information. | |
| Input | deg rotaxis element usage | The rotation angle in [degrees] ranging from -180° to 180°. The rotation axis specified by the character 'x', 'y', or 'z'. The element numbers for which this interpolation is done is applied. If no element number is given, the interpolation is done for all elements in the array. The optional parameter 'usage' can limit the rotation procedure either to the pattern or polarization. Possible values are: <ul style="list-style-type: none">• 0: Rotate both (pattern+polarization) - default• 1: Rotate only pattern• 2: Rotate only polarization |
| Output | cp | The common phase of the field pattern. |

| set_grid (azimuth_grid, elevation_grid) | | |
|---|--|---|
| Description | Sets a new grid for azimuth and elevation and interpolates the pattern This function replaces the properties ' azimuth_grid ' and ' elevation_grid ' of the antenna object with the given values and interpolates the antenna patterns to the new grid. | |
| Input | azimuth_grid elevation_grid | Azimuth angles in [rad] were samples of the field patterns are provided The field patterns are given in spherical coordinates. This variable provides the azimuth sampling angles in radians ranging from $-\pi$ to π . Elevation angles in [rad] were samples of the field patterns are provided The field patterns are given in spherical coordinates. This variable provides the elevation sampling angles in radians ranging from $-\frac{\pi}{2}$ (downwards) to $\frac{\pi}{2}$ (upwards). |

| sub_array (mask) | | |
|--------------------|--|----------------------------|
| Description | generates a sub-array with the given array indices This function creates a copy of the given array with only the selected elements specified in mask. | |
| Input | mask | A list of element indices. |

uncompress

| | |
|-------------|---|
| Description | Uncompresses an array. See: array.compress |
|-------------|---|

visualize (element)

| | | |
|-------------|---|--|
| Description | Create a plot showing the element configurations. | |
| Input | element | The element numbers for which the plot os created. If no element number(s) are given, a plot is created for each element in the array. |

2.2.3 Class “track”

One feature of the channel model is the continuous evolution of wireless channels when the terminal moves through the environment. A track describes the movement of a mobile terminal. It is composed of an ordered list of positions. During the simulation, one snapshot is generated for each position on the track.

Along the track, wireless reception conditions may change, e.g. when moving from an area with LOS to a shaded area. This behavior is described by segments, or states. A segment is a subset of positions that have similar reception conditions. Each segment is classified by a segment index (i.e. the center position of the segment) and a scenario. The scenario must be one of the supported scenarios in class `'parameter_set'`.

Properties

| | |
|-------------------------------|---|
| <code>name</code> | Name of the track |
| <code>initial_position</code> | <p>Position offset (will be added to positions)</p> <p>This position is given in global cartesian coordinates (x,y, and z-component) in units of [m]. The initial position normally refers to the starting point of the track. If the track has only one segment, it is also the position for which the LSPs are calculated. The initial position is added to the values in the positions variable.</p> |
| <code>no_snapshots</code> | Number of positions on the track |
| <code>positions</code> | <p>Ordered list of position relative to the initial position</p> <p>QuaDRiGa calculates an instantaneous channel impulse response (also called snapshot) for each position on the track.</p> |
| <code>movement_profile</code> | <p>Time (in sec) vs. distance (in m) for speed profile</p> <p>QuaDRiGa supports variable terminal speeds. This is realized by interpolating the channel coefficients at the output of the model. The variable <code>'track.movement_profile'</code> describes the movement along the track by associating a time-point with a distance-point on the track. An example is:</p> <pre> 1 t.movement_profile = [0,7 ; 5,0 ; 6,0 ; 20,20]'; 2 dist = t.interpolate_movement(1e-3); 3 ci = cn.interpolate(dist , t.get_length); </pre> <p>See also the tutorial “Applying Varying Speeds (Channel Interpolation)” in Section A.6 for more details.</p> |
| <code>no_segments</code> | Number of segments or states along the track |
| <code>segment_index</code> | Starting point of each segment given as index in the <code>'positions'</code> vector |
| <code>scenario</code> | <p>Scenarios for each segment along the track</p> <p>This variable contains the scenario names for each segment as a cell array of strings. A list of supported scenarios can be obtained by calling <code>'parameter_set.supported_scenarios'</code>. If there is only one transmitter (i.e. one base station), the cell array has the dimension [1 x no_segments]. For multiple transmitters, the rows of the array may contain different scenarios for each transmitter. For example, in a multicell setup with three terrestrial base stations, the propagation conditions may be different to all BSs. The cell arrays than has the dimension [3 x no_segments].</p> |
| <code>par</code> | <p>Manual parameter settings</p> <p>This variable contains a structure with LSPs. This can be used for assigning LSPs directly to the channel builder, e.g. when they are obtained from measurements. The structure contains the following fields:</p> <ul style="list-style-type: none"> • <code>ds</code> - The delay spread in [s] per segment • <code>kf</code> - The Ricean K-Factor in [dB] per snapshot • <code>pg</code> - The effective path gain in [dB] excluding antenna gains per snapshot • <code>asD</code> - The azimuth angle spread in [deg] per segment at the transmitter • <code>asA</code> - The azimuth angle spread in [deg] per segment at the receiver • <code>esD</code> - The elevation angle spread in [deg] per segment at the transmitter • <code>esA</code> - The elevation angle spread in [deg] per segment at the receiver • <code>xpr</code> - The NLOS cross-polarization in [dB] per segment <p>If there is only a subset of variables (e.g. the angle spreads are missing), then the corresponding fields can be left empty. They will be completed by the parameter sets. See also the method <code>'track.generate_parameters'</code> on how to fill this structure automatically.</p> |
| <code>ground_direction</code> | <p>Azimuth orientation of the terminal antenna for each snapshot</p> <p>This variable can be calculated automatically from the positions by the function <code>'track.compute_directions'</code>.</p> |

| | |
|------------------|---|
| height_direction | Elevation orientation of the terminal antenna for each snapshot |
| closed | Indicates that the track is a closed curve |

Methods

| | |
|---|---|
| <code>h_track = track(track_type, track_length, direction, street_length_min, street_length_mu, street_length_std, curve_radius, turn_probability)</code> | |
| Description | Creates a new track object. See ' <code>track.generate</code> ' for a description of the input parameters and the list of supported track types. |

| <code>compute_directions</code> | |
|---------------------------------|--|
| Description | Calculates ground and height orientations from positions This function calculates the orientations of the transmitter based on the positions. If we assume that the receive antenna array is fixed on a car and the car moves along the track, then the antenna turns with the car when the car is changing direction. This needs to be accounted for when generating the channel coefficients. This function calculates the orientation based on the positions and stored the output in the <code>ground_direction</code> and <code>height_direction</code> field of the track object. |

| <code>copy_objects</code> | |
|---------------------------|--|
| Description | A modified version of the standard physical copy function While the standard copy command creates new physical objects for each element of <code>obj</code> (in case <code>obj</code> is an array of object handles), <code>copy_objects</code> checks whether there are object handles pointing to the same object and keeps this information. |

| <code>correct_overlap(overlap)</code> | | |
|---|---|--|
| Description | Corrects positions of the segment start to account for the overlap. After the channel coefficients are calculated, adjacent segments can be merged into a time-continuous output. The merger assumes that the merging interval happens at the end of one segment, before a new segments starts. In a reality, however, the scenario change happens in the middle of the overlapping part (and not at the end of it). This function corrects the position of the segment start to account for that. | |
| Input | overlap | The length of the overlapping part relative to the segment length. It can have values in between 0 (no overlap) and 1 (ramp along the entire segment). |

| <code>generate('linear', track_length, direction)</code> | | |
|--|--|---|
| Description | Creates a linear track with given length and direction. Direction describes the travel direction along the track in [rad] in mathematical sense (i.e. 0 means east, $\pi/2$ means north, π means west and $-\pi/2$ south). If "track_length" or "direction" is not specified, then the default track is 1 m long and has a random direction. | |
| Input | track_length direction | The track length in [m]. Default length is 1 m. specifies the driving direction in [rad]. The default is random. |

| <code>generate('circular', track_length, direction)</code> | | |
|--|--|--|
| Description | Creates a circular track with given length and starting-direction. | |
| Input | track_length direction | The circumference of the circular track in [m]. Default is 62.8 m. The starting point on the circle in [rad]. Positive values define the travel direction as counter clock-wise and negative values as clock-wise. E.g. 0 sets the start point in the east of the circle, traveling north; -2π sets it in the east, traveling south. The default is random. |

| | | | | | | | | | | | | | | | | |
|---|--|--|--------------|--|-----------|--|-------------------|---|------------------|--|-------------------|--|--------------|---|------------------|--|
| generate ('street', track_length, direction, street_length_min, street_length_mu, street_length_std, curve_radius, turn_probability) | | | | | | | | | | | | | | | | |
| Description | <p>Emulates a drive route through a city grid.</p> <p>The mobile terminal starts at point 0, going into a specified direction. The trajectory grid is build from street segments. The length of each street is specified by the parameters '<code>street_length_min</code>', '<code>street_length_mu</code>', and '<code>street_length_sigma</code>'. At the end of a street (i.e. at a crossing), the terminal turns with a probability specified by '<code>turn_probability</code>'. The change of direction is in between 75 and 105 degrees either left or right. The radius if the curve is given by '<code>curve_radius</code>'. The track is set up in a way that prevents driving in circles.</p> | | | | | | | | | | | | | | | |
| Input | <table> <tr> <td>track_length</td><td>the length in [m]. Default length is 1000 m.</td></tr> <tr> <td>direction</td><td>specifies the driving direction in [rad] of the first segment in mathematical sense (0 means east, pi/2 means north). The default value is random.</td></tr> <tr> <td>street_length_min</td><td>the minimal street length in [m]. The default is 50 m.</td></tr> <tr> <td>street_length_mu</td><td>the median street length in [m]. The default is 187 m. This value was obtained from measurements in Berlin, Germany.</td></tr> <tr> <td>street_length_std</td><td>the standard deviation of the street length in [m]. The default is 83 m. This value was obtained from measurements in Berlin, Germany.</td></tr> <tr> <td>curve_radius</td><td>the curve radius during a turn in [m]. The default is 10 m.</td></tr> <tr> <td>turn_probability</td><td>the probability of a turn at a crossing. Possible values are in between 0 and 1. The default is 0.5.</td></tr> </table> | | track_length | the length in [m]. Default length is 1000 m. | direction | specifies the driving direction in [rad] of the first segment in mathematical sense (0 means east, pi/2 means north). The default value is random. | street_length_min | the minimal street length in [m]. The default is 50 m. | street_length_mu | the median street length in [m]. The default is 187 m. This value was obtained from measurements in Berlin, Germany. | street_length_std | the standard deviation of the street length in [m]. The default is 83 m. This value was obtained from measurements in Berlin, Germany. | curve_radius | the curve radius during a turn in [m]. The default is 10 m. | turn_probability | the probability of a turn at a crossing. Possible values are in between 0 and 1. The default is 0.5. |
| track_length | the length in [m]. Default length is 1000 m. | | | | | | | | | | | | | | | |
| direction | specifies the driving direction in [rad] of the first segment in mathematical sense (0 means east, pi/2 means north). The default value is random. | | | | | | | | | | | | | | | |
| street_length_min | the minimal street length in [m]. The default is 50 m. | | | | | | | | | | | | | | | |
| street_length_mu | the median street length in [m]. The default is 187 m. This value was obtained from measurements in Berlin, Germany. | | | | | | | | | | | | | | | |
| street_length_std | the standard deviation of the street length in [m]. The default is 83 m. This value was obtained from measurements in Berlin, Germany. | | | | | | | | | | | | | | | |
| curve_radius | the curve radius during a turn in [m]. The default is 10 m. | | | | | | | | | | | | | | | |
| turn_probability | the probability of a turn at a crossing. Possible values are in between 0 and 1. The default is 0.5. | | | | | | | | | | | | | | | |
| par = generate_parameters (overlap, usage, check_parfiles, verbose) | | | | | | | | | | | | | | | | |
| Description | <p>Generates large scale parameters and stores them in '<code>par</code>'</p> <p>This function extracts the LSPs for the given scenario from the '<code>parameter_set</code>' class and stores them in '<code>track.par</code>'. Hence, it automatically generates the LSPs and, thus, implements an easy-to-use interface for the '<code>parameter_set</code>' class.</p> <p>Since the track class does not handle transmitter positions, a default position of [0,0,25] is assumed. Please refer to '<code>layout.generate_parameters</code>' for a more detailed description.</p> | | | | | | | | | | | | | | | |
| Input | <table> <tr> <td>overlap</td><td>The length of the overlapping part relative to the segment length. When there are scenario transitions, KF and PG change smoothly during a predefined interval. The length of that interval is a percentage of previous segment. The parameter overlap adjusts this percentage, ranging from 0 (i.e. very hard, step-like change at the scenario boundary) to 1 (very smooth, but long transition).</td></tr> <tr> <td>usage</td><td>Changes the behavior of the method <code>usage = 0</code> Deletes all existing parameters from the track. <code>usage = 1</code> Deletes all existing parameters from the track and generates new ones. Existing LSPs will be overwritten. <code>usage = 2</code> (default) Keeps existing parameters, but generates missing ones. This is useful when, for example, the effective path gain (PG) is provided, but the other LSPs are unknown. In this case, the unknown "gaps" are filled with values which are generated from the provided scenario description.</td></tr> <tr> <td>check_parfiles</td><td><code>check_parfiles = 0 / 1</code> (default: 1) Disables (0) or enables (1) the parsing of shortnames and the validity-check for the config-files. This is useful, if you know that the parameters in the files are valid. In this case, this saves execution time.</td></tr> <tr> <td>verbose</td><td>Enables (1, default) or disables (0) the progress bar.</td></tr> </table> | | overlap | The length of the overlapping part relative to the segment length. When there are scenario transitions, KF and PG change smoothly during a predefined interval. The length of that interval is a percentage of previous segment. The parameter overlap adjusts this percentage, ranging from 0 (i.e. very hard, step-like change at the scenario boundary) to 1 (very smooth, but long transition). | usage | Changes the behavior of the method <code>usage = 0</code> Deletes all existing parameters from the track. <code>usage = 1</code> Deletes all existing parameters from the track and generates new ones. Existing LSPs will be overwritten. <code>usage = 2</code> (default) Keeps existing parameters, but generates missing ones. This is useful when, for example, the effective path gain (PG) is provided, but the other LSPs are unknown. In this case, the unknown "gaps" are filled with values which are generated from the provided scenario description. | check_parfiles | <code>check_parfiles = 0 / 1</code> (default: 1) Disables (0) or enables (1) the parsing of shortnames and the validity-check for the config-files. This is useful, if you know that the parameters in the files are valid. In this case, this saves execution time. | verbose | Enables (1, default) or disables (0) the progress bar. | | | | | | |
| overlap | The length of the overlapping part relative to the segment length. When there are scenario transitions, KF and PG change smoothly during a predefined interval. The length of that interval is a percentage of previous segment. The parameter overlap adjusts this percentage, ranging from 0 (i.e. very hard, step-like change at the scenario boundary) to 1 (very smooth, but long transition). | | | | | | | | | | | | | | | |
| usage | Changes the behavior of the method <code>usage = 0</code> Deletes all existing parameters from the track. <code>usage = 1</code> Deletes all existing parameters from the track and generates new ones. Existing LSPs will be overwritten. <code>usage = 2</code> (default) Keeps existing parameters, but generates missing ones. This is useful when, for example, the effective path gain (PG) is provided, but the other LSPs are unknown. In this case, the unknown "gaps" are filled with values which are generated from the provided scenario description. | | | | | | | | | | | | | | | |
| check_parfiles | <code>check_parfiles = 0 / 1</code> (default: 1) Disables (0) or enables (1) the parsing of shortnames and the validity-check for the config-files. This is useful, if you know that the parameters in the files are valid. In this case, this saves execution time. | | | | | | | | | | | | | | | |
| verbose | Enables (1, default) or disables (0) the progress bar. | | | | | | | | | | | | | | | |
| Output | <p>par</p> <p>The automatically generated parameters This variable contains structure of the LSPs with the following fields:</p> <ul style="list-style-type: none"> • ds - The delay spread in [s] per segment • kf - The Ricean K-Factor in [dB] per snapshot • pg - The effective path gain in [dB] excluding antenna gains per snapshot • asD - The azimuth angle spread in [deg] per segment at the transmitter • asA - The azimuth angle spread in [deg] per segment at the receiver • esD - The elevation angle spread in [deg] per segment at the transmitter • esA - The elevation angle spread in [deg] per segment at the receiver • xpr - The NLOS cross-polarization in [dB] per segment <p>An identical copy of this variable is assigned to '<code>track.par</code>'.</p> | | | | | | | | | | | | | | | |

| [len, dist] = get_length | | |
|-----------------------------------|---|---|
| Description | Calculates the length of the track in [m] | |
| Output | len | Length of a track in [m] |
| | dist | Distance of each position (snapshot) from the start of the track in [m] |

| subtracks = get_subtrack (i_segment) | | |
|---|--|--|
| Description | Splits the track in subtracks for each segment (state) | |
| | | This function returns the subtracks for the given segment indices. When no input argument is provided, all subtracks are returned. |
| | | After defining segments along the track, one needs the subtrack that corresponds only to one segment to perform the channel calculation. This new track can consist of two segments. The first segment contains the positions from the previous segment, the second from the current. This is needed to generate overlapping channel segments for the merging process. |
| Input | i_segment | A list of indices indicating which subtracks should be returned. By default, all subtracks are returned. |
| Output | subtracks | A vector of track objects corresponding to the number of segments. |

| dist = interpolate_movement (si, method) | | |
|---|--|--|
| Description | Interpolates the movement profile to a distance vector | |
| | | This function interpolates the movement profile. The distance vector at the output can then be used to interpolate the channel coefficients to emulate varying speeds. See also the tutorial “Applying Varying Speeds (Channel Interpolation)” in Section A.6 for more details. |
| Input | si | the sampling interval in [seconds]. |
| | method | selects the interpolation algorithm. The default is cubic spline interpolation. Optional are: |
| | | <ul style="list-style-type: none"> • nearest - Nearest neighbor interpolation • linear - Linear interpolation • spline - Cubic spline interpolation • pchip - Piecewise Cubic Hermite Interpolating Polynomial • cubic - Cubic spline interpolation |
| Output | dist | Distance of each interpolated position from the start of the track in [m] |

| interpolate_positions (samples_per_meter) | | |
|--|--|---|
| Description | Interpolates positions along the track | |
| | | This function interpolates the positions along the track such that it matches the samples per meter specifies in the simulation parameters. |
| | The channel model operates on a position-based sample grid. That means that the ‘channel_builder’ generates one CIR for each position on the track. In practise, however, a time continuous evolution of the CIR is often needed. This can be interpolated from the position-based grid, provided that the spatial sample theorem is not violated (i.e. the channel needs to be sampled at least twice per half wave length). In order to do that, enough sample points are needed along the track. INTERPOLATE_POSITIONS calculates the missing sample points and places them equally spaced along the track. This corresponds to a constant speed when evaluating the output CIRs. The required value for ‘samples_per_meter’ can be obtained from the ‘simulation_parameters’ object. | |
| Input | samples_per_meter | the samples per meter (e.g. from ‘simulation_parameters.samples_per_meter’). |

set_scenario (scenario, probability, seg_length_min, seg_length_mu, seg_length_std)

| | | | | |
|-------------|--|--|--|--|
| Description | Assigns random scenarios and creates segments. This function can be used to create segments along the trajectory and assign scenarios to the segments. If there are less than 3 input arguments (i.e. only 'scenario' and/or 'probability' is given), then no segments will be created. To create segments with the default settings call ' <code>set_scenario(scenario, [], [])</code> '. Alternatively, it is possible to only create segments by leaving the scenario empty, e.g. by calling ' <code>set_scenario([], [], [])</code> '. | | | |
| Input | scenario | A cell array of scenario-names. Each scenario (synonym for propagation environment) is described by a string (e.g. "MIMOSA_16-25_LOS" or "WINNER_SMa_C1_NLOS"). A list of supported scenarios can be obtained by calling ' <code>parameter.set.supported_scenarios</code> '. The scenario parameters are stored in the configuration folder "config" in the QuaDRiGa main folder. The filenames (e.g. "MIMOSA_16-25.LOS.conf") also serves as scenario name. | | |
| | probability | The probability for which the scenario occurs. This parameter must be a vector of the same length as there are scenarios. Probabilities must be specified in between 0 and 1. The sum of the probabilities must be 1. By default (or when 'probability' is set to '[]'), each scenario is equally likely. | | |
| | seg_length_min | the minimal segment length in [m]. The default is 10 m. | | |
| | seg_length_mu | the median segment length in [m]. The default is 30 m. | | |
| | seg_length_std | the standard deviation of the street length in [m]. The default is 12 m. | | |

set_speed (speed)

| | | |
|-------------|---|-----------------------------|
| Description | Sets a constant speed in [m/s] for the entire track. This function fills the ' <code>track.movement_profile</code> ' field with a constant speed value. This helps to reduce computational overhead since it is possible to reduce the computation time by interpolating the channel coefficients. | |
| Input | speed | The terminal speed in [m/s] |

split_segment (mi, ma, mu, sig, no_check)

| | | |
|-------------|---|--|
| Description | Splits long segments in subsegments of the same type. | |
| Input | mi ma mu sig no_check | Minimum length of the subsegment in [m], default: 10m Maximum length of the subsegment in [m], must be > 2*mi, default: 30m Mean length of the subsegment (mi < mu < ma), default: 15m Std of the length of the subsegment, default: 5m Disable parsing of input variables, default: false |

visualize

| | |
|-------------|------------------|
| Description | Plots the track. |
|-------------|------------------|

2.2.4 Class “layout”

Objects of this class define the network layout of a simulation run. Each network layout has one or more transmitters and one or more receivers. Each transmitter and each receiver need to be equipped with an antenna array which is defined by the array class. In general, we assume that the transmitter is at a fixed position and the receiver is mobile. Thus, each receivers movement is described by a track.

Properties

| | |
|-------------|---|
| name | Name of the layout |
| simpar | Handle of a ‘simulation_parameters’ object. See Section 2.2.1 |
| no_tx | Number of transmitters (or base stations) |
| no_rx | Number of receivers (or mobile terminals) |
| tx_name | Identifier of each Tx, must be unique |
| tx_position | Position of each Tx in global cartesian coordinates using units of [m] |
| tx_array | Handles of ‘array’ objects for each Tx. See Section 2.2.2 |
| rx_name | Identifier of each Rx, must be unique |
| rx_position | Initial position of each Rx (relative to track start) in global cartesian coordinates using units of [m] |
| rx_array | Handles of ‘array’ objects for each Rx. See Section 2.2.2 |
| track | Handles of track objects for each Rx. See Section 2.2.3 |
| pairing | An index-list of links for which channel are created. The first row corresponds to the Tx and the second row to the Rx. |
| no_links | Number of links for which channel coefficients are created (read only) |

Methods

| | | |
|---|------------------------------|---|
| <code>h_layout = layout (simpar)</code> | | |
| Description | Creates a new layout object. | |
| Input | simpar | Handle of a ‘simulation_parameters’ object. See Section 2.2.1 |

| | | |
|--|--|--|
| <code>[h_parse, h_cb] = create_parameter_sets (initialize, check_parfiles)</code> | | |
| Description | Creates ‘parameter_set’ objects based on layout specification This function processes the data in the ‘layout’ object. First, all tracks in the layout are split into subtracks. Each subtrack corresponds to one segment. Then, then scenario names are parsed. A ‘parameter_set’ object is created for each scenario and for each transmitter. For example, if there are two terrestrial BSs, each having urban LOS and NLOS users, then 4 ‘parameter_set’ objects will be created (BS1-LOS, BS2-NLOS, BS2-LOS, and BS2-NLOS). The segments are then assigned to the ‘parameter_set’ objects. In the last step, the parameter maps are created (see Section 3.1). This can be disabled by setting ‘initialize = 0’. | |
| Input | <code>initialize</code> <code>check_parfiles</code> | |
| <code>initialize</code> Enables (1, default) or disables (0) the generation of the parameter maps. If you want to adjust the parameters first, use ‘initialize = 0’, then adjust the parameters in the ‘parameter_set’ objects and call ‘update_parameters’ manually. <code>check_parfiles</code> Enables (1, default) or disables (0) the parsing of shortnames and the validity-check for the config-files. This is useful, if you know that the parameters in the files are valid. In this case, this saves some execution time. | | |
| Output | <code>h_parse</code> A matrix of ‘parameter_set’ objects. Rows correspond to the scenarios, columns correspond to the transmitters. See Section 2.2.5 <code>h_cb</code> A vector of ‘channel_builder’ objects. See Section 2.2.6 | |

| | | |
|--|--|---|
| <code>mem = estimate_memory_usage (verbose)</code> | | |
| Description | This function estimates the memory requirements for running the simulation specified by the layout. This can help to determine if the computer is equipped with enough memory before starting complex simulations. | |
| Input | <code>verbose</code> | Shows a detailed report of the memory requirements (default = 1). |
| Output | <code>mem</code> | The estimate of the required memory in [Bytes]. |

| | | |
|---|---|--|
| <code>h_layout = layout.generate ('regular', no_sites, isd, h_array)</code> | | |
| Description | generates a new multicell layout using a regular grid of BS positions. Each BS has three sectors. | |
| Input | no_sites isd h_array | the number of sites. This can be 1, 7, 19 or 37 - resulting in 3, 21, 57 or 111 sectors, respectively. the inter-site distance between the BSs in [m]. the antenna array. ' <code>h_array</code> ' is for one sector only. It will be rotated to match the sector orientations and copied to all sites. The broadside-direction of the provided antenna must be 0 (facing east). |
| Output | h_layout | The generated layout. |

| | | |
|--|--|---|
| <code>[par, h_parse] = generate_parameters (overlap, usage, check_parfiles)</code> | | |
| Description | <p>Generates large scale parameters and stores them in '<code>track.par</code>'</p> <p>Normally, parameters are handled by objects of the '<code>parameter_set</code>' class, which are generated by calling '<code>layout.create_parameter_sets</code>'. Those objects then feed the parameters to the '<code>channel_builder</code>'. However, this method is rather inflexible when the user wants to manipulate the parameters directly. As an alternative, parameters can be provided in the property '<code>track.par</code>' of the '<code>track</code>' class. This allows the user to edit parameters without dealing with the '<code>parameter_set</code>' objects.</p> <p>This function extracts the <code>LSPs</code> for the given scenario from the '<code>parameter_set</code>' class and stores them in '<code>track.par</code>'. Hence, it automatically generates the <code>LSPs</code> and, thus, implements an easy-to-use interface for the '<code>parameter_set</code>' class.</p> | |
| Input | overlap usage check_parfiles | <p>The length of the overlapping part relative to the segment length. When there are scenario transitions, KF and PG change smoothly during a predefined interval. The length of that interval is a percentage of previous segment. The parameter overlap adjusts this percentage, ranging from 0 (i.e. very hard, step-like change at the scenario boundary) to 1 (very smooth, but long transition).</p> <p>Changes the behavior of the method</p> <p><code>usage = 0</code> Deletes all existing parameters from the track.</p> <p><code>usage = 1</code> Deletes all existing parameters from the track and generates new ones. Existing <code>LSPs</code> will be overwritten.</p> <p><code>usage = 2</code> (default) Keeps existing parameters, but generates missing ones. This is useful when, for example, the effective PG is provided, but the other <code>LSPs</code> are unknown. In this case, the unknown "gaps" are filled with values which are generated from the provided scenario description.</p> <p><code>check_parfiles = 0 / 1</code> (default: 1) Disables (0) or enables (1) the parsing of shortnames and the validity-check for the config-files. This is useful, if you know that the parameters in the files are valid. In this case, this saves execution time.</p> |
| Output | par h_parse | <p>The automatically generated parameters. This cell array contains a parameter structure of the <code>LSPs</code> for each receiver with the following fields:</p> <ul style="list-style-type: none"> • ds - The delay spread in [s] per segment • kf - The Ricean K-Factor in [dB] per snapshot • pg - The effective path gain in [dB] excluding antenna gains per snapshot • asD - The azimuth angle spread in [deg] per segment at the transmitter • asA - The azimuth angle spread in [deg] per segment at the receiver • esD - The elevation angle spread in [deg] per segment at the transmitter • esA - The elevation angle spread in [deg] per segment at the receiver • xpr - The NLOS cross-polarization in [dB] per segment <p>An identical copy of this variable is assigned to '<code>track.par</code>'.</p> <p>A matrix of '<code>parameter_set</code>' objects. Rows correspond to the scenarios, columns correspond to the transmitters. See Section 2.2.5</p> |

| [h_channel, h_parse, h_cb] = get_channels (sampling_rate, check_parfiles) | | |
|--|---|---|
| Description | Calculate the channel coefficients. This is the most simple way to create the channel coefficients. This function executes all steps that are needed to generate the channel coefficients. Hence, it is not necessary to use the ' parameter_set ' or ' channel_builder ' objects. | |
| Input | sampling_rate check_parfiles | channel update rate in [s]. This parameter is only used if a speed profile is provided in the track objects. Default value: 0.01 = 10 ms Enables (1, default) or disables (0) the parsing of shortnames and the validity-check for the config-files. This is useful, if you know that the parameters in the files are valid. In this case, this saves some execution time. |
| Output | h_channel h_parse h_cb | A vector channel objects. See Section 2.2.7 A matrix of ' parameter_set ' objects. Rows correspond to the scenarios, columns correspond to the transmitters. See Section 2.2.5 A vector of ' channel_builder ' objects. See Section 2.2.6 |

| [h_channel, h_cb] = get_channels_seg (tx, rx, seg, overlap) | | |
|--|---|--|
| Description | Returns the channel coefficients for a single segment only This function can be used to obtain the channel coefficients for a single segment or single rx-tx combination only. Thus, the channel model can be run in "streaming-mode", where updates are provided on the fly. This can significantly reduce the memory requirements for long time-sequences. (However, the parameter maps still need to be generated for the entire scenario.) Features: <ul style="list-style-type: none">• Parameter maps will be deleted after the parameters were extracted to free memory before creating the channels.• Caching will be used to avoid multiple calculation of the same overlapping regions.• Preinitialization will be used to return the same coefficients for successive calls. | |
| Input | tx rx seg overlap | The index of the transmitter (e.g. the BS) The index of the receiver, or track (e.g. the BS) The segment indices on the the track. If it is not provided or empty, the entire track is returned. It is also possible to concat successive segments, i.e.: [1:3] or [3:5], etc. The opverlapping fraction for the channel merger. Default is 0.5 |
| Output | h_channel h_cb | A channel object. See Section 2.2.7 A vector of ' channel_builder ' objects. See Section 2.2.6 |

| | | |
|--|---|--|
| <pre>[map, x_coords, y_coords] = power_map (scenario, usage, sample_distance, x_min, y_max, x_max, y_min, tx_power, rx_height)</pre> | | |
| Description | <p>Calculates a power-map for the given layout. This function calculates receive power values in [W] on a square lattice at a height of 'rx_height' above the ground for the given layout. This helps to predict the performance for a given setup.</p> | |
| Input | <p>scenario</p> <p>usage</p> <p>sample_distance</p> <p>x_min</p> <p>y_max</p> <p>x_max</p> <p>y_min</p> <p>tx_power</p> <p>rx_height</p> | <p>The scenario for which the map shall be created. There are four options:</p> <ol style="list-style-type: none"> 1. A string describing the scenario. A list of supported scenarios can be obtained by calling '<code>parameter_set.supported_scenarios</code>'. 2. cell array of strings describing the scenario for each transmitter in the layout. 3. A '<code>parameter_set</code>' object. This method is useful if you need to edit the parameters first. For example: call '<code>p = parameter_set('UMaL')</code>' to load the parameters. Then edit '<code>p.scenpar</code>' or '<code>p.plpar</code>' to adjust the settings. 4. Aa array of '<code>parameter_set</code>' objects describing the scenario for each transmitter in the layout. <p>A string specifying the detail level. The following options are implemented:</p> <ul style="list-style-type: none"> • 'quick' - Uses the antenna patterns, the LOS path, and the path gain from the scenario • 'sf' - Uses the antenna patterns, the LOS path, the path gain from the scenario, and a shadow fading map • 'detailed' - Runs a full simulation for each pixel of the map (very slow) • 'phase' - Same as quick, but the output contains the complex-valued amplitude instead of the power <p>Distance between sample points in [m] (default = 10 m)</p> <p>x-coordinate in [m] of the top left corner</p> <p>y-coordinate in [m] of the top left corner</p> <p>x-coordinate in [m] of the bottom right corner</p> <p>y-coordinate in [m] of the bottom right corner</p> <p>A vector of tx-powers in [dBm] for each transmitter in the layout. This power is applied to each transmit antenna in the tx-antenna array. By default (if <code>tx_power</code> is not given), 0 dBm are assumed.</p> <p>Height of the receiver points in [m] (default = 0 m)</p> |
| Output | <p>map</p> <p>x_coords</p> <p>y_coords</p> | <p>A cell array containing the power map for each tx array in the layout. The power maps are given in [W] and have the dimensions [n_y_coords , n_x_coords , n_rx_elements , n_tx_elements].</p> <p>Vector with the x-coordinates of the map in [m].</p> <p>Vector with the y-coordinates of the map in [m].</p> |

| | | |
|--|--|---|
| randomize_rx_positions (max_dist, min_height, max_height, track_length, rx_ind) | | |
| Description | <p>Generates random Rx positions and tracks. Places the users in the layout at random positions. Each user will be assigned a linear track with random direction. The random height of the user terminal will be in between '<code>min_height</code>' and '<code>max_height</code>'.</p> | |
| Input | <p>max_dist</p> <p>min_height</p> <p>max_height</p> <p>track_length</p> <p>rx_ind</p> | <p>the maximum distance from the layout center in [m]. Default is 50 m.</p> <p>the minimum user height in [m]. Default is 1.5 m.</p> <p>the maximum user height in [m]. Default is 1.5 m.</p> <p>the length of the linear track in [m]. Default is 1 m.</p> <p>an vector containing the receiver indices for which the positions should be generated. Default: All receivers.</p> |

| [pairs, power] = set_pairing (method, threshold, tx_power, check_parfiles) | | |
|---|--|--|
| Description | <p>Determines links for which channel coefficient are generated.</p> <p>This function can be used to automatically determine the links for which channel coefficients should be generated. For example, in a large network there are multiple base stations and mobile terminals. The base stations, however, only serve a small area. If the terminal is far away from this area, it will receive only noise from this particular BS. In this case, the channel coefficients will have very little power and do not need to be calculated. Disabling those links can reduce the computation time and the storage requirements for the channel coefficients significantly. There are several methods to do this which can be selected by the input variable 'method'.</p> | |
| Methods | <p>'all'</p> <p>'power'</p> <p>'sf'</p> | |
| | | Enables the simulation of all links. |
| | | Calculates the expected received power taking into account the path loss, the antenna patterns, the LOS polarization, and the receiver orientation. If the power of a link is below the ' threshold ', it gets deactivated. |
| | | Same as ' power ', but this option also includes the shadow fading. Therefore, the LSPs have to be calculated. LSPs get then stored in ' layout.track.par '. This method is the most accurate. The actual power in the channel coefficients can be up to 6 dB higher due to multipath effects. |
| Input | method threshold tx_power check_parfiles | <p>Link selection method. Supported are: 'all', 'power', and 'sf' (see above).</p> <p>If the Rx-power is below the threshold in [dBm], the link gets deactivated.</p> <p>A vector of tx-powers in [dBm] for each transmitter in the layout. This power is applied to each transmit antenna in the tx-antenna array. By default (if 'tx_power' is not given), 0 dBm are assumed.</p> <p>Disables (0) or enables (1, default) the parsing of shortnames and the validity-check for the config-files. This is useful, if you know that the parameters in the files are valid. In this case, this saves execution time.</p> |
| Output | pairs power | <p>An index-list of links for which channels are created. The first row corresponds to the Tx and the second row to the Rx. An identical copy gets assigned to 'layout.pairing'.</p> <p>A matrix containing the estimated receive powers for each link in [dBm]. Rows correspond to the receiving terminal, columns correspond to the transmitter station. For MIMO links, the power of the strongest MIMO sublink is reported.</p> |

| pos = set_satellite_pos (rx_latitude, sat_el, sat_az, sat_height, tx_no) | | |
|---|--|--|
| Description | <p>Calculates the Tx position from a satellite orbit.</p> <p>QuaDRiGas reference coordinate system is on the surface of the earth. In order to use QuaDRiGa for satellite links, the satellite position must be set. Normally, this position is given in azimuth and elevation relative to the user's position. This function takes a satellite orbital position and calculates the corresponding transmitter coordinates.</p> | |
| Input | rx_latitude sat_el sat_az sat_height tx_no | |
| | | The receiver latitude coordinate on the earth surface in [deg]. Default is 52.5. Satellite elevation in [deg]. Default is 31.6. Satellite azimuth in [deg] given in compass coordinates. Default is 180° (south). Satellite height in [km] relative to earth surface. Default is 35786 (GEO orbit). The 'tx_no' in the layout object for which the position should be set. Default is 1. |
| Output | pos | |
| | | The satellite positions in the metric QuaDRiGa coordinate system. |

| indoor_rx = set_scenario (scenario, rx, tx, indoor_frc) | | | | | | | | | | |
|---|---|--|----------|--|----|--|----|--|------------|--|
| Description | <p>Assigns scenarios to tracks and segments.</p> <p>This function can be used to assign scenarios to tracks and segments of tracks. This takes the distance-dependent LOS probability into account for some specific scenarios. Currently, distance-dependent scenario selection is available for:</p> <ul style="list-style-type: none"> • 3GPP_3D_UMi • 3GPP_3D_UMa • mmMAGIC_initial_UMi • mmMAGIC_initial_Indoor <p>Alternatively, you can use all scenarios specified in '<code>parameter_set.supported_scenarios</code>'.</p> | | | | | | | | | |
| Input | <table> <tr> <td>scenario</td><td>A string containing the scenario name.</td></tr> <tr> <td>rx</td><td>A vector containing the receiver indices for which the scenarios should be set. Default: all receivers.</td></tr> <tr> <td>tx</td><td>A vector containing the transmitter indices for which the scenarios should be set. Default: all transmitters.</td></tr> <tr> <td>indoor_frc</td><td>The fraction of the users (number between 0 and 1) that are indoors.</td></tr> </table> | | scenario | A string containing the scenario name. | rx | A vector containing the receiver indices for which the scenarios should be set. Default: all receivers. | tx | A vector containing the transmitter indices for which the scenarios should be set. Default: all transmitters. | indoor_frc | The fraction of the users (number between 0 and 1) that are indoors. |
| scenario | A string containing the scenario name. | | | | | | | | | |
| rx | A vector containing the receiver indices for which the scenarios should be set. Default: all receivers. | | | | | | | | | |
| tx | A vector containing the transmitter indices for which the scenarios should be set. Default: all transmitters. | | | | | | | | | |
| indoor_frc | The fraction of the users (number between 0 and 1) that are indoors. | | | | | | | | | |
| Output | indoor_rx | | | | | | | | | |
| A logical vector indicating if a user is indoors (1) or outdoors (0). | | | | | | | | | | |

| han = visualize (tx , rx, show_names , create_new_figure) | | | | | | | | | | |
|--|--|--|----|--|----|---|------------|--|-------------------|--|
| Description | Plots the layout. | | | | | | | | | |
| Input | <table> <tr> <td>tx</td><td>A vector containing the transmitter indices that should be shown. Default: All</td></tr> <tr> <td>rx</td><td>A vector containing the receiver indices that should be shown. Default: All</td></tr> <tr> <td>show_names</td><td>Options: (0) shows no Tx and Rx names; (1, default) shows the Tx name and the scenario for each track segment; (2) shows the Tx and Rx name.</td></tr> <tr> <td>create_new_figure</td><td>If set to 0, no new figure is created, but the layout is plotted in the currently active figure.</td></tr> </table> | | tx | A vector containing the transmitter indices that should be shown. Default: All | rx | A vector containing the receiver indices that should be shown. Default: All | show_names | Options: (0) shows no Tx and Rx names; (1, default) shows the Tx name and the scenario for each track segment; (2) shows the Tx and Rx name. | create_new_figure | If set to 0, no new figure is created, but the layout is plotted in the currently active figure. |
| tx | A vector containing the transmitter indices that should be shown. Default: All | | | | | | | | | |
| rx | A vector containing the receiver indices that should be shown. Default: All | | | | | | | | | |
| show_names | Options: (0) shows no Tx and Rx names; (1, default) shows the Tx name and the scenario for each track segment; (2) shows the Tx and Rx name. | | | | | | | | | |
| create_new_figure | If set to 0, no new figure is created, but the layout is plotted in the currently active figure. | | | | | | | | | |

2.2.5 Class “parameter_set”

This class implements all functions that are necessary to generate and manage correlated LSPs. It also provides interfaces for the channel builder. LSPs are the shadow fading, the Ricean K-Factor, the RMS delay spread and the four angles (elevation and azimuth at the transmitter and receiver). This class implements some core functions of the channel model and the user does normally not need to interact with it. However, if parameter tables need to be changed, here is the place to do so.

Properties

| | |
|-------------------|--|
| name | Name of the 'parameter_set' object |
| simpar | Handle of a 'simulation_parameters' object. See Section 2.2.1 |
| tx_array | Handles of 'array' objects for each Tx. See Section 2.2.2 |
| rx_array | Handles of 'array' objects for each Rx. See Section 2.2.2 |
| rx_track | Handles of 'track' objects for each Rx. See Section 2.2.3 |
| scenario | Name of the scenario (text string) |
| scenpar | The parameter table. See Section 2.4 |
| plpar | Parameters for the path loss. See Section 2.4 |
| no_positions | Number of receiver positions associated to this 'parameter_set' object Note that each segment in longer tracks is considered a new Rx position. |
| positions | The list of initial positions for which LSPs are generated |
| tx_position | This variable is obtained from the properties 'track.initial_position' and 'layout.rx_position' The transmitter position obtained from the corresponding 'layout.tx_position' |
| ds | The RMS delay spread in [s] for each receiver position |
| kf | The Ricean K-Factor [linear scale] for each receiver position |
| sf | The shadow fading [linear scale] for each receiver position |
| asD | The azimuth spread of departure in [deg] for each receiver position |
| asA | The azimuth spread of arrival in [deg] for each receiver position |
| esD | The elevation spread of departure in [deg] for each receiver position |
| esA | The elevation spread of arrival in [deg] for each receiver position |
| xpr | The cross polarization ratio [linear scale] for each receiver position |
| ds_map | The RMS delay spread map in [log10(s)] |
| kf_map | The Ricean K-Factor map [logarithmic scale] |
| sf_map | The shadow fading map [logarithmic scale] |
| asD_map | The azimuth spread of departure map in [log10(deg)] |
| asA_map | The azimuth spread of arrival map in [log10(deg)] |
| esD_map | The elevation spread of departure map in [log10(deg)] |
| esA_map | The elevation spread of arrival map in [log10(deg)] |
| map_extension | Distance in [m] that is added to each direction when generating maps |
| map_extent | Extent of the mpas in x- and y-direction [xmin, xmax; ymin, ymax] in [m] |
| map_size | Number of map pixels in x and y-direction [n_x_samples; n_y_samples] |
| samples_per_meter | Resolution of the decorrelation maps in [samples/m] |
| map_valid | This value is obtained from 'simulation_parameters.map_resolution' |
| LSP_xcorr_matrix | Indicates if maps contain valid data |
| LSP_matrix_isOK | The Cross-correlation matrix for the LSPs |
| map_x_coord | Determines if the XCorr-matrix is positive definite |
| map_y_coord | The x-coordinates in [m] for each pixel of the maps |
| | The y-coordinates in [m] for each pixel of the maps |

Methods

| | | |
|--|---|---|
| h_parsest = parameter_set (scenario, positions, check_parfiles) | | |
| Description | Creates a new 'parameter_set' object. | |
| Input | scenario positions check_parfiles | The scenario name for which the parameters should be loaded. A list of supported scenarios can be obtained by calling 'parameter_set.supported_scenarios'. The list of initial positions for which LSPs should be generated. check_parfiles = 0 / 1 (default: 1) Disables (0) or enables (1) the parsing of shortnames and the validity-check for the config-files. This is useful, if you know that the parameters in the files are valid. In this case, this saves execution time. |
| Output | h_parsest | A 'parameter_set' object. |

| | | |
|---------------------|---|--|
| copy_objects | | |
| Description | A modified version of the standard physical copy function While the standard copy command creates new physical objects for each element of obj (in case obj is an array of object handles), copy_objects checks whether there are object handles pointing to the same object and keeps this information. | |

| | | |
|----------------------------|---|--|
| angles = get_angles | | |
| Description | Calculates the departure- and arrival angles of the LOS path between Tx and Rx. | |
| Output | angles | A matrix containing the four angles: <ul style="list-style-type: none">• Azimuth of Departure at the Tx (AoD, row 1)• Azimuth of Arrival at the Rx (AoA, row 2)• Elevation of Departure at the Tx (EoD, row 3)• Elevation of Arrival at the Rx (EoA, row 4) The number of columns corresponds to the number of rx-positions. |

| | | |
|---|-------------------------------------|---|
| [h_channel, h_cb] = get_channels | | |
| Description | Calculate the channel coefficients. | |
| Output | h_channel h_cb | A vector channel objects. See Section 2.2.7 A vector of 'channel_builder' objects. See Section 2.2.6 |

| | | |
|-----------------------------|---|--|
| dist = get_distances | | |
| Description | Calculates the distances between Rx and Tx. | |
| Output | dist | A vector containing the distances between each Rx and the Tx in [m]. |

| | | |
|--|---|---|
| [pl, scale_sf] = get_pl (evaltrack, i_mobile) | | |
| Description | Calculates the path loss. The path loss model is specified in the configuration files and in 'parameter_set.plpar'. | |
| Input | evaltrack i_mobile | A 'track' object for which the PL should be calculated. If 'evaltrack' is not given, then the path loss is calculated for each Rx position. Otherwise the path loss is calculated for the positions provided in 'evaltrack'. The Rx-index. If it is not given, the PL is evaluated for all Rx positions. If 'evaltrack' is given, and if 'simulation_parameters.drifting_precision' is set to 3, then this parameter is required to select the Rx antenna array (default = 1). |
| Output | pl scale_sf | The path loss in [dB] In some scenarios, the SF might change with increasing distance between Tx and Rx. Hence, the shadow fading provided by the parameter map has to be changed accordingly. The second output parameter "scale_sf" can be used for scaling the (logarithmic) SF value from the map. |

| [sf,kf] = get_sf_profile (evaltrack, i_mobile) | | |
|--|---|--|
| Description | This function returns the shadow fading and the K-factor along the given track. This function is mainly used by the channel builder class to scale the output channel coefficients. The profile is calculated by using the data in the correlation maps and interpolating it to the positions in the given track. Increasing the resolution of the maps also increases the resolution of the profile. | |
| Input | evaltrack i_mobile | A 'track' object for which the SF and KF should be interpolated. If 'simulation_parameters.drifting_precision' is set to 3, then this parameter is required to select the Rx antenna array. |
| Output | sf kf | The shadow fading [linear scale] along the track. The K-factor [linear scale] along the track. |

| set_par (name, value) | | |
|-------------------------|--|--|
| Description | Sets the parameters of all objects in 'parameter_set' arrays. This function sets all values of the parameter specified by 'name' of the 'parameter_set'-array to the given value. Example: 'set_par('ds' , 1e-9) sets all ds-values to 1 ns. | |
| Input | name value | The fieldname that should be altered. Supported are: 'ds', 'kf', 'sf', 'asD', 'asA', 'esD', 'esA', 'samples_per_meter', 'map_extension', and 'LSP_xcorr_matrix'. The value that should be assigned. If the 'LSP_xcorr_matrix' is altered, then the lower triangular part of the matrix is ignored and replaced by a transpose of the upper triangular matrix. |

| [scenarios, file_names, file_dir] = parameter_set.supported_scenarios (parse_shortnames) | | |
|--|--|---|
| Description | Returns a list of supported scenarios. | |
| Input | parse_shortnames | This optional parameter can disable (0) the shortname parsing. This is significantly faster. By default shortname parsing is enabled (1). |
| Output | scenarios file_names file_dir | A cell array containing the scenario names. Those can be used in 'track.scenario' The names of the configuration files for each scenario. The directory where each file was found. You can place configuration file also in your current working directory. |

| update_parameters (force) | | |
|-----------------------------|--|--|
| Description | Generates the LSP maps and updates the parameters for all terminals. This function calculates correlated large scale parameters for each user position. Those parameters are needed by the channel builder class to calculate initial parameters for each track or segment which are then evolved into time varying channels. By default, 'update_parameters' reads the values given in the 'track' objects of the 'layout'. If there are no values given or if parts of the values are missing, the correlation maps are generated to extract the missing parameters. | |
| Input | force | Changes the behavior of the function. force = 0 (default) Tries to read the parameters from 'layout.track.par'. If they are not provided or if they are incomplete, they are completed with values from the LSP maps. If the maps are invalid (e.g. because they have not been generated yet), new maps are created. force = 1 Creates new maps and reads the LSPs from those maps. Values from 'layout.track.par' are ignored. Note that the parameters 'pg' and 'kf' will still be taken from 'layout.track.par' when generating channel coefficients. force = 2 Creates dummy data for the maps and the LSPs. Any existing maps will be deleted. Data and maps will be declared as invalid and the next time when 'update_parameters' is called, new parameters are generated. Values in 'layout.track.par' will NOT be affected. |

2.2.6 Class “channel_builder”

This class implements all functions that are needed to generate the channel coefficients. It thus implements the core components of the channel model. The class holds all the input variables as properties. Its main function ‘get_channels’ then generates the coefficients. The procedure is summarized as follows:

The channel builder first generates a set of random clusters around each receiver. This is done by drawing random variables for the delay, the power and the departure and arrival angles for each cluster. Each cluster thus represents the origin of a reflected (and scattered) signal. The clusters are then represented as taps in the final CIR. The random variables fit the distributions and correlations defined by the ‘parameter_set’ object.

Next, antenna dependent parameters are extracted for each user. Those depend on the position of the terminal, its orientation and the equipped antennas. The polarization rotation of the NLOS taps is modeled by a random variable which fits to the distribution defined by the ‘parameter_set’. The LOS polarization is calculated from the geometric orientation of the antennas. A core function here is the interpolation of the antenna patterns which results in a specific H and V value for each subpath.

The core function then generates the coefficients themselves. This is done for each antenna element and for each snapshot separately and also includes the Doppler shift of each subpath. Finally, the K-factor and the shadow fading are applied and all the data is returned as an ‘channel’ object.

Properties

| | |
|------------------|--|
| name | Name of the ‘channel_builder’ object |
| par | The ‘parameter_set’ object for this channel builder |
| taus | The initial delays for each path in [s]. Rows correspond to the MTs, columns to the paths. |
| pow | The normalized initial power (squared average amplitude) for each path. Rows correspond to the MTs, columns to the paths. The sum over all columns must be 1. |
| AoD | The initial azimuth of departure angles for each path in [rad]. |
| AoA | The initial azimuth of arrival angles for each path in [rad]. |
| EoD | The initial elevation of departure angles for each path in [rad]. |
| EoA | The initial elevation of arrival angles for each path in [rad]. |
| xpr | The initial cross polarization power ratio in [dB] for each sub-path. The dimensions correspond to the MT, the path number, and the sub-path number. |
| pin | The initial phases in [rad] for each sub-path. |
| kappa | The phase offset angle for the circular XPR in [rad]. The dimensions correspond to the MT, the path number, and the sub-path number. |
| random_pol | Random phasors for the WINNER polarization coupling method. The dimensions correspond to polarization matrix index ‘[1 3 ; 2 4]’, the subpath number, and the MT. |
| subpath_coupling | A random index list for the mutual coupling of subpaths at the Tx and Rx. The dimensions correspond to the subpath index (1-20), the angle (AoD, AoA, EoD, EoA), the path number and the MT. |

Methods

| h_cb = channel_builder (h_parse) | | |
|---|---|-----------------------------|
| Description | Creates a new ‘channel_builder’ object. | |
| Input | h_parse | A ‘parameter_set’ object. |
| Output | h_cb | A ‘channel_builder’ object. |

| [phi_d_lm, theta_d_lm, lbs_pos, fbs_pos] = calc_scatter_positions | | |
|---|--|---|
| Description | Calculates the positions of the scatterers | This function calculates the positions of the scatterers and initializes the drifting module. The output variables are the NLOS Tx angles for the precomputation of the Tx array response. |
| Input | i_mobile | The index of the mobile terminal within the channel builder object |
| Output | phi_d_lm theta_d_lm lbs_pos fbs_pos | The departure azimuth angles for each subpath. The departure elevation angles for each subpath. The position of the last-bounce scatterer. The position of the first-bounce scatterer. |

| h_channel = get_channels | | |
|--------------------------|---|--------------------------------|
| Description | Generates the channel coefficients. This is the main function of the 'channel_builder'. | |
| Output | h_channel | An array of 'channel' objects. |

| h_channel = channel_builder.get_los_channels (h_parse) | | |
|--|---|---|
| Description | Generates channel coefficients for the LOS path only. | This function generates static coefficients for the LOS path only. This includes the following properties: |
| | | <ul style="list-style-type: none"> • antenna patterns • orientation of the Rx (if provided) • polarization rotation for the LOS path • plane-wave approximation of the phase • path loss • shadow fading <p>No further features of QuaDRiGa are used (i.e. no drifting, spherical waves, time evolution, multipath fading etc.). This function can thus be used to acquire quick previews of the propagation conditions for a given layout.</p> |
| Input | h_parse | A 'parameter_set' object (see Section 2.2.5). |
| Output | h_channel | A 'channel' object (see Section 2.2.7). The output contains one coefficient for each position in 'h_parse.position'. |

| aso = init_parameters(force) | | |
|--------------------------------|----------------------------------|---|
| Description | Generates the initial parameters | This function creates the initial parameters for the channel builder. If the parameters are already initialized, no new update is performed. The optional parameter 'force' can be used to enforce an update, even if the parameters are already given. |
| Input | force | Enforces (1) the generation of new parameters. Default: 0. |
| Output | aso | An array with angular spread values for each terminal. The rows are [AoD ; AoA ; EoD ; EoA] |

| visualize_clusters(i_mobile , i_cluster) | | |
|--|---|--|
| Description | Plots the scattering clusters for a mobile terminal | This method plots all scattering clusters for a given mobile terminal. If i_cluster is not given, then only the main paths are shown for all MPCs. If i_cluster is given, then also the subpaths are shown for the selected cluster. |
| | | The plot is in 3D coordinates. You can rotate the image using the rotate tool. |
| Input | i_mobile i_cluster | The index of the mobile terminal within the channel builder object The index of the scattering cluster. (Optional) |

2.2.7 Class “channel”

Objects of this class are the output of the channel model. They are created by the ‘`channel_builder`’. By default, channel coefficients are provided in time domain, as a list of delays and complex-valued amplitudes. However, this class also implements certain methods to postprocess the channel data. Those include:

- Transformation into frequency domain
- Interpolation in time domain (to change the terminal speed and sampling rate)
- Combining channel traces into longer segments (including birth and death of clusters)

Properties

| | |
|--------------------------------|---|
| <code>name</code> | Name of the ‘ <code>channel</code> ’ object. This string is a unique identifier of the ‘ <code>channel</code> ’ object. The ‘ <code>channel_builder</code> ’ creates one channel object for each MT, each Tx and each segment. They are further grouped by scenarios (propagation environments). The string consists of four parts separated by an underscore ‘_’. Those are: <ul style="list-style-type: none"> • The scenario name from ‘<code>track.scenario</code>’ • The transmitter name from ‘<code>layout.tx_name</code>’ • The receiver name from ‘<code>layout.rx_name</code>’ • The segment number After ‘ <code>channel.merge</code> ’ has been called, the name string consists of: <ul style="list-style-type: none"> • The transmitter name from ‘<code>layout.tx_name</code>’ • The receiver name from ‘<code>layout.rx_name</code>’ |
| <code>version</code> | Version number of the QuaDRiGa release that was used to create the ‘ <code>channel</code> ’ object. |
| <code>individual_delays</code> | Indicates if the path delays are identical on each MIMO link (0) or if each link has a different path delay (1). |
| <code>coeff</code> | The complex-valued channel coefficients for each path. The indices of the 4-D tensor are: [Rx-Antenna , Tx-Antenna , Path , Snapshot] |
| <code>delay</code> | The delays for each path. There are two different options. If the delays are identical on the MIMO links, i.e. ‘ <code>individual.delays = 0</code> ’, then ‘ <code>delay</code> ’ is a 2-D matrix with dimensions [Path , Snapshot]. If the delays are different on the MIMO links, then ‘ <code>delay</code> ’ is a 4-D tensor with dimensions [Rx-Antenna , Tx-Antenna , Path , Snapshot]. |
| <code>initial_position</code> | The snapshot number for which the initial LSPs have been generated. Normally, this is the first snapshot. However, if the user trajectory consists of more than one segment, then ‘ <code>initial_position</code> ’ points to the snapshot number where the current segment starts. For example: If ‘ <code>initial_position</code> ’ is 100, then snapshots 1-99 are overlapping with the previous segment. |
| <code>tx_position</code> | Position of each Tx in global cartesian coordinates using units of [m]. |
| <code>rx_position</code> | The receiver position global cartesian coordinates using units of [m] for each snapshot. |
| <code>no_rx</code> | Number of receive elements (read only) |
| <code>no_tx</code> | Number of transmit elements (read only) |
| <code>no_path</code> | Number of paths (read only) |
| <code>no_snap</code> | Number of snapshots (read only) |

Methods

| <code>h_channel = channel (Ccoeff, Cdely, Cinital_position)</code> | | |
|--|--|--|
| <code>Description</code> | Creates a new ‘ <code>channel</code> ’ object. | |
| <code>Input</code> | <code>Ccoeff</code> <code>Cdely</code> <code>Cinital_position</code> | The complex-valued channel coefficients for each path. The delays for each path. The snapshot number for which the initial LSPs have been generated. |
| <code>Output</code> | <code>h_channel</code> | A ‘ <code>channel</code> ’ object. |

| freq_response = fr(bandwidth, carriers, i_snapshot) | | |
|---|--|---|
| Description | Transforms the channel into frequency domain and returns the frequency response. | |
| Input | bandwidth | The baseband bandwidth in [Hz]. |
| | carriers | <p>The carrier positions. There are two options:</p> <ol style="list-style-type: none"> 1. Specify the total number of carriers. In this case, 'carriers' a scalar natural number > 0. The carriers are then equally spaced over the bandwidth. 2. Specify the pilot positions. In this case, 'carriers' is a vector of carrier positions. The carrier positions are given relative to the bandwidth where '0' is the begin of the spectrum and '1' is the end. For example, if a 5 MHz channel should be sampled at 0, 2.5 and 5 MHz, then 'carriers' must be set to [0, 0.5, 1]. |
| i_snapshot | | The snapshot numbers for which the frequency response should be calculated. By default, i.e. if ' i_snapshot ' is not given, all snapshots are processed. |
| Output | freq_response | |
| | | The complex-valued channel coefficients for each carrier in frequency domain. The indices of the 4-D tensor are: [Rx-Antenna , Tx-Antenna , Carrier-Index , Snapshot] |

| c = interpolate(dist, method) | | |
|---------------------------------|---|---|
| Description | Interpolates the channel coefficients and delays. | |
| Input | dist | <p>The channel builder creates one snapshot for each position that is listed in the track object. When the channel sampling theorem is not violated (i.e. the sample density is ≥ 2), then the channel can be interpolated to any other position on the track. This can be used e.g. to emulate arbitrary movements along the track.</p> <p>For more information see 'track.movement_profile', 'track.interpolate_movement', or the tutorial "Applying Varying Speeds (Channel Interpolation)" in Section A.6.</p> |
| | method | <p>A vector containing distance values on the track. The distance is measured in [m] relative to the beginning of the track.</p> <p>Alternatively, "dist" can be given as a 3-D tensor with dimensions [Rx-Antenna , Tx-Antenna , Snapshot].</p> <p>In this case, interpolation os done for each antenna element separately.</p> <p>Selects the interpolation algorithm. The default is linear interpolation.</p> <p>Optional are:</p> <ul style="list-style-type: none"> • linear - Linear interpolation (optimized for speed) • spline - Cubic spline interpolation of the channel coefficients and piecewise cubic hermite polynomial interpolation for the delays |
| Output | c | A ' channel ' object containing the interpolated coefficients and delays for each entry in 'dist'. |

c = merge(overlap, optimize, verbose)

| | | |
|-------------|---|---|
| Description | <p>Combines channel segments into a continuous time evolution channel.</p> <p>The channel merger implements the continuous time evolution with smooth transitions between segments. Each segment of a track is split in two parts: an overlapping area with the previous segment and an exclusive part with no overlapping. Each segment is generated independently by the channel builder. However, the distance dependent autocorrelation of the large scale parameters was considered when the parameters were drawn from the corresponding statistics.</p> <p>Transition from segment to segment is carried out by replacing taps of the previous segment by the taps of the current segment, one by one. The modeling of the birth/death process is done as published in the documentation of the WIM2 channel model. The route between adjacent channel segments is split into sub-intervals equal to the minimum number of taps in both overlapping segments. During each sub-interval the power of one old tap ramps down and one new tap ramps up. Power ramps are modeled by a modified sinus function to allow smooth transitions.</p> <p>Taps from the old and new segments are coupled based on their power. If the number of clusters is different in the channel segments, the weakest clusters are ramped up or down without a counterpart from the new/old segment. The merging is only done for the NLOS components since the LOS component has a deterministic behavior. The LOS component is thus just scaled in power.</p> | |
| Input | overlap | The length of the overlapping part relative to the segment length. It can have values in between 0 (no overlap) and 1 (ramp along the entire segment). A value of 0 disables the merging process and the channel segments are simply concatenated. A value of 1 constantly merges the channels. The default setting is 0.5. |
| | optimize | The channel merger tries to automatically optimize the pairing of the taps (i.e. one tap if the old segment ramps down and one of the new ramps up). This is enabled by default, but it is computing intensive. For quicker results, it can be disabled by setting 'optimize' to 0. |
| | verbose | Enables (1, default) or disables (0) the progress bar. |
| Output | c | An array of 'channel' objects containing the merged coefficients and delays. |

chan_out = split_snap(varargin)

| | | |
|-------------|---|--|
| Description | <p>Splits channel objects based on snapshot indices.</p> <p>This function can be used to split a channel object into sub-objects based on a list of snapshots. For example, this can be used to separate channels into LOS and NLOS parts. To split the channels, the following command can be used:</p> <pre>cs = c.split(1:100, 101:2:200);</pre> <p>This splits the channel object "c" into two sub-channels, the first containing the snapshots 1 to 100, and the second containing the snapshots 101 to 199 (at half resolution).</p> <p>Notes:</p> <ul style="list-style-type: none"> Inputs must be scalar channel objects. If there is evaluation data in the <code>par</code> field, it will be split as well. This requires the field <code>par.cluster_ind</code> which determines the small-scale-fading averaging intervals. A running index (in the format "p001", "p002", etc.) is added to the channel name, so that the sub-channels can be identified. | |
| Input | varargin | A list of snapshot indices. The number of inputs determines the number of output channels. |
| Output | chan_out | The split channel objects. |

| chan_out = split_tx(varargin) | |
|---------------------------------|---|
| Description | <p>Splits channel arrays based on transmit antenna indices.</p> <p>This function can be used to split large transmit antenna arrays into smaller arrays. For example, this can be used to calculate the channels for individual sectors at a BS.</p> <p>Example: A channel array has channels from three base stations (BSs). The first and second BS have two sectors, each with two antennas. However, the sector antennas are merged into one array. The third BS has only one sector. To split the channels into five sectors, the following command can be used:</p> <pre>cs = c.split({1:2,3:4}, {1:2,3:4}, {1:2});</pre> <p>Notes:</p> <ul style="list-style-type: none"> The method parses the name-string of the channel objects <code>channel.name</code> in order to determine the Tx-Rx relationship. There are two allowed formats: (a) "tx_rx" and (b) "scenario_tx_rx" The order of the inputs must match the transmitters in alphabetical order, i.e. the first input corresponds to "Tx01", the second to "Tx02" and so on. This is independent of the order in "layout.tx_name", which might have a different order. If only one cell is given as input, but there are several Tx's in the channel array, the same sectorization is applied to each one of them. Outputs are sorted alphabetically according to "tx_rx" (scenario names are ignored) If the input array is shaped as [Rx, Tx], the output will be shaped as [Rx, Tx * Sec] |
| Input | varargin A list of cell-arrays containing the transmit antenna indices. |
| Output | chan_out The split channel objects. |

2.3 Data Flow

The data flow of the QuaDRiGa channel model is depicted in Fig. 5. This figure shows how each of the processing steps, which are described in detail in the following sections, are linked together. The lines show, which parameters are exchanged and how often they are updated. Black lines are for parameters that are either provided by the model users or which are given in the parameter table. Those values are constant. Blue values are updated once per segment and red values are updated once per snapshot.

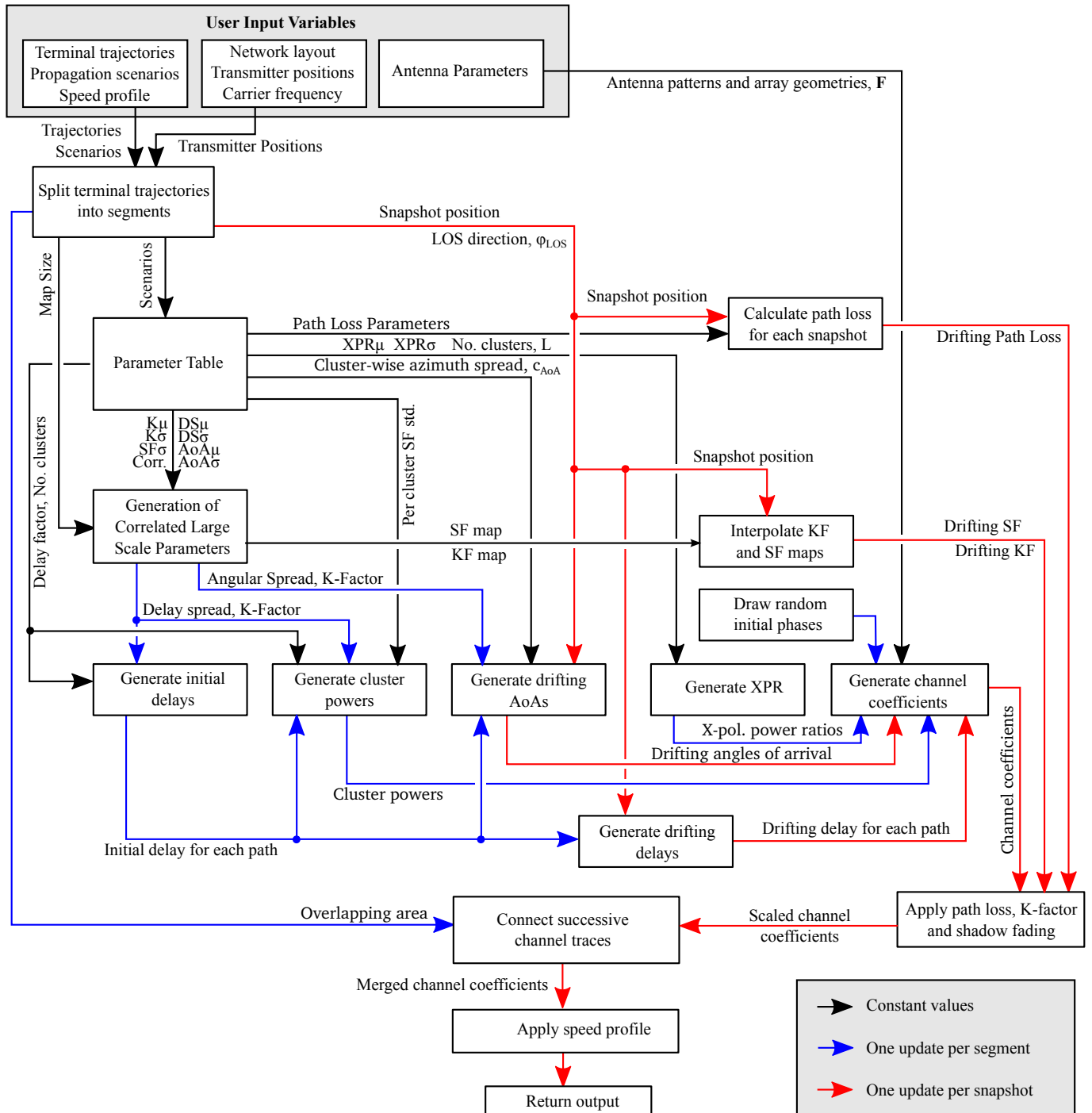


Figure 5: QuaDRiGa Data Flow

2.4 Scenario Specific Parameters

The large-scale parameters (LSPs) are defined by the parameter files which can be found in the folder 'config' of the QuaDRiGa-Core 'source' folder. The parameters are processed as follows:

- The states and segments are identified by a name. Examples are
`S1 = 'MIMOSA_10-45_LOS'`; - parameter set selected for "good state"
`S2 = 'MIMOSA_10-45_NLOS'`; - parameter set selected for "bad state"
- The name selects the related configuration file. For the given example the files
`MIMOSA_10-45_LOS.conf` and
`MIMOSA_10-45_NLOS.conf` are selected

Table 10: Parameter sets provided together with the standard software

| | |
|---------------------------|--|
| LOSonly | One LOS Path only, no Shadow-Fading, no Path-Loss |
| 3GPP_3D_UMa_LOS | 3GPP 3D Urban Macro-Cell (see 3GPP TR 36.873 V12.1.0) |
| 3GPP_3D_UMa_NLOS | For typical terrestrial base stations deployed above rooftop in densely populated urban areas. The max. cell radius is about 1 km. |
| 3GPP_3D_UMi_LOS | 3GPP 3D Urban Micro-Cell (see 3GPP TR 36.873 V12.1.0) |
| 3GPP_3D_UMi_NLOS | For typical terrestrial pico-base stations deployed below rooftop in densely populated urban areas. The max. cell radius is about 200 m. |
| WINNER_UMa_C2_LOS | WINNER Urban Macrocell |
| WINNER_UMa_C2_NLOS | For typical terrestrial base stations deployed above rooftop in densely populated urban areas. The max. cell radius is about 1 km. |
| WINNER_UMi_B1_LOS | WINNER Urban Microcell |
| WINNER_UMi_B1_NLOS | For typical terrestrial pico-base stations deployed below rooftop in densely populated urban areas. The max. cell radius is about 200 m. |
| WINNER_SMa_C1_LOS | WINNER Sub-Urban Macrocell |
| WINNER_SMa_C1_NLOS | For typical terrestrial base stations deployed above rooftop in sub-urban areas. The max. cell radius is about 10 km. |
| WINNER_Indoor_A1_LOS | WINNER Indoor Hotspot |
| WINNER_Indoor_A1_NLOS | For typical indoor deployments such as WiFi or femto-cells. |
| WINNER_UMa2Indoor_C4_LOS | WINNER Urban Macrocell to Indoor |
| WINNER_UMa2Indoor_C4_NLOS | For users within buildings that are connected to a terrestrial base station deployed above rooftop in densely populated urban areas. |
| WINNER_UMi2Indoor_B4_LOS | WINNER Urban Microcell to Indoor |
| WINNER_UMi2Indoor_B4_NLOS | For users within buildings that are connected to terrestrial pico-base stations deployed below rooftop in densely populated urban areas. |
| BERLIN_UMa_LOS | Terrestrial Urban Macrocell parameters extracted from measurements in Berlin, Germany. |
| BERLIN_UMa_NLOS | |
| MIMOSA_10-45_LOS | MIMOSA Satellite to Mobile Parameters for Urban Propagation Elevation range from 10 to 45°. Parameters were extracted from terrestrial measurement using a high-altitude platform. |
| MIMOSA_10-45_NLOS | |
| MIMOSA_16-25_LOS | MIMOSA Satellite to Mobile Parameters for Urban Propagation Elevation range from 16 to 25°. Parameters were extracted from terrestrial measurement using a high-altitude platform. |
| MIMOSA_16-25_NLOS | |
| MIMOSA_25-35_LOS | MIMOSA Satellite to Mobile Parameters for Urban Propagation Elevation range from 25 to 35°. Parameters were extracted from terrestrial measurement using a high-altitude platform. |
| MIMOSA_25-35_NLOS | |
| MIMOSA_35-45_LOS | MIMOSA Satellite to Mobile Parameters for Urban Propagation Elevation range from 35 to 45°. Parameters were extracted from terrestrial measurement using a high-altitude platform. |
| MIMOSA_35-45_NLOS | |

2.4.1 Description of the Parameter Table

The QuaDRiGa channel model is a generic model. That means, that it uses the same method for generating channel coefficients in different environments. E.g. the principal approach is exactly the same in a cellular

network and in a satellite network. The only difference is the parametrization for both cases. Each environment is described by 55 individual parameters. These parameters are stored in configuration files that can be found in the subfolder named “config” in the main channel model folder. The parameters and values can be described as follows:

- **No. Clusters**

This value describes the number of clusters. Each cluster is the source of a reflected or scattered wave arriving at the receiver. Typically there are less clusters in a LOS scenario than in a NLOS scenario. Note that the number of clusters directly influences the time needed to calculate the coefficients.

- **Path Loss (PL)**

A common path loss (PL) model for cellular systems is the log-distance model

$$\text{PL}_{[\text{dB}]} = A \cdot \log_{10} d + B \quad (1)$$

where A and B are scenario-specific coefficients. The path-loss exponent A typically varies between 20 and 40, depending on the propagation conditions, the base station height and other influences. They are typically determined by measurements. d is the distance (in units of meters) between the transmitter and the receiver. In other environments such as in satellite systems, the PL does not depend on the distance but has a constant value. In this case, A would be 0.

- **Shadow Fading (SF)**

Shadow fading occurs when an obstacle gets positioned between the wireless device and the signal transmitter. This interference causes significant reduction in signal strength because the wave is shadowed or blocked by the obstacle. It is modeled as log-normal distributed with two parameters: The standard deviation σ defines the width of the distribution, i.e. the power value (in dB) above or below the distance dependent PL and the decorrelation distance λ . This parameter defines how fast the SF varies when the terminal moves through the environment. E.g. a value of 87 means that when the terminal moves 87 m in any given direction, then the correlation of the value at this distance with the value at the initial position is $e^{-1} = 0.37$.

- **Delay Spread (DS)**

The root-mean-square (RMS) delay spread is probably the most important single measure for the delay time extent of a multipath radio channel. The RMS delay spread is the square root of the second central moment of the power delay profile and is defined to be

$$\sigma_\tau = \sqrt{\frac{1}{P_i} \cdot \sum_{l=1}^L P_l \cdot (\tau_l)^2 - \left(\frac{1}{P_i} \cdot \sum_{l=1}^L P_l \cdot \tau_l \right)^2} \quad (2)$$

with P_i is the total received power, P_l the cluster-power and τ_l the cluster delay.

In order to generate the coefficients, QuaDRiGa has to generate delays for each of the multipath clusters. I.e. the total lengths of scattered paths have to be defined. This generation of delays is governed by value of the DS in a specific environment. The DS is assumed to be log-normal distributed and defined by two parameters: Its median value μ and its STD σ . Thus, a value of DS_μ of -6.69 corresponds to 204 ns. σ then defines the range of possible values. E.g. $\text{DS}_\sigma = 0.3$ leads to typical values in the range of $10^{-6.69-0.3} = 102$ ns to $10^{-6.69+0.3} = 407$ ns. As for the shadow fading, the decorrelation distance DS_λ defines how fast the DS varies when the terminal moves through the environment.

The delay spread σ_τ is calculated from both, the delays τ_l and the path powers P_l . I.e. larger delay spreads σ_τ can either be achieved by increasing the values of τ_l and keeping P_l fixed or adjusting P_l and keeping τ_l fixed. In order to avoid this ambiguity, an additional proportionality factor (delay factor) r_τ is introduced to scale the width of the distribution of τ_l . r_τ is calculated from measurement data. See Sec. 3.2 for more details.

- **Ricean K-Factor (KF)**

Rician fading occurs when one of the paths, typically a line of sight signal, is much stronger than the others. The KF K is the ratio between the power in the direct path and the power in the other, scattered, paths. As for the DS, the KF is assumed to be log-normal distributed. The distribution is defined by its median value KF_μ and its STD KF_σ . The decorrelation distance KF_λ defines how fast the KF varies when the terminal moves through the environment.

- **Angular Spread**

The angular spread defines the distribution of the departure- and arrival angles of each multipath component in 3D space seen by the transmitter and receiver, respectively. Each path gets assigned an azimuth angle in the horizontal plane and an elevation angle in the vertical plane. Thus we have four values for the angular spread:

1. Azimuth spread of Departure (AsD)
2. Azimuth spread of Arrival (AsA)
3. Elevation spread of Departure (EsD)
4. Elevation spread of Arrival (EsA)

Each one of them is assumed to be log-normal distributed. Hence, we need the parameters μ , σ and λ to define the distributions. These spreads are translated into specific angles for each multipath cluster. Additionally, we assume that clusters are the source of several multipath components that are not resolvable in the delay domain. Thus, these sub-paths do not have specific delays, but they have different departure- and arrival angles. Thus, we need an additional parameter c_ϕ for each of the four angles that scales the dimensions of the clusters in 3D-space. See Sec. 3.3 for details.

- **Cross-polarization Ratio (XPR)**

The XPR defines how the polarization changes for a multipath component. I.e. the initial polarization of a path is defined by the transmit antenna. However, for the NLOS components, the transmitted signal undergoes some diffraction, reflection or scattering before reaching the receiver.

The XPR (in dB) is assumed to be normal distributed where μ and σ define the distribution. We translate the XPR in a polarization rotation angle which turns the polarization direction. A XPR value where a value of +Inf means that the axis remains the same for all NLOS paths. I.e. vertically polarized waves remain vertically polarized after scattering. On the other hand, a value of -Inf dB means that the polarization is turned by 90°. In case of 0 dB, the axis is turned by 45°, i.e. the power of a vertically polarized wave is split equally into a H- and V component.

The following table gives an overview of the parameters in the config files. They get converted into a structure '`parameter_set.scenpar`'.

| Parameter | Unit or type | Description |
|---|-------------------|--|
| plpar.model (PL_model) | Text string | Selects the model for average path loss. For satellite applications the pathloss is defined by the satellite distance and is assumed to be constant for the reception area. For terrestrial cases pathloss models like "Hata" or others (e.g. WINNER pathloss models) can be selected. |
| plpar.A (PL_A) | dB | For satellite applications this parameter defines the average path loss and is equivalent to the "mu" of the lognormal distribution of the shadow fading. |
| Parameters in structure '<code>parameter_set.scenpar</code>' | | |
| Large-Scale Parameters | | Those parameters describe how the large-scale parameters vary within a propagation environment. |
| SF_sigma SF_lambda | dB meter | Those parameters describe the slow fading implemented as Lognormal distribution and filtered (see "map" generation) according to the de-correlation distance "lambda". |
| KF_mu KF_sigma KF_lambda | dB dB meter | Statistical properties of the K-factor |

| | | |
|--|---------------------------------------|---|
| xpr_mu xpr_sigma | dB dB | The XPR is defined by the XPR-Antenna (see antenna pattern) and the XPR “environment”. The parameters describe the statistical properties of the XPR “environment”. For the XPR, no correlation map is calculated and the XPR is updated once per segment. Note: For the LOS component no XPR environment is assumed, only the XPR antenna is applied. Hence the overall XPR depends also highly on the K-factor. |
| DS_mu DS_sigma DS_lambda | log10([s]) log10([s]) meter | Statistical properties of the delay spread. |
| AS_A_mu AS_A_sigma AS_A_lambda | log10([deg]) log10([deg]) meter | Statistical properties of the azimuth of arrival spread at the receiver. |
| ES_A_mu ES_A_sigma ES_A_lambda | log10([deg]) log10([deg]) meter | Statistical properties of the elevation of arrival spread at the receiver. |
| AS_D_mu AS_D_sigma AS_D_lambda | log10([deg]) log10([deg]) meter | Statistical properties of the azimuth of departure spread at the transmitter. |
| ES_D_mu ES_D_sigma ES_D_lambda | log10([deg]) log10([deg]) meter | Statistical properties of the elevation of departure spread at the transmitter. |
| Cross correlations | | There are interdependencies between parameters. For example, if the K-Factor is high, the delay spread gets shorter since more power is coming from the direct component. This is expressed by the cross-correlations parameters. They can vary between -1 and 1. Negative values denote inverse correlation, e.g. a high K-Factor implies a low delay spread. Positive Value implies a positive correlation such as a high K-Factor also implies a high shadow fading. Cross-Correlations are used during the map-generation. |
| ds_kf asA.ds esA.ds ds_sf asA.kf esA.kf sf_kf esA.asA asA_sf esA_sf | | Correlation of delay spread and K-Factor. Correlation of delay spread and azimuth of arrival angle spread. Correlation of delay spread and elevation of arrival angle spread. Correlation of delay spread and shadow fading. Correlation of K-Factor and azimuth of arrival angle spread. Correlation of K-Factor and elevation of arrival angle spread. Correlation of K-Factor and shadow fading. Correlation elevation of arrival angle spread and azimuth of arrival angle spread. Correlation of shadow fading and azimuth of arrival angle spread. Correlation of shadow fading and elevation of arrival angle spread. |
| Cluster Parameter | | Those parameters influence the generation of the scattering-clusters and the distribution of the sub-paths within each cluster. |
| NumClusters | Integer | The number of clusters generated. For multipath rich environments typically more clusters are used. If the LOS component is dominant a lower number of clusters is sufficient. |
| PerCluster AS_A | deg | The azimuth angular spread of the 20 sub-paths within one cluster. |
| PerCluster ES_A | deg | The elevation angular spread of the 20 sub-paths within one cluster. |
| LOS_scatter_radius | meter | This parameter allows an additional spread of the 20 sub-paths of the LOS component by emulating scattering in the near-field of the antennas. [EXPERIMENTAL] |
| LNS_ksi | | Normally, cluster powers are taken from an exponential power-delay-profile. This parameter enables an additional variation of the individual cluster powers around the PDP. |
| r_DS | | This parameter allows the mapping of delay-spreads to delays and powers for the clusters. See section 3.2. |

2.4.2 Adding New Scenarios

The scenario parameters are set in "parameter_set.scenpar". Here, you also have the option to change individual parameters by assigning new values. The scenario "UMal", for example, uses by default 8 clusters. When the simulations should be done with 15 clusters, one can change the settings by

```
1 p = parameter_set('BERLIN_UMa_LOS');           % New parameter set
2 p.scenpar.NumClusters = 15;                    % Set new number of clusters
```

A list of currently supported scenarios is generated by:

```
1 parameter_set.supported_scenarios
```

The default settings of those scenarios are stored in config files which are located in the "config"-folder of the QuaDRiGa source path. The "UMal" config file for example looks like this:

```
1 % Config File for scenario "UMal"
2 % WINNER+ Urban Macro LOS
3 % See: CELTIC / CP5-026 D5.3: WINNER+ Final Channel Models
4 % and: IST-4-027756 WINNER II D1.1.2 v.1.1: WINNER II Channel Models
5 %
6 % Stephan Jaeckel
7 % Fraunhofer Heinrich Hertz Institute
8 % Wireless Communication and Networks
9 % Einsteinufer 37, 10587 Berlin, Germany
10 % e-mail: stephan.jaeckel@hhi.fraunhofer.de
11
12 NumClusters = 8
13 r_DS = 2.5
14
15 SF_sigma = 5
16 SF_lambda = 45
17 LNS_ksi = 3
18
19 KF_mu = 7
20 KF_sigma = 3
21 KF_lambda = 12
22
23 DS_mu = -7.39
24 DS_sigma = 0.63
25 DS_lambda = 40
26
27 AS_D_mu = 1
28 AS_D_sigma = 0.25
29 AS_D_lambda = 15
30 PerClusterAS_D = 6
31
32 AS_A_mu = 1.7
33 AS_A_sigma = 0.19
34 AS_A_lambda = 15
35 PerClusterAS_A = 12
36
37 ES_D_mu = 0.7
38 ES_D_sigma = 0.2
39 ES_D_lambda = 15 % D5.3 pp. 73
40 PerClusterES_D = 3
41
42 ES_A_mu = 0.95
43 ES_A_sigma = 0.16
44 ES_A_lambda = 15 % D5.3 pp. 73
45 PerClusterES_A = 7
46
47 xpr_mu = 8
48 xpr_sigma = 4
49
50 % Adjustments have been made to keep xcorr-matrix positive definite
51 asD_ds = 0.4
52 asA_ds = 0.7 % 0.8
53 asA_sf = -0.5
54 asD_sf = -0.4 % 0.5
```

```

55 ds_sf    = -0.4
56 asD_asA = 0.3
57 asD_kf   = 0.1
58 asA_kf   = -0.2
59 ds_kf    = -0.4
60 sf_kf    = 0.3
61 esD_ds   = -0.4 % -0.5
62 esD_asD = 0.4 % 0.5
63 esA_sf   = -0.8
64 esA_asA = 0.4
65
66 % A * log10 d + B + C * log10 f + D * log10 hBS + E * log10 hMS
67 % Two different values (first before breakpoint, last after breakpoint)
68 % Different SF coefficients
69
70 PL_model = winner_los
71
72 PL_A1    = 26
73 PL_B1    = 25
74 PL_C1    = 20
75 PL_D1    = 0
76 PL_E1    = 0
77 PL_sig1  = 4
78
79 PL_A2    = 40
80 PL_B2    = 9.27
81 PL_C2    = 6
82 PL_D2    = -14
83 PL_E2    = -14
84 PL_sig2  = 6

```

You can create your own scenario by editing this file and saving it under a new filename in the "config"-Folder. The file ending must be ".conf". The filename then is also the scenario name and the settings can be accessed from inside MATLAB as described above.

3 Technical Documentation

This chapter describes an extension of the **WINNER** model [4] where time evolution based on the ideas presented in [9] and [10] is incorporated. A reference implementation in MATLAB is available as open source [11]. The modeling approach consists of two steps: A stochastic part generates LSPs and calculates random three-dimensional (3-D) positions of scattering clusters. It is assumed that the base station (BS) is fixed and the mobile terminal (MT) is moving. In this case, scattering clusters are fixed as well and the time evolution of the radio channel is deterministic. Different positions of the MT lead to different arrival angles, delays, and phases for each multipath component (MPC). Longer sequences are generated by transitions between channel traces from consecutive initializations of the model. This allows the MTs to traverse different scenarios, e.g., move from indoors to outdoors.

Figure 6 gives an overview of the modeling steps. The user needs to configure the network layout (i.e., the positions of the BSs, antenna configurations, downtilts), the positions and trajectories of the MTs, and the propagation scenarios. The channel coefficients are then calculated in seven steps, which are described in detail in Sections 3.1 to 3.8. Major extensions concerning 3-D propagation are made in steps C and D. Time evolution is incorporated in steps D and G, and a new 3-D model of the polarization [12] is introduced in step E. In order to integrate these extensions, some changes are made in the other parts of the model as well.

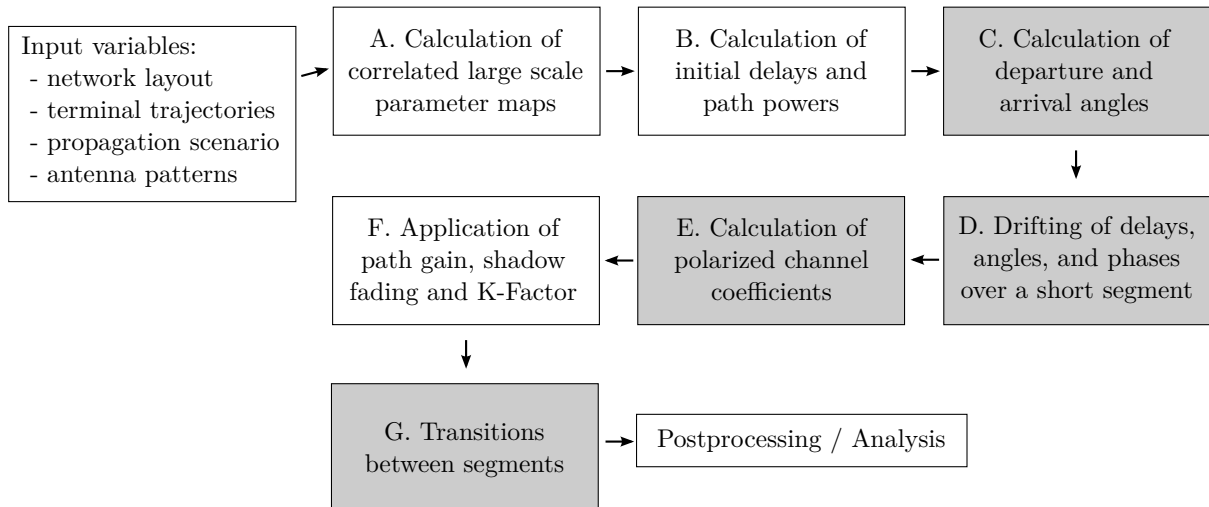


Figure 6: Steps for the calculation of time-evolving channel coefficients. Compared to the WINNER model, changes were made in the gray shaded boxes.

Time evolution requires a more detailed description of the mobility of the terminals. This is done by assigning tracks, i.e., ordered lists of positions, to each MT. In reality, this may include accelerations, decelerations, and MTs with different speeds, e.g., pedestrian and vehicular users. However, to minimize the computational overhead and memory requirements, channel coefficients are calculated at a constant sample rate that fulfills the sampling theorem

$$f_T \geq 2 \cdot B_D = 4 \cdot \max |\Delta f_D| = 4 \cdot \frac{\max |v|}{\lambda_c}, \quad (3)$$

where B_D is the width of the Doppler spectrum, Δf_D is the maximum frequency change due to the velocity v , and λ_c is the carrier wavelength. Thus, the appropriate sampling rate is proportional to the maximum speed of the MT. Since it is sometimes useful to examine algorithms at different speeds, it is unfortunate to fix the sampling rate in advance as the speed is then fixed as well. To overcome this problem, channel coefficients are now calculated at fixed positions with a sampling rate f_S measured in samples per meter. In its normalized form, it is known as sample density (SD). A time-series for arbitrary or varying speeds is

then obtained by interpolating the coefficients in a postprocessing step.

$$f_S = \frac{f_T}{\max |v|} \geq \frac{4}{\lambda_c} \quad (4)$$

$$\text{SD} = \frac{f_S}{\lambda_c/2} \geq 2 \quad (5)$$

Longer time-evolving channel sequences need to consider the birth and death of scattering clusters as well as transitions between different propagation environments. This is addressed by splitting the MT trajectory into *segments*. A segment can be seen as an interval in which the LSPs do not change considerably and where the channel keeps its wide sense stationary (WSS) properties. Thus, the length of a segment depends on the decorrelation distances of the LSPs. Hence, it might be beneficial to limit the segment length to the average decorrelation distance. In the WINNER urban macro-cell (UMa) scenario, this would be 22 m for LOS and 48 m for NLOS propagation. Channel traces are then generated independently for each segment. In Section 3.8 on Page 80, those individual traces are combined into a longer sequence that includes the birth and death of scattering clusters.

3.1 Correlated Large-Scale Parameter Maps

The positions of the scattering clusters are based on seven LSPs:

1. RMS delay spread (DS)
2. Ricean K-factor (KF)
3. Shadow fading (SF)
4. Azimuth spread of departure (ASD)
5. Azimuth spread of arrival (ASA)
6. Elevation spread of departure (ESD)
7. Elevation spread of arrival (ESA)

Their distribution properties are directly obtained from measurement data (e.g., [4–7, 13]). If some MTs or segments are close to each other, their LSPs will be correlated and they will experience similar propagation conditions. This is modeled by means of two-dimensional (2-D) maps, as illustrated in Figure 7. Our method for generating these maps is adopted from [14]. The maps are initialized with values obtained from an independent and identically distributed (i.i.d.) zero-mean Gaussian random process with desired variance. The pixels are then subsequently filtered to obtain the desired autocorrelation function, i.e., a decaying exponential function with a specific decorrelation distance. In contrast to [14], the maps are filtered also in the diagonal direction to get a smooth evolution of the values along the MT trajectory. Advanced methods going beyond this approach for generating such maps are discussed in [15]. Once the maps are generated, initial LSPs for each segment are obtained by interpolating the maps to match the exact position of the MT.

The granularity of each LSP can be described on three levels: the propagation scenario level, the link level and the path level:

- **Propagation scenario level:**

The magnitude, variance and the correlation of a LSP in a specific scenario, e.g., urban macro-cell, indoor hotspot, or urban satellite, are calculated from measurement data. Normally, LSPs are assumed to be log-normal distributed. For example, the median log-normal delay spread DS_μ in an urban cellular scenario is -6.89 which corresponds to a DS of $\sigma_\tau = 128$ ns. With a standard deviation of $DS_\sigma = 0.5$, typical values may lie in between 40 and 407 ns. The same principle applies for the other six LSPs. The decorrelation distance (e.g. $DS_\lambda = 40$ m) describes the distance-dependent correlation of the LSP. If e.g. two mobile terminals in the above example are 40 m apart of each other, their DS is correlated with a correlation coefficient of $e^{-1} = 0.37$. Additionally, all LSPs are cross correlated. A

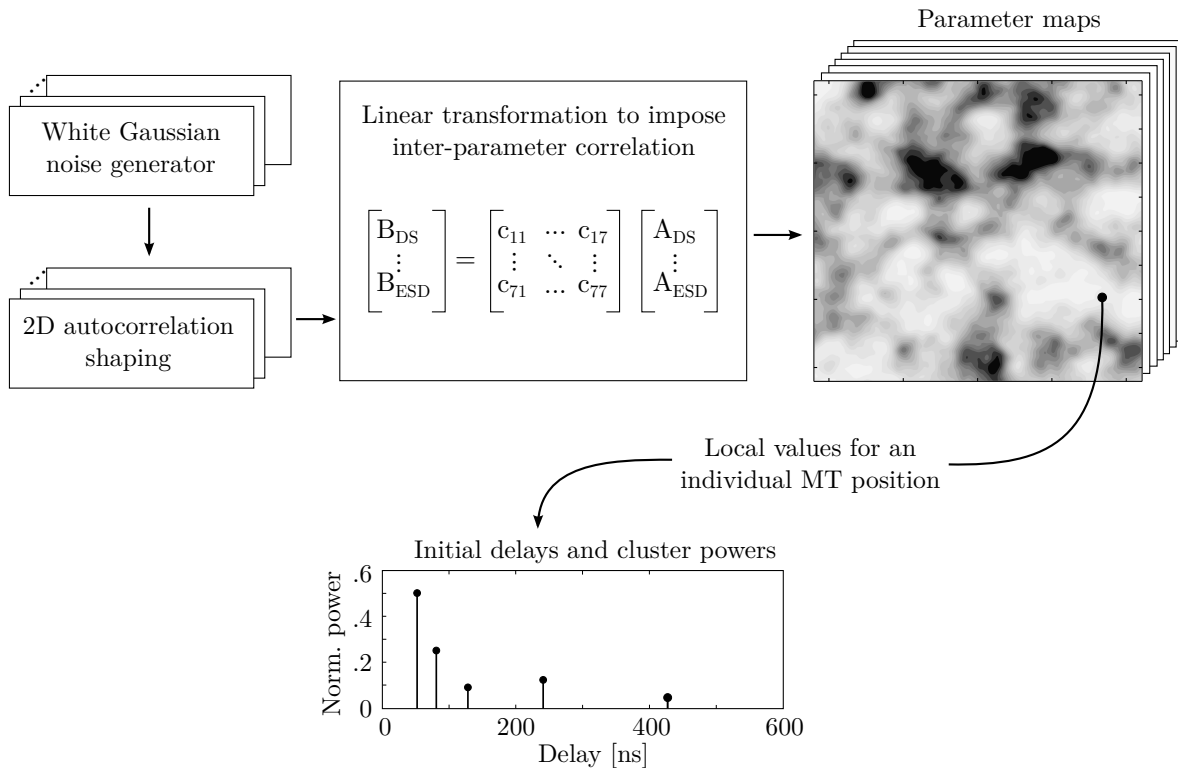


Figure 7: Principle of the generation of channel coefficients based on correlated LSPs

typical example is the dependance of the **angular spread (AS)**, e.g., the azimuth spread of arrival on the **KF**. With a large **KF** (e.g. 10 dB), a significant amount of energy comes from a single direction. Thus, the **AS** gets smaller which leads to a negative correlation between the **DS** and the **KF**.

- **Link level:**

A user terminal at a specific position (black dot on the map in Figure 7) is assigned to a propagation scenario. Depending on the position and the scenario, it experiences a radio channel which is determined by the specific values of the seven **LSPs**. Due to the autocorrelation properties, small distances between users in the same scenario also lead to high correlations in the channel statistics, e.g., a second terminal right next to the current user will experience a similar **DS**. The second granularity level thus contains the specific values of the **LSPs** for each user position. Generating those values can be seen as going backwards from the scenario-wide distribution μ, σ of a **LSP** to individual “measurement”-values for each **MT**.

- **Path Level:**

Last, the individual components of the **CIR** are calculated. This procedure takes the values of the **LSPs** into account and calculates the power and the delay of the channel coefficients. The detailed procedure for this is described in the following sections.

The correlation maps are generated at a fixed sampling grid by successively filtering a random, normal distributed sequence of numbers with a **fir** filter. The principle is depicted in Figure 8. The map is represented by a matrix **B** and one pixel of that matrix is $B_{y,x}$ where y is the row index and x is the column index. The first pixel $B_{1,1}$ is in the top left (or north-west) corner of the map. The **FIR** filter coefficients are calculated from the decorrelation distance d_λ (in units of meters). The distance dependent correlation coefficient follows an exponential function

$$\rho(d) = \exp\left(-\frac{d}{d_\lambda}\right) \quad (6)$$

with d as the distance between two positions [16]. We now calculate two sets of filter coefficients, one for the horizontal and vertical directions, and one for the diagonal elements. This is done by taking (6) and substituting the distance d by the relative distance d_{px} of two pixels.

$$a_k = \frac{1}{\sqrt{d_\lambda}} \cdot \exp\left(-\frac{k \cdot d_{\text{px}}}{d_\lambda}\right) \quad (7)$$

$$b_k = \frac{1}{\sqrt{d_\lambda}} \cdot \exp\left(-\frac{k \cdot \sqrt{2} \cdot d_{\text{px}}}{d_\lambda}\right) \quad (8)$$

k is the running filter coefficient index. The exponential decay function is cutted at a maximum distance of $4 \cdot d_\lambda$ and normalized with $\sqrt{d_\lambda}$. The map size is therefore determined by the distribution of the users in the scenario plus the length of the filter function. This is also illustrated in Figure 8 where the user terminals are placed inside the black square. The extension space is needed to avoid filter artifacts at the edges of the map. The map is initialized with random, normal distributed numbers. Then, the filter (7) is applied in vertical direction (running from top to bottom) and in horizontal direction (from left to right).

$$B_{y,x}^{[1]} = X \quad \text{with} \quad X \sim N(0, 1) \quad (9)$$

$$B_{y,x}^{[2]} = \sum_{k=0}^{\lfloor 4 \cdot d_\lambda / d_{\text{px}} \rfloor} a_k \cdot B_{y-k,x} \quad (10)$$

$$B_{y,x}^{[3]} = \sum_{k=0}^{\lfloor 4 \cdot d_\lambda / d_{\text{px}} \rfloor} a_k \cdot B_{y,x-k} \quad (11)$$

Next, the second filter (8) is applied on the diagonals of the map - at first from the top left to the bottom right, and then from the bottom left to the top right.

$$B_{y,x}^{[4]} = \sum_{k=0}^{\lfloor 4 \cdot d_\lambda / d_{\text{px}} \rfloor} b_k \cdot B_{y-k,x-k} \quad (12)$$

$$B_{y,x}^{[5]} = \sum_{k=0}^{\lfloor 4 \cdot d_\lambda / d_{\text{px}} \rfloor} b_k \cdot B_{y+k,x-k} \quad (13)$$

After the 2-D autocorrelation shaping is done, the extension space is removed and values of the remaining map are scaled to have the desired distribution μ, σ . The same procedure is repeated for all seven LSPs. However, the decorrelation distance d_λ as well as μ, σ for each LSP can be different.

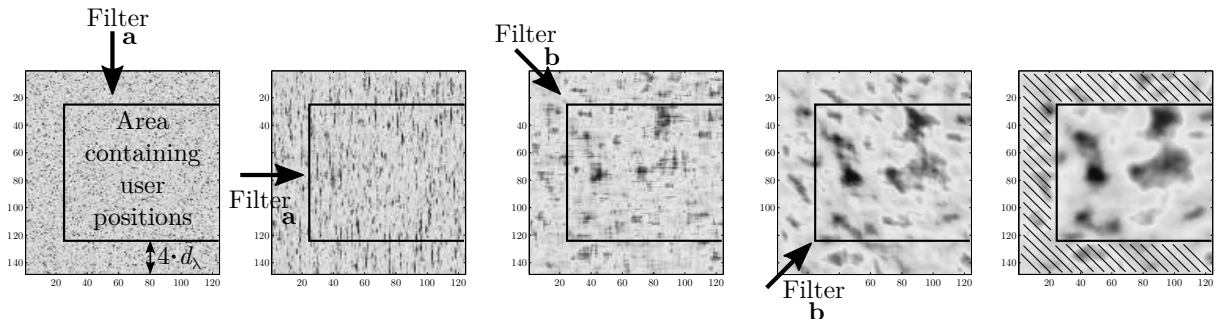


Figure 8: Map-based 2-D autocorrelation shaping using FIR filters

In order to account for the inter-LSP correlation, a matrix \mathbf{X} is assembled containing all cross-correlation values ρ between each two LSPs.

$$\mathbf{X} = \begin{pmatrix} 1 & \rho_{DS,KF} & \rho_{DS,SF} & \rho_{DS,ASD} & \rho_{DS,ASA} & \rho_{DS,ESD} & \rho_{DS,ESA} \\ \rho_{KF,DS} & 1 & \rho_{KF,SF} & \rho_{KF,ASD} & \rho_{KF,ASA} & \rho_{KF,ESD} & \rho_{KF,ESA} \\ \rho_{SF,DS} & \rho_{SF,KF} & 1 & \rho_{SF,ASD} & \rho_{SF,ASA} & \rho_{SF,ESD} & \rho_{SF,ESA} \\ \rho_{ASD,DS} & \rho_{ASD,KF} & \rho_{ASD,SF} & 1 & \rho_{ASD,ASA} & \rho_{ASD,ESD} & \rho_{ASD,ESA} \\ \rho_{ASA,DS} & \rho_{ASA,KF} & \rho_{ASA,SF} & \rho_{ASA,ASD} & 1 & \rho_{ASA,ESD} & \rho_{ASA,ESA} \\ \rho_{ESD,DS} & \rho_{ESD,KF} & \rho_{ESD,SF} & \rho_{ESD,ASD} & \rho_{ESD,ASA} & 1 & \rho_{ESD,ESA} \\ \rho_{ESA,DS} & \rho_{ESA,KF} & \rho_{ESA,SF} & \rho_{ESA,ASD} & \rho_{ESA,ASA} & \rho_{ESA,ESD} & 1 \end{pmatrix} \quad (14)$$

The matrix-square-root $\mathbf{X}^{1/2}$ of this matrix is multiplied with the values of the seven LSP maps $\mathbf{B}_{DS} \dots \mathbf{B}_{ESD}$. In order to calculate the matrix-square-root, \mathbf{X} must be positive definite to get a unique, real numbered solution.

$$\begin{pmatrix} B_{y,x,DS} \\ \vdots \\ B_{y,x,Esd} \end{pmatrix} = \mathbf{X}^{1/2} \begin{pmatrix} B_{y,x,DS}^{[5]} \\ \vdots \\ B_{y,x,Esd}^{[5]} \end{pmatrix} \quad (15)$$

Last, the MTs are placed on the maps and the corresponding values for the LSPs are obtained by interpolating the surrounding pixels of the map. In this way, initial LSPs for the following parts of the channel model are generated.

3.2 Initial Delays and Path Powers

Initial delays are drawn randomly from a scenario-dependent delay distribution as

$$\tau_l^{[1]} = -r_\tau \sigma_\tau \ln(X_l), \quad (16)$$

where $X_l \sim \mathcal{U}(0, 1)$ is an uniformly distributed random variable having values between 0 and 1, σ_τ is the initial DS from the map and r_τ is a proportionality factor (see [4]). The term r_τ was introduced in [17] because σ_τ is influenced by both the delays τ_l and the powers P_l ; r_τ is usually calculated from measurement data. Next, the delays are normalized such that the first delay is zero and then they are sorted:

$$\tau_l^{[2]} = \text{sort} \left\{ \tau_l^{[1]} - \min(\tau_l^{[1]}) \right\}. \quad (17)$$

The NLOS path powers are drawn from a single slope exponential power delay profile (PDP) depending on the DS σ_τ and a random component $Z_l \sim \mathcal{N}(0, \zeta^2)$ [4]. The term ζ is a scenario-dependent coefficient emulating an additional shadowing process. It is obtained from measurements.

$$P_l^{[1]} = \exp \left(-\tau_l \frac{r_\tau - 1}{r_\tau \cdot \sigma_\tau} \right) \cdot 10^{-\frac{Z_l}{10}} \quad (18)$$

The power of the first path is further scaled according to the initial KF from the map and path powers are normalized so that their sum power is one:

$$P_1^{[2]} = K \sum_{l=2}^L P_l^{[1]} \quad (19)$$

$$P_{2\dots l}^{[2]} = P_{2\dots l}^{[1]} \quad (20)$$

$$P_l = P_l^{[2]} / \sum_{l=1}^L P_l^{[2]}. \quad (21)$$

The scaling of the powers with the **KF** changes the **DS**. Hence, in the last step, this is corrected by calculating the actual delay spread using the scaled powers and normalizing the delays in order to obtain the desired RMS delay spread in the **PDP**. The **DS** after applying (21) is calculated to

$$\sigma_{\tau}^{[\text{actual}]} = \sqrt{\sum_{l=1}^L P_l \cdot \tau_l^2 - \left(\sum_{l=1}^L P_l \cdot \tau_l \right)^2} \quad (22)$$

With σ_{τ} being the initial **DS** from the map, path delays note

$$\tau_l = \frac{\sigma_{\tau}}{\sigma_{\tau}^{[\text{actual}]}} \cdot \tau_l^{[2]} \quad (23)$$

3.3 Departure and Arrival Angles

Four angles are calculated for each propagation path. The 2-D WINNER model [4] introduced the azimuth angle of departure (**AoD**), ϕ^d , and the azimuth angle of arrival (**AoA**), ϕ^a . In 3-D coordinates, we also need the elevation angle of departure (**EoD**), θ^d , and the elevation angle of arrival (**EoA**), θ^a . The angles share similar calculation methods but have different **ASs** σ_{ϕ^a} , σ_{ϕ^d} , σ_{θ^a} , and σ_{θ^d} . The individual angles are generated by first drawing random angles which are assigned to the already known path powers. In order to obtain the correct **ASs**, a scaling operations is used that readjusts the angles. This approach is different from the **WINNER** model, where the angels are mapped to the already known powers using a wrapped Gaussian distribution [4, 18]. A summary of the **WINNER** method together with a description of how it can be used in the new model is given in Appendix B.

Azimuth angles Here, the calculation method for the azimuth angles is described. The same calculation method is used for the **AoD** and the **AoA**. Hence, ϕ is used instead of ϕ^d or ϕ^a . Likewise, the corresponding **AS** is denoted as σ_{ϕ} .

At first, a random list of angles is created for the **NLOS** paths only, following a Gaussian normal distribution with zero-mean and a variance corresponding to the given **AS** from the **LSP** maps. The **LOS** angle is defined to be 0.

$$\phi_1^{[1]} = 0 \quad \text{and} \quad \phi_{2 \dots L}^{[1]} \sim \mathcal{N}(0, \sigma_{\phi}^2) \quad (24)$$

The so obtained angels need to be mapped to the interval $[-\pi; \pi]$. This is done by a modulo operation which wraps the angles around the unit circle.

$$\phi_l^{[2]} = (\phi_l^{[1]} + \pi \bmod 2\pi) - \pi. \quad (25)$$

The relationship between path powers and angles is random. Hence, the resulting **AS** is undefined. In the next step, the actual **AS** is calculated. This requires to calculate the power-weighted mean angle $\bar{\phi}$. This angle is subtracted from the angles $\phi_l^{[2]}$ and the wrapping around the unit circle is applied a second time. The **AS** then follows from:

$$\bar{\phi} = \arg \left(\sum_{l=1}^L P_l \cdot \exp(j\phi_l^{[2]}) \right) \quad (26)$$

$$\phi_l^{[*]} = (\phi_l^{[2]} - \bar{\phi} + \pi \bmod 2\pi) - \pi \quad (27)$$

$$\sigma_{\phi}^{[\text{actual}]} = \sqrt{\sum_{l=1}^L P_l \cdot (\phi_l^{[*]})^2 - \left(\sum_{l=1}^L P_l \cdot \phi_l^{[*]} \right)^2} \quad (28)$$

Now, with σ_ϕ being the initial AS from the map, the angles $\phi_l^{[2]}$ are updated:

$$\phi_l^{[3]} = \frac{\sigma_\phi}{\sigma_\phi^{[\text{actual}]}} \cdot \phi_l^{[2]} \quad (29)$$

If σ_ϕ is larger than $\sigma_\phi^{[\text{actual}]}$, then (25) needs to be applied again in order for account for the periodicity of the angles. However, in this case, some of the angles could be mapped to values around 0° . This could lower the AS instead of increasing it as intended by the scaling operation. A solution is to create new angles with a bias to the negative side of the circle.

$$\phi_l^{[4]} = \begin{cases} \phi_l^{[3]}, & \text{if } |\phi_l^{[3]}| < \pi; \\ \mathcal{N}(\pi, \frac{\pi^2}{4}), & \text{otherwise.} \end{cases} \quad (30)$$

$$\phi_l^{[5]} = (\phi_l^{[4]} + \pi \bmod 2\pi) - \pi \quad (31)$$

This, however, changes the AS and the calculations (26) to (31) need to be repeated iteratively until the actual AS $\sigma_\phi^{[\text{actual}]}$ converges either to the given value σ_ϕ or a maximum value. Finally, the LOS direction is applied.

$$\phi_l = \phi_l^{[5]} + \phi^{LOS} \quad (32)$$

Elevation angles Since the elevation angles can only have values in between $-\frac{\pi}{2}$ and $\frac{\pi}{2}$, the calculation method differers slightly from the method used for the azimuth angles. Again, the same method is used for the EoD and the EoA. Hence, θ is used instead of θ^d or θ^a . Likewise, the corresponding AS is denoted as σ_θ .

As for the azimuth angles, a random list of angles is created for the NLOS paths only, following a Gaussian normal distribution with zero-mean and a variance corresponding to the given AS from the LSP maps. The LOS angle is defined to be 0.

$$\theta_1^{[1]} = 0 \quad \text{and} \quad \theta_{2\dots L}^{[1]} \sim \mathcal{N}(0, \sigma_\theta^2) \quad (33)$$

Next, the LOS direction is applied. This makes sure that the elevation angles are spread around the LOS path.

$$\theta_l^{[2]} = \theta_l^{[1]} + \theta^{LOS} \quad (34)$$

The so obtained angels need to be mapped to the interval $[-\frac{\pi}{2}; \frac{\pi}{2}]$. This is done by a modulo operation which wraps the angles around the unit circle and an additional operation that mirrors the angles at the poles of the unit sphere, e.g. an elevation angle of 91° is mapped to 89° , 92° to 88° , and so on. This ensures that the previously calculated azimuth angles are not changed.

$$\theta_l^{[3]} = (\theta_l^{[2]} + \pi \bmod 2\pi) - \pi \quad (35)$$

$$\theta_l^{[4]} = \begin{cases} \pi - \theta_l^{[3]}, & \text{if } \theta_l^{[3]} > \frac{\pi}{2}; \\ \theta_l^{[3]} - \pi, & \text{if } \theta_l^{[3]} < -\frac{\pi}{2}; \\ \theta_l^{[3]}, & \text{otherwise.} \end{cases} \quad (36)$$

As for the azimuth angles, the resulting AS is undefined. Hence, we calculate the actual elevation spread $\sigma_\theta^{[\text{actual}]}$ using equations (26), (27), and (28). Then, with σ_θ being the initial elevation spread from the map, the angles $\theta_l^{[4]}$ are updated. Since the angles should be distributed around the LOS direction, we need to subtract θ^{LOS} before scaling the angles and add it again after scaling them.

$$\theta_l^{[5]} = \frac{\sigma_\theta}{\sigma_\theta^{[\text{actual}]}} \cdot (\theta_l^{[4]} - \theta^{LOS}) + \theta^{LOS} \quad (37)$$

This update, however, might shift some angles outside the allowed interval, especially if there is already a strong bias due to the LOS path which might happen e.g. in satellite scenarios when the satellite has a high elevation. Hence, angles outside the allowed range are replaced with

$$\theta_l^{[6]} = \begin{cases} \mathcal{N}\left(\frac{\pi}{2}, \frac{\pi^2}{8}\right) & \text{if } \theta_l^{[5]} > \frac{\pi}{2}; \\ \mathcal{N}\left(-\frac{\pi}{2}, \frac{\pi^2}{8}\right) & \text{if } \theta_l^{[5]} < -\frac{\pi}{2}; \\ \theta_l^{[5]} & \text{otherwise.} \end{cases} \quad (38)$$

As for the azimuth angles, equations (35) to (38) must be applied in an iterative fashion until $\sigma_\theta^{[\text{actual}]}$ converges either to the given value σ_θ or a maximum value.

Maximal achievable angular spread As already mentioned, there is an upper limit for the AS due to the wrapping around the unit circle. For two equally strong paths the maximum azimuth spread is achieved when the paths face opposite directions. Hence, in order for (26) to be zero, the two angles must be $\frac{\pi}{2}$ and $-\frac{\pi}{2}$. In this case, the AS (28) becomes $\pi/\sqrt{2} \approx 127^\circ$. For three paths, the maximum azimuth spread would be 170° , and for four paths 220° . With increasing KF, however, the maximum AS decreases since more power is allocated to the LOS path. For example, with a KF of 10 dB, the maximum azimuth spread is only 57° . However, if the angles are mapped randomly to the path powers, the realistically achievable ASs are lower. Figure 9 shows simulation results for the maximum AS depending on the KF. For NLOS propagation, the achievable azimuth spread is around 100° , and the elevation spread is around 65° . When the requested AS is larger than the maximum angle, then the angles are adjusted in a way that the AS at the output of the model is close to the maximum AS. This is illustrated in the right part of Figure 9.

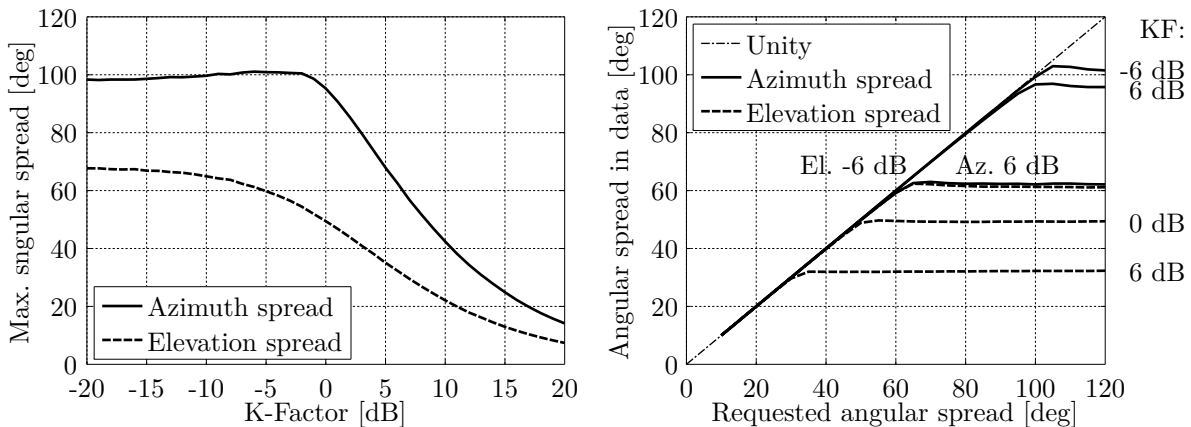


Figure 9: Maximal achievable angular spread depending on the K-factor

Subpaths Finally, the NLOS paths are split into 20 sub-paths to emulate intra-cluster ASs. The LOS path has no sub-paths.

$$\phi_{l,m} = \phi_l + \frac{\pi \cdot c_\phi \cdot \hat{\phi}_m}{180^\circ}, \quad \text{for } l > 1; \quad (39)$$

$$\theta_{l,m} = \theta_l + \frac{\pi \cdot c_\theta \cdot \hat{\phi}_m}{180^\circ}, \quad \text{for } l > 1. \quad (40)$$

Here, m is the sub-path index, c_ϕ is the scenario-dependent cluster-wise RMS AS and $\hat{\phi}$ is the offset angle of the m^{th} sub-path from Table 12. c_ϕ and $\hat{\phi}$ are given in degrees here. Furthermore, each of the 20 angle pairs $(\theta_{l,m}^d, \phi_{l,m}^d)$ at the transmitter (Tx) gets coupled with a random angle pair $(\theta_{l,m}^a, \phi_{l,m}^a)$ at the receiver (Rx) (see [4]).

Table 12: Offset Angle of the m^{th} Sub-Path from [4]

| Sub-path m | Offset angle $\hat{\phi}_m$ (degrees) | Sub-path m | Offset angle $\hat{\phi}_m$ (degrees) |
|-----------------|--|-----------------|--|
| 1,2 | ± 0.0447 | 11,12 | ± 0.6797 |
| 3,4 | ± 0.1413 | 13,14 | ± 0.8844 |
| 5,6 | ± 0.2492 | 15,16 | ± 1.1481 |
| 7,8 | ± 0.3715 | 17,18 | ± 1.5195 |
| 9,10 | ± 0.5129 | 19,20 | ± 2.1551 |

3.4 Drifting

After the path-delays, powers, and angles are known for the initial position, their values are updated for each snapshot of the segment. Thus, we get an evolution of the path-parameters over a short time interval. Drifting for 2-D propagation was already introduced in an extension of the SCM [10]. However, it was not incorporated into the WINNER model and no evaluation was reported. Here, this idea is extended towards 3-D propagation to incorporate time evolution into the new model.

Besides the initial delays, path-powers, and angles, drifting requires the exact position of each antenna element. At the MT, element positions need to be updated for each snapshot with respect to the MT orientation. The following calculations are then done element-wise. The indices r, t, l, m, s denote the index of the Rx antenna element (r) and the Tx antenna element (t), the path number (l), the sub-path number (m), and the snapshot number (s) within the current segment, respectively.

The scatterer positions are kept fixed for the time it takes a MT to move through a segment. Hence, the angles (θ^d, ϕ^d) seen from the BS do not change except for the LOS angle, which is treated separately. Based on this assumption, the angles (θ^a, ϕ^a) as well as the path delay only change with respect to the last-bounce scatterer (LBS). Hence, if the BS array size is small compared to the BS-MT distance, it is sufficient to consider only a single scatterer (the LBS) for the NLOS paths. However, if the Tx-antenna has many elements or Tx and Rx are very close together, like in indoor environments, a multi-bounce model is needed. The two approaches are described in the following.

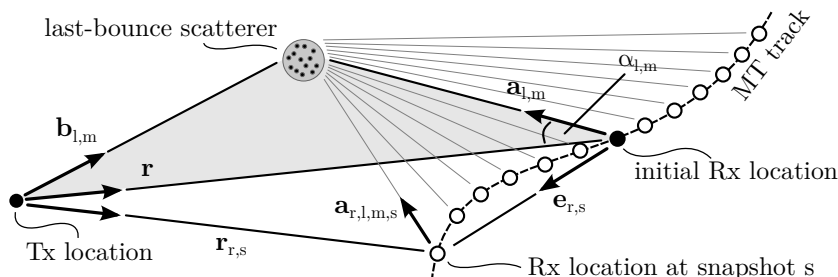


Figure 10: Illustration of the calculation of the scatterer positions and updates of the arrival angles in the single-bounce model

NLOS drifting (single-bounce model) The position of the LBS is calculated based on the initial arrival angles and the path delays. Then, the angles and path lengths between the LBS and the terminal are updated for each snapshot on the track. This is done for each antenna element separately. Figure 10 illustrates the angles and their relations. The first delay is always zero due to (17). Hence, the total length of the l^{th} path is

$$d_l = \tau_l \cdot c + |\mathbf{r}|, \quad (41)$$

where $|\mathbf{r}|$ is the distance between the Tx and the initial Rx location, and c is the speed of light. All sub-paths have the same delay and thus the same path length. However, each sub-path has different arrival angles

$(\theta_{l,m}^a, \phi_{l,m}^a)$. Those angles are transformed into Cartesian coordinates to obtain

$$\hat{\mathbf{a}}_{l,m} = \begin{pmatrix} \cos \phi_{l,m}^a \cdot \cos \theta_{l,m}^a \\ \sin \phi_{l,m}^a \cdot \cos \theta_{l,m}^a \\ \sin \theta_{l,m}^a \end{pmatrix} = \frac{\mathbf{a}_{l,m}}{|\mathbf{a}_{l,m}|}. \quad (42)$$

This vector has unit length and points from the initial Rx position towards the scatterer. Next, the length of the vector $|\mathbf{a}_{l,m}|$ is obtained. Since the drifting at the MT is modeled by a single reflection, Tx, Rx, and LBS form a triangle. We know d_l , \mathbf{r} , and $\hat{\mathbf{a}}_{l,m}$ and can thus apply the cosine theorem to calculate the length $|\mathbf{a}_{l,m}|$ between the Rx and LBS

$$|\mathbf{b}_{l,m}|^2 = |\mathbf{r}|^2 + |\mathbf{a}_{l,m}|^2 - 2 |\mathbf{r}| |\mathbf{a}_{l,m}| \cos \alpha_{l,m} \quad (43)$$

$$(d_l - |\mathbf{a}_{l,m}|)^2 = |\mathbf{r}|^2 + |\mathbf{a}_{l,m}|^2 + 2 |\mathbf{a}_{l,m}| \mathbf{r}^T \hat{\mathbf{a}}_{l,m} \quad (44)$$

$$|\mathbf{a}_{l,m}| = \frac{d_l^2 - |\mathbf{r}|^2}{2 \cdot (d_l + \mathbf{r}^T \hat{\mathbf{a}}_{l,m})} \quad (45)$$

In (44), the term $\cos \alpha_{l,m}$ is substituted with $-\mathbf{r}^T \hat{\mathbf{a}}_{l,m} / |\mathbf{r}|$ since we need the angle between $\mathbf{a}_{l,m}$ and $-\mathbf{r}$, the vector pointing from the Rx position towards the Tx. Now we can calculate the vector $\mathbf{a}_{r,l,m,s}$ for the Rx antenna element r at snapshot s . The element position includes the orientation of the antenna array with respect to the moving direction of the Rx. Hence, the vector $\mathbf{e}_{r,s}$ points from the initial Rx location to the r^{th} antenna element at snapshot s .

$$\mathbf{a}_{r,l,m,s} = \mathbf{a}_{l,m} - \mathbf{e}_{r,s} \quad (46)$$

We obtain an update of the arrival angles by transforming $\mathbf{a}_{r,l,m,s}$ back to spherical coordinates.

$$\phi_{r,l,m,s}^a = \arctan2 \{a_{r,l,m,s,y}, a_{r,l,m,s,x}\} \quad (47)$$

$$\theta_{r,l,m,s}^a = \arcsin \left\{ \frac{a_{r,l,m,s,z}}{|\mathbf{a}_{r,l,m,s}|} \right\} \quad (48)$$

Since we assume a static scattering environment, we use the same departure angles for all Tx elements. The phases and path delays, however, depend on the total path length $d_{r,t,l,m,s}$. To obtain this value, we need to calculate the vector $\mathbf{b}_{l,m}$ from the vectors \mathbf{r} and $\mathbf{a}_{l,m}$ at $r = s = 1$.

$$\mathbf{b}_{l,m} = \mathbf{r} + \mathbf{a}_{l,m} \quad (49)$$

$$d_{r,l,m,s} = |\mathbf{b}_{l,m}| + |\mathbf{a}_{r,l,m,s}| \quad (50)$$

Finally, we calculate the phases ψ and path delays τ .

$$\psi_{r,l,m,s} = \frac{2\pi}{\lambda} \cdot (d_{r,l,m,s} \bmod \lambda) \quad (51)$$

$$\tau_{r,l,s} = \frac{1}{20 \cdot c} \sum_{m=1}^{20} d_{r,l,m,s} \quad (52)$$

NLOS drifting (multi-bounce model) In the multi-bounce model, the NLOS propagation path consists of three segments as illustrated in Figure 11. In the first segment, the vector $\mathbf{b}_{t,l,m}$ points from the position of a Tx-antenna element t to the first-bounce scatterer (FBS). The Tx-element position is indicated by the vector \mathbf{e}_t . In the second segment, the vector $\mathbf{c}_{l,m}$ points from the FBS to the LBS, and in the third segment, the vector $\mathbf{a}_{r,l,m,s}$ points from the Rx-location to the LBS. The total propagation path length d_l is fixed by (41). Hence, we get

$$d_l = |\mathbf{b}_{l,m}| + |\mathbf{c}_{l,m}| + |\mathbf{a}_{l,m}|, \quad (53)$$

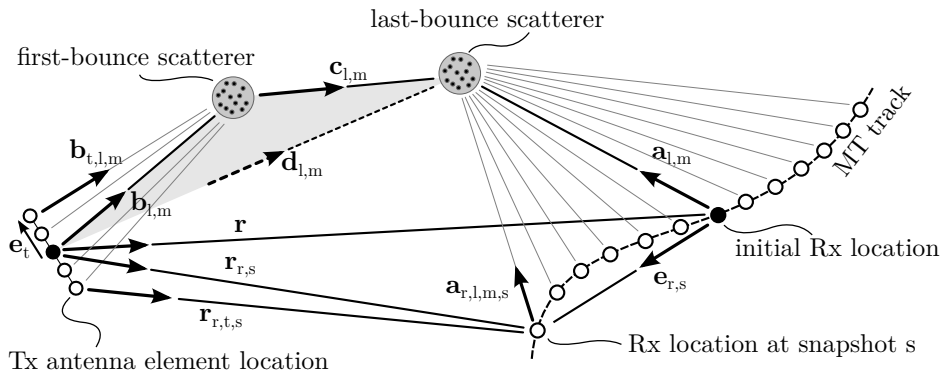


Figure 11: Illustration of the calculation of the scatterer positions and updates of the departure and arrival angles in the multi-bounce model.

where the vector $\mathbf{b}_{l,m}$ points from the Tx-array center to the FBS, i.e., where $|\mathbf{e}_t| = 0$. We also know the departure- and arrival angles, and we can calculate the unit-length vector $\hat{\mathbf{a}}_{l,m}$ using (42) and $\hat{\mathbf{b}}_{l,m}$ using

$$\hat{\mathbf{b}}_{l,m} = \begin{pmatrix} \cos \phi_{l,m}^d \cdot \cos \theta_{l,m}^d \\ \sin \phi_{l,m}^d \cdot \cos \theta_{l,m}^d \\ \sin \theta_{l,m}^d \end{pmatrix} = \frac{\mathbf{b}_{l,m}}{|\mathbf{b}_{l,m}|}. \quad (54)$$

In order to explicitly calculate the positions of FBS and LBS, we need to obtain the lengths $|\mathbf{a}_{l,m}|$ and $|\mathbf{b}_{l,m}|$. However, due to (53), there might be an infinite number of possible solutions. One idea to fix the additional degree of freedom is to minimize $|\mathbf{c}_{l,m}|$. Ideally, $|\mathbf{c}_{l,m}|$ becomes zeros and the multi-bounce model collapses to a single bounce model. The advantage of this approach is that $|\mathbf{a}_{l,m}|$ does not become too short because this would have an impact on the obtained angular spread when the MT is moving. In order to minimize $|\mathbf{c}_{l,m}|$, we need to solve an optimization problem:

$$\begin{aligned} & \underset{|\mathbf{a}_{l,m}|, |\mathbf{b}_{l,m}|}{\text{minimize}} && |\mathbf{c}_{l,m}| = d_l - |\mathbf{b}_{l,m}| - |\mathbf{a}_{l,m}| \\ & \text{subject to} && \mathbf{r} = \hat{\mathbf{b}}_{l,m} \cdot |\mathbf{b}_{l,m}| + \hat{\mathbf{c}}_{l,m} \cdot |\mathbf{c}_{l,m}| - \hat{\mathbf{a}}_{l,m} \cdot |\mathbf{a}_{l,m}|, \\ & && |\mathbf{b}_{l,m}| \geq d_{\min}, \\ & && |\mathbf{a}_{l,m}| \geq d_{\min}. \end{aligned}$$

The additional parameter d_{\min} is a minimum distance between the antenna array center and the nearest scatterer. It might be fixed according to the scenario and center frequency, e.g. 1 m for outdoor propagation and 0.1 m for indoor propagation. To solve the optimization problem we start with $|\mathbf{a}_{l,m}| = d_{\min}$ and calculate $\mathbf{c}_{l,m}$ and $|\mathbf{b}_{l,m}|$ using the cosine theorem. This is possible since the Tx, the FBS and the LBS form a triangle as indicated in Figure 11 by the gray shaded area.

$$d_l^+ = \tau_l \cdot c + |\mathbf{r}| - |\mathbf{a}_{l,m}| \quad (55)$$

$$\mathbf{d}_{l,m} = \mathbf{r} + \hat{\mathbf{a}}_{l,m} \cdot |\mathbf{a}_{l,m}| \quad (56)$$

$$|\mathbf{b}_{l,m}| = \frac{(d_l^+)^2 - |\mathbf{d}_{l,m}|^2}{2 \cdot (d_l^+ - \mathbf{d}_{l,m}^T \hat{\mathbf{b}}_{l,m})} \quad (57)$$

Now, three things might happen:

1. The value obtained for $|\mathbf{b}_{l,m}|$ might be smaller than d_{\min} or even smaller than 0. The latter would imply that the angle of departure turns around the unit sphere. However, this is not allowed since the angles are fixed. In this case, the optimization problem has no solution. This often happens when the propagation delay of a path is very short, i.e., when the path is only a little longer than the LOS path.

This case is treated by setting $|\mathbf{c}_{l,m}| = 0$ and calculating new departure angles assuming a single-bounce model only. This changes the departure angular spread. However, in most cases there will be many paths where the optimization problem has a solution. This is especially true for paths with a longer propagation delay. Hence, it is possible to mitigate the changed departure angular spread by adjusting the departure angles of the multi-bounce paths. The rationale behind this is that many measurements [5, 7] show a rather small departure angular spread of just a few degrees but a large arrival angular spread. This leaves more “room” to adjust the departure angles before they are wrapped around the unit circle. Also, paths with a short propagation delay have more power due to the exponential PDP used in (18). From a physical point of view, those paths are more likely to be scattered only once. Later paths have significantly less power and can well be the result of several scattering events.

2. The value for $|\mathbf{b}_{l,m}|$ is larger than d_{\min} and the optimization problem has a solution. In this case, there will also be a globally optimal solution, i.e., a minimal distance $|\mathbf{c}_{l,m}|$. This minimum must be in between the start point where $|\mathbf{a}_{l,m}| = d_{\min}$ and the end point where $|\mathbf{b}_{l,m}| = d_{\min}$. For each value $|\mathbf{a}_{l,m}|$ follows a value for $|\mathbf{b}_{l,m}|$ and a value for $|\mathbf{c}_{l,m}|$ which both can be calculated using the cosine theorem. Hence, we can apply standard numeric methods such as bisection to obtain the optimal solution.
3. The optimization problem has a solution, but the solution lies on one of the end points, either at $|\mathbf{a}_{l,m}| = d_{\min}$ or on $|\mathbf{b}_{l,m}| = d_{\min}$. In this case, the LBS or the FBS are very close to either the Tx or the Rx antenna. In this case, the problem is relaxed such that $|\mathbf{c}_{l,m}|$ is allowed to double in order to increase the space between scatterer and antenna array.

Once the positions of the FBS and the LBS are known, the departure angles and the total path length are updated for each antenna element of the Tx array.

$$\mathbf{b}_{t,l,m} = \mathbf{b}_{l,m} - \mathbf{e}_t \quad (58)$$

$$\phi_{t,l,m}^d = \arctan_2 \{b_{t,l,m,y}, b_{t,l,m,x}\} \quad (59)$$

$$\theta_{t,l,m}^d = \arcsin \left\{ \frac{b_{t,l,m,z}}{|\mathbf{b}_{t,l,m}|} \right\} \quad (60)$$

$$d_{r,t,l,m,s} = |\mathbf{b}_{t,l,m}| + |\mathbf{c}_{l,m}| + |\mathbf{a}_{r,l,m,s}| \quad (61)$$

The arrival angles are updated using (46), (47) and (48). The phases and delays are calculated using (51) and (52) where $d_{r,l,m,s}$ is replaced by $d_{r,t,l,m,s}$.

LOS drifting The direct component is handled differently, since we have to update the angles at both the Tx and the Rx sides. The angles are updated for each combination of Tx-Rx antenna elements based on the position of the element in 3-D coordinates.

$$\mathbf{r}_{r,t,s} = \mathbf{r} - \mathbf{e}_t + \mathbf{e}_{r,s} \quad (62)$$

$$\phi_{r,t,s}^d = \arctan_2 \{r_{r,t,s,y}, r_{r,t,s,x}\} \quad (63)$$

$$\theta_{r,t,s}^d = \arcsin \left\{ \frac{r_{r,t,s,z}}{|\mathbf{r}_{r,t,s}|} \right\} \quad (64)$$

$$\phi_{r,1,s}^a = \arctan_2 \{-r_{r,t,s,y}, -r_{r,t,s,x}\} \quad (65)$$

$$\theta_{r,1,s}^a = \arcsin \left\{ \frac{-r_{r,t,s,z}}{|\mathbf{r}_{r,t,s}|} \right\} \quad (66)$$

The vector $\mathbf{r}_{r,t,s}$ points from the location of the Tx element t to the location of the Rx element r at snapshot s . The phases and delays are determined by the length of this vector and are calculated using (51) and (52) where $d_{r,l,m,s}$ is replaced by $|\mathbf{r}_{r,t,s}|$.

3.5 Antennas and Polarization

Next, antenna patterns, polarization, and phases are combined in order to calculate initial channel coefficients for each snapshot of a segment. The antennas patterns are defined in spherical coordinates (Az-over-El) with a polar-spherical polarization basis (see [19]).

$$\mathbf{F}(\theta, \phi) = \begin{pmatrix} F^{[\theta]}(\theta, \phi) \\ F^{[\phi]}(\theta, \phi) \end{pmatrix} \quad (67)$$

The coordinate system has two angles and two poles. The elevation angle θ is measured relative to the pole axis. A complete circle will go through each of the two poles, similar to the longitude coordinate in the [world geodetic system \(WGS\)](#). The azimuth angle ϕ moves around the pole, similar to the latitude in [WGS](#). The electric field is resolved onto a polar-spherical polarization basis. The first component of the radiated field $F^{[\theta]}$ represents the case where the “*probe*”, i.e., the reference antenna which is used to measure the pattern, is polarized in θ direction. Likewise, for the second component, $F^{[\phi]}$, the probe is polarized in ϕ direction.

The channel model requires the directional antenna gains from both the [Tx](#) and [Rx](#) antennas at the previously calculated departure and arrival angles. If, in practice, $\mathbf{F}(\theta, \phi)$ is sampled once per degree in both, azimuth and elevation direction, interpolation is needed in order to obtain the exact antenna response $\mathbf{F}(\theta_{r,l,m,s}, \phi_{r,l,m,s})$. The initial channel coefficient then notes

$$g_{r,t,l,m,s}^{[1]} = \mathbf{F}_r(\theta_{r,l,m,s}^a, \phi_{r,l,m,s}^a)^T \cdot \mathbf{M}_{r,t,l,m,s} \cdot \mathbf{F}_t(\theta_{t,l,m,s}^d, \phi_{t,l,m,s}^d). \quad (68)$$

The polarization is changed along the propagation path. This is captured by the matrix \mathbf{M} . The [SCM](#), [WINNER](#), and [COST](#) models use random coefficients to handle polarization effects.

$$\mathbf{M} = \begin{pmatrix} Z_{\theta\theta} & \sqrt{1/\text{XPR}_h} \cdot Z_{\theta\phi} \\ \sqrt{1/\text{XPR}_v} \cdot Z_{\phi\theta} & Z_{\phi\phi} \end{pmatrix}, \quad (69)$$

where $Z \sim \exp\{j \cdot \mathcal{U}(-\pi, \pi)\}$ is a random phase component. However, this does not account for all effects contributing to the polarization state of a [MIMO](#) radio link. Thus, a different method for calculating \mathbf{M} based on linear transformations is proposed in the following.

3.5.1 Relation between the Polarization Model and the Jones Calculus

Jones invented a simple method to calculate polarization effects in optics [20]. In his work, he described the polarization state of a ray of light by the so-called Jones vector. Any object that changes the polarization (or the intensity) of the light is represented by a 2x2 Jones matrix. It was found that the product of the Jones matrix of the optical element and the Jones vector of the incident light accurately describes the polarization state of the resulting ray. Generally, this calculus can be used for any electromagnetic wave. It is especially interesting for the [SCM](#) and [WINNER](#) models where the paths are handled similarly like optical rays.

In the Jones calculus, the Jones vector contains the x and y components of the amplitude and phase of the electric field traveling in z -direction.

$$\begin{pmatrix} E_x(t) \\ E_y(t) \end{pmatrix} = e^{j\omega t} \cdot \underbrace{\begin{pmatrix} A_x e^{j\epsilon_x} \\ A_y e^{j\epsilon_y} \end{pmatrix}}_{\text{Jones vector}} = \begin{pmatrix} J^{[\theta]} \\ J^{[\phi]} \end{pmatrix} = \mathbf{J} \quad (70)$$

The same expression is found in the antenna pattern (67) of the [WINNER](#) model where the complex value $A_y e^{j\epsilon_y}$ from the Jones vector can be identified with the (generally also complex-valued) component $F^{[\theta]}(\theta, \phi)$ of the antenna pattern. Likewise, $A_x e^{j\epsilon_x}$ can be identified with $F^{[\phi]}(\theta, \phi)$. This implies that the polarization

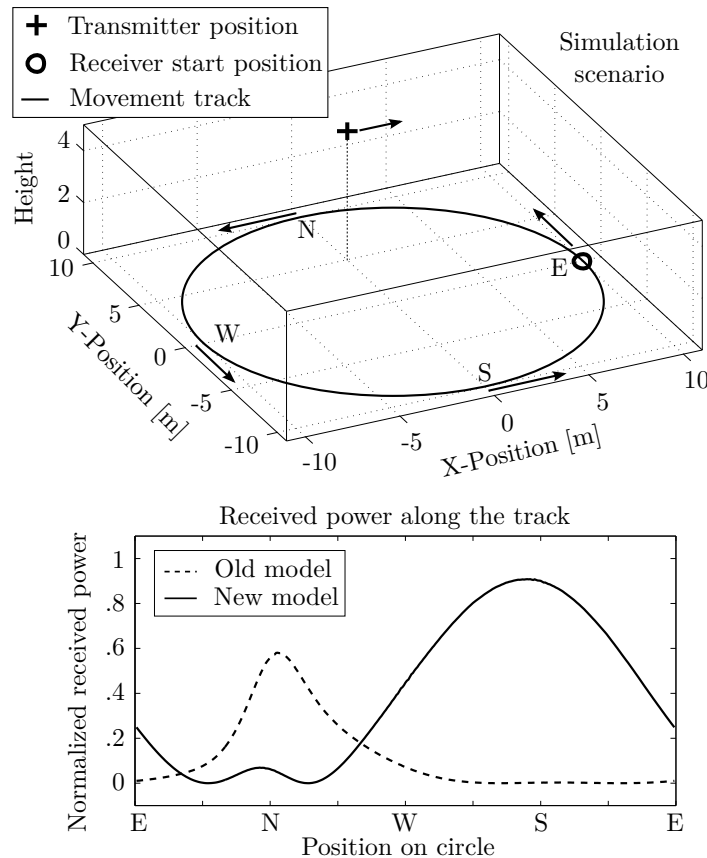


Figure 12: Example showing the effect of the new polarization rotation method

coupling matrix \mathbf{M} in (68) is a Jones matrix and that the Jones calculus could apply also to the WINNER model.

In general, \mathbf{M} can be seen as a transformation operation that maps the incoming signal on the polarization plane to an outgoing signal. If the coefficients are real valued, then linear transformations - such as rotation, scaling, shearing, reflection, and orthogonal projection as well as combinations of those operations - are possible. If the coefficients are complex valued, then the matrix shows characteristics of a Möbius transformation. Such transformations can map straight lines to straight lines or circles and *vice versa*. Since the Jones calculus allows the use of complex coefficients, it can transform linear polarized signals into circular or elliptical polarized signals and elliptical polarized signals to linear polarized signals. This implies that using (69) with complex coefficients results in a completely random polarization behavior when XPR_v and XPR_h are small (i.e., when the off-diagonal elements are large). When $XPR_{v,h}$ is large (and the off-diagonal elements are close to zero), then (69) describes a scaling operation.

Here, a different method to model the polarization based on a combination of linear transformations is proposed. In the following, \mathbf{M} will be calculated explicitly for the LOS component, taking the orientation of the antennas into account. For the NLOS components, additional operations are used to convert the XPR value from the parameter tables into Jones matrices for the linear and elliptical polarization component.

An example showing the effect of the new method is depicted in Figure 12. The upper part shows the model setup and the lower part the results. Both, the transmitter and the receiver are equipped with dipole antennas that were initially slanted by 45° around the y -axis. The transmitter is placed 5 m above ground and 5 m north of the center. The receiver moves counterclockwise around the transmitter with its antenna orientation changing in accordance with the movement direction. The orientations of transmitter and receiver (including the movement direction) are indicated by the arrows. The lower figure shows the LOS power along the track. The dashed curve comes from the WINNER approach. The new model (solid

line) calculates the change of the polarization due to the antenna orientation and adjusts the polarization accordingly.

3.5.2 Changing the Orientation of Antennas

Orientation changes are desirable in many cases, e.g., when tilting BS arrays or changing the orientation of mobile terminals. An example is depicted in Figure 13. The left side of the figure shows a dipole pattern that has only a vertical component and is in line with the global coordinate system (GCS). The right side shows the same antenna tilted by 20° around the x -axis. In order to maintain alignment with the GCS, the antenna pattern was transformed. The resulting pattern also has a horizontal component. The antenna response (67) can now be obtained by reading the polarimetric beam pattern at the given angles (θ, ϕ) .

Interpolation of the antenna pattern An antenna pattern (67) is given in spherical coordinates as a function of the elevation angle θ and the azimuth angle ϕ . When the orientation of the antenna element changes, the field pattern has to be read at different angles (Θ, Φ) which include the effect of the orientation change. Rotations in 3-D are easier in Cartesian coordinates. Therefore, the original angle pair (θ, ϕ) is transformed into a vector \mathbf{c} that describes the arrival- or departure angles in Cartesian coordinates. The three vector elements represent the x, y and z -component.

$$\mathbf{c}(\theta, \phi) = \begin{pmatrix} \cos \theta \cdot \cos \phi \\ \cos \theta \cdot \sin \phi \\ \sin \theta \end{pmatrix} \quad (71)$$

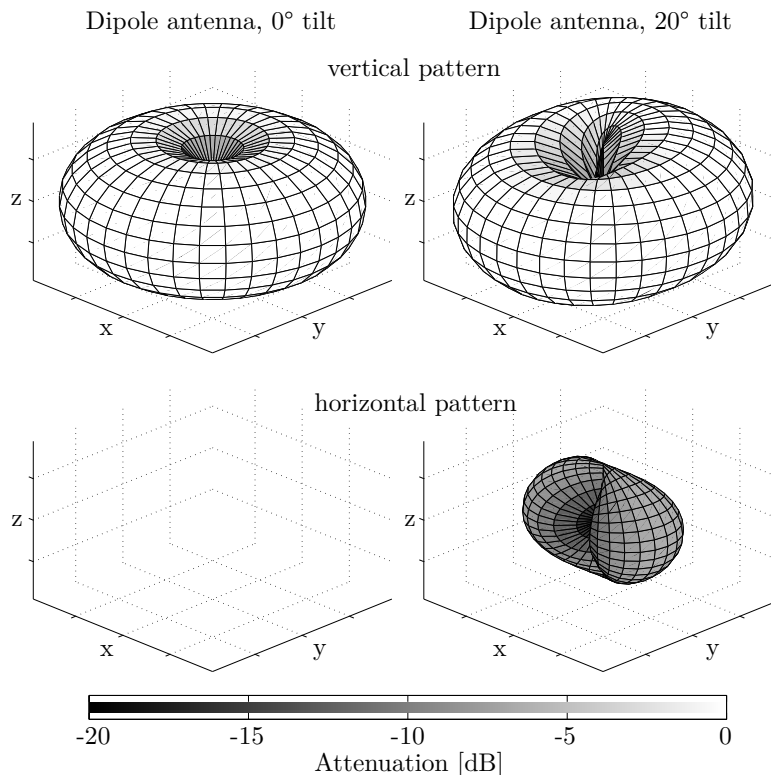


Figure 13: Example patterns for a dipole antenna

A 3x3 matrix \mathbf{R} can now be used to describe the orientation change in 3-D space. The example in Figure 13 was tilted by 20° around the x -axis of the coordinate system. The corresponding matrix is

$$\mathbf{R}_x(20^\circ) = \begin{pmatrix} 1 & 0 & 0 \\ 0 & \cos(20^\circ) & -\sin(20^\circ) \\ 0 & \sin(20^\circ) & \cos(20^\circ) \end{pmatrix} \quad (72)$$

By multiplying \mathbf{R} with (71), the orientation change is included in the vector

$$\mathbf{c}^+(\theta, \phi) = \mathbf{R}^T \cdot \mathbf{c}(\theta, \phi) \quad (73)$$

The transformed pattern $\tilde{\mathbf{F}}$ is needed in spherical coordinates. Thus, \mathbf{c}^+ is transformed back to spherical coordinates. This results in the new angles (Θ, Φ) .

$$\Theta(\theta, \phi) = \arcsin [c_z^+(\theta, \phi)] \quad (74)$$

$$\Phi(\theta, \phi) = \arctan_2 [c_y^+(\theta, \phi), c_x^+(\theta, \phi)] \quad (75)$$

c_x^+ , c_y^+ and c_z^+ are the x , y and z component of \mathbf{c}^+ , respectively. The coefficients of the rotated pattern are now obtained by reading the original pattern \mathbf{F} at the transformed angles

$$\hat{\mathbf{F}}(\theta, \phi) = \begin{pmatrix} \hat{F}^{[\theta]}(\theta, \phi) \\ \hat{F}^{[\phi]}(\theta, \phi) \end{pmatrix} = \begin{pmatrix} F^{[\theta]}(\Theta, \Phi) \\ F^{[\phi]}(\Theta, \Phi) \end{pmatrix} \quad (76)$$

Since the patterns are usually sampled at a fixed angular grid, interpolation is needed here. As a standard computationally inexpensive procedure, linear interpolation can be used. Alternatively, more advanced techniques based on the effective aperture distribution function (EADF) are possible [21].

Polarization rotation The second step takes the polarization into account. Due to the rotation of the primary antenna, the alignment with the *probe* changes. The antenna patterns are defined in a polar-spherical polarization basis. However, the rotation is defined in Cartesian coordinates. Thus, we need to perform the polarization rotation in a Cartesian basis as well. The transformation from the polar-spherical polarization basis to the Cartesian polarization basis is given by [22]

$$\begin{pmatrix} \hat{F}^{[x]}(\theta, \phi) \\ \hat{F}^{[y]}(\theta, \phi) \\ \hat{F}^{[z]}(\theta, \phi) \end{pmatrix} = \underbrace{\begin{pmatrix} \sin \Theta \cos \Phi & -\sin \Phi \\ \sin \Theta \sin \Phi & \cos \Phi \\ -\cos \Theta & 0 \end{pmatrix}}_{= \mathbf{T}(\Theta, \Phi)} \cdot \underbrace{\begin{pmatrix} F^{[\theta]}(\Theta, \Phi) \\ F^{[\phi]}(\Theta, \Phi) \end{pmatrix}}_{= \hat{\mathbf{F}}(\theta, \phi)} \quad (77)$$

The transformation matrix $\mathbf{T}(\Theta, \Phi)$ is both, orthogonal and normalized to unity. Hence, the inverse transformation matrix is equal to the matrix transpose. The rotated pattern $\tilde{\mathbf{F}}$ is obtained by using the interpolated pattern $\hat{\mathbf{F}}$ and transforming it to a Cartesian polarization basis. Then, this pattern is rotated using the rotation matrix \mathbf{R} and the resulting pattern is transformed back to the polar-spherical basis.

$$\tilde{\mathbf{F}}(\theta, \phi) = \underbrace{\mathbf{T}(\theta, \phi)^T \cdot \mathbf{R} \cdot \mathbf{T}(\Theta, \Phi)}_{= \tilde{\mathbf{M}}} \cdot \hat{\mathbf{F}}(\theta, \phi) \quad (78)$$

The entire process can be described by a 2x2 polarization rotation matrix $\tilde{\mathbf{M}}$. Due to the fact that the radiated energy in both polarizations remains constant and only the alignment with the *probe* changes, this matrix is a rotation matrix having the form

$$\tilde{\mathbf{M}}(\vartheta) = \begin{pmatrix} \cos \vartheta & -\sin \vartheta \\ \sin \vartheta & \cos \vartheta \end{pmatrix}, \quad (79)$$

where the polarization rotation angle ϑ follows from

$$\cos \vartheta = \begin{pmatrix} \sin \theta \cos \phi \\ \sin \theta \sin \phi \\ -\cos \theta \end{pmatrix}^T \cdot \mathbf{R} \cdot \begin{pmatrix} \sin \Theta \cos \Phi \\ \sin \Theta \sin \Phi \\ -\cos \Theta \end{pmatrix} \quad (80)$$

$$\sin \vartheta = \begin{pmatrix} -\sin \phi \\ \cos \phi \\ 0 \end{pmatrix}^T \cdot \mathbf{R} \cdot \begin{pmatrix} \sin \Theta \cos \Phi \\ \sin \Theta \sin \Phi \\ -\cos \Theta \end{pmatrix} \quad (81)$$

$$\vartheta = \arctan_2 [\sin \vartheta, \cos \vartheta] \quad (82)$$

3.5.3 Constructing the Polarization Transfer Matrix

Polarization of direct (LOS) path In the LOS polarization model, the *probe* is replaced by the receive antenna. Both, the transmitter and the receiver can have different orientations, e.g. due to a downtilt at the BS and a given movement direction at the MT. In addition, a reflection operation is needed to transform the outgoing polarization direction at the transmitter into an incoming direction at the receiver. Thus, a combination three linear transformations, two rotations and one reflection, is sufficient to construct the polarization transfer matrix of the LOS path.

$$\begin{aligned} \mathbf{M}_{r,t,s}^{[\text{LOS}]} &= \left[\tilde{\mathbf{M}}(\vartheta_{r,s}^{[\text{LOS}]}) \right]^T \cdot \begin{pmatrix} 1 & 0 \\ 0 & -1 \end{pmatrix} \cdot \tilde{\mathbf{M}}(\vartheta_{t,s}^{[\text{LOS}]}) \\ &= \begin{pmatrix} \cos \vartheta_{r,s}^{[\text{LOS}]} & -\sin \vartheta_{r,s}^{[\text{LOS}]} \\ -\sin \vartheta_{r,s}^{[\text{LOS}]} & -\cos \vartheta_{r,s}^{[\text{LOS}]} \end{pmatrix} \cdot \begin{pmatrix} \cos \vartheta_{t,s}^{[\text{LOS}]} & -\sin \vartheta_{t,s}^{[\text{LOS}]} \\ \sin \vartheta_{t,s}^{[\text{LOS}]} & \cos \vartheta_{t,s}^{[\text{LOS}]} \end{pmatrix} \end{aligned} \quad (83)$$

Model for the indirect (NLOS) paths For the NLOS components, the transmitted signal undergoes some diffraction, reflection or scattering before reaching the receiver. Following the common Fresnel formula in electrodynamics, the polarization direction can be changed at the boundary surface between two dielectric media. T. Svantesson [23] provided a method for modeling the polarization of a reflected wave where the polarization coupling is a function of several geometric parameters such as the orientation of the scatterers. However, these parameters are not generally available in the SCM. In addition to that, only metallic reflections keep the polarization unchanged. Reflections at dielectric media can cause changes of the polarization being a function of the complex-valued dielectric constant of the media and of the angle of incidence. Hence, not only the polarization angle might change, but also the polarization type. In order to address this issue, studies of the polarizations effects in individual scattering clusters in several outdoor- and indoor scenarios were done [24–26]. The published results indicate that, in many cases, scattering preserves the polarization quiet well. However, since only the powers of the elements in the polarization coupling matrix were analyzed, no conclusions can be drawn on how elliptic the polarization of the scattered wave becomes.

The polarization coupling matrix \mathbf{M} for the NLOS components can be described by a combination of linear transformations. Hence, it is possible to take advantage of the existing findings of the XPR. The NLOS polarization model consists of three parts: A deterministic part and two stochastic parts.

1. Deterministic part

The deterministic component is the same as for the LOS polarization. However, the wave travel direction $\mathbf{r}_{r,t,s}$ used to calculate the departure and arrival angles for LOS propagation must be replaced by $\mathbf{a}_{t,l,m,s}$, i.e., the vector pointing from the position of the transmitter to the FBS, and $\mathbf{a}_{r,l,m,s}$, i.e., the vector pointing from the position of the LBS to the Rx position. Furthermore, the calculation must be repeated for each sub-path.

2. Linear component

Individual values of the XPR for each subpath are drawn from a normal distribution

$$\text{XPR}_{l,m}^{[\text{dB}]} = \mathcal{N}(\text{XPR}_\mu, \text{XPR}_\sigma^2). \quad (84)$$

In order to model the polarization change due to scattering, $\text{XPR}_{l,m}$, we can follow the approach from [27] and calculate an additional NLOS rotation matrix $\mathbf{M}_{l,m}^{[\text{linear}]}$ as

$$\mathbf{M}_{l,m}^{[\text{linear}]} = \begin{pmatrix} m_{\theta\theta} & m_{\theta\phi} \\ m_{\phi\theta} & m_{\phi\phi} \end{pmatrix} = \begin{pmatrix} \cos \gamma_{l,m} & -\sin \gamma_{l,m} \\ \sin \gamma_{l,m} & \cos \gamma_{l,m} \end{pmatrix} \quad (85)$$

Following the notations in [28], we get

$$\text{XPR}_{l,m} = \frac{|m_{\theta\theta}|^2}{|m_{\phi\theta}|^2} = \frac{|m_{\phi\phi}|^2}{|m_{\theta\phi}|^2} = \frac{(\cos \gamma_{l,m})^2}{(\sin \gamma_{l,m})^2} = (\cot \gamma_{l,m})^2 \quad (86)$$

$$\gamma_{l,m} = \arccot \left(\sqrt{\text{XPR}_{l,m}} \right) \quad (87)$$

3. Elliptical component

Elliptic polarization is obtained, when there is a phase difference between the horizontal and the vertical component. This is included by a scaling matrix

$$\mathbf{M}_{l,m}^{[\text{elliptic}]} = \begin{pmatrix} \exp(j\kappa_{l,m}) & 0 \\ 0 & \exp(-j\kappa_{l,m}) \end{pmatrix} \quad (88)$$

The phase shift κ is calculated to

$$\kappa_{l,m} = X_{l,m} \cdot \arccot \left(\sqrt{\text{XPR}_{l,m}} \right), \quad (89)$$

where $X_{l,m} \sim \{-1, 1\}$ is the positive or negative sign.

The polarization for the NLOS paths is a combination of five linear transformations. First, any change in the transmitter orientation is included by a rotation matrix $\tilde{\mathbf{M}}(\vartheta_{t,l,m,s})$. Then, the influence of the scattering cluster is modeled by a combination of three operations: A scaling operation that introduces a phase shift between the vertical and horizontal component to obtain an elliptic XPR, a reflection operation, and a rotation operation to obtain the desired linear XPR. Last, the change in the receiver orientation is included by a second rotation matrix $\tilde{\mathbf{M}}(\vartheta_{r,l,m,s})$. The complete polarization transfer matrix notes

$$\mathbf{M}_{r,t,l,m,s}^{[\text{NLOS}]} = \left[\tilde{\mathbf{M}}(\vartheta_{r,l,m,s}) \right]^T \cdot \mathbf{M}_{l,m}^{[\text{linear}]} \cdot \begin{pmatrix} 1 & 0 \\ 0 & -1 \end{pmatrix} \cdot \mathbf{M}_{l,m}^{[\text{elliptic}]} \cdot \tilde{\mathbf{M}}(\vartheta_{t,l,m,s}) \quad (90)$$

If the same XPR is used for V and H-component, the equation can be simplified to:

$$\begin{aligned} \gamma_{l,m}^+ &= \vartheta_{r,l,m,s} - \gamma_{l,m} \\ \mathbf{M}_{r,t,l,m,s}^{[\text{NLOS}]} &= \begin{pmatrix} \cos \gamma_{l,m}^+ & -\sin \gamma_{l,m}^+ \\ -\sin \gamma_{l,m}^+ & -\cos \gamma_{l,m}^+ \end{pmatrix} \begin{pmatrix} \exp(j\kappa_{l,m}) & 0 \\ 0 & \exp(-j\kappa_{l,m}) \end{pmatrix} \begin{pmatrix} \cos \vartheta_{t,s} & -\sin \vartheta_{t,s} \\ \sin \vartheta_{t,s} & \cos \vartheta_{t,s} \end{pmatrix} \end{aligned} \quad (91)$$

Obtaining initial XPR values In the model, the simplified option 2. (a) is used to keep the compatibility with the WINNER parameter tables where the same XPR value is applied to both, the V and H-component. Statistics for the values for XPR_μ and XPR_σ are extracted from measurements. When those parameters are calculated from measured data, they are usually averaged over different propagations paths. Thus, the XPR value from the parameter tables is a LSPs having a scenario-dependent distribution, i.e., it depends on the positions of the MT. However, here, we need to draw a values $\text{XPR}_{l,m}^{[\text{dB}]}$ for individual MPCs. If this

is done using (84), then the value for XPR_σ obtained from the generated channel coefficients will effectively become zero due to the averaging over several MPC and snapshots. Therefore, a two-step approach is used here. First, a value $\text{XPR}_\mu^{[\text{LSP}]}$ is drawn from the a normal distribution

$$\text{XPR}_\mu^{[\text{LSP}]} = \mathcal{N}(\text{XPR}_\mu, \text{XPR}_\sigma^2). \quad (92)$$

This value represents the average XPR over all MPCs at the receiver positions. Then, in a second step, the XPR for the individual MPCs is drawn using $\text{XPR}_\mu^{[\text{LSP}]}$ instead of XPR_μ . This maintains the original spread XPR_σ in the generated channel coefficients.

$$\text{XPR}_{l,m}^{[\text{dB}]} = \mathcal{N}\left(\text{XPR}_\mu^{[\text{LSP}]}, \text{XPR}_\sigma^2\right) \quad (93)$$

3.6 Combining Sub-Paths into Paths

Each of the 20 sub-paths gets initialized with a random phase ψ^0 . In addition, a deterministic phase component $\psi_{r,t,l,m,s}$ (51) is obtained from the total length of the propagation path. Both components are combined to

$$\psi_{r,t,l,m,s}^+ = \exp(-j\psi_{l,m}^0 - j\psi_{r,t,l,m,s}) \quad (94)$$

The initial channel coefficients for each sub-path, including the polarization effects, are obtained by (68). Now, the 20 sub-paths get combined into a single path. However, due to the random initial phases, a simple sum will result in a random path power since it is unpredictable if the phase components add up constructively or destructively. This is compensated by normalization where first, the average power is calculated from the sup-paths as

$$P_{r,t,l,s}^{[\text{sub}]} = \sum_{m=1}^{20} \left| g_{r,t,l,m,s}^{[1]} \right|^2. \quad (95)$$

Then, the subpaths are summed up and the path power is applied

$$g_{r,t,l,s}^{[2]} = \sum_{m=1}^{20} g_{r,t,l,m,s}^{[1]} \cdot \psi_{r,t,l,m,s}^+, \quad (96)$$

$$g_{r,t,l,s}^{[3]} = \sqrt{\frac{P_l}{20} \cdot \frac{P_{r,t,l,s}^{[\text{sub}]}}{\left| g_{r,t,l,s}^{[2]} \right|^2} \cdot g_{r,t,l,s}^{[2]}} \quad (97)$$

where P_l is the initial path power from Section 3.2.

3.7 Path Gain, Shadow Fading and K-Factor

Now, we apply the path gain (PG), the shadow fading (SF), and the KF. Hata [29] presented a simple model for macro-cellular settings where the PG scales with the logarithm of the distance d (in units of meters) between BS and terminal:

$$\text{PG}^{[\text{dB}]} = -A \cdot \log_{10} d_{[\text{m}]} - B, \quad (98)$$

where A and B are scenario-specific coefficients that are typically determined by measurements. The path gain exponent A often varies between values of 20 and 40, depending on the propagation conditions, the BS height, and other factors. Combining PG and SF results in the effective path gain $\text{PG}^{[\text{eff}]}$. The values for the SF and the KF are obtained from the LSP map by an interpolation of the surrounding pixels at the position of the s^{th} snapshot. The KF at the initial position is already included due to the scaling in (21). Thus, we have to take this into account and scale the power accordingly.

$$\text{PG}_s^{[\text{eff}]} = \sqrt{10^{0.1(\text{PG}_s^{[\text{dB}]} + \text{SF}_s^{[\text{dB}]})}} \cdot \sqrt{1 + P_1 \left(\frac{K_s}{K_0} - 1 \right)} \quad (99)$$

$$g_{r,t,l,s} = \text{PG}_s^{[\text{eff}]} \cdot \begin{cases} \sqrt{\frac{K_s}{K_0}} \cdot g_{r,t,l,s}^{[3]} & \text{for } l = 1; \\ g_{r,t,l,s}^{[3]} & \text{otherwise.} \end{cases} \quad (100)$$

In the above equations, K_s and $\text{SF}_s^{[\text{dB}]}$ are the interpolated values for the KF and the SF from the map, K_0 is the KF at the initial position, $\text{PG}_s^{[\text{dB}]}$ is the path gain (without SF) at the MT position (98), and P_1 is the power of the LOS path (21).

3.8 Transitions between Segments

The calculations in Sections 3.2 to 3.7 were done independently for each segment of the MT trajectory. Here, we combine those segments into a long, time-evolving sequence of channel coefficients. The idea comes from the WINNER II model [4]. However, it was neither implemented nor tested. Our implementation requires that parts of the segments are overlapping as depicted in the top of Figure 14.

The lifetime of scattering clusters is confined within the combined length of two adjacent segments. The power of paths from the old segment is ramped down and the power of new paths is ramped up within the overlapping region of the two segments. Hence, this process describes the birth and death of scattering clusters along the trajectory. Outside the overlapping region, all paths of the segment are active. The overlapping region is further split into sub-intervals to keep the computational overhead low. During each sub-interval, one old path ramps down and one new path ramps up. The power ramps are modeled by a squared sine function:

$$w^{[\text{sin}]} = \sin^2\left(\frac{\pi}{2} \cdot w^{[\text{lin}]}\right). \quad (101)$$

Here, $w^{[\text{lin}]}$ is the linear ramp ranging from 0 to 1, and $w^{[\text{sin}]}$ is the corresponding sine-shaped ramp with a constant slope at the beginning and the end. This prevents inconsistencies at the edges of the sub-intervals. If both segments have a different number of paths, the ramp is stretched over the whole overlapping area for paths without a partner. For the LOS path, which is present in both segments, only power and phase are adjusted.

Paths need to be carefully matched to minimize the impact of the transition on the instantaneous values of the LSPs. For example, the DS increases if a path with a small delay ramps down and a similarly strong path with a large delay ramps up. Hence, the DS can fluctuate randomly within the overlapping region. To balance this out, paths from both segments are paired in a way that minimize these fluctuations. This is done by determining the values of the DS before and after the transition. Then, a target DS is calculated for each sub-interval. For example, if the old segment yields a DS of 200 ns and the new segment has 400 ns, then the target DS will be 220 ns for the first sub-interval, 240 ns for the second and so on. Then, a combination of paths is searched that best matches the target DS for each sub-interval.

3.9 Postprocessing / Variable Speeds

In the real world, MTs move at arbitrary speeds, including accelerations and decelerations. Provided that the sampling theorem is fulfilled, we can interpolate the channel coefficients to include such effects. This is illustrated in the bottom part of Figure 14. The white dots represent the snapshots at a constant distance. However, the sample points (gray stars) can have unequal spacing, e.g., for an accelerated movement. Each sample point in the time domain (given in units of seconds) has a corresponding position on the MT trajectory (in units of meters). The amplitudes and phases of the channel coefficients are interpolated separately using cubic spline interpolation. The path delays are interpolated with a piecewise cubic hermite interpolating polynomial.

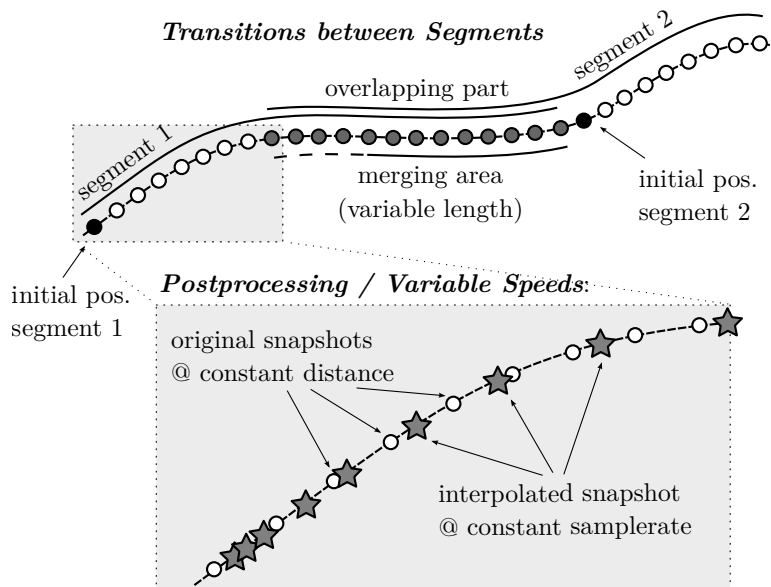


Figure 14: Top: Illustration of the overlapping area used for calculating the transitions between segments (step G), Bottom: Illustration of the interpolation to obtain variable MT speeds (step H).

4 3GPP-3D calibration results

QuaDRiGa implements all essential components of the 3GPP-3D channel model [8]. In order to qualify as a 3GPP-3D compatible implementation, and thus being eligible to evaluate 3GPP standardization proposals, the model needs to be calibrated. Individual implementations of the 3GPP contributors have to create a set of metrics which show that the model implementation fulfills the 3GPP requirements. This section summarizes the calibration steps and presents the results obtained from QuaDRiGa.

In addition to the small-scale-fading (SSF) model, which is in large parts identical to the WINNER+ model, 3GPP-3D specifies an antenna model, deployment scenarios, as well as path-loss models and parameter tables for **urban-microcell (UMi)** and **urban-macrocell (UMa)** deployments. All essential parts of the 3GPP-3D model have been implemented in QuaDRiGa as well. However, there are some differences between the two models which are explained in the following:

Differences between QuaDRiGa and the 3GPP-3D model

- **Coordinate system**

The 3GPP-3D coordinate system is defined with respect to a spherical coordinate system where the zenith angle $\theta = 0^\circ$ points to the zenith and $\theta = 90^\circ$ points to the horizon. QuaDRiGa uses the geographic coordinate system where the elevation angle $\theta = 90^\circ$ points to the zenith and $\theta = 0^\circ$ points to the horizon. The conversion between the two is straight forward. To avoid confusion between the coordinate systems, 3GPP uses the term “zenith”, i.g. zenith angle of arrival (ZoA), zenith angle of departure (ZoD), zenith angle spread of arrival (ZSA), zenith angle spread of departure (ZSD), while QuaDRiGa uses the term “elevation”, i.e. elevation angle of arrival (EoA), elevation angle of departure (EoD), elevation angle spread of arrival (ESA), elevation angle spread of departure (ESD).

- **Delays and Path Powers**

3GPP-3D uses a heuristically determined Ricean K-factor dependent scaling constant in order to adjust the delays in LOS scenarios (see [8], pp. 25). QuaDRiGa solves this differently by first assigning delays and path powers, including the KF power scaling. Then, the resulting DS is calculated and the path delays are scaled to the value from the large-scale fading (LSF) model. This avoids the heuristic

scaling. See Section 3.2 for details.

- **Intra-Cluster Delay Spread**

The 3GPP-3D model splits the two strongest clusters into three sub-clusters (per cluster), with fixed delay offsets. This is not implemented in QuaDRiGa, since it has no effect on the results obtained from the model, but adds additional complexity.

- **Departure and Arrival Angles**

3GPP-3D obtains the individual angles from mapping the path powers to a wrapped Gaussian or wrapped Laplacian power-angular spectrum (PAS). Then, heuristically determined scaling factors are used to adjust the angular values for a different number of paths and the Ricean K-factor (see [8], pp. 26, step 7 and 8). However, this approach breaks the input-output consistency of the angular spread, i.e. the angular spread calculated from the channel coefficients for an individual BS-MT link is not equal to the value given to the SSF model. Only the first-order statistics agree with each other. QuaDRiGa solves this by creating random angles, calculating the resulting angle spread, and scaling the angles to obtain the value from the LSF model (see Section 3.3). ¹

- **Polarization Model**

QuaDRiGa has its own polarization model as described in Section 3.5. However, for the calibration, the model from 3GPP was used (see [8], pp. 26, step 11). The QuaDRiGa polarization model was originally introduced to correctly model ecliptic XPRs (e.g. for satellite channels), which is not covered well by the existing approach. The 3GPP / WINNER polarization model creates additional random phase shifts which effectively destroy ecliptic polarization in NLOS channels. These effects also change phase information in the channel coefficients - leading to a different singular-value spread in cross-polarized channels.

- **Wrapping method**

QuaDRiGa does not implement a wrapping method for large deployments. Instead, MTs are only placed inside the inner ring of the BSs, which ensures that the interference from the outer rings is correctly modeled. An additional option is to add an additional ring of BS.² However, this roughly doubles the number of BSs in the deployment (111 instead of 57), adding additional memory requirements and computation time.

The 3GPP calibration consists of two phases, where the first phase tests the validity of the path-loss model and the elevation angle modeling. The second phase then tests several metrics for the SSF model. The simulation assumptions and results from different 3GPP partners are summarized in [30] and are listed in Table 13.

The antenna model is described in [8], on page 16. It consists of a 2D planar array structure with M rows and N columns of patch elements. Each element has an azimuth and elevation full width at half maximum (FWHM) of 65°. The elements can either be vertically polarized or cross-polarizes with ±45° polarization. In the latter, the number of antenna ports is doubled. Optionally, vertically stacked elements can be coupled using fixed complex-valued weights. The electric downtilt is included by a coupling matrix \mathbf{C} which maps the signal from antenna port p to transmit element m

$$c_{m,p} = \sqrt{\frac{1}{K}} \cdot \exp\left(2\pi \cdot j \cdot \frac{e_{m,p,z} \cdot \beta}{\lambda}\right), \quad (102)$$

where $e_{m,p,z}$ is the relative position of transmit element m to the array center in z direction, β is the downtilt angle in radians, and λ is the wavelength. K is the number of coupled elements in z -direction. In order to reduce computational complexity, effective antenna patterns are calculated in QuaDRiGa that include the coupling and downtilt settings.

¹The 3GPP-3D method is implemented as well and can be activated in the simulation setting of QuaDRiGa. However, there is no difference in the calibration results.

²There is an automatic function `layout.gnerate('regular',37)` for this.

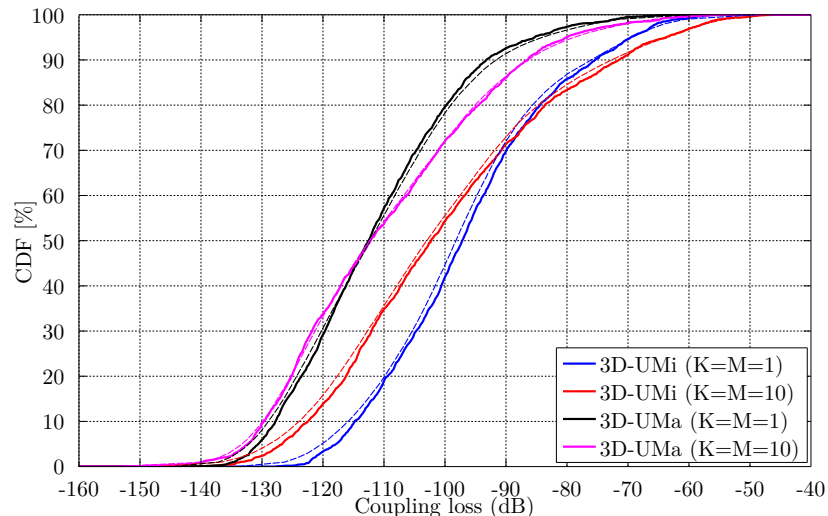
Table 13: Simulation assumptions for 3GPP-3D calibration

| Parameter | Value | |
|------------------------|---|--------|
| Scenario | 3D-UMa | 3D-UMi |
| Layout | Hexagonal grid, 19 micro sites, 3 sectors per site | |
| ISD | 500 m | 200 m |
| BS antenna height | 25 m | 10 m |
| Min. BS-MT 2D distance | 35 m | 10 m |
| MT indoor fraction | | 80 % |
| MT orientation | Random rotation around z-axis, $r_z \sim \mathcal{U}(0, 360^\circ)$ | |
| MT height in meters | General equation: $h_{MT} = 3(n_{fl} - 1) + 1.5$ Indoor users: $n_{fl} \sim \mathcal{U}(1, N_{fl})$ where $N_{fl} \sim \mathcal{U}(4, 8)$ Outdoor users: $n_{fl} = 1$ | |
| Carrier frequency | 2 GHz | |
| System bandwidth | 10 MHz, 50 Resource Blocks | |
| MT attachment | Strongest BS, based on path loss | |
| BS antenna (Phase 1) | Config 1: K=M=10, N=1, 0.5λ spacing, V-pol , 12° tilt Config 2: K=M=1, N=1, V-pol | |
| MT antenna (Phase 1) | Config 1/2: Isotropic antenna, V-pol | |
| BS antenna (Phase 2) | Config 1: K=1, M=2, N=2, 0.5λ spacing, V-pol Config 2: K=M=10, N=2, X-pol ($\pm 45^\circ$), 0.5λ spacing, 12° tilt | |
| MT antenna (Phase 2) | Config 1: N=2, Isotropic antenna, V-pol Config 2: Isotropic antenna, X-pol (0°/90°) | |

Coupling Loss (Phase 1) The coupling loss is defined as the path gain of a **MT** to its serving **BS**, i.e. the strongest **BS** seen by the **MT**. Here, the term **BS** refers to one sector of a 3-sector site. In the proposed layout, there are 19 sites, each consisting of three **BSs**. **MTs** were placed in the first ring of interferers, i.e. around the first site. The phase 1 calibration does not consider a **SSF** model, but includes the antenna patterns. Hence, the results shown in Fig. 15 were obtained by running the simulations with only one path (the **LOS** path). The thick lines were obtained using the QuaDRiGa model (v1.4), the thin dashed line are taken from [30]. They represent the median of all 3GPP calibration results. The QuaDRiGa results fit almost perfectly. The remaining differences are well within the tolerances visible in the individual result curves in [30].

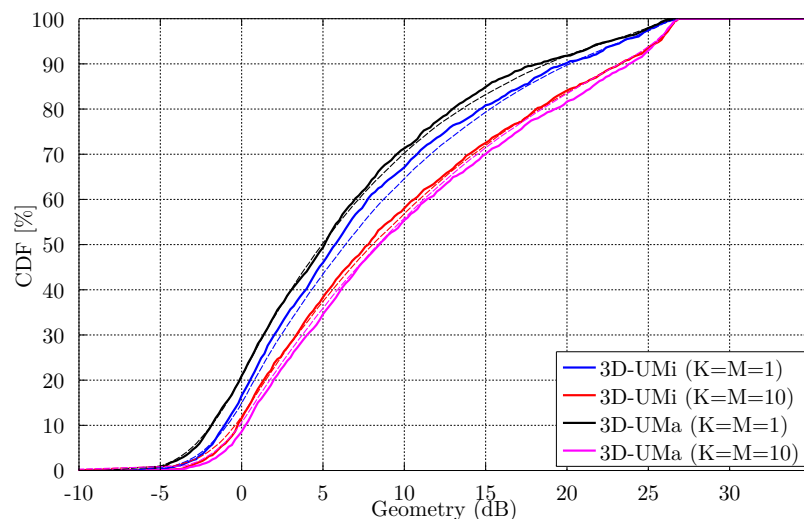
Geometry Factor (Phase 1) The geometry factor (GF) is a lower bound for the actual signal to interference and noise ratio (SINR). It is defined as the power ratio of the serving **BS** to the sum power of all interfering **BSs**. The results in Fig. 16 agree well with the 3FPP calibrations curves. Remaining tolerances are within the range of results reported in [30] (see table in Fig. 16).

Zenith Angle of Departure (Phase 1) The ZoD is calculated from the **LOS** path between the serving **BS** and the **MT** position. The values in Fig. 17 prove that the model is a 3D model. Users are placed on different floors and the serving **BS** is determined based on the power of the **LOS** path. Note that this power value changes when different antenna patterns are used. Hence, the assignment of **MTs** to **BSs** is different, depending on which antennas are used at the **BS**, which explains why the curves differ from each other. The results obtained from QuaDRiGa agree almost perfectly with the 3GPP calibration curves (tolerances are within 0.1 degree).



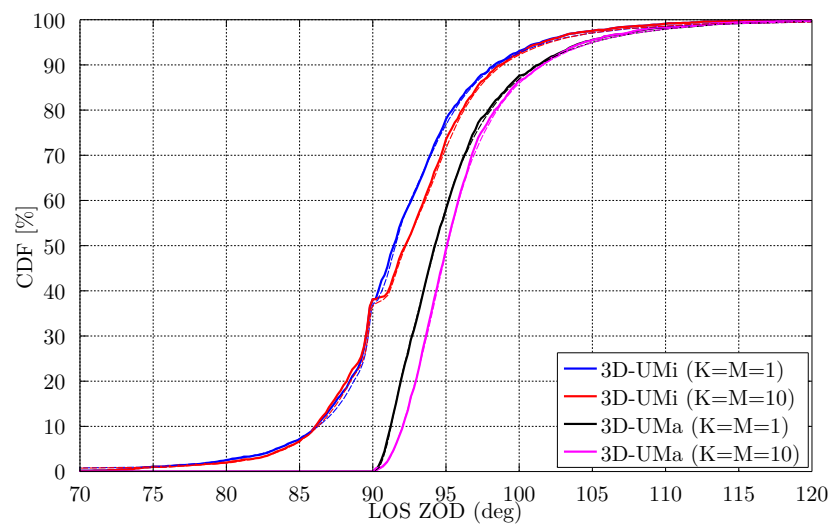
| Case | QuaDRiGa | 3GPP Median | 3GPP Min. | 3GPP Max |
|-----------------|----------|-------------|-----------|----------|
| 3D-UMi (K=M=1) | -97.1 | -98.2 | -100.8 | -96.4 |
| 3D-UMi (K=M=10) | -102.2 | -103.0 | -105.6 | -101.1 |
| 3D-UMa (K=M=1) | -112.4 | -112.3 | -114.6 | -111.1 |
| 3D-UMa (K=M=10) | -112.3 | -112.3 | -114.3 | -111.1 |

Figure 15: 3GPP-3D Calibration Results: Coupling Loss (Phase 1)



| Case | QuaDRiGa | 3GPP Median | 3GPP Min. | 3GPP Max |
|-----------------|----------|-------------|-----------|----------|
| 3D-UMi (K=M=1) | 5.9 | 6.4 | 5.7 | 7.0 |
| 3D-UMi (K=M=10) | 7.9 | 8.1 | 7.3 | 9.0 |
| 3D-UMa (K=M=1) | 5.2 | 4.9 | 4.5 | 5.3 |
| 3D-UMa (K=M=10) | 8.6 | 8.4 | 7.7 | 9.0 |

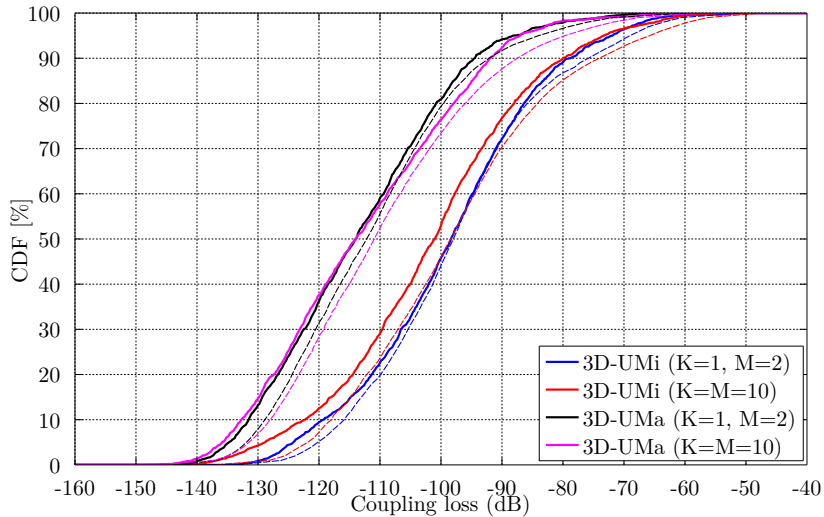
Figure 16: 3GPP-3D Calibration Results: Geometry Factor (Phase 1)



| Case | QuaDRiGa | 3GPP Median | 3GPP Min. | 3GPP Max |
|-----------------|----------|-------------|-----------|----------|
| 3D-UMi (K=M=1) | 91.5 | 91.6 | 91.2 | 91.7 |
| 3D-UMi (K=M=10) | 92.3 | 92.3 | 92.0 | 92.5 |
| 3D-UMa (K=M=1) | 94.3 | 94.3 | 93.9 | 94.6 |
| 3D-UMa (K=M=10) | 95.2 | 95.1 | 94.9 | 95.4 |

Figure 17: 3GPP-3D Calibration Results: Zenith of Departure Angle (Phase 1)

Coupling Loss (Phase 2) In the second phase of the calibration, the SSF model is enabled. Hence, all NLOS paths are included in the evaluations. For this reason, the coupling loss changes compared to phase 1. Multiple paths are now differently weighted by the antenna pattern, depending on the departure angles at the BS. The path gain is calculated by averaging the power of all sublinks of the 2×4 MIMO channel matrix. As for phase 1, the coupling loss is the path gain of the serving BS and MTs are assigned to BSs based on the maximum path gain value. Results are depicted in Fig. 18. QuaDRiGa results are within the ranges reported in [30]. However, the differences are larger as in phase 1.

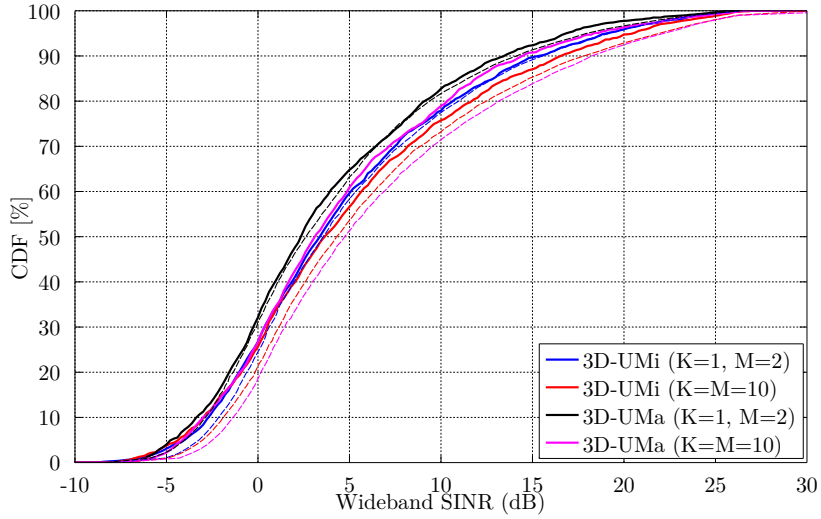


| Case | QuaDRiGa | 3GPP Median | 3GPP Min. | 3GPP Max |
|-------------------|----------|-------------|-----------|----------|
| 3D-UMi (K=1, M=2) | -98.3 | -98.0 | -99.8 | -96.2 |
| 3D-UMi (K=M=10) | -100.9 | -98.4 | -103.2 | -95.9 |
| 3D-UMa (K=1, M=2) | -113.9 | -112.2 | -114.0 | -110.5 |
| 3D-UMa (K=M=10) | -113.9 | -110.9 | -114.0 | -110.0 |

Figure 18: 3GPP-3D Calibration Results: Coupling Loss (Phase 2)

Wideband SINR The wideband SINR is essentially the same as the GF. However, the 3GPP model uses the reference signal received power (RSRP) values for the calculation of this metric. The calculation method is described in [8] on page 33. Essentially, the RSRP values describe the average received power (over all antenna elements at the receiver) for each transmit antenna port. Hence, in the phase 2 calibration, there are 4 RSRP values, one for each transmit antenna. The wideband SINR is the GF calculated from the first RSRP value, i.e. the average power for the first transmit antenna port. Results are depicted in Fig. 19.

Zenith of Departure Spread The zenith of departure spread is calculated without the influence of the antenna patterns. Only the raw value before weighting the path powers with the antenna gain is used. This is not immediately clear from [8], because the calculation method is not specified. However, a high gain pattern, such as used for the $K = M = 10$ cases, would significantly decrease the angular spread compared to the low-gain patterns ($K = 1, M = 2$) since may paths get less power due to the weighting with the antenna pattern. Hence, we conclude that the angular spreads are calculated without influence of the antenna patterns.



| Case | QuaDRiGa | 3GPP Median | 3GPP Min. | 3GPP Max |
|-------------------|----------|-------------|-----------|----------|
| 3D-UMi (K=1, M=2) | 3.5 | 3.6 | 3.2 | 4.5 |
| 3D-UMi (K=M=10) | 3.7 | 4.3 | 4.0 | 5.3 |
| 3D-UMa (K=1, M=2) | 2.4 | 2.6 | 2.2 | 3.5 |
| 3D-UMa (K=M=10) | 3.2 | 4.7 | 3.0 | 5.3 |

Figure 19: 3GPP-3D Calibration Results: Wideband SINR (Phase 2)

Unfortunately, [8] does also not define how the angular spread is calculated. Here, we extract the angles and the path powers from the QuaDRiGa SSF model and calculate the RMS angular spread as

$$\bar{\phi} = \arg \left(\sum_{l=1}^L P_l \cdot \exp(j\phi_l) \right), \quad (103)$$

$$\phi_l^{[*]} = (\phi_l - \bar{\phi} + \pi \bmod 2\pi) - \pi, \quad (104)$$

$$\sigma_\phi = \sqrt{\frac{1}{P} \cdot \sum_{l=1}^L P_l \cdot (\phi_l^{[*]})^2 - \left(\frac{1}{P} \cdot \sum_{l=1}^L P_l \cdot \phi_l^{[*]} \right)^2}, \quad (105)$$

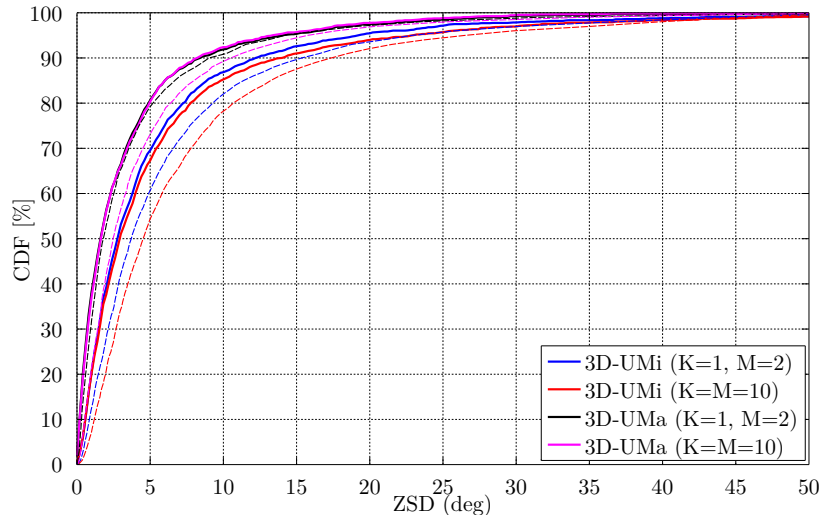
where ϕ_l is the raw departure or arrival angle of a path obtained from the model, $\bar{\phi}$ is the mean angle of all paths belonging to a CIR, and $\phi_l^{[*]}$ is the angle where the mean angle is equal to 0° . P_l is the power of a path, P is the total power in the CIR, and L is the number of paths.

To gain some information about the expected values, we can use the formulas in [8], page 32. Most of the users are in NLOS conditions and 80% of them are situated indoors. Simulation results show that the average distance between the MT and the serving BS is 0.65 times the ISD. Also, the average height for the indoor users is 9 m. With those values, the expected median ZSD for this case are:

$$\mu_{ZSD}(\text{UMa, NLOS, O2I}) = 10^{-2.1(d_{2D}/1000)-0.01(h_{MT}-1.5)+0.9} \approx 1.4^\circ \quad (106)$$

$$\mu_{ZSD}(\text{UMi, NLOS, O2I}) = 10^{-2.1(d_{2D}/1000)+0.01\cdot\max(h_{MT}-h_{BS},0)+0.9} \approx 4.4^\circ \quad (107)$$

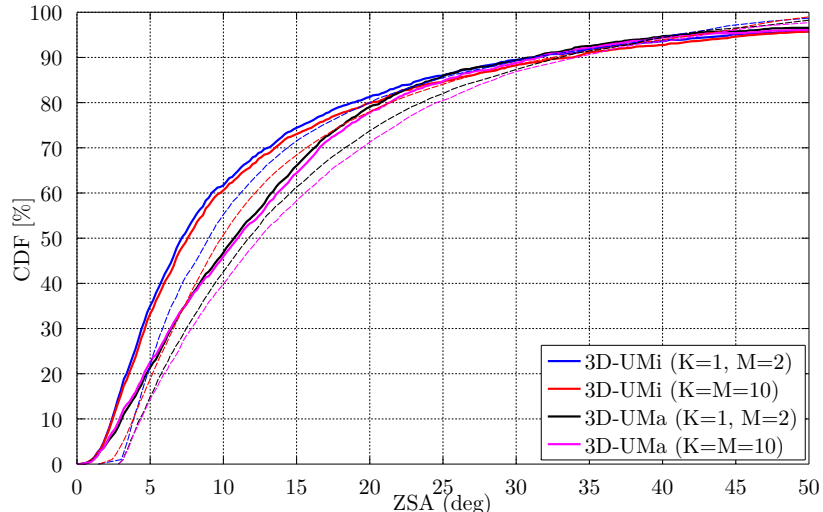
Results in Fig. 20 show that the median ZOD values for the 3GPP calibration are around 4° for UMi and 2° for UMa. However, QuaDRiGa produces smaller values of 3° for UMi and 1.7° for UMa. Those values are outside the reported ranges in [30]. At the moment, the reason for this is unclear.



| Case | QuaDRiGa | 3GPP Median | 3GPP Min. | 3GPP Max |
|-------------------|----------|-------------|-----------|----------|
| 3D-UMi (K=1, M=2) | 2.9 | 3.7 | 3.1 | 4.9 |
| 3D-UMi (K=M=10) | 3.0 | 4.5 | 3.9 | 5.7 |
| 3D-UMa (K=1, M=2) | 1.7 | 1.8 | 1.6 | 2.2 |
| 3D-UMa (K=M=10) | 1.7 | 2.5 | 1.9 | 3.0 |

Figure 20: 3GPP-3D Calibration Results: Zenith of Departure Spread (Phase 2)

Zenith of Arrival Spread The **ZSA** is calculated in the same way as the **ZSD**. It is notable here, that the for all outdoor-to-indoor (O2I) scenarios, identical values were proposed for the **ZSA** in [8]. The median value is given as $\mu_{ZSA}(O2I) \approx 10.2^\circ$. Since 80% of the **MTs** are indoors, the median value should be around 10.2 for all scenarios and antenna configurations. Surprisingly, the results show differences in the median **ZSA**, depending on the antenna and scenario settings (see Fig. 21) for both, the 3GPP-3D reference curves and the QuaDRiGa results. The reason for this is currently subject to speculation. As for the **ZSD**, QuaDRiGa tends to predict slightly lower median values compared to the 3GPP-3D reference.



| Case | QuaDRiGa | 3GPP Median | 3GPP Min. | 3GPP Max |
|-------------------|----------|-------------|-----------|----------|
| 3D-UMi (K=1, M=2) | 7.3 | 9.0 | 8.0 | 12.6 |
| 3D-UMi (K=M=10) | 7.6 | 9.9 | 8.6 | 12.0 |
| 3D-UMa (K=1, M=2) | 10.8 | 11.7 | 10.7 | 15.5 |
| 3D-UMa (K=M=10) | 11.1 | 12.4 | 11.2 | 14.5 |

Figure 21: 3GPP-3D Calibration Results: Zenith of Arrival Spread (Phase 2)

Largest and smallest singular values The singular values of a MIMO channel matrix describe how many parallel spatial data streams can be transmitted to one user and what the individual capacity of each streams is. The simulation settings propose two settings: One with four vertically polarized antennas at the BS and 2 vertically polarized antennas at the receiver (configuration 1), and one with 2 cross-polarized high-gain an antennas at the BS and an ideal cross-polarized antenna array at the receiver (configuration 2). Both configurations result in a 2×4 MIMO channel. Hence, the channel has two singular values and supports at most two streams.

The 3GPP-3D report [8] does not mention, how the singular values are calculated from the channel matrix. It was only discussed internally. The method is as follows:

1. The results are reported for the channel matrix of the serving BS. The serving BS is determined at the MT by the highest received power of all BS in the layout.
2. The calculations are done in the frequency domain. The bandwidth is set to 10 MHz, which is further split into 50 resource blocks (RBs) of 200 kHz bandwidth, each. Each RB can further be divided into n_{RB} sub-carriers. However, for the QuaDRiGa results, we only used one subcarrier per RB.
3. The singular values are reported for channels without path-gain, but with antenna patterns included. Hence, one needs to extract the path-gain at the MT position from the channel model and normalize the channel matrix accordingly, i.e.

$$\mathbf{H} = \frac{\mathbf{H}^{[raw]}}{\sqrt{10^{0.1 \cdot PG_{dB}}}} \quad (108)$$

4. The “singular values” are calculated for each RB by an Eigen-value decomposition of the receive covariance matrix as

$$s_{1,2} = \frac{1}{n_{RB}} \cdot \text{eig} \left(\sum_{n=1}^{n_{RB}} \mathbf{H}_n \mathbf{H}_n^H \right) \quad (109)$$

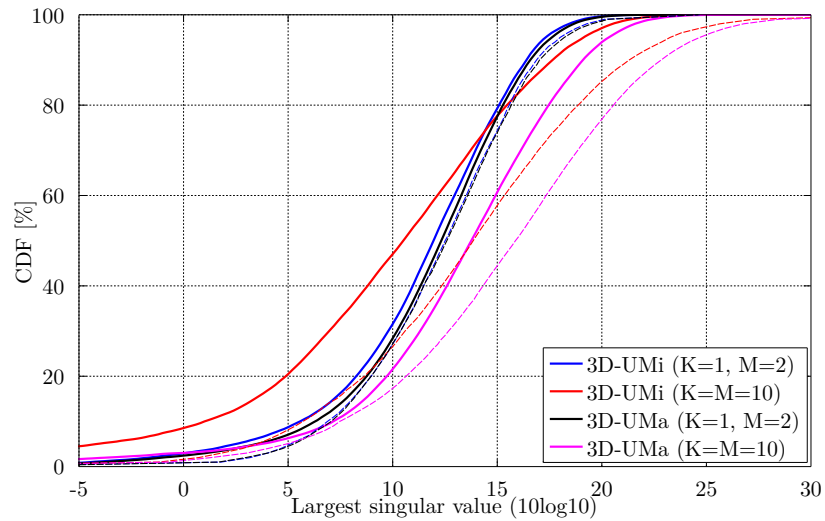
for one single carrier, the relationship between the eigenvalues of the covariance matrix and the singular values of the channel matrix is given by

$$s_{1,2} = \text{eig} (\mathbf{H}_n \mathbf{H}_n^H) = \{\text{svd} (\mathbf{H})\}^2 \quad (110)$$

5. Results are presented in logarithmic scale, i.e. as $10 \cdot \log_{10}(s_{1,2})$.

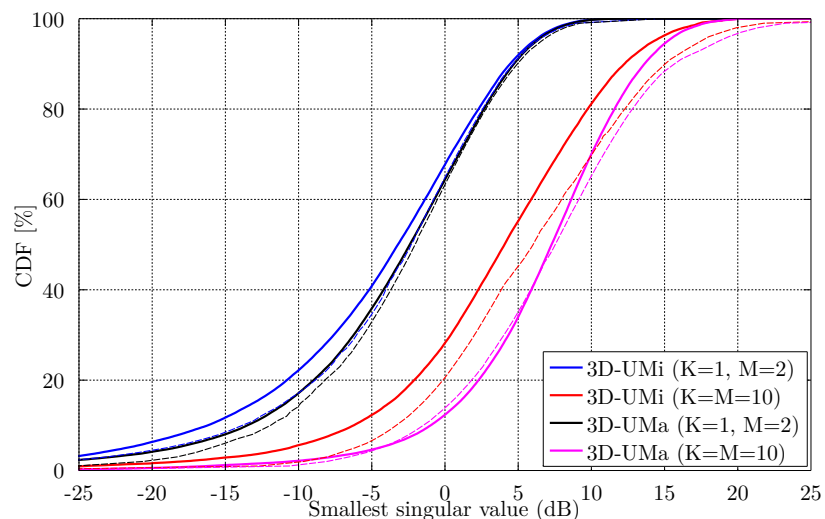
Figure 22 shows the distribution of the largest singular value. For the results with co-polar antennas (the blue and black curve), there is an almost perfect match between QuaDRiGa and the 3GPP calibration curves. The results for the cross-polar antennas (red and magenta line) show some differences. However, the results from individual partners in [30] also show a significant spread in this case. Median results for the UMi scenario (red curve) ranged from 9 to 15 dB. QuaDRiGa predicts 10.6 dB, which is still well within the reported range.

The results for the smallest singular value are shown in Figure 23. Here, QuaDRiGa performs very close to the median results reported in [30].



| Case | QuaDRiGa | 3GPP Median | 3GPP Min. | 3GPP Max |
|-----------------------|----------|-------------|-----------|----------|
| 3D-UMi ($K=1, M=2$) | 12.1 | 12.5 | 10.9 | 13.2 |
| 3D-UMi ($K=M=10$) | 10.6 | 13.8 | 9.0 | 15.0 |
| 3D-UMa ($K=1, M=2$) | 12.4 | 12.6 | 10.9 | 12.8 |
| 3D-UMa ($K=M=10$) | 13.9 | 15.9 | 11.7 | 16.2 |

Figure 22: 3GPP-3D Calibration Results: Largest Singular Value (Phase 2)



| Case | QuaDRiGa | 3GPP Median | 3GPP Min. | 3GPP Max |
|-----------------------|----------|-------------|-----------|----------|
| 3D-UMi ($K=1, M=2$) | -3.2 | -2.3 | -5.5 | -0.1 |
| 3D-UMi ($K=M=10$) | 4.1 | 6.0 | 1.3 | 7.8 |
| 3D-UMa ($K=1, M=2$) | -2.4 | -2.0 | -5.8 | 1.7 |
| 3D-UMa ($K=M=10$) | 7.3 | 7.5 | 4.6 | 9.4 |

Figure 23: 3GPP-3D Calibration Results: Smallest Singular Value (Phase 2)

Ratio of singular values Probably a more important measure than the singular values themselves is the ratio between the singular values, which is calculated as

$$SR = 10 \cdot \log_{10} \left(\frac{s_1}{s_2} \right) \quad (111)$$

This measure is closely linked to the condition number of the channel matrix $C = \sqrt{\frac{s_1}{s_2}}$. The larger this number is, the more difficult it is to invert the matrix \mathbf{H} . However, inverting this matrix is required in order to separate the two data streams at the receiver.

Results are shown in Fig. 24. As can be seen, the ratio is much higher for the co-polar antenna configuration (blue and black curve). For cross-polar channels, the ratio is about one order of magnitude lower, since an additional degree of freedom is provided by the second polarization. Results from QuaDRiGa generally agree well. However, there is one exception for the 3D-UMa cross-polar case, where QuaDRiGa predicts a SV-ratio of 6.1 dB. The lowest reported value in [30] is 6.3 dB.

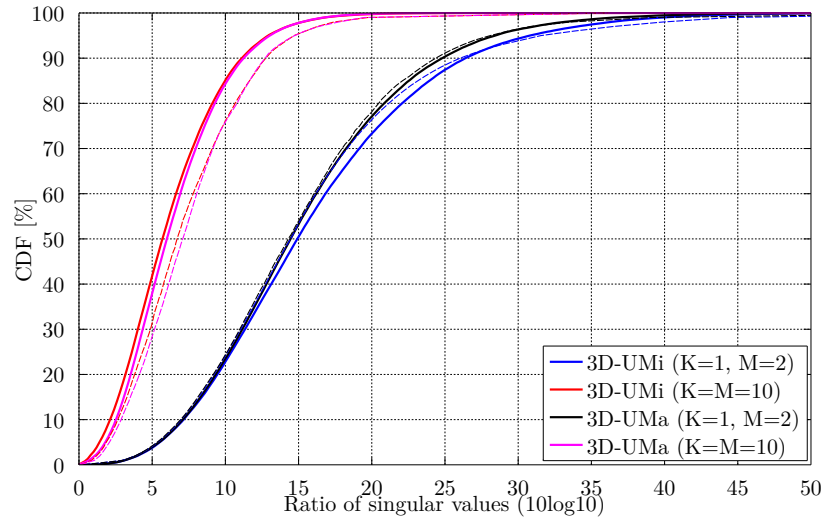


Figure 24: 3GPP-3D Calibration Results: Ratio of Singular Values (Phase 2)

A Tutorials

In the following, we provide a variety of tutorials that can get you started with QuaDRiGa. You can also use the MATLAB Help to access these files.

A.1 Network Setup and Parameter Generation

The channel model class 'parameter_set' generates correlated values for the LSPs. The channel builder then uses those values to create coefficients that have the specific properties defined in 'parameter_set'. One important question is therefore: Can the same properties which are defined in 'parameter_set' also be found in the generated coefficients? This is an important test to verify, if all components of the channel builder work correctly.

Channel model setup and coefficient generation We first set up the basic parameters. We do not need drifting here, since no time varying channels are generated.

```

1 close all
2 clear all
3
4 set(0, 'defaultTextFontSize', 14)
5 set(0, 'defaultAxesFontSize', 14)
6
7 s = simulation_parameters;
8 s.center_frequency = 2.53e9;
9 s.sample_density = 2;
10 s.use_absolute_delays = 1;
11 s.drifting_precision = 0;
```

We have one transmitter and 250 receiver positions. Each receiver gets a specific channel. However, the receivers LSPs will be correlated. We use omni directional antennas at all terminals.

```

1 l = layout( s );
2 l.no_rx = 250;
3 l.randomize_rx_positions( 200 , 1.5 , 1.5 , 1 ); % 200 m radius, 1.5 m Rx height
4 l.track.set_scenario('BERLIN_UMa_NLOS');
5
6 l.tx_position(3) = 25; % 25 m tx height
7 l.tx_array.generate( 'omni' );
8 l.rx_array = l.tx_array;
9
10 l.visualize([],[],0);
11 view(-33, 60);

```

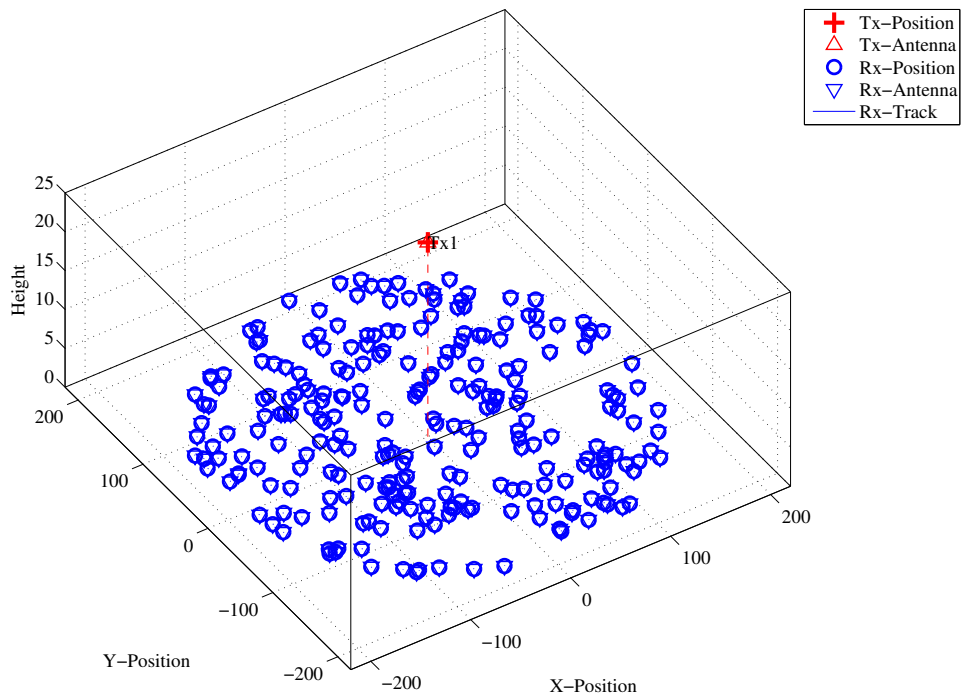


Figure 25: Distribution of the users in the scenario.

We set up the scenario such that there is no XPR. I.e. all vertical polarized paths will remain vertical after a reflection. The same result would be achieved with a perfectly X-polarized array at the receiver and summing up the power over all elements. We further increase the KF to have a wider spread. This allows us to study the parameters at a wider range when evaluating the results.

```

1 p = l.create_parameter_sets(0);
2 p.plpar = [];
3 p.scenpar.xpr_mu      = 100;          % Disable XPR
4 p.scenpar.xpr_sigma   = 0;
5 p.scenpar.KF_mu       = 5;            % Increase KF-Range
6 p.scenpar.KF_sigma    = 15;
7 p.scenpar.DS_mu       = log10(0.6e-6); % Median DS = 600 ns
8 p.scenpar.DS_sigma    = 0.3;          % 300-1200 ns range
9 p.update_parameters;
10
11 c = p.get_channels;
12
13 coeff = squeeze( cat( 1, c.coeff ) );
14 delay = permute( cat(3,c.delay) , [3,1,2] );

```

| | | |
|--------------|--|-----------|
| 1 Parameters | [oo] | 5 seconds |
| 2 Channels | [oo] | 8 seconds |

Results and discussion In the following four plots, we extract parameters from the generated coefficients and compare them with the initial ones which were generated by the 'parameter_set' object (P). The values in (P) can be seen as a request to the channel builder and the values in the generated coefficients (C) as a delivery.

We first calculate the SF from the channel data by summing up the power over all 20 taps. We see, that the values are almost identical.

```

1 sf = sum(mean(abs(coeff).^2,3),2);
2
3 figure
4 plot(-35:35,-35:35,'k')
5 hold on
6 plot([-35:35]+3,-35:35,'--k')
7 plot([-35:35]-3,-35:35,'--k')
8 plot(10*log10(p.sf'),10*log10(sf),'.')
9 hold off
10 axis([-25,25,-25,25])
11
12 legend('Equal','+/- 3dB',4)
13 xlabel('SF_P [dB]');
14 ylabel('SF_C [dB]');
15 title('Shadow Fading - Requested vs. generated value');

```

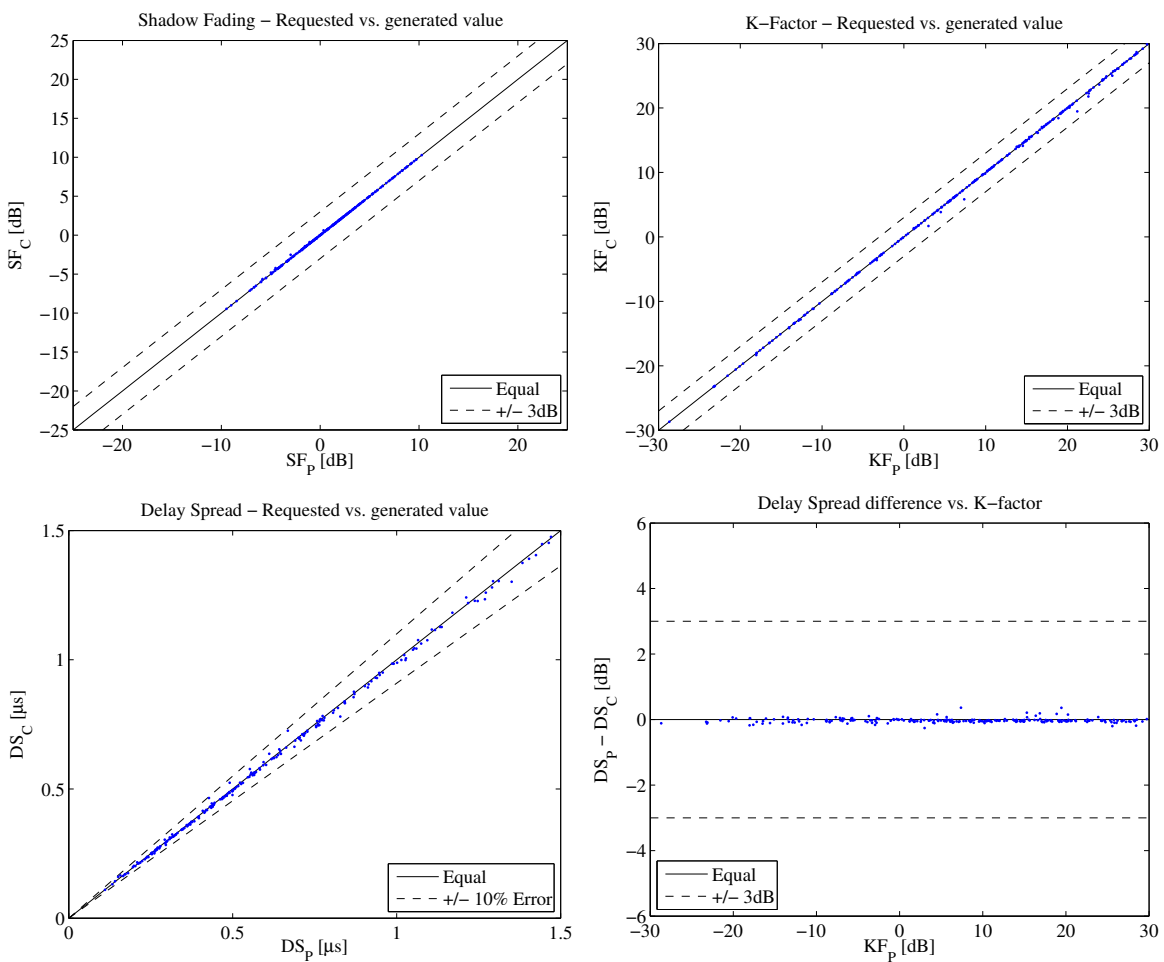


Figure 26: Comparison of input values and simulation results

Next, we repeat the same calculation for the K-Factor. Again, we see that the values are almost identical.

```

1 p_nlos = sum(mean(abs(coeff(:,2:end,:)).^2,3),2);
2 p_los = mean(abs(coeff(:,1,:)).^2,3);
3 kf = p_los./p_nlos;
4
5 figure
6 plot(-35:35,-35:35,'k')
7 hold on
8 plot([-35:35]+3,-35:35,'--k')
9 plot([-35:35]-3,-35:35,'--k')
10 plot(10*log10(p.kf'), 10*log10(kf), '.')
11 hold off
12 axis([-30, 30, -30, 30])
13
14 legend('Equal','+/- 3dB',4)
15 xlabel('KF_P [dB]');
16 ylabel('KF_C [dB]');
17 title('K-Factor - Requested vs. generated value');
18
19

```

Now we repeat the calculation for the RMS delays spread.

```

1 pow_tap = abs(coeff).^2;
2 pow_sum = sum(pow_tap,2);
3 mean_delay = sum(pow_tap.*delay,2) ./ pow_sum;
4 ds = sqrt(sum(pow_tap.*delay.^2,2)./pow_sum - mean_delay.^2);
5 ds = mean(ds,3);
6
7 figure
8 plot([0:0.1:2],[0:0.1:2],'k')
9 hold on
10 plot([0:0.1:2]*1.1,[0:0.1:2],'--k')
11 plot([0:0.1:2],[0:0.1:2]*1.1,'--k')
12 plot(p.ds'*1e6,(ds)*1e6,'.')
13 hold off
14 axis([0,1.5,0,1.5])
15
16 legend('Equal','+/- 10% Error',4)
17 xlabel('DS_P [\mu s]');
18 ylabel('DS_C [\mu s]');
19 title('Delay Spread - Requested vs. generated value');
20
21

```

The following plot shows the RMSDS of the requested and generated values (in dB) vs. the K-factor. A value of +3 means, that the RMSDS of the generated coefficients is twice a high as in the parameter_set (P). We see, that for a K-Factor of up to 30 dB, the DS difference is small (less than 3 dB).

```

1 figure
2 plot([-35,35],[0,0],'k')
3 hold on
4 plot([-35,35],[-3,-3],'--k')
5 plot([-35,35],[3,3],'--k')
6 plot(10*log10(p.kf'), 10*log10(ds./p.ds'), '.')
7 hold off
8 axis([-30, 30, -6 6])
9
10 legend('Equal','+/- 3dB',3)
11 xlabel('KF_P [dB]');
12 ylabel('DS_P - DS_C [dB]');
13 title('Delay Spread difference vs. K-factor');
14
15

```

```

1 close all
2 disp(['QuaDRiGa Version: ',simulation_parameters.version])
3

```

```

1 QuaDRiGa Version: 1.0.1-145
2

```

A.2 Simulating a Measured Scenario

This script recreates a measured drive test from the Park Inn Hotel at Berlin Alexanderplatz. The transmitter was at the rooftop of the hotel while the mobile receiver was moving south on Grunerstraße. A simplified version of the scenario is recreated in the simulation where the scenarios along the track were classified by hand.

Channel model setup and coefficient generation First, we set up the channel model.

```

1 set(0,'defaultTextFontSize', 14)
2 set(0,'defaultAxesFontSize', 14)
3 RandStream.setGlobalStream(RandStream('mt19937ar','seed',1));
4
5 close all
6 clear all
7
8 s = simulation_parameters;                                % Basic simulation parameters
9 s.center_frequency = 2.185e9;
10 s.sample_density = 2;
11 s.use_absolute_delays = 1;
12
13 t = track('linear',500,-135*pi/180);                  % Track with 500m length, direction SE
14 t.initial_position = [120;-120;0];                      % Start position
15 t.interpolate_positions( 1 );                            % Interpolate to 1 sample per meter
16
17 t.segment_index = [1    45   97   108  110  160  190  215  235  245 ...
18     280  295  304  330  400  430 ];                     % Set segments (states)
19
20 S1 = 'MIMOSA_10-45_LOS';
21 Sn = 'MIMOSA_10-45_NLOS';
22 t.scenario      = {Sn,S1,Sn,S1,Sn,Sn,S1,Sn,S1,Sn,Sn,Sn,S1};
23 t.interpolate_positions( 3 );
24
25 l = layout( s );
26 l.tx_position = [0;0;125];                             % Set the position of the Tx
27 l.track = t;                                         % Set the rx-track
28
29 l.tx_array = array('rhcp-lhcp-dipole');                % Generate Tx antenna
30 l.tx_array.rotate_pattern(30,'y');                      % 30 deg Tilt
31 l.tx_array.rotate_pattern(-90,'z');                    % point southwards
32
33 l.rx_array = array('rhcp-lhcp-dipole');                % Rx-Antenna
34 l.rx_array.rotate_pattern(-90,'y');                    % point skywards
35
36 l.visualize;
37 view(-33, 45);
38
39 lnk = [ l.tx_position, ...
40     l.track.positions(:,l.track.segment_index(2))+l.track.initial_position ];
41
42 hold on
43 plot3( lnk(1,:),lnk(2,:),lnk(3,:), '--' )
44 hold off

```

Generate channel coefficients Next, we calculate the channel coefficients.

```

1 [p,cb] = l.create_parameter_sets(0);
2 p(2).scenpar.NumClusters = 14;
3 p.update_parameters;
4
5 c = cb.get_channels;
6 cn = c.merge(0.2);

```

| | | |
|------------|--|------------|
| Parameters | [oooooooooooooooooooooooooooooooooooo] | 31 seconds |
| Channels | [oooooooooooooooooooooooooooooooooooo] | 15 seconds |
| Merging | [oooooooooooooooooooooooooooooooooooo] | 2 seconds |

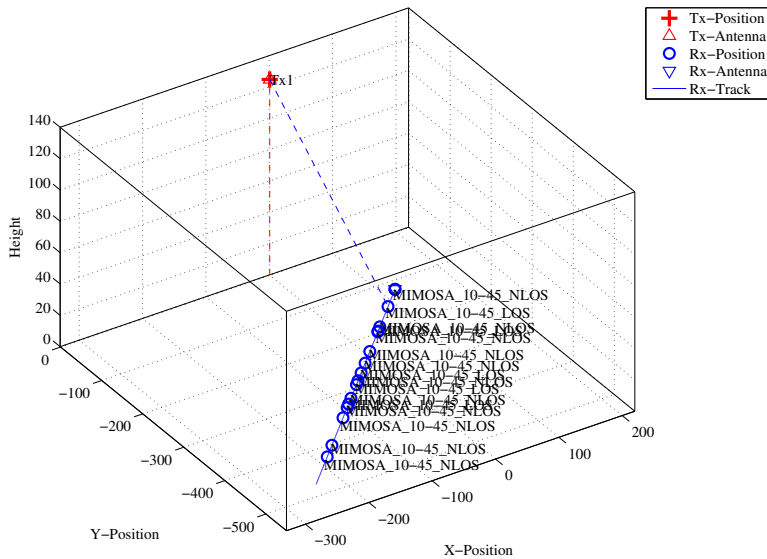


Figure 27: Scenario setup for the comparison of simulated and measured data

Results First, we plot the PDP vs distance from the start point (see Fig. 28).

```

1 h = cn(1).fr( 20e6,256 );
2 pdp = squeeze(sum(sum( abs(ifft(h,[],3)).^2 , 1),2));
3 pdp = 10*log10(pdp.');
4
5 figure
6 imagesc(pdp(end:-1:1,1:192));
7
8 cm = colormap('hot');
9 colormap(cm(end:-1:1,:));
10
11 caxis([ max(max(pdp))-60 max(max(pdp))-5 ]);
12 colorbar
13
14 title('Time variant power delay profile');
15
16 set(gca,'XTick',1:32:192);
17 set(gca,'XTickLabel',(0:32:192)/20e6*1e6);
18 xlabel('Delay [\mu s]');
19
20 ind = sort(cn.no_snap : -cn(1).no_snap/10 : 1);
21 set(gca,'YTick', ind );
22 set(gca,'YTickLabel', round(sort(500-ind / 3,'descend')) );
23 ylabel('Distance [m]');

```

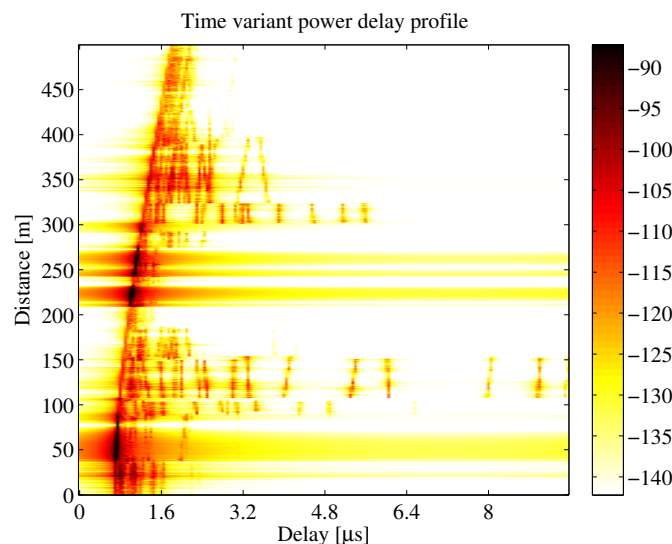


Figure 28: 2D PDP of the simulated track

The next plot shows the total received power along the path (Fig. 29, top left). Green shaded ares are LOS. The rest is NLOS.

```

1 dist = (1:cn.no_snap)*l.track.get_length/cn.no_snap;
2 ind = find(strcmp(l.track.scenario,S1));
3 los = [];
4 for n = 1:numel(ind)
5     los = [los l.track.segment_index(ind(n)) : l.track.segment_index(ind(n)+1)];
6 end
7
8 power = 10*log10( sum( reshape( abs(cn.coeff).^2 , [] , cn.no_snap ) ,1)/4 );
9 ar = zeros(1,cn.no_snap);
10 ar(los) = -200;
11
12 figure
13 a = area(dist,ar);
14 set(a(1),'FaceColor',[0.7 0.9 0.7]);
15 set(a,'LineStyle','none')
16
17 hold on
18 plot(dist,power)
19 hold off
20
21 title('Position dependent power')
22 xlabel('Track [m]');
23 ylabel('Power [dB]');
24 axis([0 500 min(power)-5 max(power)+5])
25 legend('LOS','P_{total}',4)
26 grid on

```

The following plot (Fig. 29, top right) shows the distribution (PDF) of the received power for both, the LOS and NLOS segments.

```

1 bins = -150:2:-80;
2 p_los = hist(power(los),bins)/cn.no_snap*100;
3 p_nlos = hist(power(setdiff(1:cn.no_snap,los)),bins)/cn.no_snap*100;
4
5 figure
6 bar(bins,[p_los;p_nlos])
7 axis([-124.5,-83,0,ceil(max([p_los,p_nlos]))])
8 grid on
9 colormap('Cool')
10
11 title('Empirical PDF of the \ac{LOS} and NLOS power')
12 xlabel('P_{total} [dB]');
13 ylabel('Probability [%]');
14 legend('LOS','NLOS',1)

```

The next plot shows the RMS delay spread along the path. Again, shaded ares are for the LOS segments.

```

1 pow_tap = squeeze(sum(sum(abs(cn.coeff).^2,1),2));
2 pow_sum = sum( pow_tap,1 );
3 mean_delay = sum( pow_tap.*cn.delay ,1) ./ pow_sum;
4 ds = sqrt( sum( pow_tap.*cn.delay.^2 ,1) ./ pow_sum - mean_delay.^2 );
5 ar = zeros(1,cn.no_snap);
6 ar(los) = 10;
7
8 figure
9 a = area(dist,ar);
10 set(a(1),'FaceColor',[0.7 0.9 0.7]);
11 set(a,'LineStyle','none')
12
13 hold on
14 plot( dist , ds*1e6 )
15 hold off
16
17 ma = 1e6*( max(ds)+0.1*max(ds) );
18 axis([0 500 0 ma])
19 title('Position dependant delay spread');
20 xlabel('Track [m]');
21 ylabel('Delay Spread [dB]');
22 legend('LOS','\sigma_\tau',1)
23 grid on

```

The final plot (Fig. 29, bottom right) shows the distribution (PDF) of the RMS delay spread for both, the LOS and NLOS segments.

```

1 bins = 0:0.03:3;
2 ds_los = hist(ds(los)*1e6,bins)/cn.no_snap*100;
3 ds_nlos = hist(ds(setdiff(1:cn.no_snap,los))*1e6,bins)/cn.no_snap*100;
4
5 figure
6 bar(bins,[ds_los;ds_nlos]')
7 axis([0,1.5,0,ceil(max([ds_los,ds_nlos]))])
8 grid on
9 colormap('Cool')
10
11 title('Empirical PDF of the LOS and NLOS RMSDS')
12 xlabel('\sigma_\tau [\mu\text{s}]\n');
13 ylabel('Probability [%]\n');
14 legend('LOS','NLOS',1)

```

```

1 close all
2 disp(['QuaDRiGa Version: ',simulation_parameters.version])

```

```
1 QuaDRiGa Version: 1.0.1-145
```

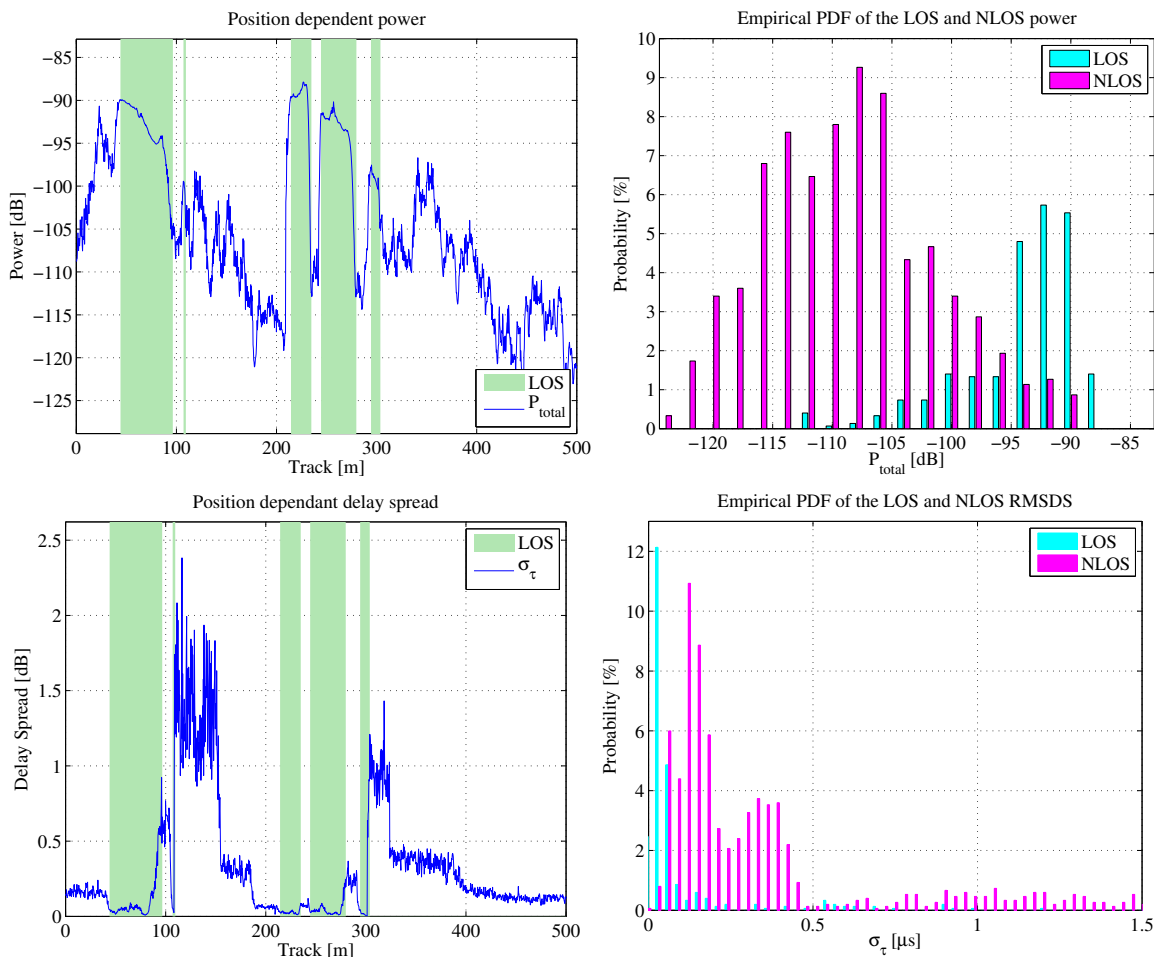


Figure 29: Results for the measurement based simulation tutorial

A.3 Generation of Satellite Channels

This script demonstrates the parametrization of the channel model to generate time-continuous sequences for a satellite scenario.

Setting up the Simulation Parameters First, we set up the general simulation parameters. We choose a center frequency of 2.1 GHz. We also want to use drifting in order to get the correct delays and angles for the time-continuous simulation. A sample density of 2.5 ensures that the channel coefficients can be interpolated to different playback speeds later on.

```

1 close all
2 clear all
3
4 s = simulation_parameters;           % Basic simulation parameters
5 s.center_frequency      = 2.185e9;
6 s.sample_density        = 0.25;
7
8 RandStream.setGlobalStream(RandStream('mt19937ar','seed',1));

```

Creating a random Track and defining states along the track Next, we generate a simulation track. A track describes the movement of a mobile terminal. It is composed of an ordered list of positions. During the simulation, one snapshot is generated for each position on the track. Later on, the generation of the track is done by the state sequence generator. Here, we implement a simple version of the sequence generator to generate a random track. We first create a set of streets with different length. We assume a normal distribution of the street length where the parameters mu and sigma were fitted from random distances between two crossings in central Berlin (measured with Google earth).

```

1 street_length_mu = 187;           % Average street length in m
2 street_length_sigma = 83;
3 min_street_length = 50;
4
5 turn_probability = 0.4;          % The prob. that the car turns at a crossing
6 curve_radius = 10;              % The curve radius in m
7 diro = rand * 2*pi;             % Random start direction

```

For the given parameters, we calculate a list of points along the track that resemble the street grid and the turns at crossings.

```

1 point = 0;                      % The start point (always at [0,0])
2 m = 1;                          % A counter for the points
3 for n = 1:3                      % We simulate 3 street segments
4
5 % Get a random street length drawn from the distribution defined above
6 street_length = randn*street_length_sigma + street_length_mu;
7 while street_length < min_street_length
8     street_length = randn*street_length_sigma + street_length_mu;
9 end
10
11 % Get 3 points along the street
12 point(m+1) = point(m) + exp(1j*diro) * street_length*0.1;
13 point(m+2) = point(m) + exp(1j*diro) * street_length*0.9;
14 point(m+3) = point(m) + exp(1j*diro) * street_length;
15 m=m+3;
16
17 % At a crossing, the car could change its direction. This is
18 % modeled here
19 if rand < turn_probability
20     dirn = diro + sign( rand-0.5 ) * pi/2 + randn*pi/12;
21     point(m+1) = point(m) + curve_radius*( exp(1j*diro) + exp(1j*dirn) );
22     diro = dirn;
23     m=m+1;
24 end
25 end

```

Next, we create a track object and pass the points along the track. We then use the internal interpolation functions to interpolate the track to 1 point per meter.

```

1 t = track;                                % Create a track object
2 t.positions = [ real(point) ; imag(point) ; zeros(1,numel(point)) ];
3 t.interpolate_positions( 1 );    % Interpolate to 1 point per meter

```

We now assemble a rudimentary state sequence generator that generates different states along the track. We first define the distribution parameters of the segment length and then calculate the segments themselves. The two possible states are "MIMOSA_10-45_LOS" which stands for LOS or good state and "MIMOSA_10-45_NLOS" for NLOS or bad state.

```

1 segment_length_mu = 30;                  % Average segment length in m
2 segment_length_sigma = 12;                % Standard deviation in m
3 min_segment_length = 10;                 % Minimum segment length in m
4
5 % Now we define the segments (the states) along the track
6 ind = 1;
7 while ind < t.no_snapshots
8
9 % Each scenario has a 50% probability
10 if rand < 0.5
11     t.scenario{ t.no_segments } = 'MIMOSA_10-45_LOS' ;
12 else
13     t.scenario{ t.no_segments } = 'MIMOSA_10-45_NLOS' ;
14 end
15
16 % Get the length of the current segment
17 segment_length = randn*segment_length_sigma + segment_length_mu;
18 while segment_length<min_segment_length
19     segment_length = randn*segment_length_sigma + segment_length_mu;
20 end
21 segment_length = round(segment_length);      % Segment length
22 ind = ind + segment_length;                  % Start of next segment
23
24 if ind < t.no_snapshots      % Exception for the last segment
25     t.no_segments = t.no_segments + 1;
26     t.segment_index( t.no_segments ) = ind;
27 end
28 end

```

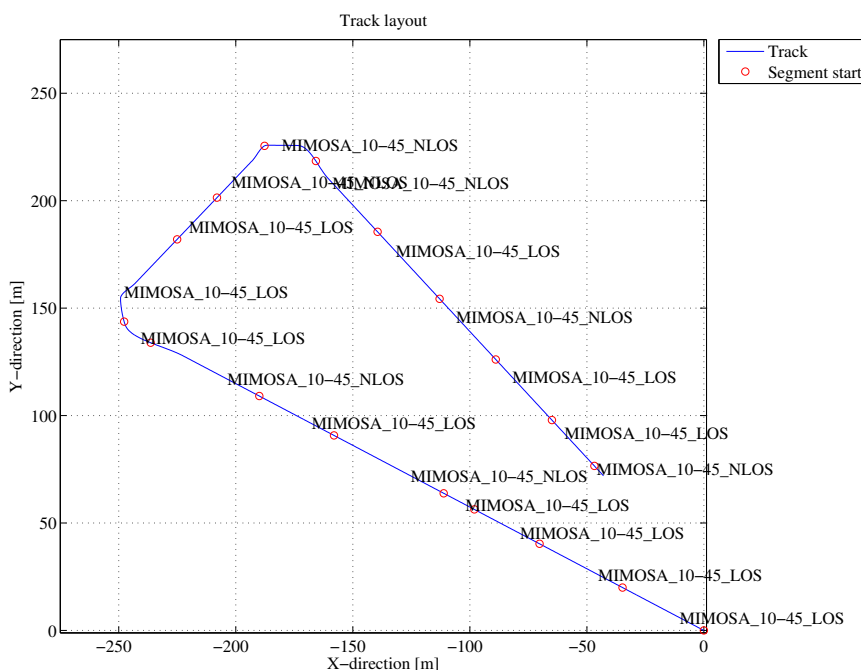


Figure 30: Receiver track for the satellite channel tutorial

Finally, we interpolate the track to the given sample density (2 samples per half-wave-length) and plot the track (see Fig. 30).

```
1 t.interpolate_positions( s.samples_per_meter );
2 t.visualize;
```

Defining Antenna Arrays In the third step, we set up our antenna arrays for the transmitter at the satellite and the receiver. We use synthetic dipole antennas for this case. Two dipoles are crossed by an angle of 90 degree. The signal is then split and fed with a 90 degree phase shift to both elements generating RHCP and LHCP signals.

```
1 % Create a patch antenna with 120 degree opening
2 a = array('custom',120,120,0);
3
4 % Copy element 1 to element 2 - the resulting antenna array has two
5 % elements, both dipoles.
6 a.copy_element(1,2);
7
8 % Rotate the second pattern by 90 degree around the x-axis.
9 a.rotate_pattern(90,'x',2);
10
11 % Set the coupling between the elements. The Tx-signal for the first
12 % element is shifted by +90 degree out of phase and put on the second element.
13 % The signal for the second element is shifted by -90 degree and copied to the
14 % first element. Both antennas thus radiate a RHCP and a LHCP wave.
15 a.coupling = 1/sqrt(2) * [1 1;1j -1j];
16
17 % Create a copy of the array for the receiver.
18 b = a.copy_objects;
19 b.coupling = 1/sqrt(2) * [1 1;1j -1j];
20
21 % Rotate the receive antenna array to face sky-wards.
22 b.rotate_pattern(-90,'y');
23
24 b.visualize; % Plot the pattern of the Rx-Antenna
```

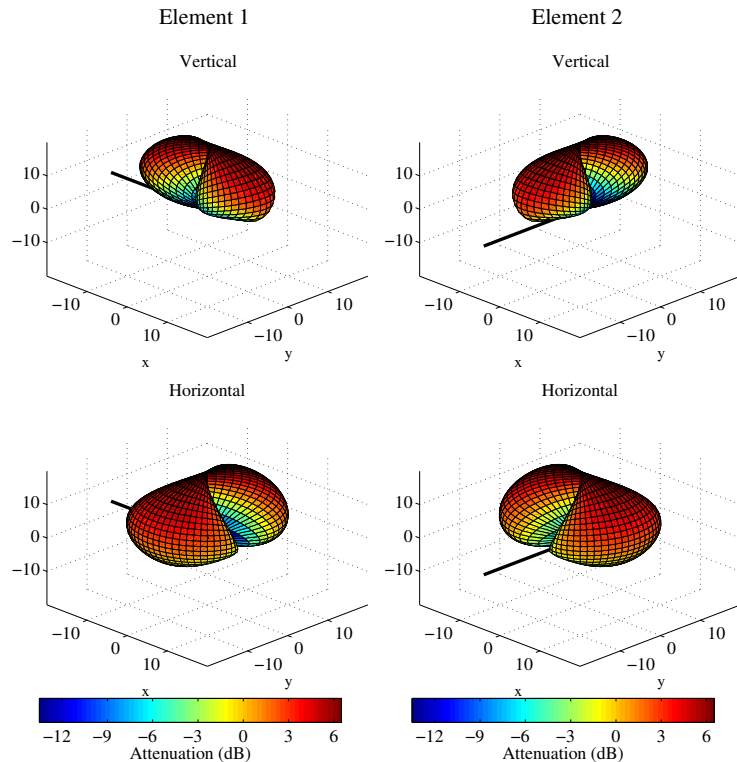


Figure 31: Antenna patterns for the satellite channel tutorial

Setting up the Layout In this step, we combine the track, the antennas and the position of the satellite into a simulation layout. A layout object contains all the geometric information that are necessary to run the simulation. First, we define the position of the satellite. Since the model uses Cartesian coordinates, we have to transform the position of the satellite first.

```

1 l = layout( s );                                % Create a new layout
2
3 % Choose a random satellite position (Astra 2, seen from Berlin).
4 % The distance only needs to be big enough to ensure insignificant changes
5 % in the reception angle on the ground.
6
7 sat_el      = 28.4;                            % Elevation angle
8 sat_az      = 161.6;                            % Azimuth angle (South = 180 degree)
9 rx_latitude = 51;                             % Latitude of the Rx
10
11 % Approximate the satellite distance for GEO orbit
12 dist_x     = 35786 + rx_latitude/90 * 6384;    % [km]
13 dist_y     = (1-rx_latitude/90) * 6384;        % [km]
14 sat_dist   = sqrt(dist_x^2 + dist_y^2);       % [km]
15 sat_dist   = sat_dist*1e3;                     % [m]
16
17 % Transform angles to Cartesian coordinates
18 sat_x = sat_dist * cosd(sat_el) * cosd(-sat_az+90);
19 sat_y = sat_dist * cosd(sat_el) * sind(-sat_az+90);
20 sat_z = sat_dist * sind(sat_el);
21
22 % We also turn the antenna of the satellite so it points to the receiver.
23 a.rotate_pattern( sat_el , 'y' );
24 a.rotate_pattern( 270-sat_az , 'z' );
25
26 % Set the satellite position in the layout
27 l.tx_position = [ sat_x ; sat_y ; sat_z ];
28
29 l.track = t;                                  % Set the track for the receiver
30 l.tx_array = a;                               % Set the tx_array
31 l.rx_array = b;                               % Set the rx_array

```

Setting up scenario parameters Next, the large scale parameters are set. The first line calls "l.create_parameter_sets", a built-in function that processes the data in the layout and returns a new "parameter_set" object "p". "p" is an array with two elements. One of them contains all the parameters for the good state (LOS) and one for the bad state (NLOS).

```
1 p = l.create_parameter_sets(0);
```

Each parameter set has two different kinds of parameters. One for the scenario and one for the current state. For example, a scenario might have an average RMS Delay spread of 158 ns plus a certain variance which defines a range for the RMSDS. In addition to that, there are cross-correlations with other parameters such as the angular spread at the transmitter. All those parameters are stored in the "scenpar" property. For the good state, that parameters are:

```
1 S1 = strcmp( { p(1).name , p(2).name } , 'MIMOSA-10-45-LOS_Tx1' ); % Select good state
2 p(S1).scenpar % Show parameter list
```

```

1 ans =
2
3
4     NumClusters: 8
5         r_DS: 2.5000
6     PerClusterAS_D: 6.2000e-07
7     PerClusterAS_A: 12
8     PerClusterES_D: 1.9000e-07
9     PerClusterES_A: 7
10    LOS_scatter_radius: 0.1000
11        LNS_ksi: 3
12        xpr_mu: 11.9000
13        xpr_sigma: 5.5000

```

```

14      DS_mu: -7.5000
15      DS_sigma: 0.3000
16      AS_D_mu: -4.6000
17      AS_D_sigma: 0.1000
18      AS_A_mu: 1.5000
19      AS_A_sigma: 0.2000
20      ES_D_mu: -5.1200
21      ES_D_sigma: 0.1000
22      ES_A_mu: 1.4000
23      ES_A_sigma: 0.1000
24      SF_sigma: 3.6000
25      KF_mu: 15.5000
26      KF_sigma: 5.9000
27      DS_lambda: 30.5000
28      AS_D_lambda: 1000
29      AS_A_lambda: 31.5000
30      ES_D_lambda: 1000
31      ES_A_lambda: 6
32      SF_lambda: 35
33      KF_lambda: 4.5000
34      asD_ds: 0
35      asA_ds: 0.6100
36      asA_sf: 0.5600
37      asD_sf: 0
38      ds_sf: 0.4300
39      asD_asA: 0
40      asD_kf: 0
41      asA_kf: -0.4400
42      ds_kf: -0.4600
43      sf_kf: -0.3000
44      esD_ds: 0
45      esA_ds: -0.0500
46      esA_sf: 0.1800
47      esD_sf: 0
48      esD_esA: 0
49      esD_asD: 0
50      esD_asA: 0
51      esA_asD: 0
52      esA_asA: 0.1500
53      esD_kf: 0
54      esA_kf: -0.0300

```

Note that the values are given for a log-normal distribution. Thus, the RMSDS in nanoseconds follows from

```
1 10^( p(S1).scenpar.DS_mu ) * 1e9
```

```

1
2 ans =
3
4 31.6228

```

Each parameter on that list can be changed by just assigning it a new value. Here, we set the number of clusters for the **LOS** scenario to 7. Note that the default settings are stored in files in the sub-folder "config" of the channel model folder. Here, the default settings can be permanently set. After a change, the parameters of the segments need to be updated. This is done by calling the "update_parameters" method.

```

1 p(S1).scenpar.NumClusters = 7;
2 p.update_parameters();

```

```
1 Parameters [oooooooooooooooooooooooooooooooooooo] 24 seconds
```

When "update_parameter" is called, the specific parameters for each segment are generated. E.g. each segment gets assigned a RMS Delay Spread and other values which are drawn from the statistics defined in scenpar. For the **LOS** segments, the individual RMSDS values for each segment are:

```

1 rmsds = p(S1).ds*1e9
2 average = mean(p(S1).ds*1e9)

```

```

1 rmsds =
2
3 Columns 1 through 7
4
5 48.8391    6.8370   55.2154   48.7273   25.9658   29.7929   22.2436
6
7 Columns 8 through 11
8
9 68.7237    13.3159   85.5425   121.5296
10
11
12 average =
13
14     47.8848
15

```

Generate channel coefficients Next, we generate the channel coefficients. This is a lengthy task. The next line then combines the channels of the individual segments into a time-continuous channel. Here, the parameter (0.2) sets the length of the overlap region between two segments. In this case, it is 20%.

```

1 c = p.get_channels; % Generate coefficients
2 cn = c.merge(0.2); % Combine segments

```

```

1 Channels      [oooooooooooooooooooooooooooooooooooooooooooo]    21 seconds
2 Merging       [oooooooooooooooooooooooooooooooooooo]    1 seconds

```

Evaluation of the data The next two plots show some basic evaluations of the generated coefficients. The first plot shows the received power for the 4 MIMO links along the track. The plot shows the differences between the LOS and NLOS segments and the cross-pol discrimination between the MIMO links. The average path loss for LOS was set to -95 dB and for NLOS -113 dB.

```

1 dist = (1:cn.no_snap)*t.get_length/cn.no_snap;
2 ind = find(strcmp(t.scenario,'MIMOSA_10-45_LOS'));
3 los = [];
4 for n = 1:numel(ind)
5     start = t.segment_index(ind(n));
6     if n==numel(ind)
7         try
8             stop = t.segment_index(ind(n)+1);
9         catch
10            stop = t.no_snapshots;
11        end
12    else
13        stop = t.segment_index(ind(n)+1);
14    end
15    los = [los start:stop];
16 end
17
18 power = reshape( 10*log10( squeeze(sum( abs(cn.coeff).^2 , 3 )) ) , 4,[] );
19
20 mi = min(reshape(power,[],1)) - 5;
21 ma = max(reshape(power,[],1)) + 5;
22
23 ar = ones(1,cn.no_snap) * ma;
24 ar(los) = mi;
25
26 figure('Position',[ 100 , 100 , 1000 , 700]);
27 a = area(dist,ar);
28 set(a(1),'FaceColor',[0.7 0.9 0.7]);
29 set(a,'LineStyle','none')
30
31 hold on
32 plot(dist,power')
33 hold off
34

```

```

35 xlabel('Track [m]');
36 ylabel('Received Power per MIMO LINK [dB]');
37 axis([0 t.get_length mi ma])
38 legend('LOS','P_{11}', 'P_{12}', 'P_{21}', 'P_{22}',4)
39 box on
40
41 title('Received power along the track')

```

The next plot shows the RMS delay spread along the path for the first MIMO element. Again, shaded areas are for the LOS segments.

```

1 pow_tap = abs(squeeze(cn.coeff(1,1,:,:,:))).^2;
2 pow_sum = sum( pow_tap,1 );
3 mean_delay = sum( pow_tap.*cn.delay ,1) ./ pow_sum;
4 ds = sqrt( sum( pow_tap.*cn.delay.^2 ,1)./ pow_sum - mean_delay.^2 );
5 ar = zeros(1,cn.no_snap);
6 ar(los) = 10000;
7
8 figure('Position',[ 100 , 100 , 1000 , 700]);
9 a = area(dist,ar);
10 set(a(1),'FaceColor',[0.7 0.9 0.7]);
11 set(a,'LineStyle','none')
12
13 hold on
14 plot( dist , ds*1e9 )
15 hold off
16
17 ma = 1e9*( max(ds)+0.1*max(ds) );
18
19 axis([0 t.get_length 0 ma])
20 xlabel('Track [m]');
21 ylabel('Delay Spread [ns]');
22 legend('LOS','\sigma_\tau',1)
23 title('Position dependant delay spread');

```

```

1 close all
2 disp(['QuaDRiGa Version: ',simulation_parameters.version])

```

```
1 QuaDRiGa Version: 1.0.1-145
```

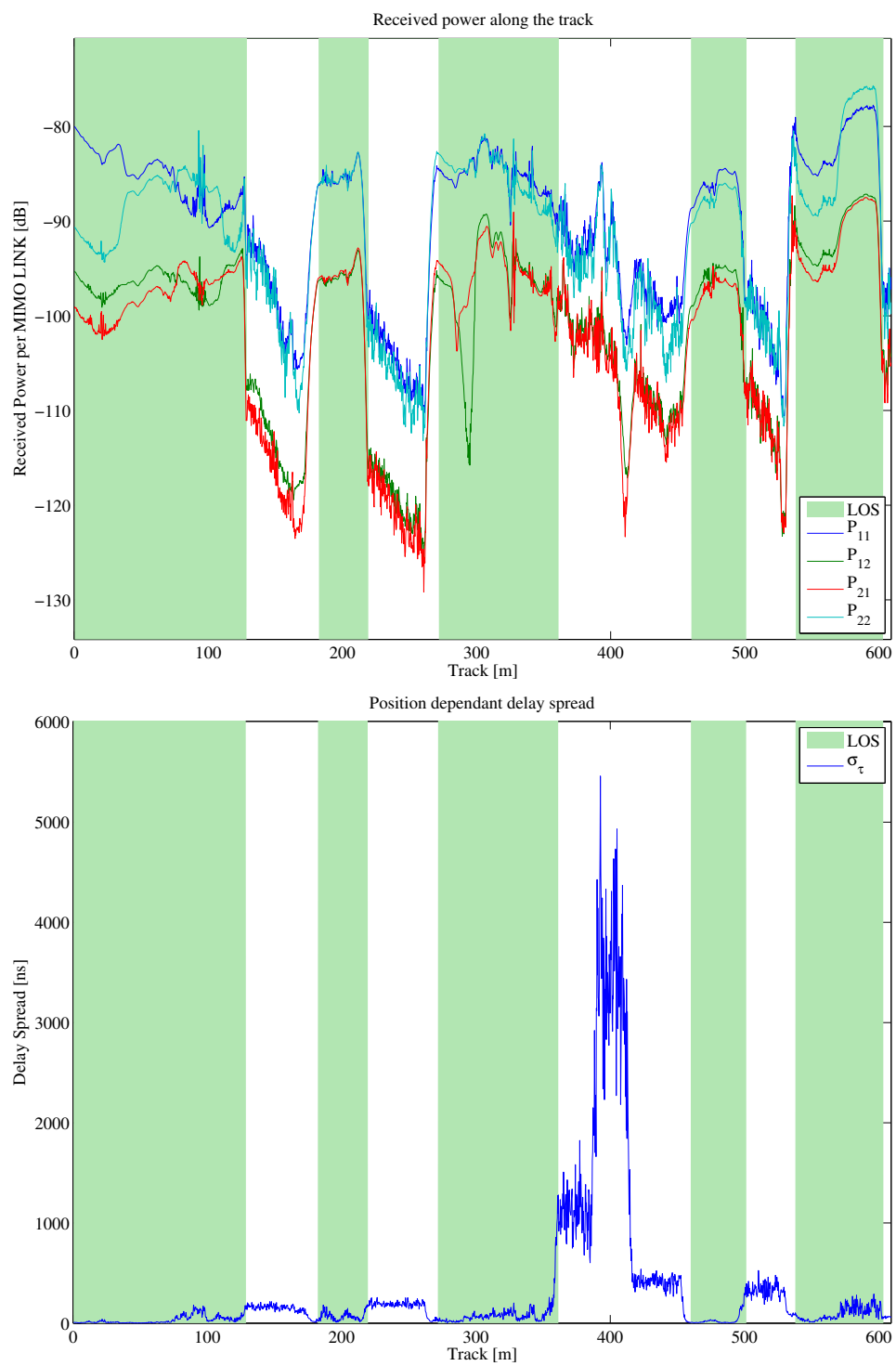


Figure 32: Results for the satellite channel tutorial

A.4 Drifting Phases and Delays

Drifting is an essential feature of the channel model. Drifting enables a continuous time evolution of the path delays, the path phases, the departure- and arrival angles and the LSPs. It is thus the enabling feature for time continuous channel simulations. Although drifting was already available in the SCME branch of the WINNER channel model, it did not make it into the main branch. Thus, drifting is not available in the WIM1, WIM2 or WIM+ model. Here the functionality is implemented again. This script focuses on the delay and the phase component of the drifting functionality.

Channel model setup and coefficient generation First, we parameterize the channel model. We start with the basic simulation parameters. For the desired output, we need two additional options: we want to evaluate absolute delays and we need to get all 20 subpaths. Normally, the subpaths are added already in the channel builder.

```

1 s = simulation_parameters;
2 s.center_frequency = 2.53e9;
3 s.sample_density = 4;
4 s.use_subpath_output = 1;
5 s.use_absolute_delays = 1;
```

Second, we define a user track. Here we choose a linear track with a length of 30 m. The track starts 20 m east of the transmitter and runs in east direction, thus linearly increasing the distance from the receiver.

```

1 l = layout( s );
2 l.tx_position(3) = 25;
3 l.track.generate('linear',30,0);
4 l.track.initial_position = [20;0;0];
5 l.track.scenario = 'WINNER_UMa_C2_LOS';
6 l.track.interpolate_positions( s.samples_per_meter );
7 l.visualize;
```

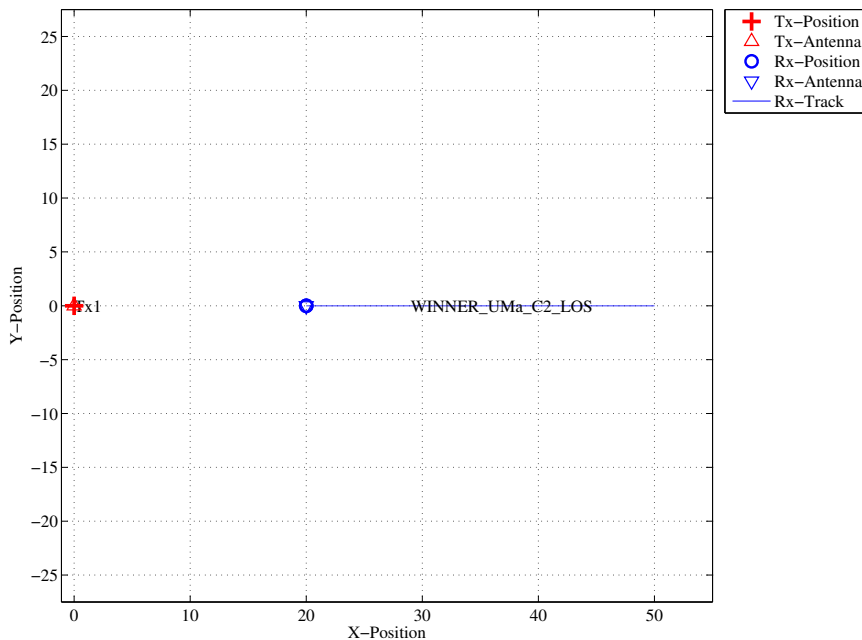


Figure 33: Scenario setup for the drifting phases tutorial

Now, we generate the LSPs. In order to get repeatable results, we set a specific random seed. This is a MATLAB internal function and is not a feature of the channel model. We also set the shadow fading and K-factor to 1 and disable the path loss model.

```

1 RandStream.setGlobalStream(RandStream('mt19937ar','seed',5));
2 p = l.create_parameter_sets;
3 p.parameter_maps(:, :, [2 3]) = 0; % Fix SF and KF to 0
4 p.plpar = []; % Disable path loss model
5 p.update_parameters;

```

| | | | |
|---|------------|--|-----------|
| 1 | Parameters | [oooooooooooooooooooooooooooooooooooo] | 1 seconds |
|---|------------|--|-----------|

Now, we generate the channel coefficients. The first run uses the new drifting module, the second run disables it. Note that drifting needs significantly more computing resources. In some scenarios it might thus be useful to disable the feature to get quicker simulation results.

```

1 s.drifting_precision = 1;
2 RandStream.setGlobalStream(RandStream('mt19937ar','seed',2));
3 c = p.get_channels;
4
5 s.drifting_precision = 0;
6 RandStream.setGlobalStream(RandStream('mt19937ar','seed',2));
7 d = p.get_channels;

```

| | | | |
|---|----------|--------------------------------|------------|
| 1 | Channels | [oooooooooooooooooooooooooooo] | 12 seconds |
| 2 | Channels | [oooooooooooooooooooooooooooo] | 7 seconds |

Results and discussion The following plots represent the results of the test.

```

1 figure
2 distance = 20+(1:c.no_snap)*l.track.get_length/c.no_snap;
3 plot( distance, c.delay(1,:)*1e9 , '-b' )
4 hold on
5 plot( distance, d.delay(1,:)*1e9 , '-.b' )
6 plot( distance, c.delay(2,:)*1e9 , '-r' )
7 plot( distance, d.delay(2,:)*1e9 , '-.r' )
8 hold off
9 xlabel('Distance from track start point')
10 ylabel('Delay [ns] ')

```

The first plot (Fig. 34) shows the delay of the LOS tap (blue) and the delay of the first NLOS tap (red) vs. distance. The solid lines are from the channel with drifting, the dashed lines are from the channel without. The LOS delay is always increasing since the Rx is moving away from the Tx. However, the increase is not linear due to the 25 m height of the Tx. Without drifting, the delays are not updated and stay constant during the segment. The position of the first scatterer is in close distance to the Rx (only some m away).

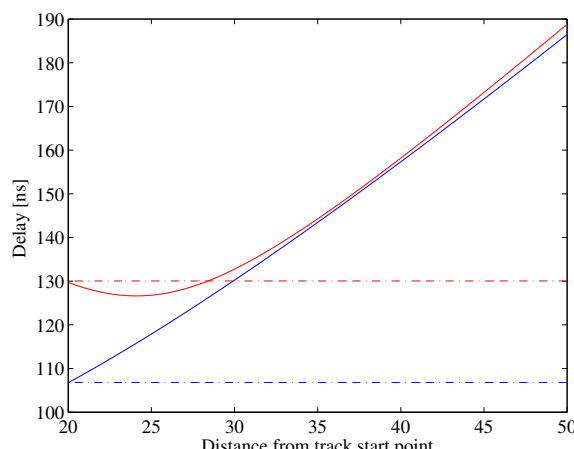


Figure 34: Cluster delays vs. Rx position (drifting phases tutorial)

When moving, the Rx first approaches the scatterer (delay gets a bit smaller) and then the distance increases again.

```

1 phase = unwrap(angle(squeeze((c.coeff(1,1,2,:,:,:)))));
2 plot( distance,phase )
3 xlabel('Distance from track start point')
4 ylabel('Continuous phase')
```

The second plot (Fig. 35, left) shows the phases of the 20 subpaths of the first NLOS tap for the drifting case. Note that the phases are not linear. This comes from the close proximity of the scatterer to the initial Rx position. The position of all 20 reflection points are calculated by the channel model. Those position mark the position of the last bounce scatterer (LBS). When moving the Rx, the distance to the LBS changes for each subpath and so does the phase. Here, the phase of each of the subpaths is calculated from the length of the path.

```

1 pow = abs(squeeze(sum( c.coeff(1,1,2,:,:,:) , 5 ))).^2;
2 plot( distance,10*log10(pow) , '-r' )
3 xlabel('Distance from track start point')
4 ylabel('Tap power (dB)')
```

This plot shows the power of the first NLOS tap along the track. The fading is significantly higher in the beginning and becomes much less strong towards the end.

```

1 phase = unwrap(angle(squeeze((d.coeff(1,1,2,:,:,:)))));
2 plot( distance,phase )
3 xlabel('Distance from track start point')
4 ylabel('Continuous phase')
```

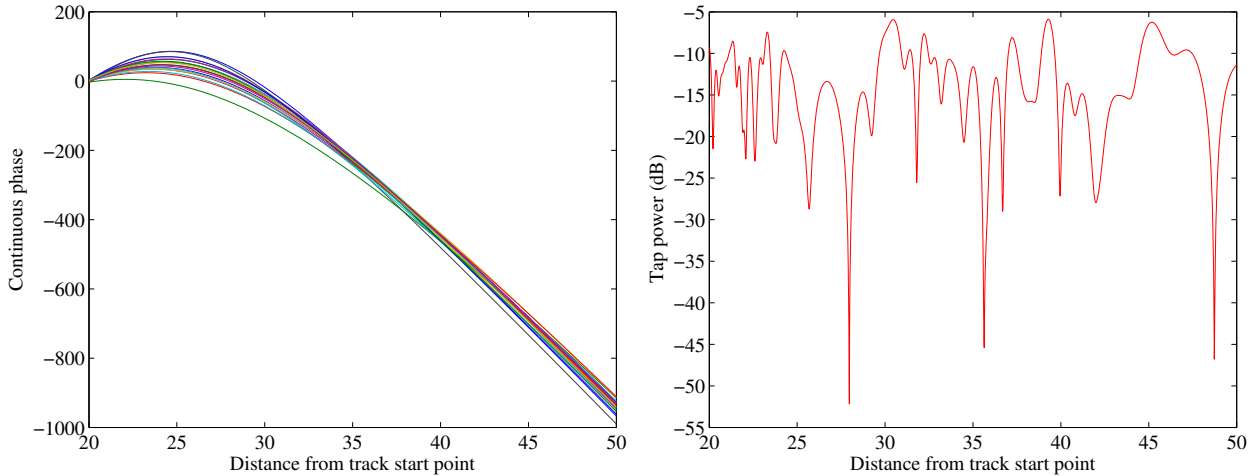


Figure 35: Drifting phases and Tx power vs. Rx position (drifting phases tutorial)

Without drifting, the phases of the subpaths are approximated by assuming that the angles to the LBSs do not change. However, this only holds when the distance to the LBS is large. Here, the initial distance is small (ca. 5 m). When the initial angles are kept fixed along the track, the error is significant. Here, the phase ramp is negative, indicating a movement direction towards the scatterer and thus a higher Doppler frequency. However, when the scatterer is passed, the Rx moves away from the scatterer and the Doppler frequency becomes lower. This is not reflected when drifting is turned off.

Note that with shorter delay spreads (as e.g. in satellite channels), the scatterers are placed closer to the Rx's initial position. This will amplify this effect. Hence, for correct time evolution results, drifting needs to be turned on.

```

1 pow = abs(squeeze(sum( d.coeff(1,1,2,:,:,:) , 5 ))).^2;
2 plot( distance,10*log10(pow) , '-r' )
3 xlabel('Distance from track start point')
4 ylabel('Tap power (dB)')

```

```

1 close all
2 disp(['QuaDRiGa Version: ',simulation_parameters.version])

```

1 QuaDRiGa Version: 1.0.1-145

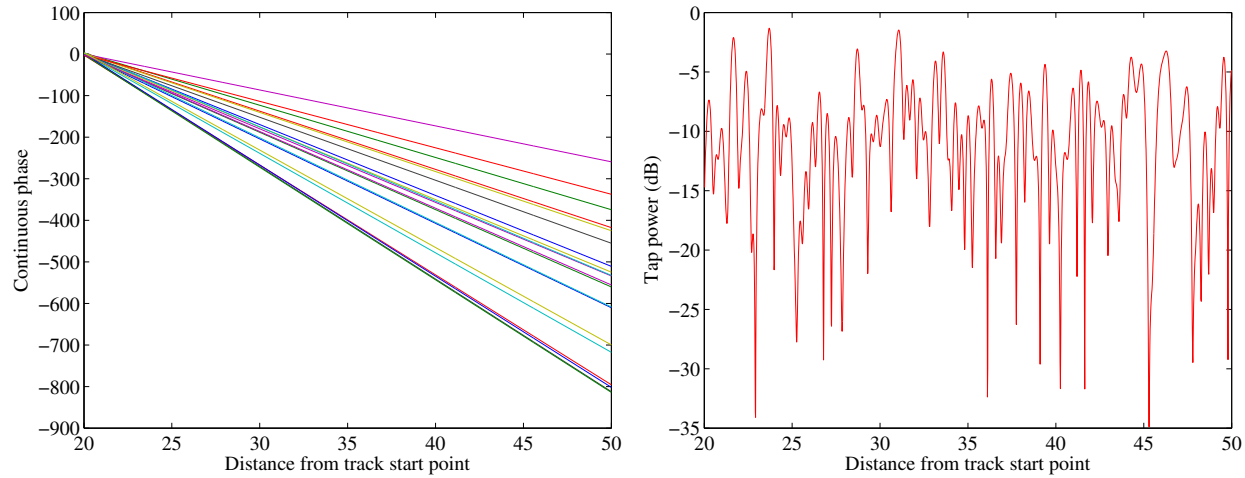


Figure 36: Phases and Tx power vs. Rx position without drifting (drifting phases tutorial)

A.5 Time Evolution and Scenario Transitions

The channel model generates the coefficients separately for each segment. In order to get a time-continuous output, these coefficients have to be combined. This is a feature originally described in the documentation of the WIM2 channel model, although it was never implemented. Since this component is needed for time-continuous simulations, it was implemented here. This script sets up the simulation and creates such time-continuous CIRs.

Channel model setup and coefficient generation First, we set up the channel model.

```

1 close all
2 clear all
3
4 set(0,'defaultTextFontSize', 14)
5 set(0,'defaultAxesFontSize', 14)
6
7 s = simulation_parameters;
8 s.center_frequency = 2.53e9;
9 s.sample_density = 4;
10 s.use_absolute_delays = 1;
```

Second, we create a more complex network layout featuring an elevated transmitter (25 m) and two receivers at 1.5 m height. The first Rx moves along a circular track around the receiver. The second receiver moves away from the Tx. Both start at the same point.

Note that each track is split into three segments. The first Rx goes from an **LOS** area to a shaded area and back. The second track also starts in the **LOS** area. Here, the scenario changes to another **LOS** segment and then to an **NLOS** segment. The **LOS-LOS** change will create new small-scale fading parameters, but the **LSPs** will be highly correlated between those two segments.

```

1 l = layout( s );                                % New layout
2 l.no_rx = 2;                                    % Two receivers
3
4 l.tx_array.generate('dipole');                  % Dipola antennas at all Rx and Tx
5 l.rx_array = l.tx_array;
6
7 l.tx_position(3) = 25;                         % Elevate Tx to 25 m
8
9 UMal = 'BERLIN_UMa_LOS';
10 UMan = 'BERLIN_UMa_NLOS';
11
12 l.track(1).generate('circular',20*pi,0);      % Circular track with 10m radius
13 l.track(1).initial_position = [10;0;1.5];       % Start east, running nord
14 l.track(1).segment_index = [1,40,90];           % Segments
15 l.track(1).scenario = { UMal , UMan , UMal };
16
17 l.track(2).generate('linear',20,0);            % Linear track, 20 m length
18 l.track(2).initial_position = [10;0;1.5];       % Same start point
19 l.track(2).interpolate_positions( 128/20 );
20 l.track(2).segment_index = [1,40,90];
21 l.track(2).scenario = { UMal , UMal , UMan };
22
23 l.visualize;                                  % Plot all tracks
24
25 l.track.interpolate_positions( s.samples_per_meter );
26 l.track.compute_directions;
```

Now we create the channel coefficients. Fixing the random seed guarantees repeatable results (i.e. the taps will be at the same positions for both runs). Note that the computing time is significantly longer when drifting is enabled.

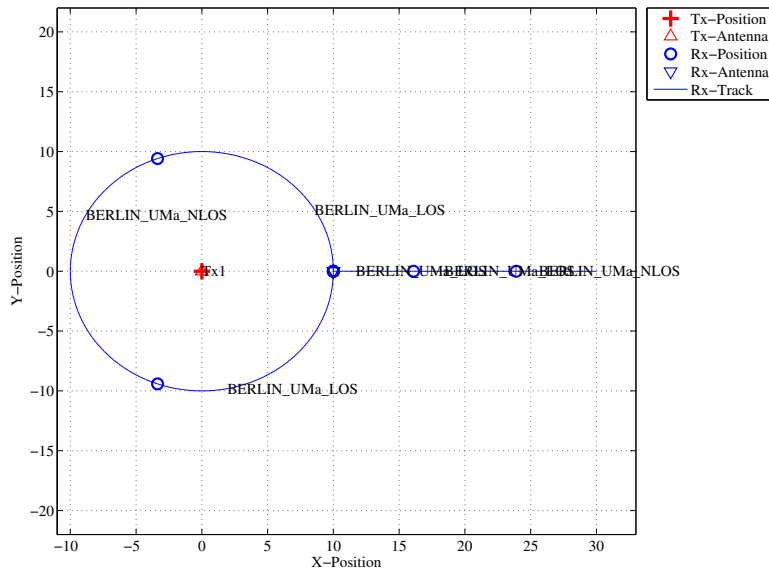


Figure 37: Scenario setup for the time evolution tutorial

```

1 RandStream.setGlobalStream(RandStream('mt19937ar','seed',2));
2 p = l.create_parameter_sets;
3
4 disp('Drifting enabled:');
5 s.drifting_precision = 1;
6 RandStream.setGlobalStream(RandStream('mt19937ar','seed',1));
7 c = p.get_channels;
8 cn = c.merge;
9
10 disp('Drifting disabled:');
11 s.drifting_precision = 0;
12 RandStream.setGlobalStream(RandStream('mt19937ar','seed',1));
13 d = p.get_channels;
14 dn = d.merge;

```

| | |
|---|------------|
| 1 Parameters [oooooooooooooooooooooooooooo] | 1 seconds |
| 2 Drifting enabled: | |
| 3 Channels [oooooooooooooooooooooooooooo] | 36 seconds |
| 4 Drifting disabled: | |
| 5 Channels [oooooooooooooooooooooooooooo] | 5 seconds |

Results and discussion Now we plot and discuss the results. We start with the power of the LOS tap along the circular track and compare the outcome with and without drifting (Fig. 38, left).

```

1 degrees = (0:cn(1).no_snap-1)/cn(1).no_snap * 360;
2 los_pwr_drift = 10*log10(squeeze(abs(cn(1).coeff(1,1,1,:))).^2);
3 los_pwr_nodrift = 10*log10(squeeze(abs(dn(1).coeff(1,1,1,:))).^2);
4
5 figure
6 plot(degrees,los_pwr_drift)
7 hold on
8 plot(degrees,los_pwr_nodrift,'-.r')
9 hold off
10
11 a = axis;
12 axis([0 360 a(3:4)]);
13
14 xlabel('Position on circle [\degree]');
15 ylabel('Power of the LOS component');
16 title('Power of the LOS component for the circular track');
17 legend('Drifting','No drifting',4);

```

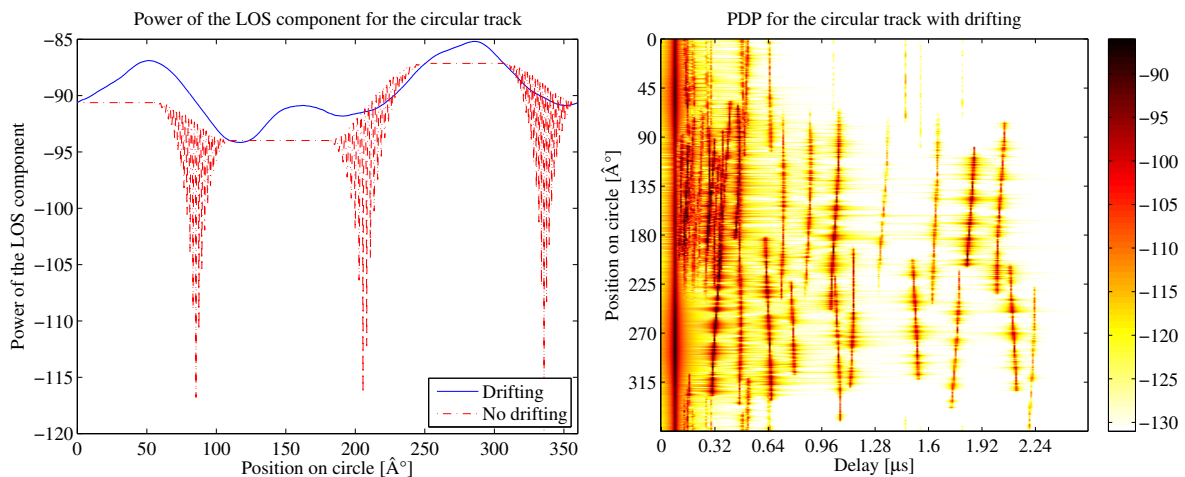


Figure 38: Received power on the circular track (time evolution tutorial)

When drifting is enabled (Fig. 38, left, blue curve), the channel output after merging is time-continuous. The variations along the track come from the drifting K-Factor and the drifting shadow fading. When drifting is disabled, these parameters are not updated and kept fixed at their initial value.

At the end of each segment, both channels are cross-faded. I.e. the power of the output of the first segment ramps down and the power of the second segment ramps up. Since drifting guarantees a time-continuous evolution of the phase, this ramping process is also time continuous and no artifacts are visible in the blue curve.

Without drifting, however, the phases are approximated based on their initial values, the initial arrival- and departure angles and the traveled distance from the start point. However, since the Rx moves along a circular track, the angles change continuously which is not correctly modeled. The phase at the end of the first segment does not match the phase at the beginning of the second. When adding both components, artifacts appear as can be seen in the red curve.

Next, we plot the power-delay profiles for both tracks. We calculate the frequency response of the channel and transform it back to the time domain by an IFFT. Then, we create a 2D image of the received power at each position of the track. We start with the circular track.

```

1 h = cn(1).fr( 100e6,512 );
2 h = squeeze(h);
3 pdp = 10*log10(abs(ifft(h,[],1)).^2);
4
5 figure
6 imagesc(pdp(:,1:256));
7 caxis([ max(max(pdp))-50 max(max(pdp))-5 ]);
8 colorbar
9
10 cm = colormap('hot');
11 colormap(cm(end:-1:1,:));
12
13 set(gca,'XTick',1:32:255);
14 set(gca,'XTickLabel',(0:32:256)/100e6*1e6);
15 xlabel('Delay [\mu s]');
16
17 set(gca,'YTick',1:cn(1).no_snap/8:cn(1).no_snap);
18 set(gca,'YTickLabel', (0:cn(1).no_snap/8:cn(1).no_snap)/cn(1).no_snap * 360 );
19 ylabel('Position on circle [degree]');
20
21 title('PDP for the circular track with drifting');

```

The X-axis (Fig. 38, right) shows the delay in microseconds and the Y-axis shows the position on the circle. For easier navigation, the position is given in degrees. 0° means east (starting point), 90° means north, 180° west and 270° south. The LOS delay stays constant since the distance to the Tx is also constant.

However, the power of the LOS changes according to the scenario. Also note, that the NLOS segment has significantly more taps due to the longer delay spread. Next, we create the same plot for the linear track (Fig. 39). Note the slight increase in the LOS delay and the high similarity of the first two LOS segments due to the correlated LSPs. Segment change is at around 6 m.

```

1 h = cn(2).fr( 100e6,512 );
2 h = squeeze(h);
3 pdp = 10*log10(abs(ifft(h,[],1)).^2);
4
5 figure
6 imagesc(pdp(:,1:256));
7 caxis([ max(max(pdp))-50 max(max(pdp))-5 ])
8 colorbar
9
10 cm = colormap('hot');
11 colormap(cm(end:-1:1,:));
12
13 set(gca,'XTick',1:32:255);
14 set(gca,'XTickLabel',(0:32:256)/100e6*1e6);
15 xlabel('Delay [\mu s]');
16
17 set(gca,'YTick',1:cn(2).no_snap/8:cn(2).no_snap);
18 set(gca,'YTickLabel', (0:cn(2).no_snap/8:cn(2).no_snap)/cn(2).no_snap * 20 );
19 ylabel('Distance from start point [m]');
20
21 title('PDP for the linear track with drifting');

```

Last, we plot the same results for the linear track without drifting (Fig. 39, right). Note that the LOS delay is not smooth during segment change. There are two jumps at 6 m and again at 13.5 m.

```

1 h = dn(2).fr( 100e6,512 );
2 h = squeeze(h);
3 pdp = 10*log10(abs(ifft(h,[],1)).^2);
4
5 figure
6 imagesc(pdp(:,1:256));
7 caxis([ max(max(pdp))-50 max(max(pdp))-5 ])
8 colorbar
9
10 cm = colormap('hot');
11 colormap(cm(end:-1:1,:));
12
13 set(gca,'XTick',1:32:255);
14 set(gca,'XTickLabel',(0:32:256)/100e6*1e6);
15 xlabel('Delay [\mu s]');
16
17 set(gca,'YTick',1:cn(2).no_snap/8:cn(2).no_snap);
18 set(gca,'YTickLabel', (0:cn(2).no_snap/8:cn(2).no_snap)/cn(2).no_snap * 20 );
19 ylabel('Distance from start point [m]');
20
21 title('PDP for the linear track without drifting');

```

```

1 close all
2 disp(['QuaDRiGa Version: ',simulation_parameters.version])

```

```
1 QuaDRiGa Version: 1.0.1-145
```

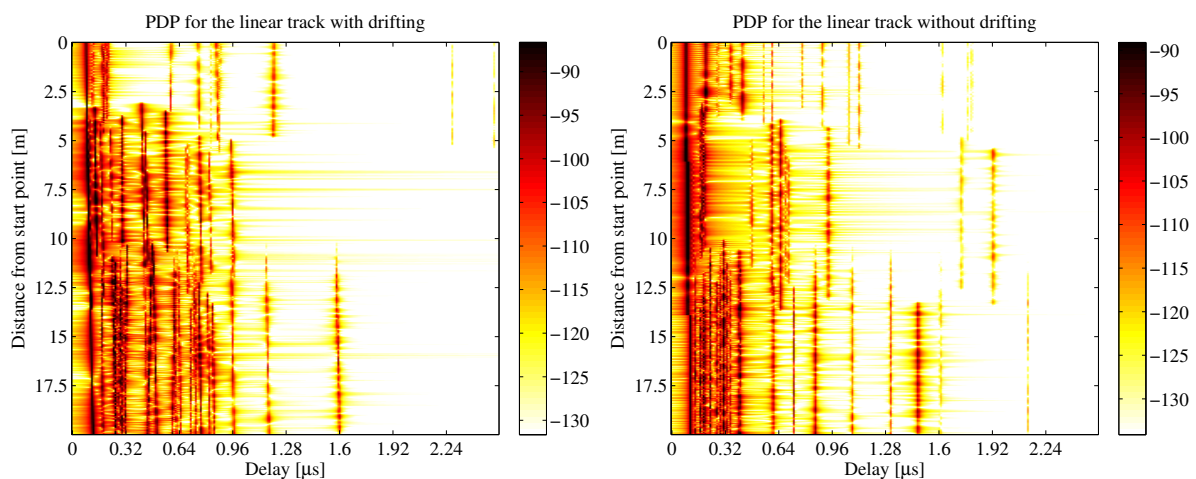


Figure 39: Received power on the linear track (time evolution tutorial)

A.6 Applying Varying Speeds (Channel Interpolation)

One new feature that makes the simulations more realistic is the function to apply arbitrary speed- and movement profiles, e.g. accelerating, breaking or moving at any chosen speed. These profiles are defined in the track class. The profiles are then converted into effective sampling points which aid the interpolation of the channel coefficients.

Channel model setup First, we set up the simulation parameters. Note the sample density of 2.5 which enables very fast simulations even with drifting.

```
1 s = simulation_parameters;
2 s.center_frequency = 2.53e9;
3 s.sample_density = 2.5;
4 s.use_absolute_delays = 1;
```

Second, we define a track. It has a length of 20 m, starts at 10 m east of the transmitter and consists of three segments (LOS, NLOS, LOS). The positions are interpolated to match the sample density defined above. The track is then plugged into a network layout with one transmitter at position (0,0,25). Both, transmitter and receiver are equipped with dipole antennas. The last three lines create the LSPs.

```
1 t = track('linear',20,0);
2 t.initial_position = [60;0;1.5];
3 t.interpolate_positions( 128/20 );
4 t.segment_index      = [1,40,90];
5 t.scenario          = { 'WINNER_UMa_C2_LOS' , 'WINNER_UMa_C2_NLOS' , ...
6   'WINNER_UMa_C2_LOS' };
7 t.interpolate_positions( s.samples_per_meter );
8
9 l = layout( s );
10 l.tx_array.generate('dipole');
11 l.rx_array = l.tx_array;
12 l.tx_position(3) = 25;
13 l.track = t;
14
15 l.visualize;
16
17 RandStream.setGlobalStream(RandStream('mt19937ar','seed',5));
18 p = l.create_parameter_sets;
```

```
1 Parameters [oooooooooooooooooooooooooooo] 2 seconds
```

Channel generation and results Next, we generate the channel coefficients. Note that the initial sample density is 2.5. We then interpolate the sample density to 20. It would take ten times as long to achieve the same result with setting the initial sample density to 20. The interpolation is significantly faster. It is done by first setting the speed to 1 m/s (default setting) and then creating a distance vector which contains a list of effective sampling points along the track.

```
1 c = p.get_channels;
2 cn = c.merge;
3
4 t.set_speed( 1 );
5 dist = t.interpolate_movement( s.wavelength/(2*20) );
6 ci = cn.interpolate( dist , t.get_length , 'spline' );
```

```
1 Channels [oooooooooooooooooooooooooooo] 5 seconds
```

The next plot shows the power of the first three taps from both, the original and the interpolated channel, plotted on top of each other. The values are identical except for the fact, that the interpolated values (blue line) have 5 times as many sample points.

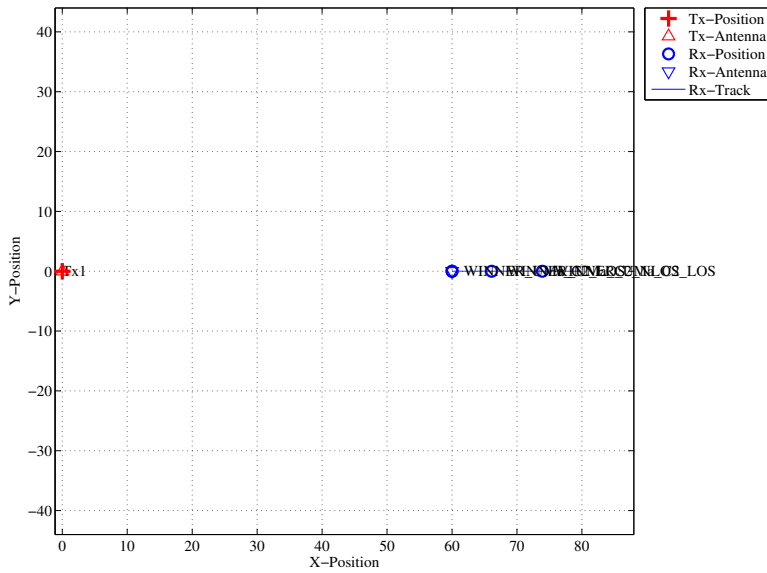


Figure 40: Scenario setup for the speed profile tutorial

```

1 pwr_orig = 10*log10(squeeze(abs(cn.coeff(1,1,1:3,:))).^2);
2 nsnap = cn.no_snap;
3 dist_orig = (0:nsnap-1) * t.get_length/(nsnap-1);
4 pwr_int = 10*log10(squeeze(abs(ci.coeff(1,1,1:3,:))).^2);
5
6 figure
7 plot( dist_orig,pwr_orig , 'r','Linewidth',2 )
8 hold on
9 plot( dist,pwr_int , 'b' )
10 hold off
11 axis( [ min(dist) , max(dist) ,...
12     min( pwr_orig( pwr_orig>-Inf ) ) , ...
13     max( pwr_orig( pwr_orig>-Inf ) )+10 ] )
14 xlabel('Distance from start point [m]');
15 ylabel('Power [dB]');
16

```

Fig. 41 (right) shows the power delay profile (PDP) for the interpolated channel. As defined in the track object, it starts with a **LOS** segment, going into a shaded area with significantly more multipath fading at around 4 seconds and then back to **LOS** at around 13 sec.

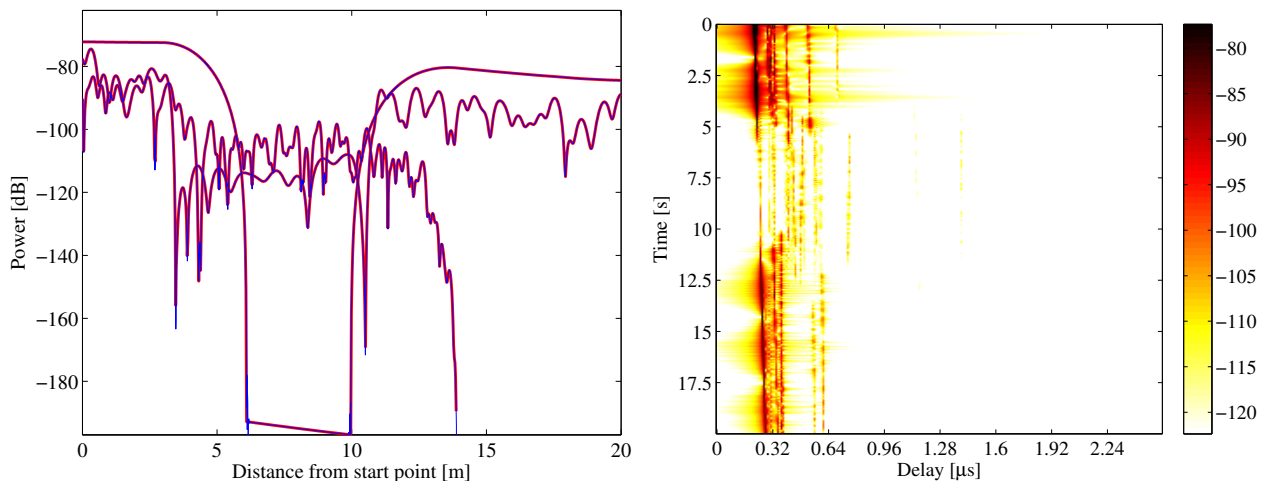


Figure 41: Received power and 2D PDP for the speed profile tutorial

```

1 h = ci.fr( 100e6,512 );
2 h = squeeze(h);
3 pdp = 10*log10(abs(ifft(h,[],1).').^2);
4
5 figure
6 imagesc(pdp(:,1:256));
7 caxis([ max(max(pdp))-50 max(max(pdp))-5 ])
8 colorbar
9
10 cm = colormap('hot');
11 colormap(cm(end:-1:1,:));
12
13 set(gca,'XTick',1:32:255);
14 set(gca,'XTickLabel',(0:32:256)/100e6*1e6);
15 xlabel('Delay [\mu s]');
16
17 set(gca,'YTick',1:ci.no_snap/8:ci.no_snap);
18 set(gca,'YTickLabel', (0:ci.no_snap/8:ci.no_snap)/ci.no_snap * 20 );
19 ylabel('Time [s]');

```

Now, we create a movement profile. It is defined by a set of value pairs in `track.movement_profile`. The first value represents the time in seconds, the second value the position on the track. Here, we start at a position of 7 m, i.e. in the second (**NLOS**) segment. We then go back to the beginning of the track. This takes 5 seconds. Then, we wait there for 1 second and go to the end of the track, which we reach after additional 14 seconds.

The next step is to interpolate the sample points. This is done by the `interpolate_movement` method. It requires the sample interval (in s) as an input argument. Here, we choose an interval of 1 ms which gives us 1000 samples per second. Fig. 42 (left) illustrates the results.

```

1 t.movement_profile = [ 0,7 ; 5,0 ; 6,0 ; 20,20 ];
2 dist = t.interpolate_movement( 1e-3 );
3 ci = cn.interpolate( dist , t.get_length );
4
5 nsnap = ci.no_snap;
6 time = (0:nsnap-1) * t.movement_profile(1,:)/(nsnap-1);
7
8 figure
9 plot( time,dist , 'r' )
10
11 xlabel('Time [s]');
12 ylabel('Position on track [m]');

```

The last plot (Fig. 42, right) shows the PDP of the interpolated channel with the movement profile applied. The channel starts in the second segment with a lot of fading, goes back to the first while slowing down at the same time. After staying constant for one second, the channel starts running again, speeding up towards the end of the track.

```

1 h = ci.fr( 100e6,512 );
2 h = squeeze(h);
3 pdp = 10*log10(abs(ifft(h,[],1).').^2);
4
5 figure
6 imagesc(pdp(:,1:256));
7 caxis([ max(max(pdp))-50 max(max(pdp))-5 ])
8 colorbar
9
10 cm = colormap('hot');
11 colormap(cm(end:-1:1,:));
12
13 set(gca,'XTick',1:32:255);
14 set(gca,'XTickLabel',(0:32:256)/100e6*1e6);
15 xlabel('Delay [\mu s]');
16
17 set(gca,'YTick',1:ci.no_snap/8:ci.no_snap);
18 set(gca,'YTickLabel', (0:ci.no_snap/8:ci.no_snap)/ci.no_snap * 20 );
19 ylabel('Time [s]');

```

```
1 close all  
2 disp(['QuaDRiGa Version: ',simulation_parameters.version])
```

```
1 QuaDRiGa Version: 1.0.1-145
```

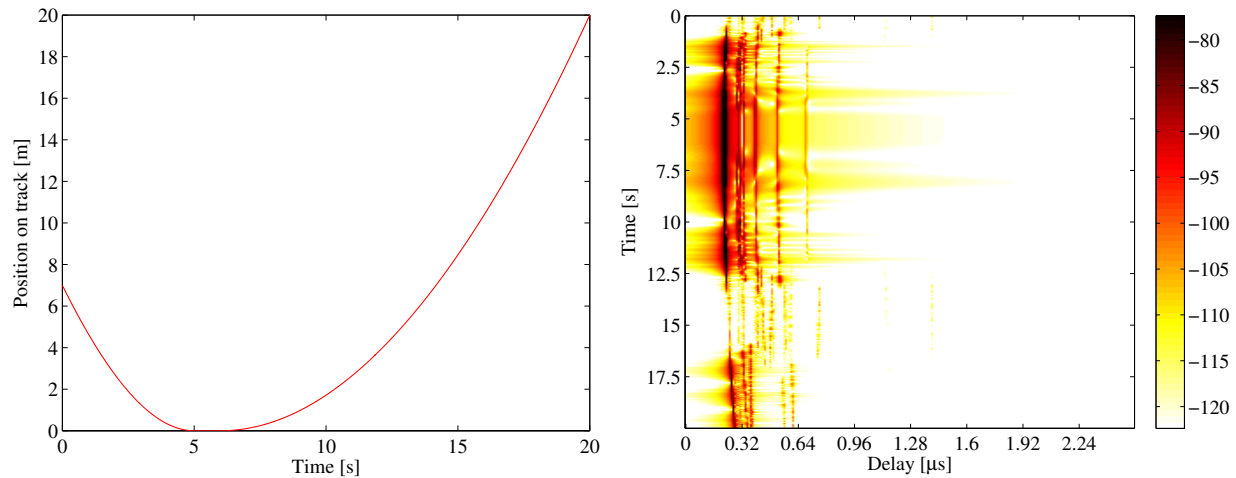


Figure 42: Movement profile (left) and interpolated PDP (right)

A.7 Geometric Polarization

Here, we demonstrate the polarization rotation model that calculates the path power for polarized antenna arrays. We do this by setting up the simulation with different H/V polarized antennas at the transmitter and at the receiver. Then we define a circular track around the receiver. When the receiver moves around the transmitter, it changes its antenna orientation according to the movement direction. In this way, all possible departure and elevation angles are sampled. Depending on the antenna orientation, the polarizations are either aligned (e.g. the Tx is V-polarized and the Rx is V-polarized), they are crossed (e.g. the Tx is V-polarized and the Rx is H-polarized) or the polarization orientation is in between those two. The generated channel coefficients should reflect this behavior.

Setting up the simulation environment First, we have to set up the simulator with some default settings. Here, we choose a center frequency of 2.1 GHz. We also want to use drifting in order to get the correct angles for the LOS component and we set the number of transmitters and receivers to one.

```

1 close all
2 clear all
3
4 set(0, 'defaultTextFontSize', 14)
5 set(0, 'defaultAxesFontSize', 14)
6
7 s = simulation_parameters; % Set the simulation parameters
8 s.center_frequency = 2.1e9; % Center-frequency: 2.1 GHz
9 s.use_polarization_rotation = 1;
10 s.samples_per_meter = 360/(40*pi); % One sample per degree
11 s.drifting_precision = 1;

```

Setting up the antenna arrays In the second step, we set up our antenna arrays. We use the synthetic dipole antennas for this case. Those antennas show perfect polarization characteristics. First, we generate a

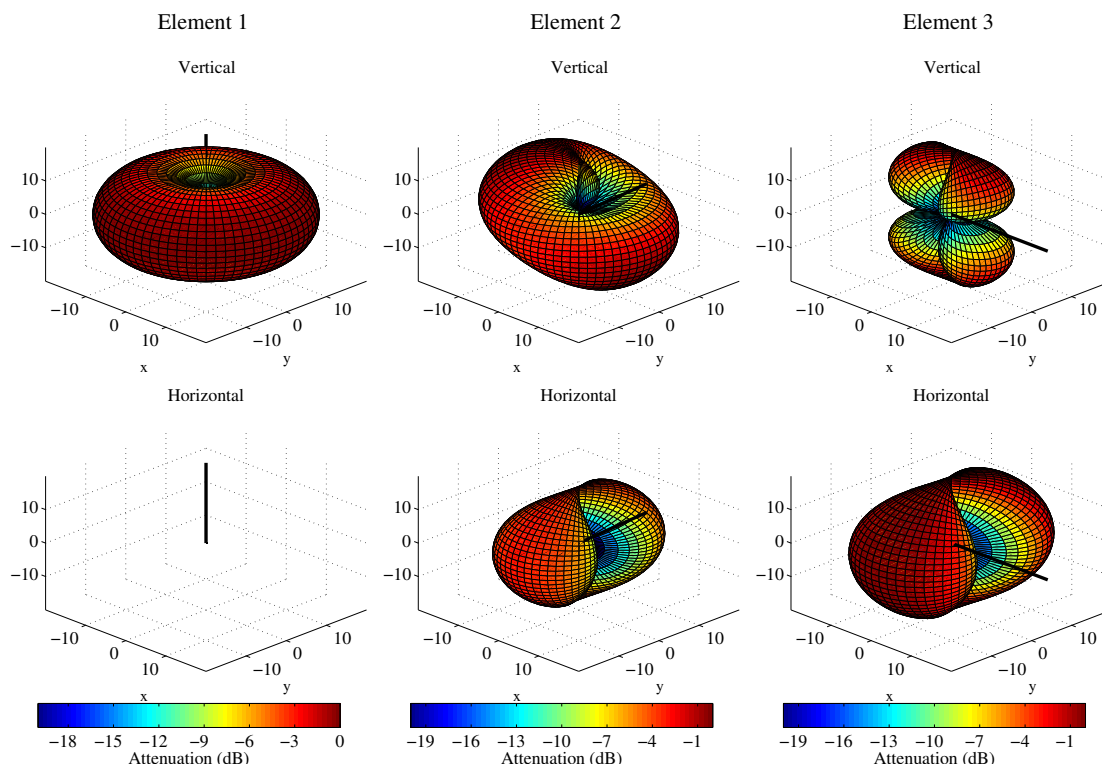


Figure 43: Polarimetric dipole antenna patterns for different orientations

single dipole with V-polarization. Then, we create multiple copies of this antenna element and rotate them by 45 and 90 degrees, respectively. We then use the same array for the receiver.

```

1 l = layout( s );                                     % Create a new Layout
2 l.tx_array.generate('dipole');                      % create V-polarized dipole
3 l.tx_array.set_grid( (-180:10:180)*pi/180 , (-90:10:90)*pi/180 );
4
5 l.tx_array.field_pattern_vertical = ...           % Normalize
6   l.tx_array.field_pattern_vertical / max(max(l.tx_array.field_pattern_vertical));
7
8 l.tx_array.set_grid( (-180:5:180)*pi/180 , (-90:5:90)*pi/180 );
9 l.tx_array.copy_element(1,2:3);                    % Duplicate the element two more times
10 l.tx_array.rotate_pattern(45,'y',2);              % 45\degree polarization
11 l.tx_array.rotate_pattern(90,'y',3);              % 90\degree polarization
12 l.tx_array.visualize;                            % Plot the array
13 l.rx_array = l.tx_array;                         % Use the same array for the Rx

```

Defining a track The third step defines the track. Here, we use a circle with 20 m diameter starting in the east, traveling north. We also choose a LOS scenario since we want to study the LOS polarization. The transmitter is located 8 m north of the center of the circle at an elevation of 2 m.

```

1 l.tx_position = [ 0 ; 12 ; 6 ];                   % Tx position
2 l.rx_position = [ 20 ; 0 ; 0 ];                   % Start position for the Rx track
3 l.track.generate('circular',40*pi,0);            % A circular track with radius 10 m
4 l.track.scenario = 'BERLIN_UMa_LOS';             % Choose the Urban Macro LOS scenario
5 l.track.interpolate_positions( s.samples_per_meter ); % Interpolate positions
6 l.visualize;                                      % Plot the track

```

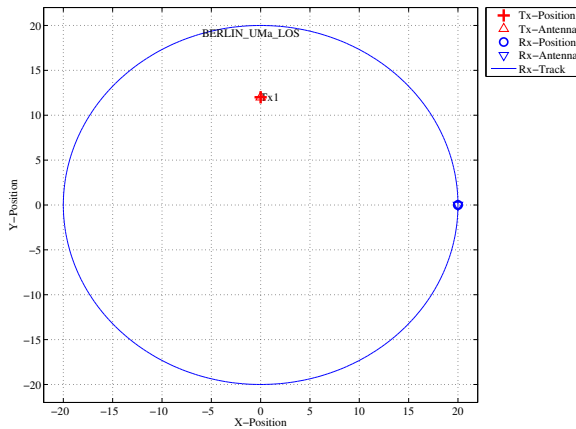


Figure 44: Scenario layout

Generating channel coefficients Now, we have finished the parametrization of the simulation and we can generate the parameters. We thus create a new set of correlated LSPs and fix the shadow fading and the K-factor to some default values. This disables the drifting for those parameters. We need to do that since otherwise, drifting and polarization would interfere with each other.

```

1 RandStream.setGlobalStream(RandStream('mt19937ar','seed',1));
2
3 p = l.create_parameter_sets;                        % Create parameter sets
4 p.parameter_maps(:,:,2) = 3;                       % Fix KF to 3 dB
5 p.parameter_maps(:,:,3) = 0;                       % Fix SF to 0 dB
6 p.plpar = [];                                     % Disable path loss model
7 p.update_parameters;
8
9 [c,cb] = p.get_channels;                          % Get the channel coefficients

```

| | | |
|--------------|--|-----------|
| 1 Parameters | [oo] | 1 seconds |
| 2 Channels | [oo] | 3 seconds |

Results and Evaluation We now check the results and confirm, if they are plausible or not. We start with the two vertically polarized dipoles at the Tx and at the Rx side.

The model creates 8 taps, which is the default for the Urban-Macro LOS scenario. Without path-loss and shadow fading ($SF=1$), the power is normalized such that the sum over all taps is 1W and with a K-Factor of 3 dB, we get a received power of 0.67W for the LOS component. The remaining 0.33W are in the NLOS components. The results can be seen in Fig. 45 (top left).

```

1 figure % New figure
2 plot(abs(squeeze( c.coeff(1,1,:,:,:) )') .^2); % Plot the graph
3 axis([0 360 -0.1 1]); % Set the axis
4 xlabel('Position [degrees]'); % Add description
5 ylabel('LOS Power, linear scale'); % Add title
6 title('Tx: Vertical , Rx: Vertical'); % Add title
7
8 disp(['LOS power: ',num2str(mean( abs(c.coeff(1,1,1,:)) .^2 , 4))])
9 disp(['NLOS power: ',num2str(mean( sum(abs(c.coeff(1,1,2:end,:)) .^2,3) , 4))])

```

```

1 LOS power: 0.52851
2 NLOS power: 0.22249

```

The LOS power is almost constant when the Rx is south of the Tx. However, in close proximity (at 90°), the power is lowered significantly. This comes from the 2 m elevation of the Tx. When the Rx is almost under the Tx, the radiated power of the Dipole is much smaller compared to the broadside direction. The average power of the LOS is thus also lowered to 0.56 W. The average sum-power of the 7 NLOS components

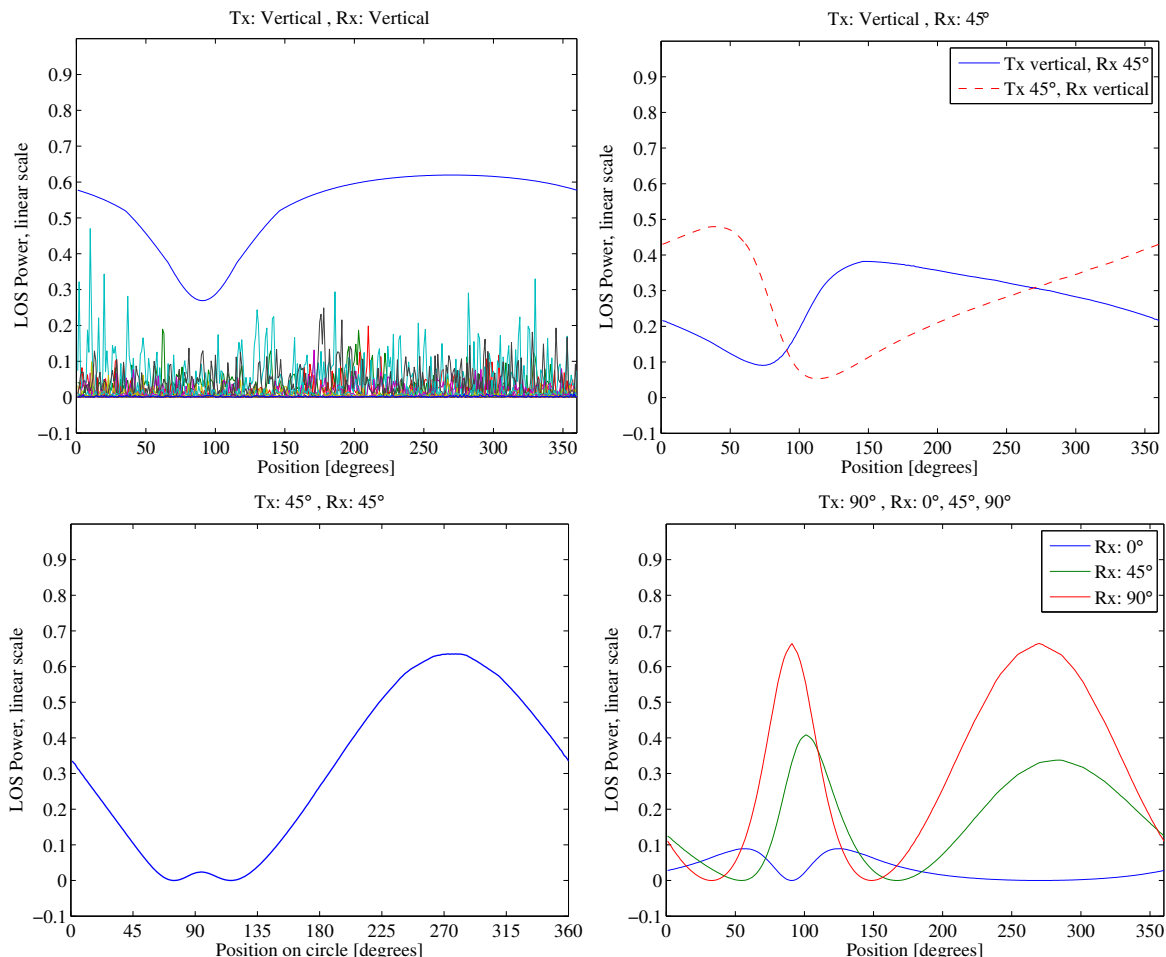


Figure 45: Results from the geometric polarization tutorial

is 0.26 W. This mainly come from the XPR which leaks some power from the vertical- into the horizontal polarization and thus reduces the received power on the vertically polarized Dipole.

Next, we study two cases. Either the Tx is vertical polarized and the Rx is at 45° or vise versa (Fig. 45, top right).

```

1 figure % New figure
2 plot(abs(squeeze( c.coeff(2,1,1,:)) .^2)); % Tx vertical, Rx 45\degree\
3 hold on
4 plot(abs(squeeze( c.coeff(1,2,1,:)) .^2, '--r')); % Tx 45\degree\, Rx vertical
5 hold off
6 axis([0 360 -0.1 1]);
7 legend('Tx vertical, Rx 45\circ', 'Tx 45\circ, Rx vertical')
8 xlabel('Position [degrees]');
9 ylabel('LOS Power, linear scale');
10 title('Tx: Vertical , Rx: 45\circ');

```

The receiver changes its direction in a way that it always has the same orientation towards the Tx. However, due to the displacement of the Tx, the radiated power towards the Tx becomes minimal at around 90°. This minimum is visible in both curves (blue and red). However, the pole of the 45°slanted dipole now points to a different direction which explains the difference in the two lines. When the Rx is at 45°and the Tx is vertical, the pole is in the right half if the circle - resulting in a lower received power. When the Rx is Vertical and the Tx is 45°, the minimum power is achieved in the left half of the circle.

Next, we evaluate the two dipoles which are rotated by 45°. When moving around the circle, the Tx stays fixed and the Rx rotates. Subsequently, at one position, we will have both dipoles aligned and at another position, both will be crossed. When they are crossed, the received power will be 0 and when they are aligned, the power will match the first plot (two vertical dipoles). This can be seen in the following figure.

```

1 figure % New figure
2 plot(abs(squeeze( c.coeff(2,2,1,:)) .^2 , 'LineWidth',1);
3 axis([0 360 -0.1 1]);
4 set(gca,'XTick',0:45:360)
5 xlabel('Position on circle [degrees]');
6 ylabel('LOS Power, linear scale');
7 title('Tx: 45\circ , Rx: 45\circ');

```

In the last figure, we rotated the transmit antenna by 90°. It is thus lying on the side and it is horizontally polarized. For the Rx, we consider three setups: Vertical (blue line), 45°(green line) and 90°(red line). Note that the Tx is rotated around the y-axis. At the initial position (0°), the Rx (45 and 90°) is rotated around the x-axis. This is because the movement direction.

```

1 figure % New figure
2 plot(abs(squeeze( c.coeff(:,3,1,:)) .^2);
3 axis([0 360 -0.1 1]);
4 legend('Rx: 0\circ','Rx: 45\circ','Rx: 90\circ')
5 xlabel('Position [degrees]');
6 ylabel('LOS Power, linear scale');
7 title('Tx: 90\circ , Rx: 0\circ, 45\circ, 90\circ');

```

When the receiver is vertical (blue line), both antennas are always crossed. There is no position around the circle where a good link can be established. When the receiver is horizontal (red line), however, there are two points where the two dipoles are aligned. For the 45°dipole, the same behavior can be observed but with roughly half the power.

```

1 close all
2 disp(['QuaDRiGa Version: ',simulation_parameters.version])

```

```

1 QuaDRiGa Version: 1.0.1-145

```

A.8 Visualizing RHCP/LHCP Patterns

The internal algorithms of the channel model only work with linear polarization. The antenna patterns are thus only stored in H/V polarization. This script defines two circular patch antennas and places them in an environment. It then rotates the transmit antenna degree by degree and thus samples all azimuth and elevation angles. The channel model is set up to record the channel response and thus record the RHCP/LHCP response like in a measurement in an anechoic chamber.

Set up the array We set up a patch antenna with an opening angle of 120° . We then copy that patch and rotate it by 90° around the x-axis to create an X-Pol array. We then set the coupling to $+/- 90^\circ$ phase to transmit circular polarized waves.

```

1 resolution = 10;           % in Degrees
2
3 a = array('custom',120,120,0);
4 a.set_grid( (-180:resolution:180)*pi/180 , (-90:resolution:90)*pi/180 );
5 a.copy_element(1,2);
6
7 b = a.copy_objects;
8
9 a.rotate_pattern(90,'x',2);
10 a.coupling = 1/sqrt(2) * [1 1;1j -1j];
11
12 b.rotate_pattern(90,'x',2);
13 b.coupling = 1/sqrt(2) * [1 1;1j -1j];

```

Place arrays in layout We place two of those arrays in a layout. The scenario 'LOSonly' has no NLOS scattering. One can see this setup as a perfect anechoic chamber.

```

1 l = layout;
2 l.simpars.show_progress_bars = 0;
3 l.simpars.drifting_precision = 0;
4
5 l.rx_position = [11;0;0];
6 l.track.no_snapshots = 1;
7 l.track.ground_direction = pi;
8 l.track.scenario = 'LOSonly';
9 l.tx_array = a;
10 l.rx_array = b;
11
12 p = l.create_parameter_sets;
13 [~,cb] = p.get_channels;
14 cb.pin = zeros( size(cb.pin) );

```

Get array response We now sample the array response for each degree in the antenna array.

```

1 pat = zeros( a.no_el , a.no_az , 2 , 2 );
2
3 values = a.no_az;
4 fprintf('Calculating ['); m0=0; tStart = clock; % A Status message
5 for n = 1:a.no_az
6     m1=ceil(n/values*50); if m1>m0; for m2=1:m1-m0; fprintf('o'); end; m0=m1; end;
7
8     a1 = a.copy_objects;
9     a1.rotate_pattern( a.azimuth_grid(n)*180/pi , 'z');
10
11    for m=1:a.no_el
12        a2 = a1.copy_objects;
13        a2.rotate_pattern( a.elevation_grid(m)*180/pi , 'y');
14        cb.tx_array = a2;
15        c = cb.get_channels;
16        pat(m,n,:,:,:) = c.coeff;
17    end
18 end
19 fprintf('] %5.0f seconds\n',round( etime(clock, tStart) ));

```

```
1 Calculating [oooooooooooooooooooooooooooo] 17 seconds
```

Plot For plotting we use the internal function of the array class. We adjust the title of the figures accordingly.

```
1 d = a.copy_objects;
2 d.field_pattern_vertical = pat(:,:, :, 1);
3 d.field_pattern_horizontal = pat(:,:, :, 2);
4 x = d.visualize;
5
6 set(x(1,11), 'String', 'RHCP-RHCP')
7 set(x(1,12), 'String', 'RHCP-LHCP')
8
9 set(x(2,11), 'String', 'LHCP-RHCP')
10 set(x(2,12), 'String', 'LHCP-LHCP')
```

```
1 close all
2 disp(['QuaDRiGa Version: ', simulation_parameters.version])
```

```
1 QuaDRiGa Version: 1.0.1-145
```

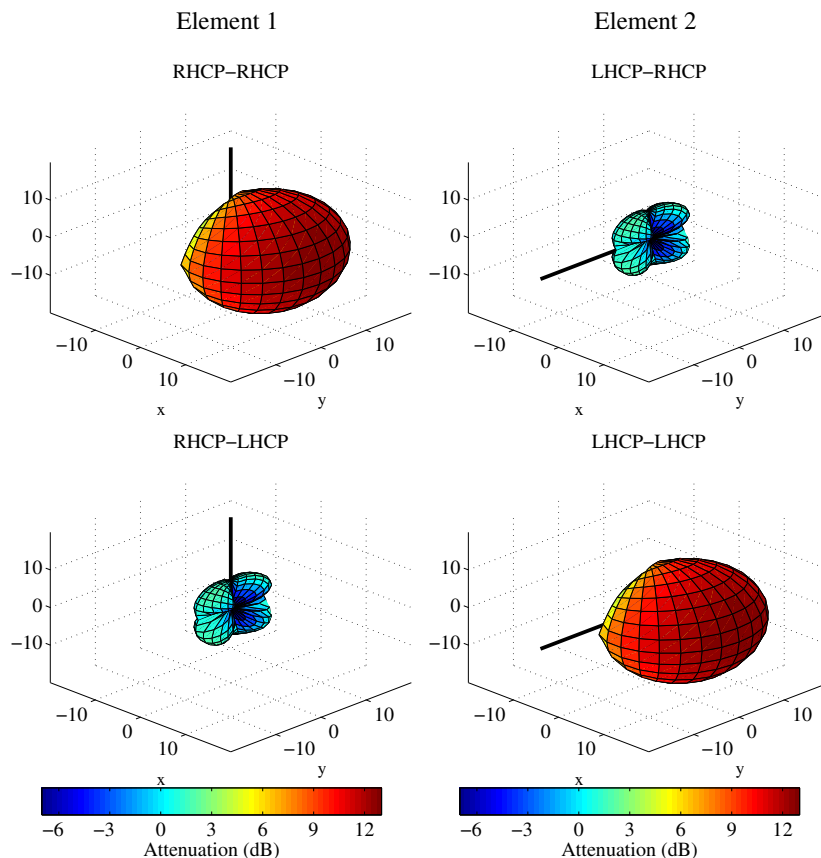


Figure 46: RHCP / LHCP antenna patterns

A.9 How to manually set LSPs in QuaDRiGa

This tutorial explains, how to generate a time-series of channel coefficients with manual selection of LSPs.

Setting general parameters We set up some basic parameters such as center frequency, sample density and the position of the transmitter.

```

1 close all
2 clear all
3
4 set(0,'defaultTextFontSize', 14)      % Set default font size for the plots
5 set(0,'defaultAxesFontSize', 14)
6
7 s = simulation_parameters;           % Basic simulation parameters
8 s.center_frequency      = 2.185e9;    % Center Frequency
9 s.sample_density        = 4;          % 4 samples / half wave length
10
11 l = layout(s);                   % Create Layout

```

Setting up a user track QuaDRiGa needs the positions of transmitter and receiver, e.g. for calculating the polarization or the arrival and departure angels. The positioning information of the Tx and Rx is essential also when the LSPs are not calculated. The following generates a linear track with 20 m length having a direction. The track is further split into 4 segments of 5 m length.

The splitting is done by calling the method 'split_segment' of the track object. The the first two arguments of that function are the minimum length of a segment (1 m) and the maximum length of the segment (6 m). Each existing segment that is longer then the maximum length is split into subsegments. The length of those segments is random where the third and fourth parameter determine the mean and the STD of the length of new subsegment. Hence, 't.split_segment(1,6,5,0)' splits all segment longer than 6 m into subsegments of 5 m length.

Each segment gets assigned a scenario. This is also essential since many parameters (such as the number of clusters, the XPR etc.) are scenario-specific. Hence, they are the same for the entire scenario. Here, we set the first the segments to **NLOS**, the third to **LOS** and the last to **NLOS**.

Last, we set a random starting position for the track in the layout.

```

1 l.tx_position = [0;0;25];                      % Set Tx-position
2
3 t = track('linear',20);                         % Linear track, 20 m length
4 t.interpolate_positions(s.samples_per_meter);   % Interpolate to sample density
5 t.split_segment( 1,6,5,0 );                      % Split in 4 segments
6
7 Un = 'WINNER_UMa_C2_NLOS';
8 Ul = 'WINNER_UMa_C2_LOS';
9 t.scenario = {Un,Un,Ul,Un};                     % Set scenarios
10
11 l.randomize_rx_positions( 500,0,0,0 );         % Random start position
12 tmp = l.rx_position;
13 l.track = t;
14 l.rx_position = tmp;
15
16 l.visualize;

```

Manual setting of the parameters Now we initialize the parameter-set objects.

The method "l.create_parameter_sets" splits the track into smaller sub-tracks, one for each segment. It further extracts the scenario informations. Each scenario gets its own parameter-set object. So we get an

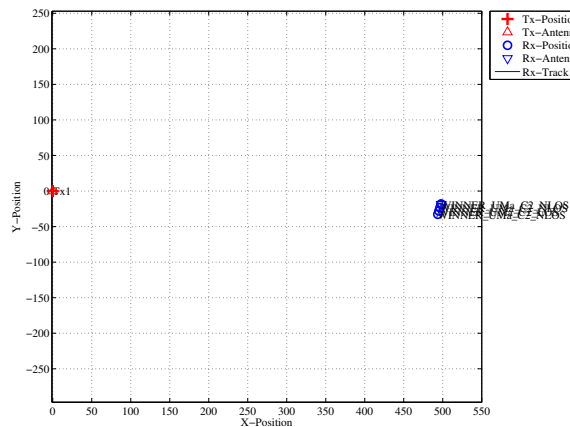


Figure 47: Scenario overview (manual parameter selection)

array of two parameter sets. The first element $p(1)$ has three positions (NLOS segments) and the second has one position (LOS segment).

```

1 p = l.create_parameter_sets(1);
2
3 p(1).name
4 p(1).no_positions
5
6 p(2).name
7 p(2).no_positions

```

```

1 Parameters      [oooooooooooooooooooooooooooo]      5 seconds
2
3 ans =
4
5 WINNER-UMa-C2-NLOS_Tx1
6
7
8 ans =
9
10    3
11
12 ans =
13
14 WINNER-UMa-C2-LOS_Tx1
15
16 ans =
17
18    1
19
20

```

We set the number of clusters for the NLOS segments to 14. Currently, it is not possible to have a different number of clusters for each segment, i.e. it is not possible for the first NLOS segment to have 14 clusters and for the second to have only 10.

```

1 p(1).scenpar.NumClusters = 14;

```

In order to manually set the parameters, we have to overwrite the original settings. We do this here for the delay spread. The automatically generated values are:

```

1 [p(1).ds(1) p(1).ds(2) p(2).ds(1) p(1).ds(3)]*1e6

```

```

1
2 ans =
3
4    0.2696    0.2433    0.0948    0.2094

```

We want to set the values of the four segments to 0.45, 0.33, 0.12 and 0.60 microseconds. This is done by:

```

1 p(1).ds(1) = 0.45e-6;
2 p(1).ds(2) = 0.33e-6;
3 p(2).ds(1) = 0.12e-6;
4 p(1).ds(3) = 0.60e-6;
```

The K-Factor and the shadow fading are read from the map during the generation of channel coefficients. This would overwrite any manual values. However, this could be deactivated. A drawback is that in this case the KF, SF and PL are only updated once per segment. This will result in a step-like function of the output power. There is currently no method to set the power manually on a per-snapshot basis.

In the following example, we want to fix the received power to -102, -97, -82 and -99 dBm. K-Factors are taken from the map.

```

1 p(1).plpar = []; % Disable path loss for NLOS
2 p(2).plpar = []; % Disable path loss for LOS
3
4 p(1).sf = 10.^0.1*[-102, -97, -99]; % Set power for NLOS segments
5 p(2).sf = 10.^0.1*[-82]; % Set power for LOS segments
6
7 p(1).map_valid = false; % Disable automatic overwrite for NLOS
8 p(2).map_valid = false; % Disable automatic overwrite for LOS
```

Calculate channel coefficients Now we calculate the coefficients and the received power along the path. The following command calculate the channel coefficients. We then check the number of clusters that have been produced for each segment.

```

1 cm = p.get_channels; % Calculate the channel coefficients
2 cat( 1, cm.no_path ) % Display the number of paths
```

```

1 Channels [oooooooooooooooooooooooooooo] 7 seconds
2
3 ans =
4
5 14
6 14
7 14
8 8
```

The first three segments have 14 clusters. This has been set earlier. The last LOS segment has 15 clusters. One can see, that the three NLOS segment come first, followed by the LOS segment. The order has been scrambled. The following command sorts and combines the segments into one fading sequence.

```
1 c = cm.merge;
```

We now plot the power along the path. You can see the power levels of around -102, -97, -82 and -99 dBm which have been set earlier. Each segment has a transition area (e.g. from 2.5m to 5m, from 7.5m to 10m and from 12.5m to 15m) where the merging took place. In those areas, the power is scaled linearly. That means that, for example, in between 7.5 and 10m, the power ramps up from -97 to -82 dBm.

```

1 power = squeeze(sum(abs(c.coeff).^2,3));
2 power = 10*log10(power);
3
4 figure
5 [~,dist] = t.get_length;
6 plot(dist,power)
7 title('Simulated Power')
8 xlabel('Distance from start point [m]')
9 ylabel('Received Power [dBm]')
10 axis([0,20,-110,-80])
11 grid on
```

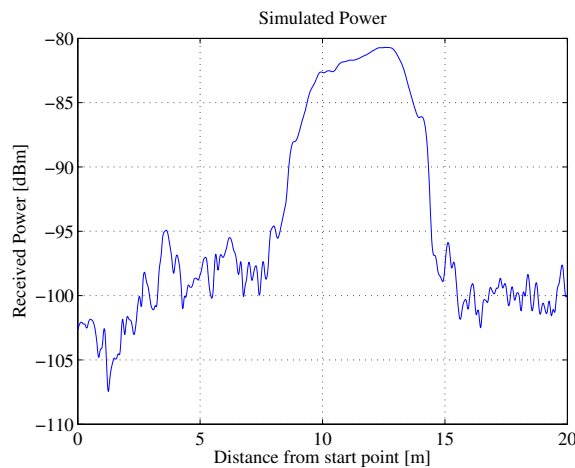


Figure 48: Power along the track (manual parameter selection)

The last plot shows the DS along the path. The results reflect the settings of 0.45, 0.33, 0.12 and 0.60 quiet well. As for the power, there is an overlap in between the segments. For example, in between 7.5 and 10m the DS drops from 0.33 to 0.12 microseconds. Additional fluctuations are caused by small scale fading.

```

1 coeff = squeeze( c.coeff );
2 delay = c.delay;
3
4 pow_tap = abs(coeff).^2;
5 pow_sum = sum(pow_tap);
6 mean_delay = sum( pow_tap.*delay) ./ pow_sum;
7 ds = sqrt( sum( pow_tap.*delay.^2)./ pow_sum - mean_delay.^2 );
8
9 figure
10 plot(dist,ds*1e6)
11 title('Simulated Delay Spread')
12 xlabel('Distance from start point [m]')
13 ylabel('RMS DS [\mu s]')
14 axis([0,20,0,1])
15 grid on

```

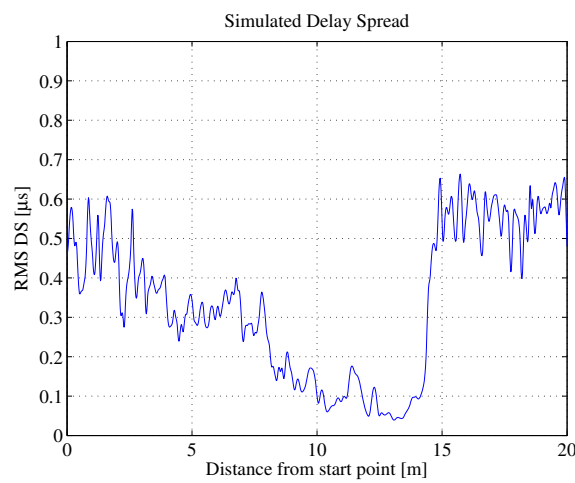


Figure 49: DS along the track (manual parameter selection)

```

1 close all
2 disp(['QuaDRiGa Version: ',simulation_parameters.version])

```

QuaDRiGa Version: 1.0.1-145

B Departure and Arrival Angles (Adopted WINNER Method)

In the **WINNER** model, the azimuth arrival and departure angles are modeled using a wrapped Gaussian distribution (see [4], page 39).

$$P(\phi) = \frac{1}{\sigma_\phi \sqrt{2\pi}} \cdot \exp\left(\frac{-\phi^2}{2\sigma_\phi^2}\right) \quad (112)$$

The wrapping is applied later by (115) when the discrete cluster angles are drawn from the statistics. Since the above formula assumes a continuous spectrum, whereas the channel model uses discrete paths, we need to correct the variance by a function $C_\phi(L, K)$. This function ensures that the input variance σ_ϕ is correctly reflected in the generated angles. The same approach was taken by the **WINNER** model. However, [4] does not explain how the correction values were obtained.

Generation of azimuth and elevation angles The individual angles ϕ_l are obtained by first normalizing the power angular spectrum so that its maximum has unit power. We can thus omit the scaling factor $1/(\sigma_\phi \sqrt{2\pi})$. The path powers P_l (21) are also normalized such that the strongest peak with unit power corresponds to an angle $\phi = 0$. All other paths get relative departure or arrival angles depending on their power,

$$\phi_l^{[1]} = \frac{\sigma_\phi}{C_\phi(L, K)} \cdot \sqrt{-2 \cdot \ln\left(\frac{P_l}{\max(P_l)}\right)}. \quad (113)$$

Next, two random variables, X_l and Y_l are drawn, where $X_l \sim \{-1, 1\}$ is the positive or negative sign and $Y_l \sim \mathcal{N}(0, (\frac{\sigma_\phi}{7})^2)$ introduces a random variation on the angle. The angles $\phi_l^{[1]}$ are then updated to

$$\phi_l^{[2]} = X_l \cdot \phi_l^{[1]} + Y_l. \quad (114)$$

If the power P_l of a path is small compared with the strongest peak, its angle $\phi_l^{[2]}$ might exceed $\pm\pi$. In this case, it is wrapped around the unit circle by a modulo operation

$$\phi_l^{[3]} = (\phi_l^{[2]} + \pi \mod 2\pi) - \pi. \quad (115)$$

In case of elevation spreads, the possible range of elevation angles goes from $-\pi/2$ to $\pi/2$. In this case, the values $\phi_l^{[3]}$ need an additional correction. This is done using (36). The positions of the **Tx** and **Rx** are deterministic, and so are the angles of the **LOS** component. This is taken into account by updating the values of the angles in order to incorporate the **LOS** angle

$$\phi_1^{[4]} = 0 \quad (116)$$

$$\phi_l^{[5]} = \phi_l^{[4]} + \phi^{LOS}. \quad (117)$$

Finally, the **NLOS** cluster-paths are split into 20 sub-paths to emulate intra cluster angular spreads.

Calculation of $C_\phi(L, K)$ The correction function $C_\phi(L, K)$ takes the influence of the **KF** and the varying number of clusters on the angular spread into account. To approximate the function, random powers P_l and angles ϕ_l are generated with the correction function set to $C_\phi = 1$. The powers are calculated as described in Section 3.2 with different values of K included. Based on those values, the actual RMS angular spread $\sigma_\phi^{[actual]}$ is calculated using equations (26), (27), and (28). The correction function follows from comparing $\sigma_\phi^{[actual]}$ with σ_ϕ . However, two aspects need to be considered:

1. Due to the randomization of the angles in (114), we have to take the average angle over a sufficiently large quantity (≈ 1000 realizations) of $\sigma_\phi^{[actual]}$. This value is denoted as $\sigma_\phi^{[avg.]}$.

2. There is a nonlinear relationship between the angular spread in the simulated data $\sigma_\phi^{[\text{avg.}]}$ and the initial value σ_ϕ . This comes from the logarithm in (113) and the modulo in (115). However, for small values, the relationship can be approximated by a linear function. The maximum angular spread σ_ϕ^{\max} is defined as the point where the error between the corrected value $\frac{\sigma_\phi}{C_\phi(L,K)}$ and $\sigma_\phi^{[\text{avg.}]}$ is 10°.

For a range of typical values $L \in [2, 42]$ and $K^{[\text{dB}]} \in [-20, 20]$, $C_\phi(L, K)$ can be numerically calculated as

$$C_\phi(L, K) = \frac{1}{\sigma_\phi^{\max}} \cdot \int_0^{\sigma_\phi^{\max}} \frac{\sigma_\phi^{[\text{avg.}]}(\sigma_\phi)}{\sigma_\phi} d\sigma_\phi, \quad (118)$$

where the σ_ϕ -dependency of $\sigma_\phi^{[\text{avg.}]}(\sigma_\phi)$ comes from the individual angles ϕ_l .

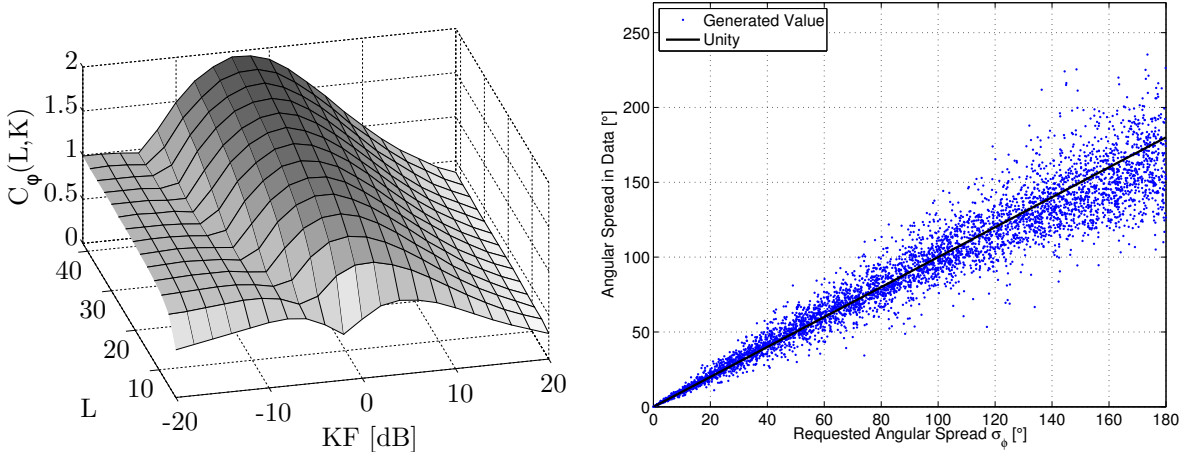


Figure 50: Visualization of the angular spread correction function $C_\phi(L, K)$. Left: Surface plot of $C_\phi(L, K)$ for different values of L and K . Right: Scatter-plot of the initial angular spread σ_ϕ vs. the output of the model (with correction).

Correction of the angular spread in the WINNER model The proposed correction function for the WINNER model (see [4], pp. 39) works as follows: The individual angles (113) are calculated by

$$\phi_l^{[1]} = \frac{2 \cdot \frac{\sigma_\phi}{1.4}}{C} \cdot \sqrt{-\ln \left(\frac{P_l}{\max(P_l)} \right)}, \quad (119)$$

where C depends on the numbers of paths (see Table 14). The **KF** is corrected by a polynomial of third grade. With the constant coefficients in (119) and the factor of 2 in the square root of (113), the correction function $C_\phi(L, K)$ of the WINNER model is

$$C_\phi^{\text{WINNER}}(L, K) = C \cdot (1.1035 - 0.028 \cdot K - 0.002 \cdot K^2 + 0.0001 \cdot K^3). \quad (120)$$

A comparison of the both functions for different values of L and K is given in Table 15. In the second column, the letter W indicates the value for the WINNER model and the letter Q indicates the value of the adopted function. The polynomial has a value of 1 at **KF** values -11.65, 3.11, and 28.54. At those points, the WINNER correction function is independent of the **KF**. The corresponding rows are highlighted in the table. Generally, both functions are similar. They agree best as **KF** values around -14, -3, and 12 but show differences at other values.

Table 14: Correction values from [4] for different numbers of paths

| L | 4 | 5 | 8 | 10 | 11 | 12 | 14 | 15 | 16 | 20 |
|---|-------|-------|-------|-------|-------|-------|-------|-------|-------|-------|
| C | 0.779 | 0.860 | 1.018 | 1.090 | 1.123 | 1.146 | 1.190 | 1.211 | 1.226 | 1.289 |

Table 15: Comparison of the correction functions

| KF [dB] | W/Q | Number of paths (L) | | | | | | | | | |
|------------|-----|---------------------|-------|-------|-------|-------|-------|-------|-------|-------|-------|
| | | 4 | 5 | 8 | 10 | 11 | 12 | 14 | 15 | 16 | 20 |
| -11.7 | W | 0.779 | 0.860 | 1.018 | 1.090 | 1.123 | 1.146 | 1.190 | 1.211 | 1.226 | 1.289 |
| | Q | 0.765 | 0.822 | 0.904 | 0.923 | 0.929 | 0.935 | 0.935 | 0.935 | 0.935 | 0.943 |
| -8.0 | W | 0.895 | 0.988 | 1.169 | 1.252 | 1.290 | 1.316 | 1.366 | 1.391 | 1.408 | 1.480 |
| | Q | 0.790 | 0.820 | 0.857 | 0.870 | 0.880 | 0.890 | 0.977 | 1.020 | 1.070 | 1.250 |
| -4.0 | W | 0.917 | 1.012 | 1.198 | 1.283 | 1.322 | 1.349 | 1.401 | 1.425 | 1.443 | 1.517 |
| | Q | 0.713 | 0.777 | 1.047 | 1.213 | 1.277 | 1.340 | 1.427 | 1.470 | 1.500 | 1.613 |
| 0.0 | W | 0.860 | 0.949 | 1.123 | 1.203 | 1.239 | 1.265 | 1.313 | 1.336 | 1.353 | 1.422 |
| | Q | 0.830 | 0.990 | 1.277 | 1.380 | 1.420 | 1.460 | 1.520 | 1.550 | 1.570 | 1.637 |
| 3.1 | W | 0.779 | 0.860 | 1.018 | 1.090 | 1.123 | 1.146 | 1.190 | 1.211 | 1.226 | 1.289 |
| | Q | 0.926 | 1.029 | 1.221 | 1.295 | 1.325 | 1.354 | 1.391 | 1.409 | 1.425 | 1.481 |
| 4.0 | W | 0.752 | 0.831 | 0.983 | 1.053 | 1.085 | 1.107 | 1.149 | 1.170 | 1.184 | 1.245 |
| | Q | 0.930 | 1.020 | 1.190 | 1.257 | 1.283 | 1.310 | 1.343 | 1.360 | 1.373 | 1.420 |
| 8.0 | W | 0.625 | 0.690 | 0.817 | 0.875 | 0.901 | 0.920 | 0.955 | 0.972 | 0.984 | 1.035 |
| | Q | 0.820 | 0.870 | 0.967 | 1.003 | 1.017 | 1.030 | 1.057 | 1.070 | 1.077 | 1.103 |
| 12.0 | W | 0.508 | 0.561 | 0.664 | 0.711 | 0.733 | 0.748 | 0.776 | 0.790 | 0.800 | 0.841 |
| | Q | 0.627 | 0.653 | 0.707 | 0.727 | 0.733 | 0.740 | 0.760 | 0.770 | 0.773 | 0.793 |
| 16.0 | W | 0.431 | 0.476 | 0.563 | 0.603 | 0.621 | 0.634 | 0.658 | 0.670 | 0.678 | 0.713 |
| | Q | 0.443 | 0.457 | 0.490 | 0.503 | 0.507 | 0.510 | 0.517 | 0.520 | 0.523 | 0.537 |
| 20.0 | W | 0.423 | 0.467 | 0.553 | 0.592 | 0.610 | 0.623 | 0.647 | 0.658 | 0.666 | 0.701 |
| | Q | 0.300 | 0.310 | 0.320 | 0.323 | 0.327 | 0.330 | 0.337 | 0.340 | 0.343 | 0.350 |